OPTIMISATION ALGORITHMS FOR ELECTRICITY LOAD MANAGEMENT

THESIS

Submitted by

GODWIN NORENSE OSARUMWENSE ASEMOTA

In Partial Fulfilment of the Requirements for the Degree of

DOCTOR OF PHILOSOPHY

AFRICAN CENTRE OF EXCELLENCE IN ENERGY FOR SUSTAINABLE DEVELOPMENT,
COLLEGE OF SCIENCE AND TECHNOLOGY,
UNIVERSITY OF RWANDA,
KIGALI - RWANDA

MAY 2023

DECLARATION

I hereby declare that the thesis titled "Optimisation Algorithms for Electricity Load Management" to be submitted for the Degree of Doctor of Philosophy is my original work andthe thesis has not formed the basis for the award of any degree, diploma, associateship, or fellowship, or similar other titles. It has not been submitted to any other University orInstitution for the award of any degree or diploma.

20th May 2022

Godwin Norense Osarumwense Asemota

Name and Signature of the student

The Thesis Committee for Godwin Norense Osarumwense Asemota

Professor Nelson M. Ijumba

Name and Signature of Main Supervisor

DEDICATION

This thesis is dedicated to the Almighty God who has given me abundant life, the grace to start and finish this research, and all good things to enjoy.

ACKNOWLEDGMENT

I am gratefully indebted to my Supervisor and Adviser, Prof. Nelson Ijumba, for his invaluable assistance and guidance in this research work.

Furthermore, he demonstrated his belief in my research capacity by breaking the strong conspiracy against my admission, when he approved my Ph.D. candidacy by the "Completed work" route in December 2016 at the College Council level, when he was mandated to be the "Caretaker Principal of CST", while he remains the substantive Deputy Vice-Chancellor (Academic Affairs and Research).

In consonance with the above, I also wish to thank the former Vice Chancellor, Prof. Philip Cotton, for strenuously trying, but being unable to keep me in the employ of UR and, for the Almighty God ultimately using him to appoint the former DVC (AAR) as the "Caretaker Principal of CST", to orchestrate my Ph.D. admission.

I wish to express my deep gratitude to my very beautiful wife Dr. (Mrs.) Olukemi Olufunmilola Asemota, for making it much easier, more congenial, and less stressful to carry on with all my diverse research endeavours, especially when there was no income generation from my end, to support the family.

I also wish to thank Eng. Mosoti Ichwara Oseko for his constant support and encouragement. The same goes for Dr. Patrick Ujwiga Anguru and Dr. Martins Onimisi for their constant urging and support. I also wish to appreciate the assistance of Eng. Dr. Katundu Imasiku, especially for helping with diagrams and formatting, and also, Engr (Dr.) Kehinde Adeseye Adeyeye for helping with registration, submitting documents and information. I wish to most sincerely thank and appreciate Dr. Omololu Akin-Ojo for his wonderful and wholesome hospitality and care for me and my family, at any time we have beaconed on him to provide us with accommodation and boarding. I would like to use this opportunity to thank the then Director of ACEESD, Prof. Etienne Ntagwirumugara for approving my full scholarship for the Ph.D. programme under the Centre and the World Bank for supporting my Ph.D. studies to enable me to complete the programmes without let or hindrance.

I wish to also thank all other people who have been of assistance in one way or another, whom I may have been unable to name. The Almighty God, bless you all richly and abundantly in Jesus Christ's precious and unchallengeable names, Amen.

ABSTRACT

The continuously-rising electricity consumption patterns worldwide and the load upsurge have imposed substantial constraints on modern and legacy power supply infrastructures. Also, optimisation algorithms are the challenging problems of determining sets of inputs to objective functions and problem parameters that result in scheduling minimum and maximum boundary conditions for each energy design constraint. The development of energy-efficient buildings minimise energy consumption through integrated energy-efficient design processes, serves as a practical guide to building designs that can lower the energy requirements, and a strategy to reduce energy consumption. Furthermore, the multivariate analysis used additive linear equations to suggest that substantial value differences exist across gender in attitude towards optimal electricity load management practices. The study also used blinds, daylighting, and geyser temperature settings to save power, and reduce electricity use, and costs for sustainable growth and development. Also, the software validation of optimal bidirectional composite conductor designs, which carry very high currents at high temperatures, vertically and horizontally in tandem, attempt to provide solutions to the composites comprising a conductor and insulating material ribbons in which the density approaches the minimum conducting area and satisfies Laplace's equation. In addition, there were materials and cost optimisation in which the horizontal and vertical currents were equal, without hotspots, or random power transfer problems in the composite conductor matrix. Adopting the findings or outcomes of the study could provide more optimal and sustainable energy consumption thereby reducing pressure on the power grid. The contributions to the knowledge of the study include (a) Residential load management predicts and modifies electricity consumption styles and attitudes by gender, (b) The Quetelet curve index is used to modify the average citizen's energy consumption behaviour, awareness, education, and target marketing, (c) A bidirectional light-weight composite conductor capable of simultaneously carrying very high vertical and horizontal currents, at high voltages, and large power-carrying capabilities were designed, and (d) The conductor-composite was proven to occupy about two-thirds of the unit square area. However, the areas for future research include the design, manufacture, and machinability of stable high-capacity composite conductors and insulators (organic or inorganic) that can withstand very high temperatures, higher voltage stresses, and much larger power-carrying capabilities.

JOURNAL ARTICLES AND CONFERENCE PAPERS FROM THIS RESEARCH

(a) Godwin Norense Osarumwense Asemota (2021). Preview: Rwanda's Off-Grid Solar Performance Targets. *Joule J.*, Volume 5, Issue 1, 20 January 2021, pages 22-23. https://doi.org/10.1016/j.joule.2020.12.016.
https://www.sciencedirect.com/science/journal/25424351. Joule, Elsevier.
Impact Factor: 46.048 (2023). Indexed by SCOPUS.

(b) Godwin Norense Osarumwense Asemota and Nelson M. Ijumba (2022). Using blinds, daylighting, and geyser temperature settings to reduce electricity consumption and pricing patterns in energy-efficient buildings, The South African Institute of Electrical Engineering Journal - Africa Research Journal, Vol. 113, No. 1, pages 4-19, March 2022.
DOI: 10.23919/SAIEE.2022.9695422. Impact Factor: 0.178 (2022). Indexed on: IEEE Xplore, Scientific Electronic Library Online (SciELO) South Africa, SCOPUS, DOAJ, and recognised by UR as a Journal we could publish our research articles. Again, SAIEE was founded in 1909 and it is the fourth oldest IEEE indexed Journal.

(c) Godwin Norense Osarumwense Asemota and Nelson M. Ijumba (2022). Software validation of optimal bidirectional composite conductor design with applications, The South African Institute of Electrical Engineering Journal - Africa Research Journal, Vol. 113, No. 1, pages 37-51, March 2022. DOI: 10.23919/SAIEE.2022.9695424. Impact Factor: 0.178 (2022). Indexed on: IEEE Xplore, Scientific Electronic Library Online (SciELO) South Africa, SCOPUS, DOAJ, and recognised by UR as a Journal we could publish our research articles. Again, SAIEE was founded in 1909 and it is the fourth oldest IEEE indexed Journal.

(d) Godwin Norense Osarumwense Asemota and Nelson M. Ijumba (2020). Gender mediated optimal multivariate electricity load management model. IEEE PES Power Africa Conference, Nairobi, Kenya, 25-28 August, 2020. 978-1-7281-6746-6/20/$31.00©2020 IEEE. DOI: 10.1109/PowerAfrica49420.2020.9219796. IEEE Proceedings Impact Factor: 14.91 (2023).

(e) Godwin Norense Osarumwense Asemota, Nelson M. Ijumba, Optimisation of the eccentricity of the pyriform diagram for balancing electrical power systems loading. 2nd East African Community Regional Science, Technology and Innovation (STI) Conference, Bujumbura, Burundi, 27-29 October 2021.

(f) Godwin Norense Osarumwense Asemota, Nelson M. Ijumba, Optimisation of the eccentricity of the pyriform diagram for balancing electrical power systems loading. The East African Journal of Science, Technology, and Innovation (EAJSTI), Vol. 3 (Special issue): February 2022, pp. 1-8. https://eajsti.org/index.php/EAJSTI/article/view/433

(g) Godwin Norense Osarumwense Asemota, Nelson M. Ijumba, Shielding and Thermostatic Control for Optimal Electricity Load Management, 13th International Conference on Applied Energy 2021, Nov. 29-Dec. 5 2021, in Bangkok, Thailand. Energy Proceedings, vol. 23, 2021, pp. 1-4. ISSN 2004-2965.
https://www.energy-proceedings.org/wp-content/uploads/icae/2021/1643308361.pdf

(h) Godwin Norense Osarumwense Asemota, Nelson M. Ijumba, Energy efficiency of a generalized optimal multidimensional electricity load management model, SAIEE – Africa Research Journal (under Review). Revised and resubmitted on the 10th of May 2022. Impact Factor: 0.178 (2022). Indexed on: IEEE Xplore, Scientific Electronic Library Online (SciELO) South Africa, SCOPUS, DOAJ, and recognised by UR as a Journal we could publish our research articles. Again, SAIEE was founded in 1909 and it is the fourth oldest IEEE indexed Journal.

(i) Godwin Norense Osarumwense Asemota, Nelson M. Ijumba, Multivariate Component Analysis Optimisation of Electricity Load Management, Energy Engineering (under Review). Revised and resubmitted on the 9th June 2022. Impact Factor: 2.027 and Indexed by: SCOPUS. It was established in 1997.

Table of contents

Contents

List of Figures

List of Tables

List of Acronyms

AAAC – All aluminium alloy conductors

ACAR – Aluminium conductor aluminium alloy reinforced

ACCC – Aluminium composite core conductors

ACCR – Aluminium conductor composite reinforced

ACSR – Aluminium conductor steel reinforced

ANOVA – Analysis of variance

APS – Anti-corrosion protective systems

ARMA – Autoregressive moving average

CIPP – Cured-In-Place pipe

CTC – Composite Technology Corporation

CTE – Coefficient of thermal expansivity

DSM – Demand-side management

DW – Durbin-Watson

ECDF – Empirical cumulative distribution function

EDP – Electrical Distribution/Maintenance Planning and Control

F-values – Fisher values

GHG – Greenhouse gases

GW - Giga Watts

HTLS – High-Temperature Low-Sag

IFL – In-Field-Linear

kV – Kilovolts

NamPower – Namibia Power Corporation

NTPT - North Thin Ply Technology

PLAT – Power Line Analysis Tool

R – Coefficient of Determination

S – Standard Error

SADC – Southern Africa Development Community

Si1 – Solar Impulse 1

Si2 – Solar Impulse 2

SPSS – Statistical Package for the Social Sciences

SRB – Sulphate-reducing bacteria

SSAC – Steel-supported aluminium conductors

TCDF – Theoretical cumulative distribution function

TLP – Tension Leg Platforms

UAE – United Arab Emirates

CHAPTER ONE

This section presents the Objective for the study, Research Problem, Hypothesis, Significance of the Study, Introduction, and Thesis outline.

1.0. Objective for the Study

The overall objective of conducting this academic research is to provide a critical overview of Electricity Load Management by contributing to an understanding of the actual and potential roles optimisation algorithms play in electricity load management.

Electricity access and availability are significant capacity requirements in the contemporary world for an improved way of life. In developing countries, electricity supply shortages, the need for load shedding and balanced loading, supply-side and demand-side management implementations, inadequate local generation, and rising electricity imports to complement the deficit in the face of rising population and higher electricity consumption requirements, necessitate the constrained optimisation of electricity and energy demand along the value chains of generation, transmission, delivery, and utilisation, in this study [1]. Increased mining sector investment with its characteristic flat load profiles, ageing infrastructure and need to strengthen the grid, high tariffs, and high unemployment rates necessitate deploying optimisation systems and procedures that allow consumers to use less energy at lower costs and also, able to supply more customers at the same time [1], [2].

Also, electricity load management regulates electricity production and consumption before and after the meter for energy efficiency, energy and cost savings, and greenhouse gases (GHG) reduction. Furthermore, blinds can be used to manage inlet summer heat and outlet winter heat. Moreover, commercial buildings consume a high percentage of the energy in buildings country-wide, day-lighting can reduce energy consumption in Schools and Colleges, and a sizeable quantity of a building's aggregate energy costs. While a substantial amount of the total energy is consumed in buildings, a portion of the cooling energy can be saved by daylighting [2].

Additionally, a building's design and energy utilisation processes can reduce energy consumption using daylighting. Also, peak demand charges can be reduced by daylighting and light-dimming raises employees' productivity, enhances building occupants' health, and saves energy. In addition, over US$60 billion was spent on energy per annum in commercial

buildings' and above 64 billion square feet of commercial buildings floor space was lit by fluorescent and/or partly by daylighting [2].

Furthermore, the optimal bidirectional composite conductor design with applications problem is to determine materials and costs optimisation. Eigenvalues solution of the inequality of the describing differential equations and proof of convergence of the expected numerical values of the vertical and horizontal currents are to be determined, using the computer software validation of the design. Also, to deduce and confirm the actual conductor materials requirements per unit area of the design and production of composites that simultaneously carries horizontal and vertical currents along their respective paths and vice versa [3].

Electricity generation deficits compelled the Southern Africa Development Community (SADC) energy services to carry out demand-side management (DSM) policies including load shedding, which negatively affected many countries' socio-economic growth [2]. The Namibian power utility was selected for the study because it has several energy needs and utilisation challenges. In addition, Namibia produces about 40% of its local power needs and the remaining 60% comes from Zambia and Zimbabwe [2].

Namibia's electricity grid is characterised by lightly loaded long lines over a vast landscape with two deserts and a small population that is spread over large distances. Namibia's power system is also subjected to high grid instability. Electricity demand increased in 2012 due to increased investment and consequent activity in the mining sector. Eskom sometimes supplies over 80% of electricity at high prices, which makes Namibia's electricity tariffs to be high especially at peak periods [2]. Namibia's electricity price and industrial tariffs are higher than South Africa's rates. Also, indigent, jobless, and peasant Namibians cannot afford high electricity expenses. Besides, Namibia has severe weather, an arid environment, and dire water deficiency problems [2].

The specific objectives are:

(a) To investigate how gender influences electricity consumption for optimal electricity load management using multidimensional interactions of electricity consumers of a residential load management questionnaire designed and administered in Windhoek, Namibia to predict and modify electricity consumption styles and attitudes by gender.

(b) To develop energy-efficient buildings that abate energy consumption using predictive analytics and integrated energy-efficient design procedures to evaluate how drapes, daylighting, and heater regulators lower energy demands, electricity consumption, and pricing arrangements of households, commercial, and industrial properties.

(c) To validate an optimal bidirectional composite conductor design with applications, using the minimum conducting area of a conductor-insulator matrix to satisfy Laplace's equation that simultaneously allows very high vertical and horizontal currents at high temperatures to flow through the composite conductor without local heating, galvanic corrosion, or metal solution problems.

1.1. Research Problem

The natural increase in population and the need for more access are driving electricity demand worldwide. The consequent rapid growth in power systems networks and complexity in power systems operational economics, have exacerbated security and supply reliability difficulties. Also, optimal power systems planning scope and associated constraints have introduced additional complications set by the requirement that power utilities remain profitable, react quicker, offer higher quality products and services, and use fewer people at lower costs.

In this work, the software validation of a bidirectional composite conductor which simultaneously allows horizontal and vertical currents to flow and to follow in their respective paths or vice versa, using the least conducting area was considered. The optimisation solution to the minimum area problem of a conductor composite consisting of an appropriate mixture of conductors and insulators microstructure can be obtained using conductance that has the requisite conductor characteristics. The design problem is such that the least composite conductor area, can handle the greatest horizontal and vertical currents in tandem [1]. Furthermore, isotropic composites employing conducting rings or anisotropic composites deploying ellipses could be used for the optimal designs.

Consequently, the ensuing relations for describing and possibly, modelling electricity load management, are nonlinear. These constrained nonlinear equations may not be easy to solve, even if, it can be shown that these equations exist in the first place. Nevertheless, if a physical system can be modelled, there should be a solution, even if it cannot be solved, yet. Arguably, the systems of equations may not have exact solutions, so, approximations, bounds,

convexity, iterations, and numerical analyses, which border and depend on optimisation techniques could be used [3], [4], [5], [6], [7].

Furthermore, a class of computable convex functions used the least search minimisation conditions to solve operations management and electricity load and demand-side management optimisation problems. Convex functions are important because one minimum point exists within the space of convexity. Also, data points on a convex function graph are always on the epi-graph and the supremum of convex functions is always convex. The twice differentiable convex function is not greater than the Taylor series expansion boundaries and it is also convex when the Hessian matrix is positive semi-definite in the right-hand plane. Also, convexity is the curvature that imputes value to real number sequences. They are used to obtain fundamental solutions to complex and constrained physical nonlinear problems using easy and straightforward reasoning [3].

In this study, valid electricity load management was based on the production, transmission, delivery, and interrelated grids of appropriately planned and sufficiently gauged conductors using convexity. The constrained composite conductor used polyconvexity, Lagrange multipliers, Green's criterion, and Laplace's boundary conditions for costs and materials minimisation. The designed composite conductors are applicable in modern power systems with greater energy-carrying capabilities, lower sags, raised current and temperature capacities, the ability to service more electricity consumers at higher voltage levels, and also capable of postponing multi-billion dollar new energy installations for many years [4].

Deregulated electricity markets trade energy between production, transportation, and delivery systems functionaries or controllers, districts, commercial, and industrial customers that depend on probabilistic energy forecasts and predictions in terms of the fuel costs and energy prices, grid usage expenses, reserve capacity constraints, risk premium margins, and traders earnings. The future pricing optimisation algorithm used difference equations of the spectral density of autoregressive moving average (ARMA) processes to predict the sigmoid graph of expected electricity pricing patterns. Also, the sigmoid introduces nonlinearity, exponential enlargement, jump discontinuities, and bounded electricity price elasticity that lies within a certain range [5].

Communality denotes special difference factors of the respective item's aggregate discrepancy of distributed variables. It measures composite variables of hidden parameters in any multidimensional electricity load management design. Communalities assess the

reliability criteria of developed models whenever communalities approach unity. Also, how communalities derive the number of factors to assess in any sample is a difficult question to answer. Therefore, either Kaiser's eigenvalues or the scree diagrams could be used to determine the electrical load management factors extracted in each case based on the different assumptions.

Furthermore, communalities comprise loadings of allowed deviations and exclusive components that are weights of the observed or measured estimates. Again, mean communalities indicate the proportion of the variation described by the developed model. The scree indicates residuals or remainders while the communalities are the least score estimates similar to convex functions of lower bound solutions or optimisation solutions of the electricity load management problem [6].

The calibre, amount, and consistency of the power or energy used by the population in any nation categorise peoples by their living standards as advanced, not developed, emerging, or growing. Electricity trading using either the commodities exchange or electric power consortia of electricity networks traversing nations, regions, and continents has brought extra entanglements to the electricity load management equation. The skilful management of efficient and profitable electricity service businesses results in a lack of knowledge of how leading power systems operations should be managed for effectiveness, conformance to regulatory practices, and performance. Consequently, multivariate analyses enable power utilities to create knowledge for effective management that enhances policy and decision-making. Multidimensional analyses comprise statistical procedures that meaningfully analyse several measurements on discrete, features, and targeted electricity load management parameters in tandem. Hence, multidimensional analyses gauge, clarify, and forecast the quality of interdependence between and among electricity load management variables that are weighted composites of the load management variables [7].

In addition, between 1.7 and 2.0 billion people do not have access to grid electricity around the world, and the majority of them live in rural settlements, especially in Sub-Saharan Africa. The low distribution of grid electricity could be due to difficult terrain, sparsely populated human settlements that are very far apart, and highly expensive and uneconomical power generation investments [8]. In addition, rural electrification has been limited because over 1.0 billion people globally cannot access electricity and above 600 million are in sub-Saharan Africa [9]. Furthermore, over 625 million people in sub-Saharan Africa have no access to

electricity and eighty percent of this population live in rural communities where grid electricity connectivity is prohibitively high or very expensive [10]. Also, research has shown that electrification has grown globally in the recent decade where an estimated 770 million population suffer from energy poverty and about 577.5 million are in sub-Saharan Africa [11].

In order to contribute to an understanding of the actual and potential roles optimisation algorithms play in electricity load management through this research, conductor optimisation is necessary for electricity network expansion planning, which secures transmission lines infrastructure that can carry rising electricity generation and consumption capacities worldwide. Other benefits or advantages are to support, enhance, and strengthen optimal power systems operators' response in emergencies, increase and maximise benefit-cost ratios, which enhance reliability improvements, and reduce operational costs against initially high optimal bidirectional composite conductor investments. Also, to adaptively strengthen the interdependence between electricity conductor infrastructures and renewable energy uncertainties, minimise total investment costs, and transmission line losses, and optimally and efficiently engage electricity production units. These requirements are also to satisfy future load growth with additional security and operational constraints, and minimise transmission lines' right-of-way difficulties [1], [12].

Also, policy was used to analyse consumer behaviour, attitudes of the average citizen, and behaviour modification of consumers through the Quetelet curve. Use blinds to conserve heat in cold weather and significantly cuts down electricity used for heating in summer, and a combination of blinds, daylighting, and geyser temperature settings at medium to lessen electricity consumption. Also, manage high electricity prices, where incessant price increases could engender strife, which could lead to strikes, and lockouts including social and political upheavals at the detriment of the economy. In addition, manage the problem of water stress and water use in thermal electricity generation fleets, whose optimised costs and generation technologies are required to deliver future demand for secure and affordable electricity, and make energy bills as low as possible. Other benefits include achieving internal order, external independence, or economic growth, and balancing demand with secure (domestic) supply is the major energy policy of nations [13], [14], [15], [16], [17], [18], [19], [20], [21].

Furthermore, it is necessary to implement demand side management objectives that include: (i) Carbon emission reduction, (ii) Energy security, (iii) Increase energy efficiency uptake, (iv) New resources and markets, (v) Regulatory compliance, (vi) Economic

Efficiency, (vii) Public awareness, (viii) Improve knowledge, (ix) Consumer affordability, (x) Jobs and economic development, (xi) Reduce costs, (xii) Defer investments, (xiii) Improve collaboration, (xiv) Health and safety, (xv) Self-sufficiency, (xvi) Consumer trust, (xvii) Change consumer behaviour, (xviii) Local air pollution reduction and (xix) Lead by example [13], [14], [15], [16], [17], [18], [19], [20], [21].

Moreover, multivariate analyses are used to gauge the attitudes and behaviours of people towards electricity load management, in which small F-values less than unity suggest that the variance was due to error and Type-I errors are in the sample. The low Wilks' lambda values suggest substantial differences exist across respondents' attitudes toward optimal electricity load management practices and lowering thermostats at night or anytime the house was vacant, drawing blinds over windows and doors, locking all windows and doors tightly in winter were all seen to save energy, reduce overall energy costs and minimise inconveniences [13], [14], [15], [16], [17], [18], [19], [20], [21].

Also, good and adequate house insulation, using shutters, and spreading underlay were seen to reduce sunlight into the house by between 50 and 75% in summer and reduce heat outlet by over 25% in winter. Furthermore, rarely opening refrigerator and freezer compartments in summer, cooking with little water, keeping the bottom of pots clean and shining, and boiling liquids in tight containers can minimise spoilage and save energy by over 20%, more than normally used [13], [14], [15], [16], [17], [18], [19], [20], [21].

1.2. Hypotheses

The hypotheses proposed for the study are:

(a) Substantial differences exist across gender in the attitudes and behaviours of people toward optimal electricity load management practices

(b) The optimised composite conductor can carry larger power ratings and higher voltage profiles than conventional conductors of the same size

(c) Blinds, daylighting, and heater temperature settings can save energy and reduce losses

(d) Optimisation can enable more electricity consumers to be served

1.3. Significance of the Study

This research is of great importance and also a contribution to the power systems grids along the value chain of generation, transmission, delivery, and utilisation of electrical power. This is

so because the composite conductor design would lead to better energy efficiency, ultralight materials, more effective power systems design, enhanced renewable energy production, improved energy storage cycle, and more efficient electric motors. The benefits also include the optimisation of production from existing assets, focus on innovation, cost-effective technology, delaying assets replacement, extending service life, better strength-to-weight ratios, lower thermal expansivity coefficients, and higher moduli of elasticity (or stiffness), and lower electrical resistance. Also, larger spans with greater currents, temperature, power, and voltage capacities.

Furthermore, blinds reduce heat loss in winter and heat inlet in summer. Optimisation of electricity load management is used to lower electricity consumption, lower prices, and modify electricity consumption attitudes and behaviour for affordable, reliable, and sustainable supply. In addition, it could lead to optimal and viable production, transportation, distribution, and utilisation of electrical power, worldwide. It also contributes to the least cost and optimal solutions to the rising electricity consumption and pricing patterns problem with population growth by reducing pressures on the power grids. It equally saves energy and reduces operational costs through avoided production, minimises loss, and mitigates greenhouse gas emissions and global heating.

Moreover, the pyriform will serve as the globally optimised solution to the electricity consumption balanced loading problem. A balanced electrical power systems loading enables utilities to supply more customers, increases operational efficiencies, and places less stress on electricity generators, transmission, and distribution networks. Also, optimisation of electrical power systems loading will lead to lower-cost operations and balanced light loading of electrical power systems components that facilitates optimal unit commitment at lower economic and social costs. Whenever service taxes are reduced because of cheaper electricity prices, utilities witness flatter load curves and avoided production costs across power systems operations, which further, lessens blackouts and extends the life of utility facilities.

1.4. Literature Review

The optimised bidirectional composite conductor design employs the mesh network and a unit square of conducting area A, such that the minimum area occupied by the insulator material is 1 – A. Also, a unit voltage is permitted to act from the left-hand side to the right-hand side and up and across the unit square to measure the two currents (vertical and horizontal) [22].

The connected conductor problem was homogenised and converted to a variational problem having similar solutions using convex functions [1],[3],[4],[22],[23],[24]. Very slender ribbons of both the conductor and insulator were interwoven and used to form a matrix for the design such that the vertical and horizontal currents can flow through or follow either path, as the conductor ribbons or strips are almost indistinguishable [1], [3], [4], [22], [23], [24].

Furthermore, convex functions are uneven [25] optimisation algorithms for obtaining important and superior results like in software validation of optimal bidirectional composite conductor design with applications using the smallest area principle [1],[4],[22],24]. A thoroughly combined composite of conductor and insulator ribbons results from conductance of the smallest area of the boundary conditions [1],[22],[26]. Also, isotropic composites deploying conducting rings encircling insulator disks were used to produce optimal design [27], and anisotropic composites used ellipses for optimal design [28]. References [27] and [28] proved that no optimal design could be better, and [1] also proved that the optimal conductor area was two-thirds the unit area.

Electricity is a vital resource in the contemporary world for an enhanced way of life. In addition, inadequate generation, transmission, and distribution infrastructure of energy lead to power blackouts, load shedding, and supply- and demand-side management strategies caused by insufficient local generation amid rising population and electricity demand. Also, expensive electricity imports from neighbouring countries and within the regional power pool are likely to be used to augment the shortfall [2],[17],[21],[29],[30]. The mining sector investment expansion in Australia and Namibia and their symbolic stable load profiles are important for electricity load management because a smelter can consume the power supplied to a city or municipality. This situation also calls for the need to replace or refurbish ageing infrastructure or strengthen the grid [1], [2], [31], [32].

Electricity generation deficits constrained the Southern Africa Development Community (SADC) energy services to affect demand-side management (DSM) policies that included load shedding, which negatively affected many countries' socio-economic growth [2],[17],[21],[29]. The Namibian power utility was chosen as a part of the study because it has many power shortages and utilisation challenges. It was also able to secure power availability till August of 2016 and thereafter, without load shedding. Furthermore, Namibia generates 40% of its domestic energy needs and imports the balance 60% from South Africa, Zambia, and Zimbabwe [2], [30].

Namibia's electricity grid is lightly loaded with long lines stretching over an extensive landmass containing two deserts and a sparse population that is prone to outages and supply disruptions from equipment failures, insufficient generation capacity, and transmission and distribution constraints [33]. The power system is also characterised by relatively high network instability, voltage fluctuations, and fluctuating temperatures that negatively impact the network [34]. Electricity requirements rose in 2012 because of investments in mining and Eskom at times provides over 80% of electricity during peaks at exorbitant prices [2], [31], [32], [35]. Namibia's electricity rates and industrial charges are greater than South Africa's tariffs [2], [15], [19], [21]. Also, needy, unemployed, and subsistence-level Namibians cannot bear high electricity prices [20]. Moreover, Namibia has extreme weather, desert environments, and severe water shortage problems [2], [35].

Also, electricity load management controls energy generation and utilisation behind and after the meter for enhanced energy efficiency, energy and cost savings, and hothouse gases (GHG) mitigation [2]. Consequently, drapes permit 50.0% inlet heat in summer and 25.0% heat outlet in winter. About 75.0% of the energy in buildings country-wide was consumed in commercial buildings [36]. Also, energy consumption in commercial buildings hovered between 35.0% and 50.0% [37], [38]. In 2023, using the commercial buildings energy consumption survey (CBECS) of 2018, 60.0% of electricity and 34.0% of natural gas were consumed in commercial buildings [39]. Furthermore, over 5.9 million commercial buildings were surveyed in the U.S. covering about 96 billion square feet of floor space, and used over 6.8 quadrillion British thermal units (BTU) of energy, and spent over US$ 141 billion. Between 1979 and 2018 (inclusive), commercial floor space increased by 89.0% and the number of buildings increased by 59.0%. In the same period under reference, utilisation of all the major fuels increased by 17.0% [39]. Although large buildings (over 100,000 square feet) constitute only about 2.0% of commercial buildings, they consumed over a third of the total energy consumed in commercial buildings. While space heating utilised about two-thirds of end-use energy for natural gas, fuel oil, and district heat, electricity was mostly used for cooling, lighting, ventilation, and other end uses [39]. Daylighting reduces energy consumption by 24.0% in Los Angeles Schools and by a third of a building's overall energy costs. Although between 35.0% and 50.0% of the aggregate energy is consumed in buildings [40], the 10.0% to 20.0% of the energy used in cooling can be saved by day-lighting [2], [36], [37], [38], [39], [40].

Furthermore, daylighting can reduce a building's energy utilisation between 20.0% and 80.0% [2], [40]. Also, daylighting can lower peak demand charge and lights-dimming can improve employees' productivity, enhance building occupants' well-being, and save energy [2], [41]. Additionally, over US$60 billion was expended on energy annually in commercial buildings while above 64 billion square feet of commercial buildings floor space was either lit by fluorescent or day lighting [2], [42], [43].

1.5. THESIS OUTLINE

The Thesis outline comprises three published articles to be embedded as three separate chapters, namely: (a) Gender mediated optimal electricity load management (in Chapter two), (b) Using blinds, day-lighting, and geyser temperature settings to reduce electricity consumption and pricing patterns in energy-efficient buildings (in Chapter three), and (c) Software validation of optimal bidirectional composite conductor design with applications (in Chapter four).

Furthermore, chapter five presents the overall conclusions and contributions to the knowledge of the research. Also, the details of journal articles and conference papers from the research were presented just after the "ABSTRACT" of the study.

The last section comprises three published articles and two unpublished manuscripts (under review) to be embedded as five different appendices, namely: (a) Rwanda's Off-Grid Solar Performance Targets (in Appendix D), (b) Optimisation of the eccentricity of the pyriform diagram for balancing electrical power systems loading (in Appendix E), (c) Shielding and Thermostatic Control for Optimal Electricity Load Management (in Appendix F), (d) Energy Efficiency of an Optimal Multidimensional Electricity Load Management Model (in Appendix G – unpublished manuscript), and (e) Multivariate Component Analysis Optimisation of Electricity Load Management (in Appendix H – unpublished manuscript).

REFERENCES

[1] G. N. O. Asemota and N. M. Ijumba, "Software validation of optimal bidirectional composite conductor design with applications," *SAIEE –Africa Res J* 2022, vol. 113, no. 1, pp. 37-51.

[2] G. N. O. Asemota and N. M. Ijumba, "Using blinds, daylighting, and geyser temperature

settings to reduce electricity consumption and pricing patterns in energy-efficient buildings," *SAIEE –Africa Res J* 2022; vol. 113, no. 1, pp. 4-19.

[3] G. N. O. Asemota, On a class of computable convex functions. *Can J Pure Appl Sc* 2009; 3(3): 959-65.

[4] G. N. O. Asemota, Optimal two-way conductor design using computable convex functions approach. *Adv Mat Res* 2012; 367: 75-81

[5] G. N. O. Asemota, A prediction model of future electricity pricing in Namibia. *Adv Mat Res* 2013; 824: 93-99. Doi: 10.4028/www.scientific.net/AMR.824.93.

[6] G. N. O. Asemota, Communality performance assessment of electricity load management model for Namibia. IEEE-AIMS 2014: 252-7. 2nd International Conference on Artificial Intelligence, Modelling and Simulation.

[7] G. N. O. Asemota, Multivariate parsimony model of electricity load management. WSEAS 2015: 77-86 Energy & Environ Proc. 10th International Conference on Energy & Environment.

[8] J. Dekker, S. Chowdhury, and S. P. Chowdhury, Economic viability of PV/diesel hybrid power systems in different climatic zones in South Africa. *IEEE* 2010: 1-8.

[9] J. D. D. Niyonteze, F. Zou, G. N. O. Asemota, S. Bimenyimana, and G. Shyirambere, Key technology development needs and applicability analysis of renewable energy hybrid technologies in off-grid areas for the Rwanda power sector. *Heliyon* 2020; 6: 1-14. Doi:10.1016/j.heliyon.2020.e03300.

[10] J. P. Ihirwe, Z. Li, K. Sun, S. Bimenyimana, C. Wang, G. N. O. Asemota, A. Nduwamungu, and C. K. Mesa, Solar PV minigrid technology: peak shaving analysis in the East African community countries. *International J Photoenergy* 2021; 2021, Article ID 5580264: 1-40. Doi:10.1155/2021/5580264.

[11] S. Bimenyimana, C. Wang, G. N. O. Asemota, A. Nduwamungu, C. K. Mesa, J. P. Ihirwe, J. D. D. Niyonteze, S. Bora, C-L. Ho, N. Hagumimana, and Y. Mo, A technoeconomic feasibility analysis for affordable energy system in the East African community countries. *International J Photoenergy* 2021; 2021, Article ID 9921940: 1 -19. Doi:10.1155/2021/9921940

[12] Y. Hu, Z. Bie, T. Ding, and Y. Lin, An NSGA-II based multi-objective optimization for combined gas and electricity network expansion planning. *Appl Energy* 2016; 167: 280 -293.

[13] H. Pohamba, Former President of Namibia: "Reliable electricity is crucial to socio -economic development". In: Namibia's power is in your hands: use it wisely (NamPower). A documentary compiled by *The Republikein*, Windhoek, Namibia: April 23, 2008. [Accessed 14 February 2019] https://www.republikein.com.na/nuus/nampower-namibias-power-is-in-your-hands-use-it-wisely/

[14] P. I. Shilamba, Managing Director of NamPower: Save now to prevent load shedding. In: Namibia's power is in your hands, Use it wisely, (NamPower), A documentary compiled by *The Republikein*, Windhoek, Namibia: April 23, 2008. https://www.republikein.com.na/nuus/nampower-namibias-power-is-in-your-hands-use-it-wisely/ [Accessed 14 February 2019]

[15] E. Brandt, Namibia's high electricity price. New Era Newspaper, Namibia; 14 November, 2014. Available: http://allafrica.com/stories/201411140794.html [Accessed 29 March, 2017]

[16] G. Jahoda, Quetelet and the emergence of the behavioral sciences. SpringerPlus 2015; 4:473. https://www.ncbi.nlm.nih.gov/pmc/articles/PMC4559562/ [Cited 30 July 2018]

[17] P. I. Shilamba, Update on the current power supply and progress made on NamPower projects and initiatives to ensure security of supply in Namibia. Media Briefing, Windhoek; 13 April, 2015.

[18] A. Cherp, V. Vinichenko, J. Jewell, M. Suzuki, and M. Antal, Comparing electricity transitions: A historical analysis of nuclear, wind and solar power in Germany and Japan. *Energy Policy* 2017; 101: 612-28.

[19] D. Murrant, A. Quinn, L. Chapman, and C. Heaton, Water use of the UK thermal electricity generation fleet by 2050 Part 2. *Energy Policy* 2017; 108: 859-874.

[20] CIA world factbook. Namibia Economy2018. [Cited 30 July, 2018] https://theodora.com/wfbcurrent/namibia/namibia_economy.html

[21] P. Warren, Demand-Side Policy: Global evidence base and implementation patterns. *Energy & Environ* 2018; 0(0): 1-26.

[22] G. Strang and R. Kohn, "Optimal design of a two-way conductor," in *Topics in Nonsmooth Mechanics*, J. J. Moreau, P. D. Panagiotopoulus, and G. Strang, Eds. Basel: Birkhauser Verlag, 1988, pp. 143-155.

[23] S. Takriti, "The unit commitment problem," in *Operational research in industry*, T. A.

Ciriani, S. Gliozzi, E. L. Johnson, and R. Tadei, Eds. London, UK: MacMillan, pp. 299 -322, 1999, Doi: 10.1057/9780230372924.

[24] G. N. O. Asemota, "Optimal two-way conductor design using computable convex functions approach," in *Proc.3rd ICERD*, Benin City, Nigeria, 2010.

[25] J. J. Moreau, "Bounded variation in time," in *Topics in Nonsmooth Mechanics*, J. J. Moreau, P. D. Panagiotopoulus, and G. Strang, Eds. Basel: Birkhauser Verlag, 1988.

[26] C. H. Edwards and D. E. Penney, *Calculus*. New Jersey, NJ, USA: Prentice-Hall, 2002.

[27] Z. Hashin and S. Shtrikman , "A variational approach to the theory of the elastic Behaviour of multiphase materials," *J. Mech. & Phys. Solids.*, vol. 11, no. 2, pp. 127 -140, Mar.-Apr. 1963, 10.1016/0022-5096(63)90060-7.

[28] F. Murat and L. Tartar, *Optimality conditions and homogenization: nonlinear variational problems*. (Isola de'Elba, 1983). London, UK: Roman Publishing, pp. 1-8, 1985.

[29] S. Bimenyimana, A. Ishimwe, G. N. O. Asemota, C. M. Kemunto, and L. Li, "Web -based design and implementation of smart home appliances control system," in ICRET, Kuala Lumpur, Malaysia. *IOP Conf. Series: Earth and Env. Sci.*, vol. 168, pp. 1-9, 2018, 10.1088/1755-1315/168/1/012017

[30] Anon., "No power cuts expected in Namibia-Energy Minister," *New Era Newspaper*, Windhoek, Namibia. 24 Mar. 2016. [Online]. Available: https://www.newera.com.na/2016/03/24/power-cuts-expected-namibia-energy-minister/, Accessed on: Mar. 29, 2017

[31] W. Isaaks. Energy situation in Namibia. Presented at AEF2013 Africa Energy Forum, Barcelona, Spain. [Online]. Available: www.energynet.co.uk/system/files/Private_23, Accessed on: Mar. 29, 2017

[32] P. Simshauser and D. Downer, 2012. "Dynamic pricing and the peak electricity load problem," *Australian Econ. Rev.*, vol. 45, no. 3, pp. 305-324, 2012, 10.1111/j.1467-8462.2012.00687.x.

[33] Sinalda. "Voltage in Namibia," 2021. [Online]. Available: www.sinalda.com, Accessed On: May 19, 2023

[34] I. Hoeck, E. Steurer, Ö. Dolunay, and H. Ileka, "Challenges for off-grid electrification in rural areas: assessment of the situation in Namibia using the examples of Gam and Tsumkwe," Energ. Ecol. Environ., vol. 7, no. 5, pp. 508-522, 2012, 10.1007/s40974-021-00214-5.

[35] G. N. O. Asemota, *Electricity Use in Namibia*. Bloomington, IN, USA: iUniverse, 2013.

[36] Solatube "Daylighting Facts & Figures" [Online]. Available: 150516 Daylighting Facts & Figures-plain.pdf, Accessed on: Feb. 24, 2020

[37] G. Ander, "Day-lighting: Whole building design guide," 2011. [Online]. Available: http://www.wbdg.org/resources/daylighting.php, Accessed on: Feb. 24, 2020

[38] G. D. Ander, "Daylighting", 2016. [Online]. Available: wbdg.org/resources/daylighting Accessed on: May 22, 2023

[39] EIA, "2018 Commercial Buildings Energy Consumption Survey final Results," 2023. [Online]. Available: https://www.eia.gov/cbecs, Accessed on: May 22, 2023

[40] N. Stauffner, "Daylight Device Lightens Electricity Cost," *MIT News*, 2007. [Online]. Available: http://newsoffice.mit.edu//2007/techtalk51-26.pdf, Cited: Feb. 24, 2020

[41] D. Kozlowski, "Using daylighting to save on energy costs," *FacilitiesNet,* 2006. [Online]. Available: http://www.facilitiesnet.com/energyefficiency/article/Harnessing-Daylight-For-Energy-Savings-Facilities-Management-EnergyEfficiency-Feature—4267# Accessed on: Feb. 24, 2020,

[42] T. Mocherniak, "Lighting technologies produce energy savings," *Energy and Power Mgt.,* 2006. [Online]. Available: www.highbeam.com/doc/1G1-146346289.html Accessed on: Feb. 24, 2020

[43] R. P. Leslie, R. Raghavan, O. Howlett, and C. Eaton, "The potential of simplified concepts for daylight harvesting," *Lighting Research and Technology,* 2005. [Online]. Available: http://www.lrc.rpi.edu/programs/daylighting/pdf/simplifiedConcepts.pdf Accessed on: Feb. 24, 2020

CHAPTER TWO

This section describes how Gender mediated optimal multivariate electricity load, management model. The optimised multidimensional analyses used four metrics obtained from the analyses (Wilks' lambda, Pillai's trace, Hotelling's trace, and Roy's largest root). Multidimensional analyses in power systems load management produce knowledge for management and effective policy decision-making. They consist of regular distribution of real number sequences of interdependent and disparate electricity load management variables that cannot be meaningfully and independently interpreted. Also, multidimensional analyses assess, describe, and forecast loaded links among composite parameters for lower error.

Furthermore, Wilk's Lambda accounts for the substantial differences that exist between male and female gender attitudes and behaviour towards optimal electricity load management principles and practices. Pillai's trace is the aggregation of deviances explained by bias and acts as a defence against Type 1 error for a limited specimen. It also indicates the divergence among independent variables. Hotelling's trace provides two dimensions of the most important composite parameters that contribute the most to the model. In addition, Roy's largest root indicates the greatest loading unto an electricity load management variable. It was also shown that females were less likely to use electricity optimally.

2.1. Gender mediated optimal multivariate electricity load, management model.

This is the title of the contents in this part of the thesis under consideration in this study.

2.2. Abstract

Electricity load management embraces optimal power generation, transmission, distribution, and utilisation, while demand-side management considers electricity consumption after the meter. The multivariate analysis uses Wilks' lambda, Pillai's trace, Hotelling's trace, and Roy's largest eigenvalue to obtain multi-dimensional additive linear equations. A load management questionnaire having 54 predictors was randomly distributed to around 300 residents in a Windhoek suburb. The 127 questionnaire responses were analysed using a statistical package for social sciences. Results indicate there was no statistical difference between predictors. Low Wilks' lambda values suggest substantial differences exist across gender in attitude towards optimal electricity load management and females were less likely to use electricity optimally. It is recommended for the least costs and minimal resources

deployment in power utilities that, the female gender is sensitised, encouraged, and urged to adopt optimal multivariate electricity load management strategies proposed in this study for affordable and sustainable electricity generation, supply, utilisation, growth, and overall development.

2.3. Keywords

ANOVA, Hotelling's trace, Pillai's trace, Roy's largest root, Wilks' lambda. These are the important keywords for this portion of the thesis.

2.4. Introduction

Electricity load management provides control for electricity generation and consumption before and after the meter. Demand-side management (DSM) and automated control of electricity consumption occur after the meter to boost energy efficiency and carbon emission reduction [1],[2],[3],[4]. While energy consumption in households is useful in energy savings, energy consumption increases with population, quality of life, and electricity consumption behaviour. DSM expresses governmental policies for controlling energy consumption that could positively influence environmental, security, demand response, and carbon emissions [5],[6].

Multivariate analyses are used to logically analyse more complex simultaneous relationships between many independent and dependent variables. They measure each association based on the same model to obtain proportionate reductions of error. Therefore, a larger association leads to a larger reduction in error [7]. Multivariate analysis of variance (MANOVA) examines the discrepancy within independent variables to determine whether it is below the discrepancy between dependent variables. If the within-subjects variance is below the between-subjects variance, the independent variable has significant effects on the dependent variables. MANOVAs assess multiple independent and dependent variables within the same model for greater complexity. They do not use F-values for levels of significance but multivariate measures (Wilks Lambda, Pillai's Trace, Hotelling's Trace, and Roy's Largest Root) [8],[9],[10].

MANOVAs combine multiple dependent variables linearly to produce optimally separate independent variable groups. Thereafter, an ANOVA is performed on newly developed dependent variables. Independent variables relevant to each main effect are weighted to give

them priority in the calculations transmitted. During interactions, independent variables are weighted equally to examine if they exhibit additive effects on the combined variance of dependent variables [7],[8],[9],[10].

The main effects of independent variables and their interactions are evaluated while keeping other parameters constant. The effects of each independent variable are tested separately. Multiple interactions are tested separately from each other and also, from any significant main effects. For equal sample sizes, both in main effects and interactions, each test will be independent of the next or previous computation (except for error term calculated across independent variables) [7],[8],[9],[10]. Moreover, the researchers decide which variables are included in MANOVA to address the research questions or hypotheses. Also, they are to interpret the significant results. Although a statistical main effect of the independent variable indicates independent variable groups are significantly different in their scores on the dependent variable, it is not a statement that the independent variable caused the changes in the dependent variable [7],[8],[9],[10],[11].

The difference between the four multivariate metrics depends on how each combines the dependent variable to examine the amount of variation in data. Wilks Lambda is the amount of variation allowed in the dependent variable by the independent variable. Smaller values indicate larger differences between the groups analysed. One minus Wilks Lambda is the proportion of variance in the dependent variable allowed by the independent variable [7],[8],[9],[10],[11],[12],[13]. Pillai's Trace is the most reliable because it offers protection against Type I errors with small samples. It is the sum of variance explained by the computation of discriminant variables. It computes the proportion of variance in the dependent variables allowed by the greatest separation of independent variables. It ranges between 0 and 1. Increasing values suggest those effects contribute more to the model and we reject the null hypothesis for large values. Hotelling-Lawley Trace is converted to Hotelling's T-square. Hotelling's T is used when independent variables form two groups and represent the most significant linear combination of the dependent variables. It is also the sum of eigenvalues of the test matrix in which increasing values suggest effects that contribute most to the model [7],[8],[9],[10],[11],[12],[13].

Roy's Largest Root or Roy's largest eigenvalue is determined like Pillai's Trace except it considers the largest eigenvalue, which is the largest loading onto a vector. As sample sizes increase, parameters produced by Pillai's Trace, Hotelling-Lawley Trace, and Roy's Largest

Root become similar. Thus, Wilks Lambda is the easiest to understand and most frequently used metric [7],[8],[9],[10],[11],[12],[13].

The objective of the study is to investigate how gender influences electricity consumption for optimal electricity load management. A residential load management questionnaire was designed and administered in Windhoek, Namibia to elicit consumption responses from electricity consumers. Predictors on the questionnaire and their multidimensional interactions were used to select the most appropriate predictors that successfully modulate electricity consumption patterns and behaviour by gender. Multivariate analysis was used to evaluate the relative strengths of the developed optimal multivariate electricity load management model. Above all, the four multivariate measures select and combine each admissible predictor from data to weave a linear addition of multidimensional independent variables using gender to mediate the optimal multivariate electricity load management model, at least costs and minimal resources.

However, this part of the thesis is divided into Introduction, Methodology, Results and Discussion, and Conclusion.

2.5. Methodology

A questionnaire on electricity load management was, after validation randomly administered to over 300 residential electricity consumers in Windhoek to obtain responses on each of the 54 predictors in the questionnaire. The responses from the 127 respondents were analysed using the statistical package for social sciences (SPSS), especially employing multivariate analysis for the study. Also, a sample size of about 385 is used for the population of over 10,000 [14],[15],[16],[17].

2.5.1. Test Statistics

MANOVA probes the degree of variance among between-subjects and within-subjects independent variables, in which slight differences suggest independent variables have significant effects on dependent variables. Further, they do not use F-values to determine the levels of significance, but multivariate indices of Wilks lambda, Pillai's trace, Hotelling's trace, and Roy's largest eigenvalue [7],[8],[9],[10],[11],[12],[13].

Also, if p-value $> \alpha$: The association is not statistically significant. Additionally, if p-value is greater than the significance level, we do not conclude there is a statistically significant

relationship between the response variable and that term. We could refit the model without the term. Thus, if multiple predictors exist without statistically significant relationships with the response, the model can be reduced by removing terms one at a time [7],[8],[9],[10],[11],[12],[13]. The hypotheses for mean vectors become:

$$H_0: v_1 = v_2 \ldots = v_m = 0$$
$$H_A: v_k \neq v_l \tag{2.1}$$

$k < l, k, l = 1,2, \ldots, m.$

where H_0 is the null hypothesis, which is due to chance alone, and H_A is the alternative or researchers hypothesis which is due to some experimental treatment, which shows the groups are different [18].

The most commonly used metrics for multivariate analyses are Wilks' lambda, Pillai's trace, Hotelling's trace, and Roy's largest root [7],[8],[9],[10],[11],[12],[13].

2.5.1.1. Wilks' Lambda Test Statistics

Comparing mean vectors of q number of variables and h number of groups, the matrices become [8],[9]:

$$C = \sum n_k (\bar{x}_k - \bar{x})(\bar{x}_k - \bar{x})$$
$$V = \sum_{k=1}^{h} (n_k - 1) R_k \tag{2.2}$$

where C is the total square matrix between groups, V is the total square matrix within groups, h is the number of compared mean vectors, $\bar{x}_k$ are observations of the k-th group, $\bar{x}$ is the general mean vector, n_k are observations of the k-th group, and R_k is the covariance matrix of the k-th group. Thus, Wilks' lambda definition becomes [8],[9]:

$$\Lambda = \frac{|V|}{|C+V|} \tag{2.3}$$

is the ratio between two determinant matrices. In the limit, the ratio suggests there are differences between mean vectors.

For λ_k, CV^{-1} is singular and forms the roots of matrix and r is the number of nonzero matrices. Then, Wilks' lambda transforms to [8],[9]:

$$\Lambda = \prod_{k=1}^{t} \frac{1}{1+\lambda_k} \approx \cup_{q,h-1,N-h} \tag{2.4}$$

where h is the number of groups, q is the number of variables in each group, N is observations, λ_k is k-th root of CV^{-1}, and $r = \min\ (h-1, q)$. Equation (2.4) simplifies to [8],[9]:

$$\Lambda = \prod_{k=1}^{n}(1+\lambda_k)^{-1} \tag{2.5}$$

The critical lambda value is $\big((1-\lambda)(\sum n_1 - h)\big)/\lambda(h-1)$.

But, the Bartlett method is used for large samples, as:

$L = -\big[\big(N-1-(q+h)\big)/2\big]\ln\Lambda$. It is a chi-square (χ^2) distribution with $q(h-1)$ degrees of freedom.

2.5.1.2. Hotelling's Trace Metric

The Hotelling-Lawley statistic determines $\lambda_{k's}$ from the roots of the CV^{-1} matrix [8],[9]:

$$T = \sum_{k=1}^{t}\lambda_k \tag{2.6}$$

whenever $T > \chi^2_{Table[q(h-1)];\alpha}$, there are differences between mean vectors. Therefore, F distribution is used to test T statistics.

2.5.1.3 Pillai's Trace Test Statistics

It is defined as [8],[9]:

$$T = \sum \frac{\lambda_k}{1+\lambda_k} \tag{2.7}$$

The F_T is an F distribution with degrees of freedom $t(2m+t+1)$ and $(2n+t+1)$. For $t=1$, it is a full F distribution [8],[9]:

$t = \min\ (h-1, q)$

$$m = \frac{|q-(h-1)|-1}{2}$$

$$n = \frac{N-q-h-1}{2}$$

$$F_T = \frac{2n+t+1}{2m+t+1} \times \frac{T}{t-T} \tag{2.8}$$

2.5.1.4. Roy's Largest Root Metric

Roy's largest root is represented by λ_{max} and deduced as [8],[9]:

$$T = \sum_{k=1}^{t} \frac{\lambda_{max}}{1+\lambda_{max}} \tag{2.9}$$

The value is compared with the Heck graph using t, m and n as parameters. If T statistic is larger than the Heck graph value, there are differences between mean vectors [9].

2.6. Results and Discussion

Table 2.I indicates the multivariate results of the four metrics (Wilks' lambda, Pillai's trace, Hotelling's trace, and Roy's largest root) used for simultaneous multidimensional analyses in the study. It comprises Intercept, 24 independent electricity load management variables using gender as moderator [7],[8],[9],[10],[11],[12],[13],[14].

Figure 2.1 is Gender mediated optimal multivariate electricity load management model developed in the study. Multivariate tests are significant mean vector metrics that assume correlations between variables in data are essentially the same [18]. Although each metric reports the same F value for every independent variable, none was statistically significant.

Further, F-ratio is variance due to the manipulation of a factor by variance from error. The Intercept [F(1,8) = 2.344(a), p = 0.468; Wilks' λ = 0.051], indicates there was a substantial difference between male and female behaviours in relationship to optimal electricity load management. Pillai's trace is one minus Wilks' λ, and a smaller Wilks' λ is preferable for analyses [7],[8],[9],[10],[11],[12],[13],[14].

Q32-Turn off radiators or close air ducts in vacant guest rooms [F(1,8) = 0.425(a), p = 0.837; Wilks' λ = 0.227], shows a positive influence on optimal electricity load management. Q33-Lowering thermostats at night or anytime the house is vacant [F(1,8) = 0.080(a), p = 0.992; Pillai's trace = 0.390], substantially and positively influences optimal electricity load management. The Wilks' λ is greater than Pillai's trace and was used because it is the trace of the covariant matrix. It is also, the sum of eigenvalues in the diagonal matrix. The small F value indicates over 12.5 times the variance or proportion of saving energy and reducing money loss in the expectation of lowering thermostats at night or when the house is vacant.

Q34-Draw or open blinds over windows during the evening or sunlight hours [F(1,8) = 0.414(a), p = 0.841; Wilks' λ = 0.232], conserves electricity consumption throughout the day

or night by reducing space heating or cooling, thereby saving energy and costs. The F-value is attributable to error. Q35-Lock all windows tightly in winter to cut down heat losses [F(1,8) = 0.317(a), p = 0.887; Wilks' λ = 0.283]. Although the noticeable effect seems due to error variance because of the small F-value, common sense demands that we should do all within our confines to conserve available energy resources, especially in times of scarcity.

Q36-Insulate house to save energy and money [F(1,8) = 0.756(a), p = 0.717; Wilks' λ = 0.142], seems due to an error from small F-value. But good and adequate insulation is worthwhile in saving energy, and money and reducing inconveniences. Q37-Using blinds reduce heat inlet during summer and heat outlet during winter [F(1,8) = 0.490(a), p = 0.809; Wilks' λ = 0.203], though the F-value seems likely due to error, it conserves energy (reducing inlet heat by 50.0% in summer and preventing outlet heat by 25.0% in winter) [1]. Q38-Spreading underlay or carpets over windows or doors reduce 75.0% sunlight heat into the house [19] in summer [F(1,8) = 0.550(a), p = 0.786; Wilks' λ = 0.185]. The small F-value seems due to an error that may have arisen probably from a poor understanding of the question or sampling error or both. Q39- Shutting off air-conditioners when leaving the house for some hours [F(1,8) = 0.312(a), p = 0.889; Wilks' λ = 0.286], has a small F-value it is nonetheless a very credible optimal electricity load management predictor. This is so because, it reduces wasted energy, and money and minimises the occurrence of fires [1],[19].

Q40-Keeping air conditioners clean and not blocked by drapes or furniture [F(1,8) = 0.706(a), p = 0.732; Wilks' λ = 0.150], is a very good approach to saving energy. Unclean air conditioners overwork compressors and operate at lower efficiency. Any obstacle before air conditioners distorts ambient temperatures leading to irregular heating and cooling.

Q41-Keep windows closed and open doors when necessary, if air-conditioners are operating [F(1,8) = 0.358(a), p = 0.867; Wilks' λ = 0.259], seems to be an error in variance, but in practice is an excellent optimal electricity load management strategy. This makes air conditioners work more efficiently by not operating in an open system, thereby unable to cool as desired because of energy leakage. Q42-Keep heat-producing appliances away from thermostats to obtain accurate readings [F(1,8) = 0.240(a), p = 0.924; Wilks' λ = 0.342], shows a lack of understanding of basic Physics. It is a very good practice for achieving optimal electricity load management daily. This is so because incorrect ambient temperature measurements by thermostats make air conditioners overwork and burn their motors as a result [1],[19].

Q43-All rooms' air conditioners and outside compressors protected from the sun [F(1,8) = 0.888(a), p = 0.680; Wilks' λ = 0.123], show there is a great difference across gender in following through on the practice. This is so because, most females were less likely to understand these practices to be optimal electricity load management values, as they are very few in the field. Q44-Setting water heaters at medium enables energy to be optimally utilised. Q45-Turning off heaters if away for a few days is another useful cost-saving mechanism that equally avoids overcapacity and fire risks. Q46-Opening refrigerators and freezers rarely, especially in summer, enables materials kept in them to be adequately stored and minimise spoilage.

The Q47-Maintaining proper temperature in refrigerator and freezer compartments has differences by gender. Further, Q48-Cooking with little water has significant differences biased towards females. Q49-Boiling liquids in tight containers to save 20% energy, was also biased towards females [1],[19]. Q50-Keeping bottom of pots and pans shining to reduce energy wastage was also biased towards females. Q51-Pots and pans the same sizes as burners were equally biased towards females. Q52-Use fluorescent lamps when practicable were heavily biased towards females. Q53-Install automatic switches in closets to switch off when the door closes which was also biased towards females. Q54-Should not switch on fluorescent lamps within 15 minutes of switching them off, was equally biased towards females. Q2-Gender was biased towards females. Therefore, a credible optimal electricity load management model should sensitise, encourage, remind, and prod females in society to embrace sustainable optimal electricity management practices.

2.7. Conclusion

Multivariate analyses were used to gauge the attitudes and behaviours of people toward electricity load management in the study. For all selected predictors, Hotelling's trace, Roy's largest root, and F-values were the same for each predictor class. There was no statistically significant predictor in the decoupled multivariate model. Small F-values less than unity suggest variance was due to error, which indicates Type-I errors in the sample. Further, the many low Wilks' lambda values suggest substantial differences exist across gender in attitude toward optimal electricity load management practices and females were generally less likely to use electricity optimally. Lowering thermostats at night or anytime the house was vacant, drawing blinds over windows and doors, and locking all windows and doors tightly in winter were all seen to save energy, reduce overall energy costs and minimise inconveniences. Good

and adequate house insulation, using shutters, and spreading underlay were seen to reduce sunlight into the house by between 50.0 and 75.0% in summer and reduce heat outlet by over 25.0% in winter.

Rarely opening refrigerator and freezer compartments in summer, cooking with little water, keeping the bottom of pots clean and shining, and boiling liquids in tight containers can minimise spoilage and save energy by over 20.0%, more than normally used. It is, therefore, strongly recommended for the least costs and minimal resources deployment in power utilities that the female gender could be sensitised, encouraged, prodded, and urged to adopt optimal multivariate electricity load management practices proposed in this study for affordable and sustainable electricity generation, supply, utilisation, growth, and overall development.

Table 2. 1: Multivariate Tests(b)

Effect		Value	F	Hypothesis df	Error df	Sig.
Intercept	Pillai's Trace	.949	2.344(a)	8.000	1.000	.468
	Wilks' Lambda	.051	2.344(a)	8.000	1.000	.468
	Hotelling's Trace	18.750	2.344(a)	8.000	1.000	.468
	Roy's Largest Root	18.750	2.344(a)	8.000	1.000	.468
Q32TODRG	Pillai's Trace	.773	.425(a)	8.000	1.000	.837
	Wilks' Lambda	.227	.425(a)	8.000	1.000	.837
	Hotelling's Trace	3.396	.425(a)	8.000	1.000	.837
	Roy's Largest Root	3.396	.425(a)	8.000	1.000	.837
Q33LTWHV	Pillai's Trace	.390	.080(a)	8.000	1.000	.992
	Wilks' Lambda	.610	.080(a)	8.000	1.000	.992
	Hotelling's Trace	.640	.080(a)	8.000	1.000	.992
	Roy's Largest Root	.640	.080(a)	8.000	1.000	.992
Q34DCEOD	Pillai's Trace	.768	.414(a)	8.000	1.000	.841
	Wilks' Lambda	.232	.414(a)	8.000	1.000	.841
	Hotelling's Trace	3.309	.414(a)	8.000	1.000	.841
	Roy's Largest Root	3.309	.414(a)	8.000	1.000	.841
Q35LWTDW	Pillai's Trace	.717	.317(a)	8.000	1.000	.887
	Wilks' Lambda	.283	.317(a)	8.000	1.000	.887

	Hotelling's Trace	2.532	.317(a)	8.000	1.000	.887
	Roy's Largest Root	2.532	.317(a)	8.000	1.000	.887
Q36IHSEM	Pillai's Trace	.858	.756(a)	8.000	1.000	.717
	Wilks' Lambda	.142	.756(a)	8.000	1.000	.717
	Hotelling's Trace	6.048	.756(a)	8.000	1.000	.717
	Roy's Largest Root	6.048	.756(a)	8.000	1.000	.717
Q37DSRHM	Pillai's Trace	.797	.490(a)	8.000	1.000	.809
	Wilks' Lambda	.203	.490(a)	8.000	1.000	.809
	Hotelling's Trace	3.921	.490(a)	8.000	1.000	.809
	Roy's Largest Root	3.921	.490(a)	8.000	1.000	.809
Q38UCWDR	Pillai's Trace	.815	.550(a)	8.000	1.000	.786
	Wilks' Lambda	.185	.550(a)	8.000	1.000	.786
	Hotelling's Trace	4.397	.550(a)	8.000	1.000	.786
	Roy's Largest Root	4.397	.550(a)	8.000	1.000	.786
Q39SOACO	Pillai's Trace	.714	.312(a)	8.000	1.000	.889
	Wilks' Lambda	.286	.312(a)	8.000	1.000	.889
	Hotelling's Trace	2.499	.312(a)	8.000	1.000	.889
	Roy's Largest Root	2.499	.312(a)	8.000	1.000	.889
Q40KACFB	Pillai's Trace	.850	.706(a)	8.000	1.000	.732
	Wilks' Lambda	.150	.706(a)	8.000	1.000	.732
	Hotelling's Trace	5.647	.706(a)	8.000	1.000	.732
	Roy's Largest Root	5.647	.706(a)	8.000	1.000	.732
Q41KWCDA	Pillai's Trace	.741	.358(a)	8.000	1.000	.867
	Wilks' Lambda	.259	.358(a)	8.000	1.000	.867
	Hotelling's Trace	2.867	.358(a)	8.000	1.000	.867
	Roy's Largest Root	2.867	.358(a)	8.000	1.000	.867
Q42KHAAT	Pillai's Trace	.658	.240(a)	8.000	1.000	.924
	Wilks' Lambda	.342	.240(a)	8.000	1.000	.924

	Hotelling's Trace	1.924	.240(a)	8.000	1.000	.924
	Roy's Largest Root	1.924	.240(a)	8.000	1.000	.924
Q43RACCP	Pillai's Trace	.877	.888(a)	8.000	1.000	.680
	Wilks' Lambda	.123	.888(a)	8.000	1.000	.680
	Hotelling's Trace	7.108	.888(a)	8.000	1.000	.680
	Roy's Largest Root	7.108	.888(a)	8.000	1.000	.680
Q44STHAM	Pillai's Trace	.858	.755(a)	8.000	1.000	.717
	Wilks' Lambda	.142	.755(a)	8.000	1.000	.717
	Hotelling's Trace	6.037	.755(a)	8.000	1.000	.717
	Roy's Largest Root	6.037	.755(a)	8.000	1.000	.717
Q45TOHAD	Pillai's Trace	.790	.470(a)	8.000	1.000	.817
	Wilks' Lambda	.210	.470(a)	8.000	1.000	.817
	Hotelling's Trace	3.763	.470(a)	8.000	1.000	.817
	Roy's Largest Root	3.763	.470(a)	8.000	1.000	.817
Q46OFFDR	Pillai's Trace	.818	.561(a)	8.000	1.000	.781
	Wilks' Lambda	.182	.561(a)	8.000	1.000	.781
	Hotelling's Trace	4.489	.561(a)	8.000	1.000	.781
	Roy's Largest Root	4.489	.561(a)	8.000	1.000	.781
Q47MPTRF	Pillai's Trace	.860	.770(a)	8.000	1.000	.713
	Wilks' Lambda	.140	.770(a)	8.000	1.000	.713
	Hotelling's Trace	6.160	.770(a)	8.000	1.000	.713
	Roy's Largest Root	6.160	.770(a)	8.000	1.000	.713
Q48CWLWP	Pillai's Trace	.694	.284(a)	8.000	1.000	.903
	Wilks' Lambda	.306	.284(a)	8.000	1.000	.903
	Hotelling's Trace	2.269	.284(a)	8.000	1.000	.903
	Roy's Largest Root	2.269	.284(a)	8.000	1.000	.903
Q49BLQTC	Pillai's Trace	.828	.600(a)	8.000	1.000	.767
	Wilks' Lambda	.172	.600(a)	8.000	1.000	.767
	Hotelling's	4.804	.600(a)	8.000	1.000	.767

	Trace					
	Roy's Largest Root	4.804	.600(a)	8.000	1.000	.767
Q50KBPPS	Pillai's Trace	.736	.349(a)	8.000	1.000	.871
	Wilks' Lambda	.264	.349(a)	8.000	1.000	.871
	Hotelling's Trace	2.795	.349(a)	8.000	1.000	.871
	Roy's Largest Root	2.795	.349(a)	8.000	1.000	.871
Q51PPSSB	Pillai's Trace	.544	.149(a)	8.000	1.000	.968
	Wilks' Lambda	.456	.149(a)	8.000	1.000	.968
	Hotelling's Trace	1.193	.149(a)	8.000	1.000	.968
	Roy's Largest Root	1.193	.149(a)	8.000	1.000	.968
Q52UFLWP	Pillai's Trace	.932	1.714(a)	8.000	1.000	.533
	Wilks' Lambda	.068	1.714(a)	8.000	1.000	.533
	Hotelling's Trace	13.713	1.714(a)	8.000	1.000	.533
	Roy's Largest Root	13.713	1.714(a)	8.000	1.000	.533
Q53ASCLD	Pillai's Trace	.652	.235(a)	8.000	1.000	.927
	Wilks' Lambda	.348	.235(a)	8.000	1.000	.927
	Hotelling's Trace	1.876	.235(a)	8.000	1.000	.927
	Roy's Largest Root	1.876	.235(a)	8.000	1.000	.927
Q54NSFWF	Pillai's Trace	.758	.392(a)	8.000	1.000	.851
	Wilks' Lambda	.242	.392(a)	8.000	1.000	.851
	Hotelling's Trace	3.132	.392(a)	8.000	1.000	.851
	Roy's Largest Root	3.132	.392(a)	8.000	1.000	.851
GENDER	Pillai's Trace	.555	.156(a)	8.000	1.000	.965
	Wilks' Lambda	.445	.156(a)	8.000	1.000	.965
	Hotelling's Trace	1.248	.156(a)	8.000	1.000	.965
	Roy's Largest Root	1.248	.156(a)	8.000	1.000	.965

Notes:

a Exact statistic

b Design:

Intercept+Q32TODRG+Q33LTWHV+Q34DCEOD+Q35LWTDW+Q36IHSEM+Q37DSRH

M+Q38UCWDR+Q39SOACO+Q40KACFB+Q41KWCDA+Q42KHAAT+Q43RACCP+Q44STHAM+Q45TOHAD+Q46OFFDR+Q47MPTRF+Q48CWLWP+Q49BLQTC+Q50KBPPS+Q51PPSSB+Q52UFLWP+Q53ASCLD+Q54NSFWF+GENDER

REFERENCES

[1] G. N. O. Asemota, *Electricity use in Namibia*, Indiana: iUniverse, 2013.

[2] C. Eid et al., "Market integration of local energy systems: Is local energy management compatible with European regulation for retail competition," *Energy*, vol. 114, pp. 913-922, 2016.

[3] S. Bimenyimana, A. Ishimwe, G. N. O. Asemota, C. M. Kemunto, and L. Li, "Web-based design and implementation of smart home appliances control system," *in Proc. 2018 IOP Earth and Environmental Science Conf.*, vol. 168, pp. 1-9.

[4] H. Shiraki, S. Nakamura, S. Ashina, and K. Honjo, "Estimating the hourly electricity profile of Japanese households-Coupling of engineering and statistical methods," *Energy*, vol. 114, pp. 478-491, 2016.

[5] S. Simoes, W. Nijs, P. Riuz, A. Sgobbi, and C. Thiel, "Comparing policy routes for low-carbon power technology deployment in EU- an energy systems analysis," *Energy Policy*, vol. 101, pp. 353-365, 2017.

[6] P. Warren, "Demand-Side policy: Global evidence base and implementation patterns," *Energy & Environment*, pp. 1-26, 2018.

[7] E. Babbie, J. Mouton, P. Vorster, and B. Prozesky, The practice of social research, Cape Town: Oxford, 2003.

[8] J. Foster, E. Barkus, and C. Yarvosky, Understanding and using advanced statistics, London: Sage, 2006.

[9] C. Ates, O. Kaymaz, H. E. Kale, and M. A. Tekindal (2019). Comparison of test statistics of nonnormal and unbalanced samples for multivariate analysis of variance in terms of Type-I error rates. *Hindawi Comp. Math. Methods in Medicine*. Vol. 2019, pp. 1-8. Available: https://doi.org/10.1155/2019/2173638

[10] J. Frost (2017). Understanding interaction effects in statistics. [Online]. Available: Statisticsbyjim.com/regression/interaction effects/, Accessed on: Jan. 23, 2019

[11] J. J. Foster, Data analysis using SPSS for windows: a beginner's guide, London: Sage, 1998.

[12] IBM. SPSS tutorials. Available: https://ibm.com, Accessed on: Jan. 9, 2016

[13] Minitab. P-values. Available: support.minitab.com, Accessed on: Oct. 28, 2020

[14] G. N. O. Asemota (2013). A prediction model of future electricity pricing in Namibia. *Adv. Mat. Res.*, vol. 824, pp. 93-99. 10.4028/www.scientific.net/AMR.824.93.

[15] G. N. O. Asemota, "Multivariate parsimony model for electricity load management," in Proc. 2015 WSEAS Energy and Environment Conf., pp. 77-86.

[16] G. N. O. Asemota, "Communality performance assessment of electricity load management model for Namibia," in Proc. 2014 IEEE Artificial Intelligence, Modelling and Simulation Conf., pp. 252-257.

[17] P. D. Leedy and J. E. Ormrod, Practical research: planning and design, 8th ed., New Jersey: Pearson, 2005.

[18] N. Brace, R. Kemp, and R. Snelgar, SPSS for psychologists: a guide to data analysis using SPSS for windows, New Jersey: Lawrence Erlbaum Associates, 2000.

[19] P. Jones, How to cut heating and cooling costs: save money and energy in your home, New York: Butterick Publishing, 1979.

CHAPTER THREE

This section of the thesis describes how blinds, day lighting, and geyser temperature settings reduce electricity consumption and pricing patterns in energy-efficient buildings. An electricity household consumer questionnaire was designed, validated, and used in Windhoek, Namibia to gather data that were subjected to the statistical package for the social sciences (SPSS). Namibia was chosen as the test laboratory because the power systems network comprises long lines with very light loads that are distributed to a sparse population, which is far apart, and also over a very wide landscape. Also, the country contains two deserts (Namib and Kalahari), extremes of weather, and water stress situations.

Predictive analytics was also used to evaluate the research data. The sample size was also proven to be suitable for the study. Both the Enter and Stepwise regression methods, Durbin-Watson statistics, analyses of deviation, and residuals were also used to assess the precision, overall model fit, and whether there were interdependence effects in the data. There were also interactional effects, Quetelet curve, and price discontinuities used to save energy, enhance the energy efficiency, modify consumer behaviour and attitudes, loss reduction, reduce stress on utility facilities during peak electricity consumption periods, and capacity to supply more consumers.

3.1. Using blinds, day-lighting, and geyser temperature settings

To reduce electricity consumption and pricing patterns blinds, day-lighting, and geyser temperature settings reduce electricity consumption and pricing patterns in energy-efficient buildings. This is the title of the second section of this thesis.

3.2. Abstract

Depending on the building architecture, usage, and energy consumption patterns, over US$ 60 billion was expended annually on electric lighting in commercial buildings. Therefore, the study focuses on the development of energy-efficient buildings that minimise energy consumption through integrated energy-efficient design processes. This can serve as a practical guide to designing buildings that can lower the energy requirements and a strategy to reduce energy consumption. In this study, predictive analytics were used to examine how blinds, daylighting, and geyser temperature settings can reduce electricity consumption and pricing patterns. A panel of expert judges like electrical engineers, economists, linguists, and planners

was used to validate the 5-point Likert scale residential electricity load management questionnaire used to gather survey data for the statistical analysis in a Windhoek suburb, Namibia. The main goal of this study was to investigate how blinds, day-lighting, and geyser temperature settings can be used to save energy, and reduce electricity consumption, and costs for sustainable growth and development. The results from this investigation indicate a reasonably good Gaussian distribution histogram of 15 electricity price jumps confirming 15 four-way stepwise interaction effects. The optimal 0.5 Quetelet curve index offers average citizen energy efficiency awareness, education, and behaviour modification for affordable electricity. Females generally set hotter geyser temperatures and are higher energy consumers. Blinds reduce electricity consumption by 50% in summer, 25% in winter, and day-lighting by 25%. These were the least cost and optimal solutions to the rising electricity consumption and pricing patterns problem. Adopting the findings or the outcomes of this study could provide more optimal and sustainable energy consumption thereby reducing pressure on the power grid.

3.3. Keywords

Cost-saving, electricity consumption, energy-saving, loss, and waste minimisation.

3.4. INTRODUCTION

Electricity supply shortages forced the Southern Africa Development Community (SADC) utilities to implement the demand-side management (DSM) programmes [1],[2] with load shedding negatively impacting some countries' socio-economic development [3]. The Namibian power utility was able to guarantee power till August 2016 with the occurrence of load shedding. Currently, Namibia generates 40% of its power locally, and the remaining 60% is from Zambia and Zimbabwe [4]. Namibia's electricity demand doubled in 2012 because of investment in the mining sector, and Eskom supplies over 80% of electricity at significantly increased prices [5]. Liquid fuel constitutes over 63% of total net energy consumption [6] while mining expansion leads to flat load curves [7].

Namibia's electricity price and industrial tariffs are high while South Africa's rates are 20 to 25% lower [8]. Reference [9] indicates electricity price increases were to modernise aging infrastructure. The majority of the poor, unemployed, and rural-dwelling Namibians [10] cannot afford high electricity prices. Namibia has harsh weather, a dry environment, and acute

water shortage problems. The Van Eck dry-cooling power station in Windhoek was built to reduce the water used for cooling [11]. Also, the cooling water needed for the United Kingdom's thermal electricity generation fleet is equivalent to that used to cool the Van Eck power plant [12].

Load management (LM) is used to effectively optimise and successfully operate any power utility. Load growth, increasing generation capacity constraints, rising electricity imports, and electricity demand beyond supply capacity in Namibia and the Southern African Development Community (SADC), necessitated new generation capacities or LM to supply the shortfall [11]. High energy intensity caused rising electricity tariffs in Namibia [13]. Cost-reflective electricity tariffs were anticipated in 2011/2012, and a high supply dependence on South Africa hampers the Namibian electricity supply sector [14].

Blinds systems that comprise curtains, shutters, and shade over windows and doors could reduce inlet heat by 50.0% in summer and 25.0% in heat outlets in winter [11]. Daylighting is the regulated admission of natural light to reduce electric lighting and save energy. Daylighting controls provide commercial benefits in the United States (US) because around 75.0% of electricity is consumed in buildings nationwide. Platinum-level-rated tubular skylights use 25.0% less energy than conventional lighting fixtures, which incorporates daylighting to achieve uniform light distribution while limiting electric lighting. Furthermore, daylighting provides a 24.0% energy reduction in Los Angeles schools and reduces by a third of total building energy costs [15].

Total electric energy consumed in commercial buildings is between 35.0% and 50.0%, while between 10.0% and 20.0% of the energy used for cooling buildings can be saved by employing day-lighting. Thus, optimisation of daylighting stratagems can reduce total energy costs by a third [16]. Depending on building architecture, usage, and energy consumption patterns, daylighting could reduce electric lighting between 20.0% and 80.0% [17]. Employing daylighting at utility peak demand hours can reduce demand charges. Turning off and dimming lights when not needed [1], saves between 10.0% and 20.0% of energy used for cooling a building. This also increases employees' productivity and improves the health of building occupants [18].

Further, above US$60 billion was expended annually for electric lighting which constitutes over 37.0% of average commercial buildings' total energy consumption [19]. Also, over 64 billion square feet of commercial buildings' floor space was lit by fluorescent systems in

which between 30.0% and 50.0% of the spaces can access daylight either by skylights or through windows. Thus, millions of electric lighting fixtures could be turned off for some periods of the day for energy-saving advantages [20].

The objective of the study was to determine how blinds, day-lighting, and geyser temperature settings can be used to save energy, and reduce electricity consumption, and costs for sustainable growth and development.

Namibia was the test laboratory. The results, conclusions, and recommendations of the study could be applicable globally. This study was organised into Introduction, Materials and Methods, Results and Discussion, and Conclusions.

3.5. Materials and Methods

A panel of expert judges was used to validate the 5-point Likert scale residential electricity load management questionnaire used to gather survey data for analysis in Windhoek City, Namibia. Over 300 self-report questionnaires were randomly distributed in Windhoek, Namibia. The 127 returned questionnaires were analysed using the statistical package for social sciences (SPSS) version 11.5. Also, the 127 sample size sufficiency and adequacy criterion were proved by [21].

The Enter, and Stepwise regression analyses, residuals, analysis of variance (ANOVA), Durbin-Watson statistics, and other methods determined the correctness, model fit, autocorrelation, and overall quality of model development [22-23]. The study was limited to using blinds, day-lighting, and geyser temperature settings variables to reduce electricity consumption and pricing patterns employing interactional predictive statistics without considering actual electricity consumption measurements of households or other consumers.

The analysis sub-section that applies more complex computational and rational tools to study four tables and eight graphs purely from statistical perspectives can be found in Appendix A. Also, the questionnaire is shown in Appendix B.

3.5.1. Sample Size Determination

The Cochran formula was used to obtain the sample size, as:

$$n_0 = \frac{Z^2 pq}{e^2}$$
$$\Rightarrow \frac{(1.96)^2 (0.5)^2 (0.5)^{22}}{(0.05)^2} = 384.16 \approx 385 \quad (3.1)$$

where Z is ± 1.96 (Z-score values), $p = q = 0.5$ are probabilities or likely outcomes, e is an error (0.05), and the study sample size was approximately 385. Also, model diversity decreases with increasing sample size, and a local optimum occurs between 300 and 350 samples [24].

Table 3. 1: RESIDUAL STATISTICS

	Minimum	Maximum	Mean	Std. Deviation	N
Predicted Value	-1.8139	5.0000	1.7641	1.36459	46
Residual	-2.6168	4.8139	.2359	1.14898	46
Std. Predicted Value	-3.977	3.185	-.216	1.434	46
Std. Residual	.	.	.	.	0

Note: Dependent Variable: Uncontrolled electricity use makes the utility increase electricity cost

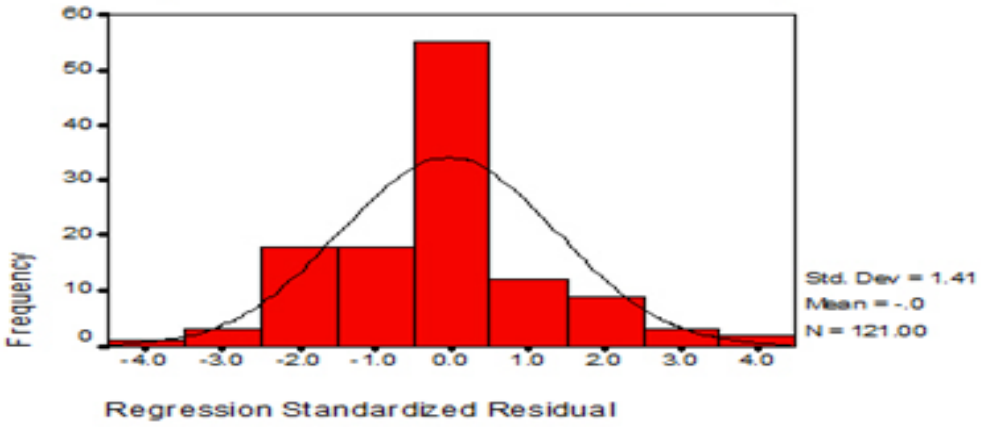

Figure 3. 1: Frequency Vs Regression of Standardised Residual Dependent variable: Blinds lessen heat inlet by 50% in summer and 25% heat outlet in winter [1].

3.5.2. Residual Statistics

Table 3.1 indicates the estimates of the disparity between observed and predicted values in regression analyses. The leftover effects test skews, accuracy, and adequacy of statistical predictions in the data. The histogram of standardised residuals is shown in Fig. 3.1.

Table 3. 2: VARIABLES ENTERED/REMOVED [1]

Model	Variables Entered	Variables Removed	Method
1	Setting geyser temperature at medium	.	Stepwise (Criteria: Probability-of-F-to- enter $\leq .050$, probability-of-F-to-remove $\geq .100$).
2	Electricity consumption-don't care	.	Stepwise (Criteria: Probability-of-F- to-enter $\leq .050$, Probability-of-F-to-remove $\geq .100$).
3	Draw blinds over all windows in the evenings and open them during sunlight hours	.	Stepwise (Criteria: Probability-of-F- to-enter $\leq .050$, Probability-of-F-to-remove $\geq .100$).
4	Energy-efficient buildings and lighting conserve the earth's resources	.	Stepwise (Criteria: Probability-of-F- to-enter $\leq .050$, Probability-of-F-to-remove $\geq .100$).

Note: Dependent Variable: Uncontrolled electricity use makes the utility increase electricity cost.

Table 3. 3; MODEL SUMMARY [1]

Model	R	R Square	Adjusted R Square	Std. Error of the Estimate	Change Statistics					Durbin-Watson
					R Square Change	F Change	df1	df2	p-value F Change	
1	.658(a)	.433	.415	.72770	.433	23.707	1	31	.000	
2	.757(b)	.573	.545	.64196	.140	9.833	1	30	.004	
3	.829I	.687	.655	.55904	.114	10.560	1	29	.003	
4	.864(d)	.747	.710	.51212	.059	6.557	1	28	.016	1.994

Note

a Predictors: (Constant), Setting geyser temperature at medium

Predictors: (Constant), Setting geyser temperature at medium, Electricity consumption-don't care

c Predictors: (Constant), Setting geyser temperature at medium, Electricity consumption-don't c , Draw blinds over all windows in the evenings and open them during sunlight hours

d Predictors: (Constant), Setting geyser temperature at medium, Electricity consumption-don't care, Draw blinds over all windows in the evenings and open them during sunlight hours, energy-efficient buildings and lighting conserve earth resources

3.5.3. Stepwise Regression

Table 3.2 was used to present four overall best models. Logistic regression is a stepwise method for selecting the best variables at the lowest error rates. The sample size independent response variable is binary (0 and 1). The four-factor method interprets 15 interdependent interaction effects using $(2^k - 1)$, where k is variables number [24].

3.5.4. Model Summary

Table 3.3 has one variable and three composite-variable models. Standard error measures model precision using dependent variable units. The R^2 change measures advancement in R^2 upon adding the second evaluator. F change predicts variable addition improvements while the p-value of F change is the alternative hypothesis acceptance probability. Statistical shifts exist between dependent and independent variables [25].

3.5.5. Analysis of Variance

Table 3.4 is the ANOVA that confirms, validates, verifies, and strengthens estimates in Tables 3.1-3.3. The sum of squares adds deviations of observations from their mean. The mean square is the variation in the model's measurements. The model is perfect if the model line passes through all the observations [21].

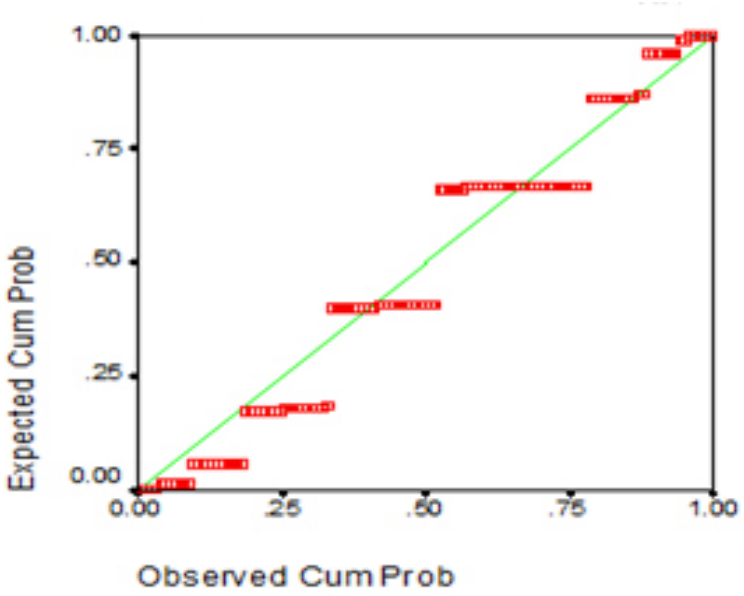

Figure 3. 2: Expected cumulative probability Vs Observed Cumulative probability [1].

3.5.6. Normal Probability Plots

Fig. 3.2 was used to present the probability-probability plots of standardised residuals. The 0.05 statistical power [26] measures central tendency, point-fit, subtle deviations from normality, and the Gaussian determines the characteristic behaviour of increasing electricity prices and consumption patterns.

Table 3.4 was used to present the ANOVA and we determine values of R^2 and R, for each composite model 1-4.

Model 1: From equation (A.22), the sample square correlation (R_1^2) was 0.4333, and the sample model correlation R_1 was 0.6583. The $F(1,32)$ distribution was below 0.0001probability of observing the values over 23.707 and shows strong evidence against the null hypothesis. Thus, (R_1^2) indicates a 43.3% variability and a 65.8% moderately strong correlation for increasing the price and electricity consumption with hotter geyser temperature settings.

Model 2: From equation (A.22), the sample square correlation (R_2^2) was 0.5732, and the sample model correlation R^2 was 0.7571. The F (2,30) distribution was below 0.0001 probability of observing values over 20.148 and indicates strong evidence for the alternative hypothesis. Thus, R_2^2 indicates a 57.3% variability and 75.7% strong correlation for increasing the price and electricity consumption from combined hotter geyser temperature settings and electricity consumption-don't care variables. Thus, model 2 is an improvement over the one-variable model.

Model 3: From equation (A.22), the sample square correlation (R_3^2) was 0.6871, and the sample model correlation R_3 was 0.8289. The F (3,29) distribution was below 0.0001 probability of observing values over 21.232 and strong evidence against the null hypothesis. Thus, R_3^2 suggests a 68.7% variability and 82.9% strong correlation at increasing the price and electricity consumption from combined hotter geyser temperature settings, electricity consumption-don't care, and daylighting variables. There was an improvement over the model having two variables.

Model 4: From equation (A.22), the sample square correlation (R_4^2) was 0.7465, and the sample model correlation R_4 was 0.8640. The F (4,28) distribution was below 0.0001

probability of observing values over 20.615 and strong evidence for the alternative hypothesis. Thus, R_4^2 indicates 74.6% variability and 86.4% very strong correlation between increasing the price and electricity consumption explained by hotter geyser temperature settings, electricity consumption-don't care, daylighting and, energy-efficient buildings and lighting conserve earth resources variables. Thus, model 4 was an improvement over all the other three models.

3.7. Results and Discussion

The results are tabulated in Tables 3.1-3.4 and Figures 3.1-3.8. Figure 3.9 is the methodology flowchart. Table 3.1 shows residual statistics and Table 3.2 indicates stepwise regression results. Table 3.3 is a model summary for statistics ranging from the coefficient of determination to DW statistics. Table 3.4 is ANOVA for developed models.

3.7.1. Histogram of Standardised Residuals

Fig. 3.1 is a histogram of standardised residuals assessing normality [27]. It cannot detect subtle deviations but tests for normality [28]. The X-axis is Observed Cumulative Probability percentiles in the residuals frequency distribution. The Y-axis is a Standardised Residual (Z-score) for computing the Cumulative Density from the Normal distribution. The normally distributed residuals are on the diagonal of the identity line. Results show 1.41 standard deviations, 0 mean, 0 median, 121 nonmissing samples, and 61st point of 0 value were the mean and median of the perfect histogram.

3.7.2. Normal Probability-Probability Plot

Fig. 3.2 compares the empirical cumulative distribution function (ecdf) of the variable with the defined theoretical cumulative distribution function (tcdf). The proportion of the nonmissing ecdf observations below their heights [29] are sorted according to increasing order. They determine the deviations from normality in the distribution centre, whether Gaussian or not [28]. Linear data distribution point patterns on the P-P plot through the origin are proof that measurements are normally distributed [30]. Therefore, the unit slope in Fig. 3.2, in square format, is normally distributed [29].

Errors in the Normal P-P plot follow Gaussian normal distributions for parameters [31]. Results in Fig. 3.2 are non-uniform discrete staircase jump function discontinuities. They are random outcomes in the interval (0, 1) of time distances t. It is a convex set with one minimum point [32-33].

Interchanging axes of $F(x)$, determine the graph of x_u, the median of x is the smallest number *m* on the 61st term in Fig. 1 (*m* is *0.5* percentile of x). Empirical interpretation of u percentile x_u is the Quetelet curve [34-35]. This optimisation point was n line segments of lengths x_i, separated vertically in order of increasing lengths. Thus, jump distribution functions occur at 15 points as a countable sequence in Fig. 3.2.

3.7.3. Residual Statistics

Table 3.1 is residual statistics that test the remaining variability and the disparity between observed dependent and predicted values in regression analysis. They show the prediction accuracy of models, assumptions, heteroscedasticity, and dispersion in data [36]. Residuals measure the risk premium for operating power systems that affect increasing electricity consumption and pricing patterns [30]. The p-value below 0.0005 suggests a reasonably good model development of statistical significance.

3.7.4. Variables Entered/Removed Based on Stepwise Regression Analyses

The stepwise method fits models automatically by selecting predictive variables using two significance levels for the removal/addition of variable [37]. The probability of adding variables is lower than of removing variables based on *t*-statistics [38].

Table 3.2 Stepwise criteria have: Probability-of-F-to-enter below $0.05(\leq .050)$ and Probability-of-F-to-remove variables $(\geq .100)$ exceeded 0.10. The model variables were removed in one step: set geyser temperature at medium, electricity consumption-don't care, daylighting, and energy-efficient buildings and lighting conserve earth resources.

Setting high geyser temperatures increases electricity consumption and drives electricity prices higher. Not drawing blinds over windows causes higher inlet heat in summer and larger heat outlets in winter. Both factors drive electricity consumption and prices higher for space cooling/heating as shown by the steps/jumps in Fig. 3.2.

Don't care electricity consumption accentuates higher electricity consumption patterns, higher bills, creates hardship. and a vicious spiral for the majority of the population living below the poverty trap [35,39].

However, stepwise analyses significantly strengthen the most economical overall model that contains important variables [40], having minimum predictors [24].

3.7.5. Model Summary

R measures the relationship between observed and predicted values of the criterion variable. R^2 tests the criterion variable variance and predictors' goodness-of-fit. Favourable model outcomes could be overestimated. Adjusted R^2 is the most useful model success indicator [23].

Both R^2 and standard error (S) measure goodness-of-fit and how the model best fits sample data. S measures the model precision of the absolute data points spread around the regression line. S is a rough estimate of a 95% prediction interval extending between $+/-2$ standard errors of the fitted regression line [25].

The R^2 values are relative measures of higher variance percentages, while larger R^2 indicates closely fitted data points. R^2 is valid for linear models [25], but independent variables collectively explain the variance of the dependent variable. R^2 measures the relationship strength between the model and the dependent variable on a 0-100% scale. It tests the data scatter points about the fitted regression line [41]. It also contains the precise number of independent variables in regression models [42]. R^2 change enhances R^2 by adding a second evaluator. F-test determines the R^2 change, while significant F-change suggests that the added variables remarkably enhanced the prediction [43].

The limitations of R^2 include prescription bias when the linear model was underspecified. Further, significant independent variables, polynomials, or interaction terms are present [41].

3.7.5.1. Model 1 Setting Geyser Temperatures at Medium

The 65.8% correlation and 43.3% variance accounted for in model 1, occurred between setting geyser temperatures at medium against increasing electricity consumption and pricing patterns. Overall model fit improved by 41.5%, with 0.73% standard distance between observation and regression lines, 95% of data points are between the regression line and, $+/-$ 1.5% of geyser temperature settings. Hence, Model 1 is statistically significant

$(F_{(1,31)} = 23.707 ; p \text{ p } 0.0005)$.

3.7.5.2. Model 2 Combined Effects of Geyser Temperature Settings and Electricity Consumption-Don't Care

Over 75.7% correlation and above 57.3% variance were allowed in Model 2. Overall model fit improved by 54.5%, with 0.64% standard distance between observation and regression lines, 95% of data points of the model lie between the regression line and, $\pm$ 1.3% of combined effects of geyser temperature settings and electricity consumption–don't care. Model 2 improved by 14.0% by adding a second predictor. It was statistically significant $(F_{(1,30)} = 9.833; p \text{ p } 0.0004)$.

3.7.5.3. Model 3 Combined Effects of Geyser Temperature Settings, Electricity Consumption-Don't Care and Day-lighting

Above 82.9% correlation and over 68.7% variance were allowed in Model 3. About 65.5% overall model fit sufficiency, 0.56% standard distance between observation and regression lines, 95% model precision of data points lie between the regression line and $\pm$ 1.12% of geyser temperature settings, electricity consumption-don't care, and day-lighting. An incremental 11.4% model improvement was achieved by adding the third predictor. Model 3 was statistically significant $(F_{(1,29)} = 10.560 ; p \text{ p } 0.0003)$.

3.7.5.4. Model 4 Combined Effects of Geyser Temperature Settings, Electricity Consumption-Don't Care, Day-lighting, and Energy-Efficient Buildings and Lighting Conserve Earth Resources

About 86.4% correlation and over 74.7% variance were allowed in Model 4. Above all, the 71.0% overall model goodness-of-fit, 0.51% standard distance of observation and regression lines, occurred while 95% of the model data precision points lie between the regression line and $\pm$ 1.0% of the geyser temperature settings; electricity consumption-don't care; day-lighting and energy-efficient buildings and lighting conserve earth resources. Model 4 achieved a 5.9% incremental improvement by adding four predictors and was statistically significant $(F_{(1,28)} = 6.557 ; p \text{ p } 0.016)$.

3.8. The Durbin-Watson Statistic

Overall, the 71.0% model goodness-of-fit mirrors increasing electricity consumption and pricing patterns. Therefore, the researchers accept the null hypothesis of the DW statistic because the effective DW (2.006) was higher than the upper limit of the DW statistics $(d_U = 1.73)$. We also conclude that there were no autocorrelation effects in the model. This was so because the determined DW (1.994) was close to the ideal DW statistic (Since $4 - 1.994 = 2.006 \approx 2.0$). Therefore, errors in the model were uncorrelated, without autocorrelation effects, and without violating the independent errors assumption of the Durbin-Watson statistic [44-45]. The two (2) DW statistics suggest a reasonably good model and also strengthen the significance, quality, and adequacy of this and the other four (4) developed models, in this part of the thesis.

3.9. Multivariate Interaction Effects

Interaction effects occur whenever one variable effect depends on another and affect statistical design outcomes. They show how a third variable influences links between dependent and independent variables [46]. The p-values are the statistical significance of fitted interaction plots. Several lines indicate the values of the second independent variable [46], while the parallel lines show no interaction effects. Different slopes suggest interaction effects. The cross-lines on the graph indicate that the interaction effects have significant p-values and so, the main effects are interpreted [46].

Logistic regression models use stepwise to select the best model, give the lowest error rates, broad usage, and sample size independence. The model diversity evaluates the model quality for reproducibility and each interaction effect indicates the compound power index [24].

3.9.1. Model 1a Setting Geyser Temperatures at Medium-Main Interaction Effect (A)

Model 1a: This factor is highly significant in electricity load management because the specific heat capacity of water is high, and setting the geyser temperature at medium reduces energy wastage [1,47]. In this work, the ideal geyser temperature setting is between 50 and 55^0C in summer and between 60 and 65^0C in winter. This geyser temperature setting should not be

lower than 50^0C so as not to increase bacterial growth in the water [48]. A geyser temperature setting of 140^0F (60^0C) is usually used for homes with an immunocompromised person, a dishwasher that does not pre-heat, and multi-occupant because of a higher number of family members. If the competition for hot water is fierce in the home across family members or washing machine or dishwasher, one might be tempted to raise the temperature of the water heater [49]. Although 120^0F (49^0C) is the safety recommendation against scalding, 140^0F (60^0C) is the common default setting. Again, both the Department of Energy and manufacturers have divergent opinions, and most experts agree that temperatures below 120^0F (49^0C) create a risk for bacteria to develop in the water heater from stagnant water, such as Legionella species that cause Legionnaire's disease [49].

Furthermore, a variety of factors are considered in setting geyser temperature: (a) Stick to 120^0F (49^0C) if the home has young children and/or elderly who are susceptible to third-degree burns within seconds or single occupant because of lower demand on hot water, and (b) Consider 140^0F (60^0C) if the home has an immunocompromised person, a dishwasher that does not pre-heat, and multi-occupant because of higher demand on hot water [49]. Water heaters consume between 14 and 18% of a home's energy on average and it could be tempting to decrease temperature for savings. It was noted that a 10^0F (5.6^0C) reduction in temperature is connected with between a 3 and 5% reduction in energy. But, Legionella bacteria can multiply just below 122^0F (50^0C). So, a balance of risk acceptance level and energy consumption goals must be struck [49]. In addition, many water heaters have a temperature dial that can be used to adjust the temperature. If yours does not, the temperature can still bump up in small increments to your taste or probably engage a service provider [49].

A water tank booster that keeps the temperature of water at 140^0F (60^0C) to avoid pathogens and mixes cold water to deliver a lower temperature at the tap could be a solution to homes that need to balance a higher hot water temperature for health and safety along mitigating the risk of scalding [49]. Heating water in a geyser can be expensive if not done correctly. This is so because water geysers need a lot of energy to heat water and high electricity consumption shoots up bills in winter. Most geysers or water heaters are equipped with thermostats that maintain the water temperature at the desired levels and cut off the power supply whenever the desired water temperatures are achieved [50]. Whenever the water temperature drops to a certain preset level, the thermostat switches on and makes sure that the water is heated until the preset temperature. Moreover, two types of geysers are available in the market: (a) One with thermostat settings outside and changeable, and (b) Others in which the thermostat is not visible from outside and cannot be changed. Although water geysers have a temperature range of between 40 and 75^0C, most geysers available in the market have a default thermostat setting of 60^0C or higher [50].

That means water in the geyser will be heated till it reaches a temperature of 60^0C or higher. Water at this temperature is extremely hot and needs to be mixed with a lot of cold water before use. The amount of electricity used in heating the water depends upon the temperature of the water entering the geyser and the temperature setting of the thermostat. The more the difference between these two temperatures, the more the amount of electricity required to heat water. Also, several energy-saving groups suggest that water heated up to between 40 and 45^0C is good for use. So, if one has a geyser with an outside thermostat setting, one can change it from 60^0C to between 40 and 45^0C. For the right heating amount and electricity saving, the thermostat knob must be kept around the middle position [50].

Several persons have the tendency of leaving the geyser "ON" all the time which leads to a lot of electricity wastage. Whenever the water is heated, the power supply is automatically switched "OFF" by the thermostat. After some time, the hot water begins to lose the heat through the body of the geyser and once the water temperature goes down to a certain preset value, the thermostat switches on the power supply and the water heating process starts all over again. This on-and-off process repeats itself throughout the day and consumes electricity [50]. Also, the size of a geyser is selected based on the requirements because an oversized geyser entails heating extra water that is not needed so that electricity is not wasted. The 5-star rated geysers consume less electricity, have much less heat loss, and reduce monthly electricity bills [50].

Further, the Y-axes for Figs. 3.3-3.8 are response figures on a 5-point Likert scale. The 9-point Likert scale on Y-axis for Fig. 3.5 arose because 9 was used to represent missing responses on the questionnaire (attached). The X-axes for Figs. 3.3-3.8 were supposed to have 1 and 2 only because each represents male and female. The fractional or decimal values on X-axis arose because of the limitations and drawing errors of automatically using the preset scaling graph algorithms in SPSS software. Therefore, decimal figures on the X-axes for Figs. 3.3-3.8 should be ignored as machine errors because males and females are binary and there are no fractions in human beings.

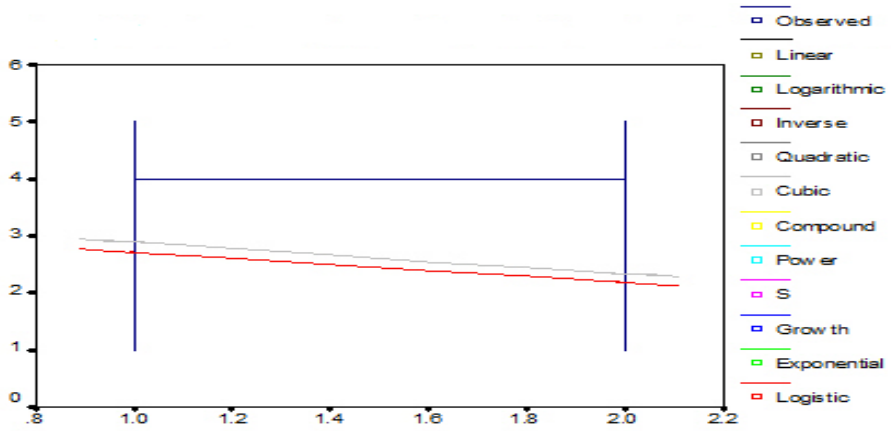

Respondents' gender

Figure 3. 3: Setting geyser temperatures at medium against respondents' gender [1].

Fig. 3.3 suggests an H-pole with parallel decreasing logistic and cubic regression cross-lines. The graph shows females set higher geyser temperatures, causing higher electricity consumption and higher prices. This assertion is corroborated by [51] indicating that women and teenagers are suspected to use more electricity in the home. Also, women have a larger carbon footprint compared to men, which derives from the kinds of activities reported. However, qualitative and quantitative research concludes that women would be affected more by load-shifting and lessening programmes. In addition, [52] indicates that real energy consumers do not have adequate specialised energy backgrounds, knowledge, and training in nearly all cases.

Furthermore, women are trice more engaged in domestic schedules than men in practically all countries, thereby consuming more energy than men on the homestead. The growth regression cross-line plateaued [46] at level four (4), which means hotter geyser temperature settings by both genders lead to higher electricity consumption, higher electricity prices, and higher utility penalty payments. However, the vertical parallel lines on points 1 and 2 of the X-axis indicate there were no interaction effects [24] between the gender and everyone (male or female) was at liberty to set hotter geyser temperatures.

3.9.2. Model 1b Electricity Consumption-Don't Care-Main Interaction Effect (B)

Model 1b: works directly into the economic objectives of utility and could negatively impact electricity supply efficiency and usage, electricity bills, and loss reduction. This behavioural attitude in electricity consumption stresses utility facilities, and provides a strong

economic basis for electricity price increases, which supports utility production inefficiencies and could jeopardise the public good, in terms of energy efficiency [1].

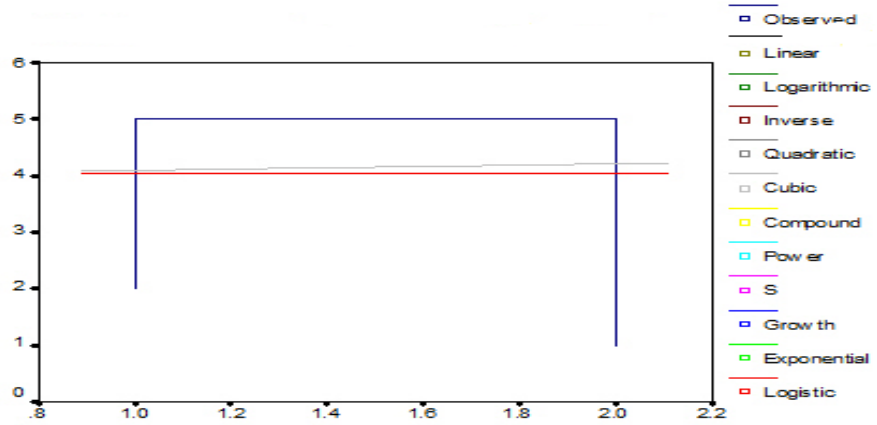

Figure 3. 4: Electricity consumption-don't care Vs Respondents gender [1].

Fig. 3.4 indicates an eta-shaped or table-like plateau of growth regression interaction cross-lines. It has high and slowly rising logistic and cubic regression gradients by gender. The graph shows the highest rates of electricity consumption and penalty payments by both genders. The interaction cross-lines of logistic and cubic regressions, as well as the entitled electricity consumer groups, were gender independent [46]. This was so because the vertical parallel lines on points 1 and 2 on the X-axis (respondents' gender) indicate no interaction effects across gender in electricity consumption. Further, the figures on Y-Axis indicate (1-strongly agree, 2-agree, 3-not sure, 4-disagree, and 5-strongly disagree) the strength of respondents agreeing with the propositions on the questionnaire.

3.9.3. Model 1c Day-lighting-Main Interaction Effect (C)

Model 1c conserves heat, and lowers energy or electricity consumption, and electricity bills paid for home heating by natural convection. These reduce wasted energy, greenhouse gases (GHG) emissions, fuel burnt for electricity production, and avoided production [1,47], defer high-cost power plants, transmission, and distribution network systems [30].

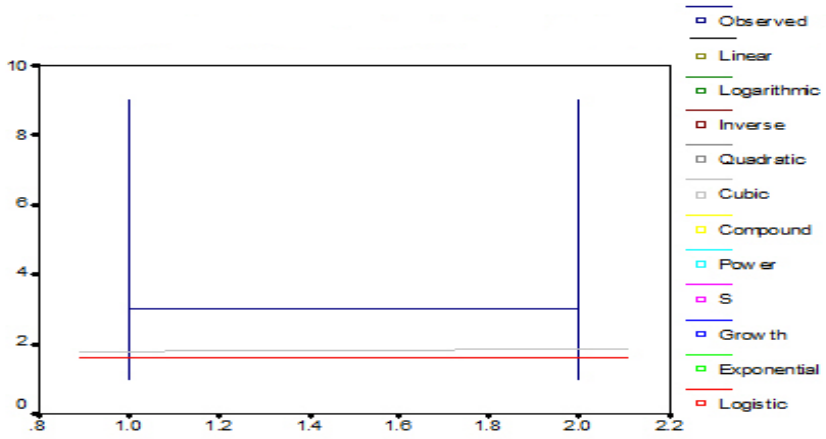

Respondents' gender

Figure 3. 5: Draw/open blinds over windows (Daylighting) Vs Respondents' gender [1].

Fig. 3.5 suggests indecision in using day lighting to reduce electricity consumption as shown by the horizontal crossbar of H-pole growth regression cross-lines. Day-lighting practice hovers between strongly agree and agree for logistic and cubic regression interaction patterns. Therefore, day-lighting indicates the optimal solution to reducing electricity consumption and pricing patterns problems by gender, because there were no gender interactions in using it to reduce consumption and costs. Additionally, [15] indicates that day-lighting reduces electricity consumption by 25%.

Therefore, daylighting is one of the best strategies for keeping electricity consumption and price increases to the barest minimum. It could be pivotal in any electricity load management model for securing optimal and sustainable production, transmission, distribution, and utilisation of electrical power, globally.

3.9.4. Model 1d Energy-Efficient Buildings and Lighting Conserve Earth Resources-Main Interaction Effect (D)

Model 1d: directly relates the stress on utility facilities with power consumed always. Electricity consumers' gender, economic power, and age determine preferences in an electrical appliance used and times of use for households, lighting, or electric motors in commerce and industry. The quantity and cost of electricity used depend on the application [1], which affects electricity pricing [30] and stresses placed on utility facilities [47].

Electricity production technologies use coal, natural gas, diesel, nuclear, hydro, wind, and solar while increasing electricity consumption worldwide increases global warming. Utilities

unable to cope with overloads lead to power systems failures, instability, unreliable performance, and nonconformance with regulatory requirements [1].

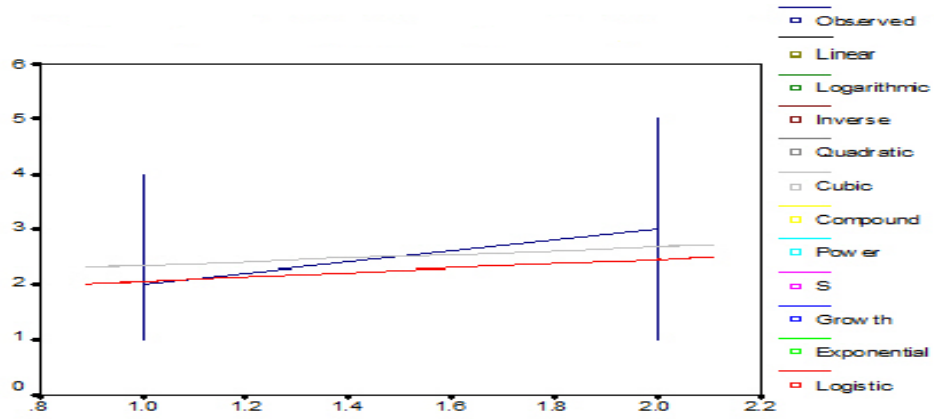

Respondents' gender

Figure 3. 6: Energy-efficient buildings and lighting conserve earth resources [1].

Fig. 3.6 suggests wheel and axle-type interaction plots for logistic, cubic, and growth regressions. Male electricity consumers prefer energy-efficient buildings and lighting. Although the spread is gender-independent, females have a larger scatter. Electricity consumption patterns were equal at mid-points for cubic and growth regressions (1.5) and logistic and growth regressions were close to 1.1. Thus, males were more favourably disposed to energy-efficient building and lighting principles and practices.

3.9.5. Using Blinds Reduce Heat Inlet through Windows by 50% in Summer and Heat Outlet by 25% in the Winter-Main Interaction Effect

Fig. 3.7 is an H-pole growth regression with almost parallel logistic and cubic interaction cross-lines. Blinds reduce inlet heat through windows by 50.0% in summer while not running air conditioners or other cooling devices. It reduces heat exchanges between warmer inside ambience with much colder outside temperatures by 25.0% in winter, while heaters are on [1]. This reduces electricity consumption for room and space heating/cooling. Electricity prices were stable, even during heavy, persistent, and universal electricity consumption. The plateau [46] between the H-pole cross-line indicates virtually no increases in electricity consumption or prices and no interaction effects across gender.

However, both the logistic and cubic interaction cross-lines show increasing electricity consumption and pricing patterns if those using blinds were male.

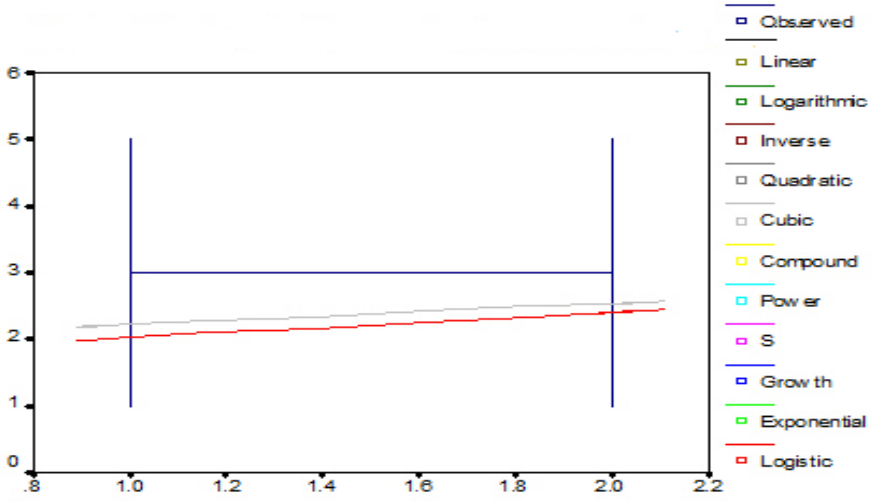

Respondents' gender

Figure 3. 7: Using blinds reduces heat inlet through windows by 50% in summer and heat outlet by 25% in winter against Respondents' gender [1].

3.9.6. Uncontrolled Electricity Use Makes NamPower Increase Electricity cost-Main Interaction Effect

Fig. 3.8 is a J-shaped interaction plot of growth, logistic, and cubic regression cross-lines. The parallel lines [46] indicate no interaction effects across gender that controls rising electricity consumption and cost patterns, but high electricity consumption and pricing patterns are prevalent if consumers are female.

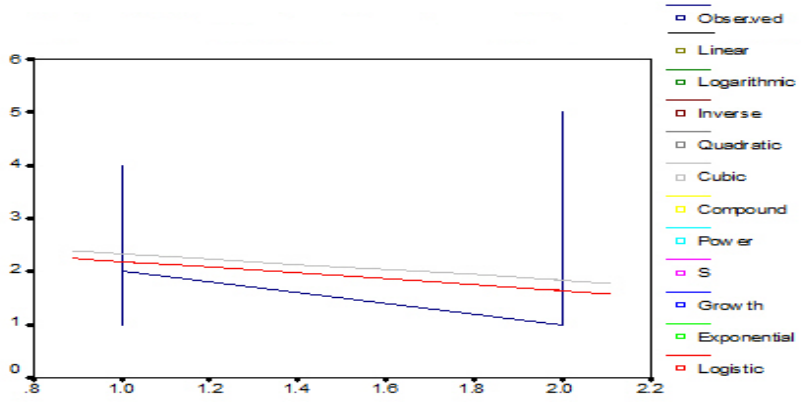

Respondents' gender

Figure 3. 8: Without electricity use control the utility will increase cost Vs Respondents' gender [1].

However, the rate of increase is much higher for the growth regression line than either the

logistic or cubic regression interaction cross-lines. Thus, costs are managed by reducing consumption, peak load management, peer comparison, and energy efficiency identification projects, utility invoice management that optimise facility, and involvement in rate-making processes [53].

3.9.7. One-Way Effects for each of the Four (4) Main Interaction Effects- A, B, C, D

The model of each main effect predicts how their combined effects encourage rising electricity consumption and pricing patterns. The adjusted R^2 value indicates the quality of the model and accounts for over 41.5% variance. Thus, rising prices and electricity consumption depend on geyser temperature settings (A), electricity consumption-don't care (B), Day-lighting (C), and energy-efficient buildings and lighting to conserve earth resources (D).

3.9.8. Two-Way Effects $(A, B, A \times B)$

Model 2 is the interaction and predictive relationships of setting high geyser temperatures and electricity consumption-don't care. The adjusted R^2 value accounts for over 54.5% variance in total overall model development. The three major relationships were: (a) main effect (A), (b) main effect (B), and (c) single two-way interaction of items A and $B(A \times B)$ .The additional 13% variance was a combination of items A and B, each acting alone and in concert $(A \times B)$ [1],[22],[23]. To avoid repetition, the single two-way interaction $(A \times B)$ is discussed. Hence, rising prices and electricity consumption patterns depend on the combined effects of hotter geyser temperature settings and electricity consumption–don't care $(A \times B)$.

3.9.9. Three-Way Effects of Combining the First Three (3) Main Effects (Seven Model Effects in All)

Model 3 is the interaction and predictive relationships among three variables: (i) setting high geyser temperatures (A), (ii) electricity consumption-don't care (B), and (iii) day-lighting (C).

There were seven models: (a) main effect (A), (b) main effect (B), (c) main effect (C), (d) two-way effect $(A\times B)$, (e) two-way effect $(A\times C)$, (f) two-way effect $(B\times C)$, and (g) single three-way effect $(A\times B\times C)$.

Adjusted R^2 value accounts for over 65.5% variance in total overall model development. This suggests an additional 11.0% variance above the model with only two interacting predictors [1].

To avoid repetition, only the three two-way effects and one three-way effect are discussed. Therefore, rising price and electricity consumption patterns depend on the combined effects of high geyser temperature settings and electricity consumption-don't care $(A\times B)$, high geyser temperature settings, and day-lighting $(A\times C)$, electricity consumption-don't care and day-lighting $(B\times C)$ and high geyser temperature settings, electricity consumption-don't care and day-lighting $(A\times B\times C)$.

3.9.10. Four-Way Effects Combine the Four (4) Models Selected by the Stepwise Regression (15 Models)

The four-way effects of model 4 indicate relationships between four predictors: (i) setting high geyser temperatures (A); (ii) electricity consumption-don't care (B); (iii) day-lighting (C), and (iv) energy-efficient buildings and lighting conserve earth resources (D).

The fifteen models were: (a) main effect (A), (b) main effect (B), (c) main effect (C), (d) main effect (D), (e) two-way effect $(A\times B)$, (f) two-way effect $(A\times C)$, (g) two-way effect $(A\times D)$, (h) two-way effect $(B\times C)$,(i) two-way effect $(B\times D)$, (j) two-way effect $(C\times D)$, (k) three-way effect $(A\times B\times D)$; (l) three-way effect $(A\times B\times C)$, (m) three-way effect $(B\times C\times D)$, (n) three-way effect $(A\times C\times D)$, and one four-way effect $(A\times B\times C\times D)$.

The final adjusted R^2 value accounts for over 71.0% variance in the total overall model developed. The result shows an additional 5.5% variance contribution over the model with three interacting predictors. The trend indicates that additional variance contributions from higher-order interacting predictor variables continuously improved upon the quality of model fit in the study (71.0% model fit with 4 predictors). To avoid repetition we discuss only the combined effects.

Thus, rising price and electricity consumption patterns depend on: high geyser temperature settings and electricity consumption-don't care $(A\times B)$, high geyser temperature settings and day-lighting$(A\times C)$, high geyser temperature settings and energy-efficient buildings and lighting conserve earth resources$(A\times D)$, electricity consumption-don't care and day-lighting $(B\times C)$, electricity consumption-don't care and energy-efficient buildings and lighting conserve earth resources $(B\times D)$, day-lighting with energy-efficient buildings and lighting conserve earth resources $(C\times D)$, high geyser temperature settings, electricity consumption-don't care and day-lighting $(A\times B\times C)$, high geyser temperature settings, electricity consumption-don't care and energy-efficient buildings and lighting conserve earth resources $(A\times B\times D)$, high geyser temperature settings, day-lighting and energy-efficient buildings and lighting conserve earth resources$(A\times C\times D)$, electricity consumption-don't care, day-lighting with energy-efficient buildings and lighting conserve earth resources $(B\times C\times D)$, and high geyser temperature settings, electricity consumption-don't care, day-lighting with energy-efficient buildings and lighting conserve earth resources $(A\times B\times C\times D)$.

Nevertheless, the 15 jump discontinuities in Fig. 3.2 corroborate the 15 four-way effects developed by the stepwise regression in Table 3.3. The same trend of reinforcements and validations are visible from the parameter estimates in Tables 3.1, 3.3, and 3.4, which have all worked in tandem to strengthen the claims of very good model development having the requisite accuracy, precision, and reliability in this thesis.

3.10. Analysis of Variance (Table 3.4)

Table 3. 4: ANALYSIS OF VARIANCE [1]

Model		Sum of Squares	Df	Mean Square	F	p-value
1	Regression	12.554	1	12.554	23.707	.000(a)
	Residual	16.416	31	.530		
	Total	28.970	32			
2	Regression	16.606	2	8.303	20.148	.000(b)
	Residual	12.363	30	.412		
	Total	28.970	32			
3	Regression	19.906	3	6.635	21.232	.000I

	Residual	9.063	29	.313		
	Total	28.970	32			
4	Regression	21.626	4	5.407	20.615	.000(d)
	Residual	7.343	28	.262		
	Total	28.970	32			

Note

a Predictors: (Constant), Setting geyser temperature at medium

b Predictors: (Constant), Setting geyser temperature at medium, Electricity consumption-don't care

c Predictors: (Constant), Setting geyser temperature at medium, Electricity consumption-don't care, Draw blinds over all windows in the evenings and open them during sunlight hours

d Predictors: (Constant), Setting geyser temperature at medium, Electricity consumption-don't care, Draw blinds over all windows in the evenings and open them during sunlight hours, Energy-efficient buildings and lighting conserve earth resources

e Dependent Variable: Uncontrolled electricity use makes the utility increase electricity cost.

ANOVA splits observed variance for significance and test whether linear relationships exist between dependent and independent variables [54]. The error sum of residuals is a portion of total variability not explained by the model and nonlinear portions of the dependent variable [22],[23],[45],[54]. Although the F-test does not indicate which parameters (β_k) is not zero, only that at least one of them is linearly related to the response variable. Further, the square root of R^2 is the multiple association coefficient R between observations y_i and fitted values $\hat{y}_i$ [55].

The distribution F(1,32) has below 0.0001 probability of observing a value over 23.707 and is strong evidence for the alternative hypothesis. Thus, R_1^2 indicates 43.3% variability and 65.8% moderately strong correlation explained by increasing price and electricity consumption patterns for high geyser temperature settings. Also, the distribution $F_{(2,30)}$ has below 0.0001 probability of observing a value over 20.148 and strong proof for the alternative hypothesis. Thus, R_2^2 suggests 57.3% variability and 75.7% strong correlation explained by increasing price and electricity consumption patterns for the combined high geyser

temperature settings and electricity consumption-don't care variables. This was 14.0% better than the one-variable linear model.

The distribution $F_{(3,29)}$ has below 0.0001 probability of observing a value over 21.232 and a strong indication against the null hypothesis. Thus R_3^2 implies 68.7% variability and 82.9% strong correlation explained by rising price and electricity consumption patterns for the combined high geyser temperature settings, electricity consumption-don't care, and day-lighting variables. There was an 11.0% enhanced performance over the two variables model.

The distribution $F_{(4,28)}$ has below 0.0001 probability of observing a value exceeding 20.615 and strong evidence against the null hypothesis. Thus, R_4^2 stipulates over 74.6% variability and 86.4% very strong correlation explained by increasing price and electricity consumption patterns for combined high geyser temperature settings, electricity consumption-don't care, day-lighting with energy-efficient buildings and lighting conserve earth resources variables. There was an extra 5.9% refinement over all the other models and especially that having only three variables.

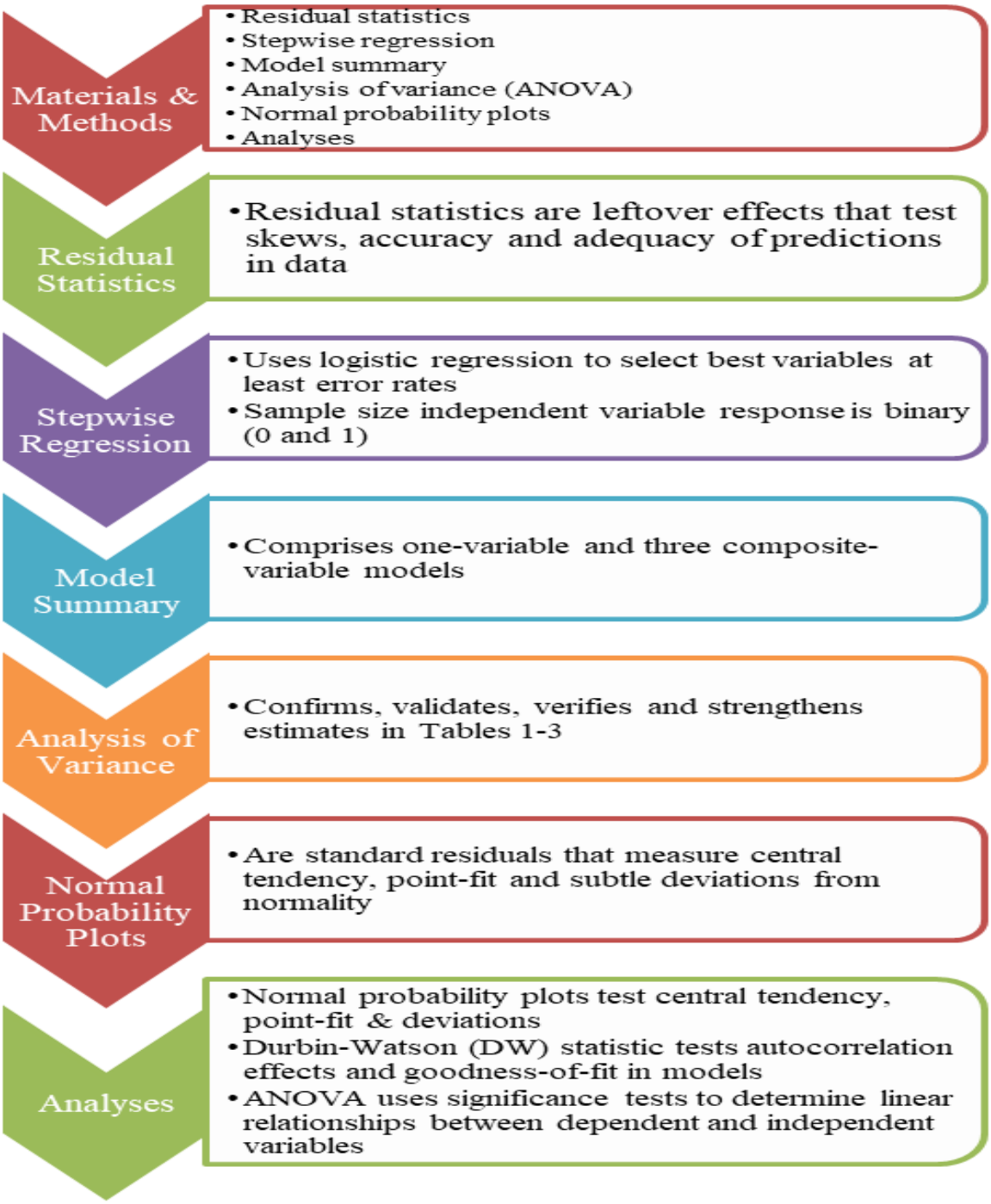

Figure 3. 9: Flowchart.

3.11. Conclusions

Using blinds, shutters, or shades significantly reduced inlet heat through windows by 50.0% in summer and heat outlet by 25.0% during winter, while day-lighting reduced

electricity consumption by 25.0% as electricity prices were stable, even during heavy, persistent, and widespread electricity consumption.

Both electricity price jump discontinuities and stepwise regression four-factor interaction analyses were 15 each, and the 0.5 Quetelet curve index at the median percentile was the optimal solution to the empirical electricity consumption and net pricing distribution patterns problem. Furthermore, the Quetelet index is used to create awareness, education, and behaviour modification, especially among the average citizens on energy efficiency for affordable, reliable, and sustainable supply.

Logistic and cubic interaction cross-lines for the study sample in Namibia show males prefer using blinds over windows than females. Blinds and day-lighting were the least costly and optimal strategies for curtailing electricity consumption and latching price increases. Therefore, blinds and day-lighting could lead to optimal and more sustainable production, transmission, distribution, and utilisation of electrical power, worldwide. Daylighting tends to raise the ambient temperatures of the interior environments, especially in summer. The temperature rise may not warrant switching air conditioning equipment or fans except when it is absolutely necessary. So, daylighting would not inadvertently raise electricity consumption but to lower it. On that score, however, daylighting is still a credible energy reduction mechanism that is worth embracing. This is especially so because Namibia experiences extremes of temperature at different times of the year: It can be extremely hot (up to 45^0C or higher) and bitterly cold (as low as -10^0C or lower).

Future research should consider actual electricity consumption measurements by the electrical appliances category to ascertain quantifiable energy savings using any of the methods proposed in the study. Consequently, actual electricity consumption measurements of appliances in households and other consumers could be used to better understand the cause-effect relationships and to determine specific energy savings from particular and specialised consumer categories.

II. APPENDIX B

B.1. Analyses

This section contains the analyses of the study.

B.1.1. Normal probability-probability plot

Fig. 3.2 is a Normal P-P plot that compares the variable empirical cumulative distribution function (ecdf) with the theoretical cumulative distribution function (tcdf) F(.). The ecdf $F_n(x)$ is the nonmissing observation proportion equivalent to *x*, because $x_{(i)} \le x_{(2)} \le ...x_{(n)}$. Furthermore, the *n* nonmissing values follow an increasing order [29]:

$$x_{(1)} \le x_{(2)} \le ...x_{(n)} \tag{B3.1}$$

The i^{th} ordered value $X_{(i)}$ on the P-P plot in the X-coordinate is $F\left(x_{(i)}\right)$, and in the Y-coordinate is [*i/n*].

Errors in the Normal P-P plot follow Gaussian normal distributions for parameters [27],[31].

Fig. 3.2 was used to present the results of discrete non-uniform staircase jump functions. They lie along with electricity consumption against the net pricing distribution curve. Electricity switching and consumption patterns are random intervals (0, 1). Their time distances, *t* occur between 0 and 1. The probability *t* is between t_1 and t_2 [34]:

$$P\{t_1 \le t \le t_2\} = t_2 - t_1 \tag{B3.2}$$

The random variable X is

$$x(t) = t....0 \le t \le 1 \tag{B3.3}$$

The variable has double meanings: Experimentation outcome and also, corresponding value x(t) of random variable X. We show the ramp distribution function, F(x) of X [34]:

If $x > 1$, then $x(t) \le x$ for every outcome:

$$F(x) = P\{X \le x\} = P\{0 \le t \le 1\} = P(S) = 1..x > 1 \quad \text{(B3.4)}$$

If $0 \le x \le 1$, then $X(t) \le x$ for every t in interval $(0, x)$ Thus:

$$F(x) = P\{X \le x\} = P\{0 \le t \le x\} = x...0 \le x \le 1 \quad \text{(B3.5)}$$

If $x < 0$, then $\{X \le x\}$ is the impossible event because $X(t) \ge 0$ for every t. Whence,

$$F(x) = P\{X \le x\} = P\{\Phi\} = 0...x < 0 \quad \text{(B3.6)}$$

Established as, required.

Percentile η of the random variable X is the smallest number X_u because [34]:

$$u = P\{X \le x\} = F(x_u) \quad \text{(B3.7)}$$

Hence, X_u is the inverse of the function $u = F(x)$, in interval $0 \le u \le 1$, on the X-axis. We interchange the axes of F(x) to determine the graph of X_u. The median of X is the smallest number *m* as F(m) = 0.5, which is the 61st term of Fig. 3.1, where *m* is the 0.5 percentile of X.

The frequency interpretation of F(x) and X_u follows: we perform the experiment n times and observe n values $X_1,\ldots,X_n$ random variables X [34]. If these numbers on the *x*-axis form the staircase function $F_n(x)$; the steps are located at points x_i, and their height equals 1/n [29]. It starts at the smallest value x_{min} of x_i and $F_n(x) = 0$ for $x < x_{min}$.

The function $F_n(x)$ is the empirical distribution of random variable X. For any specific X, the number of $F_n(x)$ steps equals the number n_x of x_{is} smaller than X. Hence, $F_n(x) = n_x/n$. But, $n_x/n \cong P\{x \le x\}$ for large $n_x/n \cong P\{x \le x\}$, so we conclude that [34]:

$$F_n(x) = \frac{n_x}{n} \to P\{X \le x\} = F(x) \text{ as } n \to \infty \quad \text{(B3.8)}$$

The empirical interpretation of the u percentile x_u is the Quetelet curve. This derives from n line segments of lengths x_i, separated vertically in order of increasing length, by distance 1/n. It forms the staircase function with corners at the endpoints of those segments.

Empirically, x_u equals the empirical distribution of $F_n(x)$, if the axes were interchanged. We know that [34]:

$$P\{X > x\} = 1 - F(x) \tag{B3.9}$$

$$F(x^+) = F(x) \tag{B3.10}$$

$$P\{x_1 \le x_2\} = F(x_2) - F(x_1) \tag{B3.11}$$

$$P\{X = x\} = F(x) - F(x^-) \tag{B3.12}$$

At a discontinuity, both the left and right-hand limits are different, and equation (B3.12), becomes:

$$P\{X = x\} = F(x) - F(x^-) > 0 \tag{B3.13}$$

The only discontinuities of a distribution function $F_n(x)$ are jumps, which occur at points x_0 where equation (B3.13) is satisfied. Also, these points are listed as a sequence and can be counted [34]. The countable jump discontinuities [56] in Figure 3.2 were fifteen (15).

We deduce the staircase function using nonnegative real numbers corollary [34],[56]:

As $x_i \le x < x_{i+1}$,then $\{X(n) \le x\} = U_{x_k \le x}\{X(n) = x_k\} = U_{k=1}^{i}\{X(n) = x_k\}$, and therefore,

$$F(x) = P\{X(n) \le x\} \sum_{k=1}^{i} p_k \ldots . x_i \le x < x_{x+1} \tag{B3.14}$$

F(x) is a staircase function having an infinite number of steps, where i-th step size equals p_i, $p_i,\ i = 1, 2, .. \infty$.

If $F_x(x)$ is constant except for a finite number of jump discontinuities, then X is a discrete random variable. Such x_i is a discontinuity point, and from equation (B3.13), becomes [34],[57]:

$$P\{X = x_i\} = F_x(x_i) - F_x(x_i^-) = p_i \tag{B3.15}$$

At discontinuity:

$$P\{X=a\}=F_x(a)-F_x(a^-)=1-0=1 \quad \text{(B3.16)}$$

At such discontinuity:

$$P\{X=0\}=F_x(0)-F_x(0^-)=q-0=q \quad \text{(B3.17)}$$

The following Durbin-Watson statistic confirms the quality of interpretations of the study.

B.1.2. Durbin-Watson (DW) statistic

The 1.994 calculated Durbin-Watson (DW) statistic in model 4 (Table 3.3), was used for the model analyses [45]:

Decision rules for testing between the two hypotheses include: If $D > d_{U,}$ we conclude H_0. If $D > d_L$, we conclude H_a. If $d_L \leq D \leq d_U$, DW test is inconclusive: where D is the computed DW value, d_U is the upper D limit, d_L is the lower D limit, ρ is the autocorrelation parameter estimate, H_0 is the null hypothesis, and H_a is the alternative hypothesis.

The DW statistic was evaluated using each residual value, e_t and its previous value, e_{t-1} [58],[59]:

$$DW=\frac{\sum_t^T(e_t-e_{t-1})^2}{\sum_t^T e_t^2} \quad \text{(B3.18)}$$

Where T is the number of time-series observations. Also, small D values indicate that $\rho > 0$ especially because neighbouring error terms e_t and e_{t-1} have similar magnitudes, and are positively autocorrelated. If the residual differences $e_t - e_{t-1}$ are small when $\rho > 0$, we have a small D numerator and a small test statistic.

Using parameters: $k = 4$; n = df + 1(32 + 1) = 33 and $\alpha = 0.05$, where: df is the degree of freedom, n is the number of Cronbach's Reliability test predictors.

Reject H_0 if $DW < d_L$ (B3.19)

Fail to reject H_0 if $(4 - DW) > d_U$ (B3.20)

But, 4 – DW = 4 – 1.994

(= 2.006) > d_U (= 1.73).

So, we fail to reject the Null hypothesis. Thus, the goodness-of-fit closely mimics the electricity consumption and pricing model by 71.0%. The model is significant at 70.0% cut-off without autocorrelation effects or independent error assumption violations [59].

B.1.3. ANOVA

ANOVA partitions observed sample variance and the sum of squares into the minimum number of different significance tests to determine linear relationships between dependent and independent variables. Imperfect models have unexplained observed total variability [45],[54].

Basic regression line concept [55]: Data = Fit + Residual

$$\left(y_i - \bar{y}\right) = \left(\hat{y} - \bar{y}\right) + \left(y_i - \hat{y}_i\right) \tag{B3.21}$$

The first term in equation (B3.21) is total y response variation, the second term is mean response variation, and the third term is the residual value.

Simplifying equation (B3.21):

$$\sum\left(y_i - \bar{y}\right)^2 = \sum\left(\hat{y} - \bar{y}\right)^2 + \sum\left(y_i - \hat{y}_i\right)^2 \tag{B3.22}$$

Equation (B3.22) becomes: $SS_T = SS_M + SS_E$, where SS is a sum of squares, T, M, and E, are total, model, and error symbols, respectively.

The sample square correlation is the ratio between the sum of squares and the total sum of squares: $r^2 = SS_M/SS_T$. Thus, r^2 is the variability fraction in the data explained by the regression model and sample variance [54],[55]:

$$s_y^2 = \sum \frac{\left(y_i - \bar{y}\right)^2}{n-1} = \frac{SS_T}{DF_T} \tag{B3.23}$$

MS_M (model mean square) = $s_y^2 = \sum \frac{\left(\hat{y}_i - \bar{y}\right)^2}{(1)} = \frac{SS_M}{DF}$.

The linear regression model has one variable X. Mean square error:

$$(MS_E) = \frac{\sum\left(y_i - \hat{y}_i\right)^2}{n-2} = \frac{SS_E}{DF_{Estimate}} \tag{B3.24}$$

estimates variance about the population regression line σ^2

$F\left(\frac{MS_M}{MS_E}\right)$-value tests hypothesis: $\beta_1 \neq 0$ against the null hypothesis: $\beta_1 = 0$, β_i parameter estimates and F is Fisher-value). A test statistic is the ratio $\left(\frac{MS_M}{MS_E}\right)$. When MS_M is large, and the test ratio is large, there is evidence against the null hypothesis [23],[55].

Multiple linear regressions use ANOVA computations to adjust the minimum number of explanatory variables in the model [55]. The test statistic $\left(\frac{MS_M}{MS_E}\right)$ has $F_{(q,n-q-1)}$ distribution. The null hypothesis states: $(\beta_1 = \beta_2 = ... = \beta_q = 0)$, alternative hypothesis indicates at least one parameter $\beta_k \neq 0$, $SS_M/SS_T = R^2$, k = 0,1, …, q. However, F-test does not indicate which parameters $\beta_k \neq 0$ are not zero. But, one parameter linearly depends on the response variable [55].

The ratio $\frac{SS_M}{SS_T} = R^2$ is the squared multiple correlation coefficient. Its square root is the multiple correlation coefficient R, and tests the relationship between observations y_i and the fitted values $\ddot{y}_i$ [55].

APPENDIX C

I. ELECTRICITY LOAD MANAGEMENT QUESTIONNAIRE (PUBLIC)

Generally, electricity load management is the control of electricity consumption after the meter. This electricity consumption pattern involves several switching processes undertaken by the consumer. Consequently, it is to your advantage to be recognised as a resident in Namibia, which has an excellent reputation for quality housing development. Houses and building complexes are increasing in number, so also is the increasing need for satisfying electricity requirements.

In the light of the foregoing, therefore, we would like to please request you to give your candid opinion about efficient lighting and use of electricity in Buildings. We would also like you to please complete the following questionnaire with your permission, which we believe will not take more than fifteen minutes of your valuable time to answer.

Thank you for your willingness to cooperate by answering this questionnaire.

The questions follow:

1. Name:

(Optional)……

2. Respondents Gender: Male Female Age: 18-25, 26-35, 36-45, 46-55, Above 55

3. Region:……Occupation……

E-mail ……Tel:……

The key to answering the questions that follow in this questionnaire: SA-Strongly Agree A-Agree U-Not Sure DA-Disagree SD-Strongly disagree

S/N	Description	SA	A	U	DA	SD
4	Electricity is meant to be enjoyed as long as I can pay for it					
5	I should always switch off lights that I am not using					
6	Control switches should be used on geysers, air conditioners, and other high energy consuming house appliances					
7	"Energy savers" reduce the cost of electricity consumed					
8	I feel I can live comfortably anywhere in Windhoek city					
9	Energy savers are not bright enough and are very costly					
10	Reduced electricity consumption decreases money paid to Municipality or NAMPOWER					
11	The smaller amount of electricity I use helps NAMPOWER to regularly supply electricity to all					
12	I will only use efficient lighting bulbs or lamps if supplied					

	by ECB or Municipality					
13	I can only live in some areas of Windhoek city if asked to do so by law or legislation					
14	I can live in some areas of Windhoek city if asked to do so by law or legislation					
15	I do not need to reduce the electricity consumed since I can pay the amount charged by Municipality or ECB or NAMPOWER					
	If you have a washing machine with a dryer, please answer the following questions					
16	I prefer to use a dryer than the clothesline in drying my clothes					
17	Controlled electricity consumption reduces stress on NAMPOWER facilities					
18	Increased electricity consumption increases global warming					
19	I will like to buy energy-efficient equipment to reduce the amount of money spent on electricity bills					
20	Whatever affects NAMPOWER does not necessarily affect me					
21	Reducing electricity consumption reduces global warming					
22	Engineers are there to produce enough energy for me to enjoy					
23	More daylighting in buildings reduce electricity use					
24	NAMPOWER should be allowed to charge any amount for electricity supply to consumers					
25	Reducing wasted electricity is good for development					
26	Increasing electricity use does not affect the environment					
27	Energy-efficient buildings and lighting protect the globe and earth resources					
28	If electricity use is not controlled NAMPOWER will					

	continue to increase the cost of electricity					
29	Efficient use of electricity will enable delay in building new power generation stations					
30	Building new electricity generation stations reduce global warming					
31	Allowing my television to be "on" without anyone watching it, is a good energy use method					
	How much do you agree that any of the following actions can reduce your energy and electricity bills?					
32	I turn off radiators or close air ducts in rooms used for guests					
33	I lower the thermostat at night or any time the house is vacant					
34	I draw curtains over all windows in the evenings and open them during sunlight hours					
35	I lock all windows tightly during winter to cut down on heat loss					
36	I insulate my house as much as I can to save energy and money					
37	Using blinds, shutters or shades can reduce the heat coming through windows by 50% during summer and reduce heat loss by 25% in cold months. These actions can save me money and reduce energy wastage					
38	Installing underlay or carpets over windows and doors can reduce about 75% sunlight heat from getting into the house					
39	I shut off my air conditioner whenever I leave home for more than one hour or two					
40	I keep air conditioners clean and do not block them with drapes or furniture					
41	I keep windows closed and only open doors when necessary if the air conditioner is operating					

42	I keep heat-producing appliances away from the thermostat so that it can give accurate readings					
43	All rooms air conditioners and outside compressors are protected from the sun					
44	I set the temperature of my water heater at a medium					
45	I turn off the heater if I go away for more than a few days in winter					
46	I should open refrigerator and freezer doors rarely, especially in hot weather					
47	I maintain proper temperature in refrigerator and freezer compartments					
48	I cook with as little water as possible					
49	I boil liquids quickly in tightly closed pans and save about 20% of energy, if otherwise					
50	I keep the bottom of my pans and pots shining to reduce energy wastage					
51	My pots and pans should be the same sizes as the sizes of burners I put them upon					
52	I use fluorescent lamps whenever practicable					
53	I install automatic switches in closets for the lights to go off whenever the door is closed					
54	I should not switch on fluorescent lamps within 15 minutes of switching off					

N.B. Please feel free to make any comments on any of the points covered or on any other point, you feel necessary for more clarification in the space provided below or at the back of this questionnaire.

THANK YOU ONCE AGAIN FOR YOUR TIME AND COOPERATION

ACKNOWLEDGMENT

This is an extended and updated version of an unpublished paper (not published in IEEExplore), originally accepted for the IEEE International Conference on Industrial Technology (IEEE ICIT 2013) held in Cape Town, South Africa between 25 and 27 February 2013.

REFERENCES

[1] S. Bimenyimana, A. Ishimwe, G. N. O. Asemota, C. M. Kemunto, and L. Li, "Web-based design and implementation of smart home appliances control system," in ICRET, Kuala Lumpur, Malaysia. *IOP Conf. Series: Earth and Env. Sci.*, vol. 168, pp. 1-9, 2018, 10.1088/1755-1315/168/1/012017

[2] P. Warren, "Demand-side policy: Global evidence base and implementation patterns," *Energy and Env.*, pp. 1-26, 2018, 10.1177/0958305X18758486

[3] P. I. Shilamba, "Update on the current power supply and progress made on NamPower projects and initiatives to ensure security of supply in Namibia," Media Briefing, Windhoek, Namibia. 13 April, 2015.

[4] Anon., "No power cuts expected in Namibia-Energy Minister," *New Era Newspaper*, Windhoek, Namibia. 24 Mar. 2016. [Online]. Available: https://www.newera.com.na/2016/03/24/power-cuts-expected-namibia-energy-minister/, Accessed on: Mar. 29, 2017

[5] W. Isaaks. Energy situation in Namibia. Presented at AEF2013 Africa Energy Forum, Barcelona, Spain. [Online]. Available: www.energynet.co.uk/system/files/Private_23, Accessed on: Mar. 29, 2017

[6] V. Manuel, "Energy demand and forecasting in Namibia: Energy for economic development." Office of the President, National Planning Commission, Windhoek, Namibia, 2013.

[7] P. Simshauser and D. Downer, 2012. "Dynamic pricing and the peak electricity load problem," *Australian Econ. Rev.*, vol. 45, no. 3, pp. 305-324, 2012, 10.1111/j.1467-8462.2012.00687.x.

[8] E. Brandt, "Namibia's high electricity price," *New Era Newspaper*, Windhoek, Namibia. 14 Nov. 2014. [Online]. Available: http://allafrica.com/stories/201411140794.html, Accessed on: Mar. 29, 2017

[9] P. Warren, "Demand-side policy: Global evidence base and implementation patterns," *Energy and Env.*, pp. 1-26, 2018, 10.1177/0958305X18758486

[10] CIA World Factbook, "Namibia Economy 2018," [Online]. Available: https://theodora.com/wfbcurrent/namibia/namibia_economy.html Accessed on: Jul. 30, 2018

[11] G. N. O. Asemota, *Electricity Use in Namibia*. Bloomington, IN, USA: iUniverse, 2013.

[12] D. Murrant, A. Quinn, L. Chapman, and C. Heaton, "Water use of the UK thermal electricity generation fleet by 2050: Part 2 quantifying the problem," *Energy Policy,* vol. 108, pp. 859-874, 2017, 10.1016/j.enpol.2017.03.047

[13] Electricity Control Board, "2005 Electricity Control Board Annual Report." ECB, Windhoek, Namibia, Annual Report, 2006.

[14] D. von Oertzen, "Namibia's Electricity Supply." VO Consulting, Swakopmund, Namibia. 2009. [Online]. Available: https://www.voconsulting.net/pdf/Namibia's%20Electricity%20Supply%20%20VO%20CONSULTING.pdf Accessed on: Mar. 29, 2017

[15] Solatube,"Daylighting Facts & Figures," [Online]. Available: 150516 Daylighting Facts & Figures-plain.pdf, Accessed on: Feb. 24, 2020

[16] G. Ander, "Day-lighting: Whole building design guide," 2011. Accessed on: Feb. 24, 2020, http://www.wbdg.org/resources/daylighting.php

[17] N. Stauffner, "Daylight Device Lightens Electricity Cost," *MIT News*, 2007. [Online]. Available: http://newsoffice.mit.edu//2007/techtalk51-26.pdf, Cited: Feb. 24, 2020

[18] D. Kozlowski, "Using daylighting to save on energy costs," *FacilitiesNet,* 2006. Cited: Feb. 24, 2020, http://www.facilitiesnet.com/energyefficiency/article/Harnessing-Daylight-For-Energy- Savings-Facilities-Management-EnergyEfficiency-Feature-4267#

[19] T. Mocherniak, "Lighting technologies produce energy savings," *Energy and Power Mgt.,* 2006. Accessed on: Feb. 24, 2020, www.highbeam.com/doc/1G1-146346289.html

[20] R. P. Leslie, R. Raghavan, O. Howlett, and C. Eaton, "The potential of simplified concepts for daylight harvesting," *Lighting Research and Technology,* 2005. Accessed : Feb. 24, 2020, http://www.lrc.rpi.edu/programs/daylighting/pdf/simplifiedConcepts.pdf

[21] G. N. O. Asemota, "Communality performance assessment of electricity load management model for Namibia," Presented at2nd IEEE-AIMS Int. Conf., Madrid, Spain, pp. 252-257, 2014, 10.1109/AIMS.2014.20

[22] J. J. Foster, *Data analysis using SPSS for Windows: a beginner's guide*. 2nd ed., London, UK: Sage Publication, 1998.

[23] N. Brace, R. Kemp, and R. Snelgar, *SPSS for Psychologists: a guide to data analysis using SPSS for Windows*. New Jersey, NJ, USA: Lawrence Erlbaum Associates, 2000.

[24] T. Heckmann, K. Gegg, A. Gegg, and M. Becht, "Sample size matters: investigating the effect of sample size on a logistic regression susceptibility model for debris flows," *Nat. Hazards Earth Syst.Sc.*, vol.14, pp. 259-278, 2014, 10.5194/nhess-14-259-2014.

[25] J. Frost, "Standard error of the regression vs r-squared,". 2017a. [Online]. Available: Statisticsbyjim.com/regression/standard-error-regression-vs-r-squared/, Accessed on: Jan. 23, 2019

[26] G. N. O. Asemota, "Evidence-based wind-felled recovery of plantains," *Afr. J. Plant Sci. Biotech.*, vol. 4, no. 1, pp. 84-89, 2010.

[27] M. Beasley, "BST 622 regression assumptions-graphs," [Online]. Available: www.soph.uab.edu/statgenetics/People/MBeasley/Courses/BST622RegressionAssumptions-Graphs.pdf, Accessed on: Mar. 29, 2017

[28] K. Grace-Martin, "Anatomy of a normal probability plot: The analysis factor," [Online]. Available: http://www.theanalysisfactor.com/a natomy-of-a-normal-probability-plot/ Accessed on: Mar. 29, 2019

[29] SAS Institute Inc, "Construction and interpretation of P-P plots," 1999. [Online]. Available: https://v8doc.sas.com/sashtml/qc/chap8/sect8.htm, Accessed on: Mar. 29, 2017

[30] G. N. O. Asemota, "A prediction model of future electricity pricing in Namibia," *Adv. Mat. Res.*, vol. 824, pp. 93-99, 2013, 10.4028/www.scientific.net/AMR.824.93.

[31] D. George and E. A. Huerta, "Deep neural networks to enable real-time Multimessenger Astrophysics," *ArXiv:1701.00008v2 [astro-ph.IM]*, 4 Jan. 2017.

[32] G. N. O. Asemota, "On a class of computable convex functions," *Can. J. Pure and Appl. Sci.*, vol. 3, no. 3, pp. 959-965, 2009.

[33] G. N. O. Asemota, "Optimal two-way conductor design using computable convex functions approach," *Adv. Mat. Res.*, vol. 367, pp. 75-81, 2012, 10:4028/www.scientific.net/AMR.367.75

[34] A. Papoulis and S. U. Pillai, *Probability, random variables and stochastic processes*. 4th ed., New Delhi, India: Tata McGraw-Hill, 2008.

[35] G. Jahoda, "Quetelet and the emergence of the behavioral sciences," *SpringerPlus*, vol. 4, pp. 473, 2015. [Online]. Available: https://www.ncbi.nlm.nih.gov/pmc/articles/PMC4559562/, Accessed on: Jul. 30, 2018

[36] J. J. Taylor, "Confusing stats terms explained: residual," 2011. [Online]. Available: www.statsmakemecry.com/smmctheblog/confusing-stats-terms-explained-residual.html, Accessed on: Jan. 5, 2019

[37] NCSS statistical software, "Stepwise regression: Chapter 311," [Online]. Available: https://ncsswpengine.netdnassl.com/wpcontent/themes/ncss/pdf?procedures/NCSS/stepwise_Regression.pdf, Accessed on: Jan. 5, 2019

[38] R. Nau, "Stepwise regression and all-possible-regressions-Duke people," 2014. [Online]. Available: https://people.duke.edu/~rnau/regstep.htm, Accessed on: Jan. 5, 2019

[39] CIA World FactBook, "Namibia Economy 2018," [Online]. Accessed on: Jul. 30, 2018. https://theodora.com/wfbcurrent/namibia/namibia_economy.html

[40] E. Marshall, "The statistics tutor's quick guide to commonly used statistical tests," Accessed on: Jan. 9, 2019, [Online]. Available: www.statstutor.ac.uk/resources/uploaded/tutorquickguidetostatistics.pdf

[41] J. Frost, "How to interpret r-squared in regression analysis," 2018. [Online]. Available: Statisticsbyjim.com/regression/interpret-r-squared-regression/, Accessed on: Jan. 23, 2019

[42] J. Frost, "How to interpret adjusted–r-squared and predicted r-squared in regression analysis," 2017b. [Online]. Available: Statisticsbyjim.com/interpret-adjusted-r-squared-predicted-r-squared-regression/, Accessed on: Jan. 19, 2019

[43] J. T. Newsom, "Lecture 20: more on multiple regression," 2007. [Online]. Available: Web.pdx.edu/~newsomj/PR551/lecture20.htm, Accessed on: Jan. 29, 2019

[44] M. R. Braun, H. Altan, and S. B. M. Beck, "Using regression analysis to predict the future energy consumption of a supermarket in the UK," *Appl. Energy*, vol. 130, pp. 305-313, 2014, 10.1016/j.apenergy.2014.05.062

[45] G. N. O. Asemota, "Multivariate parsimony model of electricity load management," WSEAS-10th Energy and Env. Int. Conf., Budapest, Hungary, 2015, pp. 77-86.

[46] J. Frost, "Understanding interaction effects in statistics," 2017c. [Online]. Available: Statisticsbyjim.com/regression/interaction-effects/, Accessed on: Jan. 30, 2019

[47] P. Jones, *How to cut heating and cooling Costs: save money and energy in your home.*

New York, NY, USA: Butterick Publishing, 1979.

[48] Geezers.co.za, "Ideal Geyser Temperature Setting – Geezers Plumbing", 2020. [Online]. Available: https://www.geezers.co.za.ideal-ge... Accessed on: Jun. 23, 2023

[49] Gopreferred.com, "What's The Best Water Heater Temperature Setting?", 2023. [Online] Available: https://www.gopreferred.com > blog Accessed on: Jun. 23, 2023

[50] D. Mishra, "4 tips to use your hot water geyser correctly and reduce the sky high electricity bill", 2014. [Online]. Available: https://www.mrright.in > appliances, Accessed on: Jun. 23, 2023.

[51] P. Grünewald and M. Diakonova, "Societal differences, activities, and performance: Examining the role of gender in electricity demand in the United Kingdom," *Energy Res. & Soc, Sc.*, vol. 69, 2020. DOI:10.1016/j.erss.2020.101719

[52] B. Shrestha, S. R. Tiwari, S. B. Bajracharya, M. Keitsch, and H. B. Rijal, "Review on the importance of gender perspective in household energy-saving behavior and energy transition," *Energies*, vol. 14, no. 22, pp. 1-18, 2021. DOI: 10.3390/en14227571

[53] Energywatch, "Why your electricity bills increase despite low power pricing," 2019. [Online]. Available: https://energywatch-inc.com/electricity-bills-increase-despite-low-power-pricing/, Accessed on: Feb. 8, 2019

[54] Weibull.com, "Reliability hot wire: Analysis of variance," [Online]. Available: https://www.weibull.com/hotwire/issue95/relbasics95.htm, Accessed on: Feb. 11, 2019

[55] M. Lacey, "ANOVA for regression," [Online]. Available: www.stat.yale.edu/Courses/1997-98/101/anovareg.htm, Accessed on: Feb. 11, 2019

[56] F. B. Hildebrand, *Advanced calculus for application.* 2nd ed., New Delhi, India: Prentice-Hall of India Private Limited, 1977.

[57] J. Waldvogel, "Circuits in power electronics," in *Solving problems in scientific computing using Maple and MATLAB*, 4th ed., W. Gander and J. Hrebicek, Eds. Berlin, Germany: Springer, 2004, pp. 314.

[58] J. Netter, M. H. Kutner, C. J. Nachtsheim, and W. Wasserman, *Applied linear regression.* 3rd ed., USA: Irwin, 1996.

[59] A. H. Kvanli, S. C. Guynes, and R. J. Pavur, *Introduction to business statistics: A computer integrated approach*. 4th ed., St. Paul, Minneapolis, MN, USA: West Publishing Company, 2002.

CHAPTER FOUR

This section comprises the Software validation of optimal bidirectional composite conductor design and its applications. The optimal bidirectional composite conductor was designed using the unit area principle. The conductor and insulator were cut into strips or ribbons and then interwoven into a matrix with the provision that the conductor composite was to carry vertical and horizontal electrical currents at the same time up and across the unit square area.

The advantages of a bidirectional composite conductor under real loading conditions comprise an increase in current carrying capacity, ability to withstand higher temperature and higher voltage stresses, higher power carrying capacity, better insulation capacity, less sag and lower coefficient of thermal expansivities, and ability to limit aeolean vibrations to safe levels.

Other advantages include eliminating galvanic corrosion and metal solution problems, ability to withstand higher corona breakdown voltages, increase in strength/weight ratio, extended service life, lower maintenance frequency, and costs, delay in asset replacement, higher moduli of elasticity, reduced overall installation costs, and sustainable and less expensive alternative composite conductors in the longer terms, and fewer losses.

Convex functions were used to minimise the area, currents, sags, and losses. In addition, the Hessian matrix and the Jacobian determinants were used to maximise the temperature, power, and voltage profiles.

The Python open-source software was used to validate the analytical correctness and robustness of the describing partial differential equations of the optimal bidirectional composite conductor design using Green's identity, Laplace's equation boundary conditions, and minimum area principle. Also, the conductor component of the conductor composite was proven to occupy about two-thirds of the unit square area in this research. This part of the thesis is presented in the subsequent sub-sections.

4.1. Software validation of optimal bidirectional composite conductor design with applications

. This is the title of this part of the thesis.

4.2. Abstract

The ever-increasing electricity consumption patterns worldwide and the very many drivers of load growth have placed heavy burdens on new and existing power supply infrastructures, globally. The measurement of standards of living based on the quantity and quality of electricity consumed has further exacerbated power systems transmission network problems. Software validation of optimal bidirectional composite conductor designs, which carry very high currents at high temperatures, vertically and horizontally in tandem, attempt to provide solutions to the above problems. Composites comprising a conductor and insulating material strips in which the density approaches the minimum conducting area and satisfies Laplace's equation was considered. The variational problem was homogenised and polyconvexified using Lagrange multipliers and Green's identity, while the Hessian was used to relax the minimised characteristic function for convexification. The results indicate materials and costs optimisation. Both the horizontal and vertical currents were equal, without hotspots or irregular power transfer problems in the composite conductor matrix. The vertical and horizontal gradients along the composite were equal and optimal, and their respective directions of highest change were uniform along their lines of equal energy. The conductor materials occupied about two-thirds area of the composite. The high-temperature low-sag cable is light in weight, strong, and bendable. Its larger diameter reduces corona effects, which makes it useful for voltages beyond 300 kV and can minimise the incidence of power blackouts, globally.

4.3. Index Terms

Balanced loading, cables, composites, Green's identity, Hessian, Lagrangian.

4.4. INTRODUCTION

The optimal bidirectional composite conductor used the series-parallel combination that is subject to competition for the design. The problem was made continuous to measure the currents across a unit square of conducting area A, in which the area of insulating material without current flowing through it, is 1-A. A unit voltage difference between the left- and right-hand sides of the square or from the top to bottom; enables measurement of the currents [1].

The problem was to design a single conductor that carries currents flowing in both directions up and across the unit square surface, which are measured, separately. A voltage difference between the x-axis produces a horizontal current, while the voltage between the y-axis of the conductor produces a vertical current.

The present bidirectional composite conductor design problem was to software validate the constrained solutions to the already developed computable convex functions [2] algorithm, applied to the minimum conductor area A [1], having the desired conductor characteristics [3].

The continuous problem was relaxed to a variational problem having reasonable solutions and the same minimum. The bidirectional current-carrying composites were obtained from the original materials by homogenisation, which changes the original nonconvex problem into a new and more readily solved problem.

Further, the one-current conductor case is naturally convex, because there is no competition and it is the smallest current that can flow in one direction only. Similarly, the two-current case is polyconvex and can be solved [1].

Adopting extremely thin strips for the design, and in the limit; the density and direction of the strips determine the conducting area A. The foregoing harmonises with the macroscopic properties of the composites themselves. The Physics of relaxation of variational problems leads to homogenisation and convexification, which yield optimal solutions with simple reasoning [1],[2],[3],[4]. The addition of a constant or linear function to a convex function does not affect convexity, and a convex function is below its interpolation [2],[3],[4],[5]. Further, convex functions are nonsmooth [6] optimisation algorithms for obtaining high-quality results in applications like the optimal bidirectional composite conductor design using the minimum area criterion.

A completely mixed composite of conductor and insulator strips is obtained using conductances of the minimum area in the limit [1],[7]. Reference [8] used isotropic composites to deduce optimal design employing conducting rings around smaller insulated disks. In contrast, ellipses were used to obtain the optimal design for anisotropic composites. References [8] and [9] have also proved that no other design could be better.

Our contributions to the optimal bidirectional composite conductor design problem include materials and costs optimisation, eigenvalues solution of inequality of the describing differential equations, proof of convergence of the expected numerical values of the vertical

and horizontal currents, and computer software validation of the design. Also, deducing and confirming the actual conductor materials requirements per unit area of the design and production of composites that simultaneously carry horizontal and vertical currents along their respective paths and vice versa.

This part of the thesis is organised into an Introduction, Materials and methods, Simulation and validation, Results and Discussion, Applications of conductor composites, and Conclusion.

4.5. Materials and Methods

The materials required for this study are thorough mixtures of conductor and insulating material strips interwoven to obtain a mat pattern. The optimal cross-sectional area minimisation of the composite was used to enable the conductor designed to carry maximum vertical and horizontal currents, simultaneously and along their respective paths. The 0-1, nonlinear variational problem was convexified using the Lagrange multipliers and Green's function identity.

Lagrange multipliers provide optimal solutions to constrained nonlinear problems, subject to specialised boundary conditions. The variational problems were convexified and homogenised using multilinearisations because convex functions provide one minimum point for convexity. The sum of convex functions is convex. Adding a constant or linear function to a convex function does not affect convexity, and a convex function is below its interpolation [2],[3],[4],[5].

Further, convex functions are nonsmooth optimisation algorithms [6] that provide simple and elegant results in applications like the optimal bidirectional composite conductor software validation design problem, under investigation in this thesis.

Python algorithm design and simulation were used to maximise and minimise the constrained composite conductor parameters to obtain an optimal bidirectional composite conductor, which carries maximum vertical and horizontal currents, at the same time. Also, the smallest cross-sectional area possible was used in the analyses. The sub-sections that follow have been organised into Problem formulation, Mat design, Variational problem, Bidirectional optimal conductor problem, and Convergence tests for vertical and horizontal currents. The Python open-source computer codes used for the study are in Appendix A.

4.5.1. Problem Formulation

How do we obtain a software validation of a bidirectional horizontal current $C < 1$ and a vertical current $D < 1$, using the least conducting area A of the composite conductor, in which the vertical currents can follow the horizontal paths and vice versa?

The solution to the minimum area (A) problem is obtained in the limit, from a composite material containing suitable conductors and insulators as their microstructure, when they are thoroughly mixed. Also, the constrained composite conductor conductances are, C and D, respectively [1],[7]. Consequently, the design problem was to obtain the least composite area, that can carry the highest horizontal and vertical currents simultaneously (Fig. 1), and have the required conductor attributes [3],[5].

In isotropic composites $(C = D)$, [1] indicates [8] obtained the optimal design using conducting rings around smaller insulated disks. For anisotropic composites $(C \neq D)$, ellipses were used to obtain the optimal design. Since [8] and [9] have proved that no other design could be better; we shall then use this result without proof in this part of the thesis.

4.5.2. Mat Design

Adopting the Mat pattern makes it easy and possible for the vertical currents to flow through the horizontal strips as their conducting paths and vice versa [1]. When the density of the vertical strip is G and the height of those strips is $1 - C$, the vertical resistance of the composite becomes $(1 - C)/G$ [3],[5].

Since the composite is in series with a conducting resistance strip C (to the vertical flow), the effective conductor properties become [1]:

Vertical resistance $= C + (1 - C)/G$

Horizontal resistance $= 1/C$

Conducting area $A = C + G\,(1 - C)$

The desired vertical resistance value $1/D$, produces a current D with unit voltage drop [5]. Hence [1],

$$C + \frac{(1-C)}{G} = \frac{1}{D} \text{ or } G = \frac{D-CD}{1-CD} \tag{4.1a}$$

Consequently, the total conducting area becomes

$$A = C + \left[\frac{D-CD}{1-CD}\right][1 - C] = \frac{C+D-2CD}{1-CD} \tag{4.1b}$$

Equation (4.1b) above is the optimal area of the composite conductor. Coincidentally, and for small currents, the optimal area is near $C + D$. Furthermore, the economics of the interleaving composite matrix ensures that both the horizontal and vertical current modes can use each other's conducting paths because these conducting paths are fine, compact together, and rather indistinguishable [10].

4.5.3. Variational Problem

Suppose Q is the open unit square of the composite, having a unit voltage between $x = 0$ and $x = 1$, and a current flows. The vector has zero divergences because there are no sources or sinks inside the square. The vector describes a current function: $u(x, y)$ by $(\partial u/\partial y, -\partial u/\partial x)$.

For any u, this vector has divergence [11]:

$$\left(\frac{\partial^2 u}{\partial x \partial y} - \frac{\partial^2 u}{\partial y \partial x}\right) = 0 \tag{4.2}$$

The above divergence equation (4.2) gives both the magnitude $|\nabla u|$ and direction of the current at each point. For the insulated region, the magnitude $|\nabla u| = 0$ and the current function are constant. Hence, $\partial u/\partial n = 0$ is the normal derivative from both sides of the boundary. At the lower boundary of the square, $u = 0$ and the upper boundary of the square $u = C$, so that current C can flow from left to right [1],[5].

The increase in $u(O) - u(P)$ is the current function that flows from O to P [12],[13]. Since the conducting material has a unit-specific resistance, the heat loss, I^2R in a single resistor, is [1],[11]:

$$\iint |\nabla u|^2 dxdy = C \times 1 \text{ (current} \times \text{voltage)} \tag{4.3}$$

The current is obtained in the smallest possible conducting area A when it is flowing, because $\nabla u \neq 0$.

Then, the optimal bidirectional composite conductor problem becomes:

Minimise the area in which $\nabla u \neq 0$, subject to:

$$\iint |\nabla u|^2 dxdy = C, u(x, 0) = 0;\ u(x, 1) = C. \tag{4.4}$$

The above one-dimensional problem in equation (4.4) is solved using a horizontal conducting strip of height C [1]. The current function is $u = y$ for $y \leq C$; and $u = C$ for $y \geq C$ [12],[13]. Therefore, $|\nabla u| = 1$ inside the strip and $|\nabla u| = 0$, elsewhere. Thus, meeting the above constraints ensures that the conductor strip area C has the least value.

The constraint $\iint |\nabla u|^2 dxdy = C$ indicates that the actual current minimises the above integral and satisfies Laplace's equation in the conducting area [12],[13].

Physically, the heat loss relationship is replaced by Green's identity to ease transformation, simplicity in representation, and solution to the problem [1],[7].

$$\iint |\nabla u|^2 dxdy = \iint u\left(-u_{xx} - u_{yy}\right) + \int u \frac{\partial u}{\partial n} ds \tag{4.5}$$

On the right side of equation (4.5) above, the only nonzero integral term is $u(\partial u/\partial n)$ along the top of the square, where $u = C$ and $\int u(\partial u/\partial n)\, ds =$ voltage drop $\equiv 1$. Therefore:

$$\iint |\nabla u|^2 dxdy = C \tag{4.6}$$

The above unidirectional conductor problem is simple to solve and realise, and it is not convex. Consequently, the minimisation of the area is the minimisation of $\iint 1_{\{\nabla u \neq 0\}} dxdy = C$, where 1_k is a characteristic function (Fig. 1) [1],[11],[12],[13]. The step function equals unity in the set K, wherever $\nabla u \neq 0$, and zero outside the set K, wherever $\nabla u = 0$.

Naturally, the Lagrange multiplier (λ) constraints minimise the $0-1$ nonconvex integral problem whenever we can make $\nabla u = 0$, as often as, practicable.

Therefore, the Lagrange multiplier functional is [1],[13]:

$$L(u, \lambda) = \iint \left[1_{\{\nabla u \neq 0\}} + \lambda |\nabla u|^2\right] dxdy - \lambda C \tag{4.7}$$

Fortunately, the integrand in equation (4.7) above has the Hessian functionals: $H = 1 + \lambda |\nabla u|^2$ or $H = 0$, that is relaxed, to realise acceptable solutions.

Moreover, for an unknown scalar, the relaxation is the same as its convexification [1],[2],[3],[4].

We use convex functions because there is one minimum point in the convex interval [14],[15]. Convexity unifies a wide range of phenomena [2],[3],[16], like the optimal bidirectional composite conductor software design validation problem under investigation in this thesis.

Furthermore, every convex combination of points is in its epigraph. Therefore, a function is convex iff its epigraph is a convex set [2],[17],[18]. Hence, a convex function on a convex set A is converted to a convex function on R^n [17]. Similarly, a differentiable function f on a convex domain is convex, and the divergence of a convex function f, $\nabla f(x) = 0$, indicates that the x is a global minimum. Also, if f is differentiable twice on a convex domain A, it is convex iff the Hessian matrix $H(x)$ is positive semi-definite for all $x \in A$ [2].

We replace H by the greatest convex function satisfying $H_c \leq H$ without changing the minimum integral value (Fig. 4.2). Thus, the minimising function u^* is significantly changed, but the original L may not exist. In the one-conductor problem, H_c grows linearly from its virtual bifurcation point having $|\nabla u|$ up to where $\lambda|\nabla u|^2 = 1$ and H_c is tangent to H. But, before that point, the convexified functional is [1],[2],[3],[4]:

$$L_c(u,\lambda) = \iint H_c dxdy - \lambda C = \iint 2\lambda^{1/2}|\nabla u| dxdy - \lambda C \quad (4.8)$$

Minimising u^*, grows from zero at $y = 0$ to C at $y = 1$, and it is linear because $u^* = yC$. Hence, $|\nabla u^* = C|$ and the Lagrange functional is [1],[2],[3],[4]:

$$L_c(u^*,\lambda) = 2\lambda^{1/2}C - \lambda C \quad (4.9)$$

The maximum over λ occurs wherever $\lambda^* = 1$, and gives the least area subject to the constraint: Optimal area $= C$.

But, $\lambda^*|\nabla u^*|^2 = C^2 < 1$. Consequently, the least conductor area appears where H_c, is lower than H. This homogenisation condition ensures that the composite conductor mat structure swings between $H = 0$, and $H = 1 + \lambda|\nabla u|^2$. This is so because the average of H is H_c [1]. Although the unidirectional conductor problem uses relaxation, the least area C is obtained without relaxation. However, the proof indicates that the least area used convexification, where $\lambda = 1$ and for any u:

$$\text{Area} = \iint \left[1_{\{\nabla u \neq 0\}} + |\nabla u|^2\right] dxdy - C \geq \iint 2|\nabla u| dxdy - C \geq C \quad (4.10)$$

4.5.4. Bidirectional Optimal Conductor Problem

The bidirectional variational conductor problem requires two current functions $u(x,y)$ and $w(x,y)$. The simple convexification procedure is not applicable, because the unknown vector quantity has magnitude and direction [13]. The mat design is divided into two regions R_1 and R_2 (Fig. 4.3). Using Green's identity, which is horizontally and vertically, simple, we divided the boundaries C and D of R into $C_1 \cup D_1$ for boundary R_1 and $C_2 \cup D_2$ boundary R_2 [7]. The increase $u(O) - u(P)$ is the current function [7],[8], that provides the flow from O to P (Fig. 4.3).

Additionally, the first part is constrained by $u(x,0) = 0$ and $u(x,1) = C$, while $\iint |\nabla u|^2 dxdy = C$, as in the unidirectional conductor case [1]. Similarly, the second part w

shows that a vertical current D flows through the mat composite when a unit voltage is applied between the highest and lowest portions of the unit square [1],[3].

Also, wherever the horizontal and vertical currents are respectively zero, $\nabla u = 0$ and, $\nabla w = 0$, there is no need for conducting materials at such locations. Therefore, the bidirectional composite conductor problem occupies the set K values in the minimised area [1],[4],[7]:

$$K = \{\nabla u \neq 0\} \cup \{\nabla w \neq 0\} \tag{4.11}$$

Minimise area $(K) = \iint 1_k dxdy$

Subject to: $\iint |\nabla u|^2 dxdy \leq C$, $\iint |\nabla w|^2 dxdy \leq D$,

$u(x,0) = 0, u(x,1) = C, w(0,y) = 0, w(1,y) = D.$

It was shown that the strips/mat design had minimal area: $A = \frac{C+D-2CD}{1-CD}$.

But, the $0-1$ bidirectional composite conductor problem is not convex and is converted by the Lagrange multipliers λ and μ, into the unrelaxed functional: $L(u, w, \lambda, \mu) =$

$$\iint [1_K + \lambda |\nabla u|^2 + \mu |\nabla w|^2] dxdy - \lambda C - \mu D \tag{4.12}$$

Equation (4.12) is convexified because the least value, L_c is small, since it is below L. The pseudoconvexification L_r is the greatest functional below L, which shows the relaxation is small and partly continuous. Therefore, the minimising functions u^*, w^* are feeble oscillation boundaries for L [1],[3],[4],[7].

Pseudoconvexity is laborious to test, but polyconvexity exists and can be tested. The relaxation [1],[3],[4],[7], $L_r = \iint H_r(\nabla u, \nabla w) dxdy$, is polyconvex because H_r is a convex function of $|\nabla u|$ and $|\nabla w|$, while the Jacobian determinant is

$$J = |\nabla u \nabla w| \tag{4.13}$$

The Jacobian is not a convex $0-1$ characteristic function of 1_K. It is made polyconvex by relaxation, homogenisation, and multilinearisations to form a family of upper envelopes of linear functions in $J, |\nabla u|$, and $|\nabla w|$. Convex functions are envelopes of linear functions of $|\nabla u|$ and $|\nabla w|$, but, a polyconvex function may not be convex. The unrelaxed integrand [1],[2],[3],[4],[7]:

$$H = \begin{cases} 0 \\ 1 + |\nabla \bar{u}|^2 + |\nabla \bar{w}|^2 \end{cases} \begin{cases} If\ \nabla \bar{u} = \nabla \bar{w} \\ Otherwise \end{cases} \tag{4.14}$$

Equations (4.14) above are vector transformations included in the Lagrange multipliers λ and μ into $\bar{u} = \lambda^{1/2} u$ and $\bar{w} = \mu^{1/2} w$. The Lagrange multipliers are positive parameters and

the inequality constraints satisfy the design objectives. This is so because the bidirectional composite conductor design presents a lower resistance to either of the currents.

Also, the bidirectional composite conductor design obeys $\iint|\nabla u|^2 = C$, and $\iint|\nabla w|^2 = D$. The relaxation of H is [1],[3]:

$$H_r = \begin{cases} 2\sigma - 2|\bar{J}| & If\ \sigma \leq 1 \\ 1 + |\nabla\bar{u}|^2 + |\nabla\bar{w}|^2 & If\ \sigma \geq 1 \end{cases} \tag{4.15}$$

where $\sigma = (|\nabla\bar{u}|^2 + |\nabla\bar{w}|^2 + 2|\bar{J}|^2)^{1/2}$ and $\bar{J} = |\nabla\bar{u}\nabla\bar{w}|$. We shall show that H_r is polyconvex and $H_r \leq H$. We know that no pseudoconvex functions are between H and H_r, provided that, the constraints are satisfied in the conducting area $A' = \frac{C+D-2CD}{1-CD}$. And, the area is not greater than A [1].

Interestingly, the variational bidirectional composite conductor design problem is solved because H_r is polyconvex. Hence, [1],[2],[3]:

Minimise $\iint H_r dxdy$ subject to:

$$\begin{cases} \bar{u}(x,0) = 0;\ \bar{u}(x,1) = \lambda^{\frac{1}{2}}C \\ \bar{w}(0,y) = 0;\ \bar{w}(1,y) = \mu^{\frac{1}{2}}D \end{cases} \tag{4.16}$$

The above constraints satisfy linear functions:

$\bar{u} = \lambda^{\frac{1}{2}}Cy$ and $\bar{w} = \mu^{\frac{1}{2}}Dx$

The Jacobian functions are constant, which is the necessary and sufficient condition for pseudoconvexity. This is so because they satisfy the boundary conditions by producing the lowest possible solutions [1],[2],[3].

Additionally, the lowest value of $\iint H_r dxdy$, after integration of a constant over the unit square, is [1],[2],[3]:

$$2\sigma - 2|\bar{J}| = 2\left(\lambda C^2 + \mu D^2 + 2\lambda^{\frac{1}{2}}\mu^{\frac{1}{2}}CD\right)^{\frac{1}{2}} - 2\lambda^{\frac{1}{2}}\mu^{\frac{1}{2}}CD = 2\left(\lambda^{\frac{1}{2}}C + \mu^{\frac{1}{2}}D - \lambda^{\frac{1}{2}}\mu^{\frac{1}{2}}CD\right) \tag{4.17}$$

We realise that the final terms $-\lambda C - \mu D$ in equation (4.18) below are as in the Lagrangian of equation (4.12), and we are left with a maximisation over λ and μ. Therefore,

$$A' = \max_{\lambda,\mu}\min_{u,w} L_r = \max_{\lambda,\mu} 2\left(\lambda^{\frac{1}{2}}C + \mu^{\frac{1}{2}}D - \lambda^{\frac{1}{2}}\mu^{\frac{1}{2}}CD\right) - \lambda C - \mu D \tag{4.18}$$

Differentiating equation (4.18) above with respect to λ and μ, and rearranging, the Lagrange multipliers become:

$\lambda^{\frac{1}{2}} = \frac{1-D}{1-CD}$ and $\mu^{\frac{1}{2}} = \frac{1-C}{1-CD}$

Substituting the above functionals into equation (4.18), we have

$$A' = \frac{C+D-2CD}{1-CD} \tag{4.19}$$

which is equal to area A, and this minimum occurs at $\sigma \leq 1$.

However, σ is equal to the density of the conducting material, and it is equal to A ($\sigma = A$). This is so because the density is a constant value over the unit square [1],[3].

Consequently, the area of the bidirectional composite conductor design is not less than A', because:

(a) $H_r \leq H$ since, $L_r \leq L$ for each positive λ and μ, and (b) H_r is polyconvex, because its associated functional is least.

The constrained minimum area A' is equal to area A, as the mat design is approached.

Hence, the proof of polyconvexity using the computable convex functions technique will show that multilinear functions, having H_r envelopes are below H. And, they produce the lowest possible solutions. Thus, the results come very simply and elegantly, as:

$$c(\tau) = \begin{cases} 2\tau, & 0 \leq \tau \leq 1 \\ 1 + \tau^2, & \tau \geq 1 \end{cases} \tag{4.20}$$

We then consider the two functions as:

$$H_{\pm}(\nabla u, \nabla w, J) = c\left(\left[|\nabla u|^2 + |\nabla w|^2 \pm 2det[\nabla u \nabla w]\right]^{1/2}\right) \mp \mu 2J \tag{4.21}$$

For either sign, the parameters in brackets are positive quadratic forms in $\nabla u, \nabla w$, and a sum of squares. The square root τ, $c(\tau)$, and constituents of $c\big(\tau(\nabla u, \nabla w)\big)$ are convex [2]. The linear Jacobian terms $\mp\mu 2J$, make $H_{\pm}$ convex functions have supplementary parameters. Since H_r is the larger of the two functions ($H_{\mp}$), when J is equal to $det[\nabla u \nabla w]$, then H_r is polyconvex [1],[2],[3].

We see that for $c(\tau) = 1 + \tau^2$ and large τ, the $H_{\pm}$ functions are: $1 + |\nabla u|^2 + |\nabla w|^2$. Besides, for small τ, the difference between H_+ and H_- depends on:

$$2(m+n)^{1/2} - n \geq 2(m-n)^{1/2} + n \tag{4.22}$$

Equation (4.22) exists when $m \geq n \geq 0$, and $m + n \leq 1$.

Our interest in this part of the thesis is to provide optimal solutions to the bidirectional composite conductor design problem; conduct a software validation study and discuss some composite conductor applications.

Hence, $m = |\nabla u|^2 + |\nabla w|^2$ and $n = 2|J|$ (4.23)

Therefore, the best solution occurs when $\pm det[\nabla u \nabla w]$ is equal to the absolute value $|J|$. Consequently, the parameter τ is equal to ƀ in defining H_r, where max $H_{\mp}$ is equal to H_r.

Solving equations (4.22) and (4.23) by applying the constraints, shows that: $m = n$, and $m + n = 1$, and the optimisation conditions become:

$$m = n = ½$$

Therefore,

$½ = |\nabla u|^2 + |\nabla w|^2$ (4.24a)

$½ = 2|J| = 2|\nabla u \nabla w| \Rightarrow ¼ = |\nabla u \nabla w|$ (4.24b)

Hence,

$\nabla u \equiv \nabla w$ (4.25a)

$\nabla \bar{u} = \nabla \bar{w}$ (4.25b)

$\nabla u = C = ½$ (4.25c)

$\nabla w = D = ½$ (4.25d)

$C = D = ½$ (4.25e)

$m - n = 0$ and $m + n = 1$ (4.25f)

$A = A' = \frac{C+D-2CD}{1-CD} = \frac{½}{¾} = ⅔$ (4.25g)

This $(0,1)$ convex set is an optimal solution to the computable convex functions design of a bidirectional composite conductor software validation problem.

Also, the half $(½)$ is a local maximum for grad (∇u), and the other half $(½)$ is also a local maximum for grad w (∇w). Furthermore, any local optimum is also a global optimum, provided the constraints define a convex region. This optimisation is so because it describes linear functional [18].

Moreover, the gradient shows the direction of the greatest change along the line of equipotential or equal energy or of the value of $F(x, y)$ [19]. Also, the Jacobian (J) tracks the distortion, whenever there is a change of coordinate system. It also mirrors the symmetry of the changes made in the coordinate system by substitution. It further measures the stretching, shrinking, or twisting of the substitution, which may result in a larger determinant of the representative matrix [20].

Although the gradient and Hessian analytically compare a derived gradient for correctness, the Hessian matrix computes the confidence interval values of parameters in maximum likelihood estimation. While the Hessian matrix as a minimiser should be positive definite, one of the eigenvalues of a semi-definite Hessian matrix will necessarily, be zero [21].

However, H_r is below H simply because 2τ is smaller than $1+\tau^2$. The difference between the unit square and the area occupied by insulator strips is the savings in the conductor area that was achieved by homogenisation [1],[3],[22],[23].

4.5.5. Convergence Tests for Vertical and Horizontal Currents

Suppose each wire composite conductor matrix can accommodate two kinds of currents C and D, where the total number of currents in each wire adds up to N. If the wire is in state e_k, $k = 0,1,2,\dots,N$ and consists absolutely k currents of type C and $N-k$ currents of type D [24]. The probability that a new wire is in the state e_l is given by the hypergeometric distribution

$$p_{kl} = \frac{\binom{2k}{l}\binom{2N-2k}{N-l}}{\binom{2N}{N}},\ k,l = 0,1,\dots,max(0,2k-N) \le l \le min(2k,N) \tag{4.26}$$

Let e_k be the present state and probability of choosing the current type C in the next stage be $p = k/N$. If the N currents in the next stage are randomly chosen from N Bernoulli measurements, the C-current probability is equal to p. The transition probability that the next stage current has moved to state e_l (l currents of type C and $N-l$ currents of type D) from the state e_k is the binomial distribution

$$p_{kl} = \binom{N}{l}\left(\frac{k}{N}\right)^l\left(1-\frac{k}{N}\right)^{N-l} \quad k,l = 0,1,\dots,N \tag{4.27}$$

The limiting behaviour of total current based on these models after many stages can be determined because models e_0 and e_N contain currents of the same type and no exit from these states is possible [11],[13],[24]. Absorption probability transition matrices can be used to represent finite-chain Martingales. A martingale is a Markov chain when the expectation of probability distribution $\{p_{kl}\}$ equals k:

$$\sum_k l p_{kl} = k \tag{4.28}$$

Let $e_0, e_1, \dots, e_N$ be the states in a martingale and the system is absorbed either into e_0 or e_N. If $k = 0$ and $k = N$ in equation (4.28), we have $p_{00} = p_{NN} = 1$, because e_0 and e_N are absorbing states [24]. Assuming these two are all the persistent states in the sequence, then $e_1, e_2, \dots, e_{N-1}$ are transient states, and the arrangement is absorbed into either e_0 or e_N. From equation (4.28), and by induction we have,

$$\sum_{k=0}^{N} l p_{kl}^{(n)} = k \tag{4.29}$$

for all n. Actually, $p_{kl}^{(n)} \to 0$ for every transient state e_l, $l = 1,2,\dots,N-1$ and for $k > 0$, equation (4.29) provides the only solution

$$p_{kN}^{(n)} \to \frac{k}{N} \tag{4.30}$$

Because there are only two absorbing states, give

$$p_{k,0}^{n} \to 1 - \frac{k}{N} \tag{4.31}$$

If the current starts from e_k, the probability of the final absorption into e_0 and e_N are $1 - \frac{k}{N}$ and $\frac{l}{N}$. If all current states are equally likely to start with and then, finally be absorbed into e_N, then:

$$\lim_{n\to\infty} \sum_{k=0}^{N} p_k^{(0)} p_{k,N}^{(n)} = \sum_{k=1}^{N} \frac{1}{N+1} \frac{k}{N} = \frac{1}{2} \tag{4.32}$$

Therefore, for a randomly selected initial distribution, final absorption into either e_0 or e_N are both equally likely events for limited state martingale [24]. It follows that regardless of the actual process of the model, beginning from an initial state e_k the final absorption probabilities into e_0 (all C currents) and e_N (all D currents) are $1 - k/N$ and k/N, respectively. Consequently, currents $C = D = \frac{1}{2}$, which corroborate equation (4.25e). It follows that and by similar reasoning (substituting values into equation (4.19)) the optimal area A' tends to be two-thirds the unit area of the composite conductor design $\left(A = A' \to \frac{2}{3}\right)$, which is in perfect agreement with equation (4.25g).

4.6. Simulation and Validation

Simulation is the mimicking of one system by another. It is used in two ways: (a) when uncertainty is high because of sparse or limited data, (b) for experimentation in a low-cost, low-risk environment. Furthermore, simulation is conducted by researchers before the validation of their forecasts in the expensive real world. Although simulation applications are useful, they have advantages and disadvantages.

The advantages of simulation include: (a) Studying the behaviour of a system without building it, (b) Results are accurate in general compared to analytical models, (c) Helping to find unexpected phenomena and behaviour of the system, (d) Easy to perform, using "what-if" analyses, (e) Forecasting under uncertainty, (f) Able to answer several questions, (g) Use low data requirements to model, (h) Low cost and (i) Innovative approaches can be applied [25],[26],[27].

The disadvantages of simulation include (a) Expensive to build a simulation model, (b) Expensive to conduct a simulation, (c) Sometimes, it is difficult to interpret the simulation results, (d) Good theories are needed, (e) No standardised approach, (f) Challenging to validate, (g) Potential scope encroaches into projects, and (h) Political entanglements [25],[26],[27].

Also, simulation is an elegant approach to analysing problems with limited data. It is so because we do not need data to design or construct a simulation. However, validating a simulation demands several data sources for a reliable representation of the real world. Thus, the process of validation is a disadvantage to simulation because validating simulations is usually more laborious to design [25],[26],[27].

4.6.1. Why Carry Out Bidirectional Composite Conductor Optimisation Study?

We embarked on Python software validation of the earlier work [3] in this study because [3],[28]:

(a) Conductor optimisation is necessary for electricity network expansion planning

(b) To secure transmission lines infrastructure able to evacuate rising electricity generation and consumption capacities worldwide

(c) To support, enhance, and strengthen optimal power systems operators' response in emergencies

(d) To increase and maximise benefit-cost ratios, which enhance reliability improvements, reduce operational costs against initially high optimal bidirectional composite conductor investments

(e) To adaptively strengthen the interdependence between electricity conductor infrastructures and renewable energy uncertainties

(f) To minimise total investment costs, transmission lines losses, and optimally and efficiently engage, electricity production units

(g) To satisfy future load growth having additional security and operational constraints

(h) To minimise transmission lines rights-of-way difficulties

4.6.2. Policy Problem Formulation

The policy is to address some recurrent questions and challenges of the electricity industry [29]:

(a) To determine which and where optimal electricity lines are built for minimum investment costs that satisfy future energy requirements

(b) Transmission infrastructure directly and considerably impact optimal operations of electricity networks by the ability to efficiently convey large quantities of power at high voltages over long distances from various generation plants to distribution centres to satisfy consumers demand. Transmission performance is measured by the efficiency of the network where nonlinearity-equality constraints exist because electricity flows along the lines and voltage drops in the transmission systems. Also, the available feasible limits to carry extra power beyond the present demand are nonconvex and nonlinear constraints to be considered for future transmission network expansion planning

(c) To minimise electricity production costs of power generation, which depend on fuel sources, technology, and transmission infrastructure for the supply

(d) Increasing future demand requires significant investments in electricity generators and transmission systems, which need additional capacities

(e) To develop and deploy more efficient and sustainable electricity transmission systems

(f) To educate and encourage energy suppliers to embrace new, efficient, and more sustainable transmissions systems infrastructure

4.7. Results and Discussion

4.7.1. Results and Discussion of Mathematical Model Analysis

Table 4.1 in Appendix A indicates the results of the convexified variational bidirectional composite conductor software validation study. The study, software validated the composite conductor designs that carry high currents both horizontally and vertically. It used the minimum area without hotspots because of balanced loading. The density of conductor strips determines the vertical and horizontal resistances of the unit square. The divergence of the current functions of the variational problem evaluates the heat loss in the resistor. The minimised constrained currents satisfy Laplace’s equation and Green’s function identity.

Both the Lagrangian multipliers and the Hessian matrix convexified the scalar characteristic function. The convexified Hessian of the relaxed problem served as inputs to the software validation study. The Python open-source computer codes of the results in Table 4.1 are shown in Appendix A.

The results in Table 1 show that a half (½) each was a local maximum for grad (∇u), and grad w (∇w). Further, any local optimum is also a global optimum, provided the constraints define a convex region. Also, these optimisation results describe linear functional [18]. In addition, the gradient indicates the direction of the greatest change along the lines of equipotential, or equal energy, or the value $F(x, y)$ [19]. The Jacobian (J), which is a quarter (¼) tracks the distortion, whenever there is a change in the coordinate system. It mirrors the symmetry of the changes made in the coordinate system by substitution. It also measures the stretching, kinking, shrinking, or twisting of the new coordinate system leading to an alteration of the determinant of the representative matrix [20].

Additionally, the gradient (½) and Hessian $[H^{+} = 1½;\ H^{-} = ½]$ analytically compare the derived gradients for correctness. The Hessian matrix determines the confidence interval values on parameters in maximum likelihood estimation. Although the Hessian matrix as the minimiser should be positive definite, one of the eigenvalues of a semi-definite Hessian matrix will necessarily be zero [21].

The above semi-definite Hessian matrix condition was satisfied in this study because the eigenvalues were 0 and 1 (Convex functions). Additionally, the conductor materials occupied about two-thirds (⅔) of the unit square area A of the designed optimal bidirectional composite conductor proposed in the study.

However, both the vertical and horizontal currents flowing in the designed bidirectional composite conductor were half (½) each. The equality of currents between the horizontal and vertical components of the composite conductor matrix resulted in balanced current loading that does not create hotspots nor localised heating.

Moreover, Fig. 4.1 shows the characteristic function of the unit square. It used the Lagrangian multipliers, Green's function, homogenisation, multilinearisations, polyconvexity, and Hessian matrices to achieve the minimisation of conductor strips. Fig. 4.2 shows the representations of the convex function of the gradients and the convexified Hessian functionals used to achieve one minimum point in the interval of convexity, which was also a global optimum. It also supports the claim and objective of using the minimum conductor area

to show that, the bidirectional composite conductor design was optimal. Fig. 4.3 shows the mat structure of the proposed optimal bidirectional composite conductor that was homogenous in the interleaving of insulator and conductor strips able to conduct high currents vertically and horizontally, in which the vertical currents can follow the horizontal paths and vice versa. Fig. 4.4 shows the methodology flowchart for the study. It also represents the step-by-step operations used to realise the body of work in this thesis.

Furthermore, Table 4.2 shown in the Appendix indicates the contribution of the bidirectional composite conductor software validation design in this study. The next subsection 4.7.2 discusses software validation.

4.7.2. Software Validation

Although the bidirectional optimal composite conductor design has been built around the minimisation criteria for the conductor area, the ability to carry maximum currents both vertically and horizontally, at the same time, remains the major contributions and benefits of the study. While simulation is used to mimic a system by another because of the paucity of data, validation of design requires ample data for a reliable representation of the real world. Therefore, verification and validation of the results of differential equations become vital for simulation processes. Thus, verification determines if the result of the simulation approximates the precise solutions to the differential equations of the original model. In contrast, validation determines if the chosen model is an adequate representation of the real-world system for the simulation [25],[26],[27].

Verification is divided into (a) solution verification, and (b) code verification. Hence, solution verification confirms that the output of the intended algorithm approximates the precise solutions to the differential equations of the original model. However, code verification confirms that the code as it is written performed the intended algorithm. More importantly, benchmarking solutions are premised on verifying solutions, which compare the computed output with analytical solutions [25],[26].

From the epistemology of simulation, the dichotomy between verification and validation is not so subtle. There are overlaps and sometimes, real difficulties arise in defining one without the other. A help emanates from [30] as quoted by [26], that: “Verification deals with mathematics and addresses the correctness of the numerical solutions to a given model.

Validation, on the other hand, deals with physics and addresses the appropriateness of the model in reproducing experimental data. Verification can be thought of as solving the chosen equations correctly, while validation is choosing the correct equations in the first place."

Further, simulation results show that any local optimum is also a global optimum in the region of convexity. Hence, both local maxima and global maxima occurred for the: (a) Horizontal currents, (b) Vertical currents, (c) Gradient of the vertical functional, (d) Gradient of the horizontal functional, and (e) Constraints. Moreover, the gradient, which is the direction of the greatest increase maximises the varying tradeoffs, while the Jacobian tracks the distortion, stretching, or kinking of the change in the coordinate system [2],[18],[19],[20]. The next section discusses composite conductors and their applications.

4.8. Applications of Composite Conductors

4.8.1. Earlier Composite Conductors

Earlier composite conductors were designed from two separate wires considering their physical and electrical properties. Aluminum conductors steel reinforced (ACSR), aluminum conductors aluminum alloy reinforced (ACAR), and all-aluminum-alloy conductors (AAAC) are long-span used in overhead transmission and distribution lines [31]. Air-expanded ACSR is an increased hollow diameter conductor used to create air spaces for cooling and minimise corona effects. Its increased current-carrying capacity, better skin effects, and using lesser metal enable it to operate at higher temperatures above 300 kV [32]. Self-supporting ACSR limits aeolian vibrations to safe levels, ACSR/TW because of its smaller diameter and smooth surface experiences lower wind loading. T2 conductors comprise two spiral windings from twisted standard ACSRs and significantly reduce wind-induced galloping because ice cannot form along conductor length. Steel-supported aluminium conductors (SSAC) have high electrical conductivity at high temperatures and better sag-tension properties [32].

4.8.2. Power Blackouts

Electrical transmission and distribution lines outages mostly come from thermal sags, when the current passing through the conductor exceeds transmission capacity. Overheated wires elongate to cause sags, which potentially violate minimum ground clearances leading to arcing faults, short circuits, and cascading failures [3],[33]. Thermal sags caused the August

14, 2003, US East Coast blackout, leaving over 50 million people without power [34]. The July/August 2012 India blackout that made over 710 million people of the Indian sub-continent without power was due to sags [35]. A combination of weak monsoon, low hydropower generation, high temperatures, high humidity, and increasing electricity consumption to cool the heat and discomfort experienced, caused the monumental collapse of the Indian power system [36].

On 2nd July 1996, a Western US power blackout occurred because of a short circuit in transmission lines from the Bridger coal-fired generator of Idaho Power affecting over 7.5 million people. A disconnection of three 500 kV lines caused heavy power flow North-South. Consequent overload caused 230/115 kV lines to disconnect leading to voltage declines, tripping power units, power oscillations, cascading separations, and power blackout [37]. North Eastern U.S. and Canada blackout of 14th August 2003 affecting over 50 million people occurred like those of 1996. A 500 kV line disconnected causing heavy power flow South-North. Another 500 kV line sags into a tree and disconnects making 230/115 kV lines to disconnect. Several 345 kV lines trip, voltage declines, power units trip, and power oscillates causing voltage declines and cascading separations leading to blackout, later [37].

Over 57 million people were affected in the Italy 2003 power failure because 6 GW heavy power import to Italy caused one 380 kV line to sag into a tree and disconnect. Parallel 220/110 kV line sags into another tree because of overload to completely isolate Italy. Consequent voltage declines, power units trip, power oscillates, voltage further declines to cause cascading separations, and blackouts [37]. However, using the proposed optimal bidirectional composite conductor designs validated in this study can drastically reduce thermal and cable sags in power systems networks, worldwide.

4.8.3. High-Temperature Low-Sag Composite Conductors (HTLS)

HTLS conductors retain their shape integrity at higher temperatures, lower thermal expansivity coefficients (CTE), and higher ampacity (ampere capacity) for transmission. CTC Global hybrid carbon/glass fibre aluminium composite core conductors (ACCC), have low CTE, low sag, operational temperatures between 180^0 and 210^0C, and can carry twice ACSR current and less sag [3],[33]. Between 2006 and September 2012 over 14,806 km of ACCC were installed in over 220 projects worldwide. Also, ACCC re-conductored 345 kV 2,680 km

American Electric Power (Columbus, Ohio), 893 km power line in Texas, and 18 mm diameter ACCC conductors replaced 69 kV 32 km long, old copper conductors, in Nevada in 2009 [33]. Lightweight and fire resistance made felled conductors to be re-energised after replacing the burnt H-frame. They have been installed in over 24 countries, including Russia [33].

3M's aluminium conductor composite reinforced (ACCR) cable uses a metal-matrix composite core design. Its CTE is half that of steel. 3M doubled manufacturing capacity and supplied over 2,575 km ACCR conductors to 13 countries except for Australia and Antarctica. By 2013, 3M manufactured 135 to 828 mm^2 product lines using alumina ceramic oxide (Al_2O_3) powder made into a gel. It is extruded through spinnerets to form embedded core fibres in high-purity aluminium. Customer size/strength requirements enable 7 to 19 core aluminium zirconium (Al-Zr) stranded wires as twisted cable to operate continuously at 210^0C and peaks at 240^0C [3],[33].

EDP Escelsa (Brazil) in 2012 replaced its sagging power lines over the Rio Doce River in Linhares (918 m span) by ACCR and doubled the 138 kV line ampacity with a better line clearance, without requiring new rights-of-way permits and new construction efforts. Georgia's power saved between US$ 15 and 20 million to upgrade a 54.7 km 230 kV power transmission line using ACCR. It served Savannah Power for 10 weeks in the fall and 10 weeks in the spring, during low-demand periods between 2011 and 2012 [33]. Utah Power Utility cost-effectively reconductored a section of its transmission lines with CTC cables and replaced only 7 instead of 150 support towers, if it used conventional ACSR to strengthen its transmission capacity. It could meet projected electricity demand for the next 15 years without building new transmission lines [3],[33].

4.8.4. Power Line Analysis Tool (PLAT)

Although many benefits derive from composite conductors, the equivalency of composite-for-steel-cored cable conversions in the power industry has faced acceptance difficulties. Reference [38] indicates despite the upfront cost of developing and commercialising composite conductors, the equivalency of composite-for-steel-cored cable is the most difficult aspect of their sale to customers long used to some other technology. To break that barrier, Composite Technology Corporation (CTC) designed Power Line Analysis Tool (PLAT)

software to compare, contrast, and evaluate the electrical and physical performance characteristics of available cable products based on twelve linked screens. It helps engineers, project managers, and other professionals in the power industry to select cable sizes (diameters), power capacity, cable sags, seasonal weather performance features, estimated installation costs, and computation of cost savings over the expected useful life of the cable [38].

4.8.5. Linking Composite Conductors with Cabling

Conductor composites connect seamlessly with the physical, electrical, and mechanical characteristics for specialised applications. These include power systems transmission cables, subsea cables on off-shore platforms, standing-to-rig on yachts, cable stays on bridges, solar-powered cars, and solar-powered aircrafts. These occur because of composite for metal replacement processes. These have also proved very useful and economical especially when viewed from structural and components integrity considerations [39].

Overheating and sag have plagued conventional ACSR cables. Replacing them with composite HTLS conductors provides long-term durability, little or low maintenance, removes rights-of-way permit problems, corrosion resistance, higher ampacity, higher working temperatures, little or no tower replacements, fewer losses, longer spans, higher electrical loads, and significantly reduced installation cost. The global market for composite cored cables is over US$ 50 billion annually to strengthen the existing power infrastructure [3],[39].

Further, ACCC is constructed using a pultrusion process in which carbon fibres are drawn unidirectionally along 0^0-axis to form, the cylindrically shaped core around E-glass oriented fibres at the exterior. They are wetted out with high-temperature resistant epoxy resin to separate carbon from conductive aluminium overwrap that prevents metal solution and galvanic corrosion [3],[5],[39]. The process makes brittle carbon more malleable, and enhances the flexibility and robustness of the composite ACCC core. This same carbon structure makes the tail section of the Boeing 777 jet [3] that is intricately linked to its efficient braking system. Thus, the wet ACCC fibre bundle is cured at 260^0C, and core conductor sizes range from 12.7 mm to over 69.85 mm. They carry between 300 and over

3500 amps per line in ampacity range and these high currents are suitably controlled at high tension of 18,597 kg [39].

While fibre availability, lack of standards, testing/inspection methodologies, customers continued adherence to ACSR cables, quality, and very high upfront costs are disadvantages of composite cables [39], price, weight reduction, processing renewable resources, production using low investment, thermal recycling possibility, good thermal and acoustic insulating properties are advantages of using natural fibre composites for technical applications [40]. However, lower impact strength, weather-dependent quality variability, hygroscopic swelling, limiting maximum processing temperature, poor fire resistance, harvest-dependent price fluctuations or on agricultural politics, thinning, knots, ties, voids, and imperfections in natural fibres are the major drawbacks [40].

4.8.6. Subsea Cables

Subsea composite cables used in offshore oil rigs for continuous movements from shallow waters to deep waters up to 2,000 miles (3,220 km) deep have low weight, high stiffness/strength-to-weight ratio to support high stiffness/low sag and low elongation properties. Further, offshore operators need to avoid paying the higher costs for carbon fibre with termination difficulties made Aker Kvaeman Subsea, Norway, and Conoco Philip (Houston, Texas) develop carbon-composite cables used in steel for anchor tension leg platforms (TLPs). It is used in carbon-stiffened, hollow-umbilical cables, to carry electrical, fibre-optic sensing, and other service lines [39].

4.8.7. Bridge Cable Stays

Bridge cable stays are supports for deck or girder systems. They use a series of cables attached at regular intervals, strung diagonally to attachment points on one or more vertical supports. Bridge cable stays are durable in the longer term, corrosion-resistant, and low need for maintenance. These advantages offset the initially great upfront capital outlay [39].

4.8.8. Yacht Rigging

The major objective for composite conductor use in Yacht rigging is weight reduction. For every 0.45 kg weight removed from the top of the mast, about 3.6 kg of ballast is removed

from the yacht keel. Many tonnes of yacht structural strength requirements are reduced to minimise material costs, and yacht becomes faster and more responsive without losing stability, thereby saving between 60 and 70 percent in weight compared to the steel they replace, without compromising strength. The disadvantage of fibre elongation is eliminated by increased composite rigging cross-section [39].

Element C6 carbon cables are bundles of 1 mm diameter rods with 227 kg tensile strength capable of customised performance requirements. They are 50% stronger than stainless steel at a fraction of its density. About 34 bundled rods have a breaking strength of 5,715 kg and a maximum stress capability of 2,551 MPa. They are encased in carbon or aramid brand protective jackets for better grip because cable tensions increase simultaneously with an increase in the compressive load of the terminus plug, which is distributed evenly along the full length of the rod bundle [39].

4.8.9. Custom Composite Rigging Cable

Custom composite rigging (CCR) cable design assembles parallel nested hexagonal tension rods pultruded (pulling through) using 60 to 70% carbon volume fibre and epoxy resin binder. Complementary dual tapering along their lengths removes stress concentrations at load points. Stainless steel or titanium-coated shanks at end terminals prevent corrosion between metal and carbon [39].

4.8.10. Petroleum Pipelines Anti-Corrosion Control Systems

A new lease of life was given to internally corroded petroleum oil pipelines earmarked for closure using Anti-Corrosion Protective Systems (APS) in 2013. In-Field-Liner (IFL) is an innovative composite liner system of the corrosion-resistant barrier, between highly corrosive hydrogen sulphide medium produced by sulphate-reducing bacteria (SRB) in crude oil that causes damage or rupture to steel pipeline structures [40]. In 2014, gas pipelines totaling 4 km were installed in four other PETRONAS Cargali locations in the West Lutong fields of Sarawak in Malaysia. The service lives of pipelines were extended beyond 30 years saving over 50% of pipeline capital replacement costs [41].

The success of APS's IFL technology for oil, gas, crude, and multiphase mixtures, enabled the rehabilitation of over 10 subsea pipelines running between platforms operating at

temperatures up to 110^0C. PETRONAS saved over US$ 100 million using IFL technology [42]. In 2015, PETRONAS Malaysia awarded two multi-year contracts to APS (Dubai, UAE) worth US$ 150 million to rehabilitate many subsea crude oil gathering and high-pressure gas and condensate lines.

4.8.11. Cured-In-Place Pipe (CIPP)

Alternative on-land rehabilitation and repair lining using cured-in-place pipe (CIPP) resulted in significant time and cost savings for sewer lines (on-and-offshore fields), petrochemical plants, drinking water, foul outflow, gas, and pressurised water distribution. Although CIPP has great potential in the rehabilitation/repair composite market, IFL has future potential in the rehabilitation/repair market for undersea/underwater applications [41].

4.8.12. Solar-Powered Car Design

Composite technology consistently made solar-powered composite car designs win racing competitions, consecutively. The redesigned 190 kg carbon composite car ran its fourth race in Australia for a total of 3,000 km from Darwin in the North to Adelaide in the South of Australia in October 2007. The race had no blaring engines, screeching tires, smell of fuel, or smoke. Everything was quiet but powered by the strong Australian sun [44].

All Nuna1-3 designs were carbon composites instead of aluminium. Weight advantages, higher specific strength, and stiffness led to better fatigue properties and significantly reduced parts. Nuna4 was a semimonocoque design. Its aircraft wing-like shape experienced only one-sixth drag of a comparable automobile. Solar cells on top of the relatively flat horizontal surface produced enough energy to power the electric motor on the rim of the rear wheel, about 100 km/h [44].

The rear suspension system was infused with carbon fibre and Turane urethane resin cured at 80^0C. The thermal resistance of Turane resin was adjusted to withstand Australia's ambient temperature between -20^0C and 60^0C. The urethane is stable dimensionally, but the composite begins to soften between 95^0C and 150^0C. Air-sprung shock-absorbers design combines dampers and springs systems. The front wheels are aluminium while the rim of the rear wheel is composite strengthened with carbon and aramid fibre. However, C-profile stiffeners

incorporated into the chassis and top shell of the driver's seat provide needed strength, and to further reduce weight [44].

Although it is not clear if solar-powered cars can replace petroleum inland transportation systems, solar power is being sustainably and inexpensively used in residential heating and electricity supply [45] as in space exploration of using rovers for Mars exploration [44].

4.8.13. Solar-Powered Aircraft Design

Solar Impulse 2 is the second generation of Si2 first solar-powered aircraft. Solar Impulse sought North Thin Ply Technology (NTPT), Switzerland assistance to make very thin unidirectional carbon fibre spread because NTPT offered outstanding composite strength, homogeneity, and machinability for rigid commercial applications demanding high performance and low weight [46].

In July 2010, Decision built Solar Impulse 1 (Si1), the first solar-powered aircraft that stayed a total of 26 hours in the air solely on solar power (even after dark). Si2 construction began in 2011 and included an increased payload. Electrical circuitry was isolated to enable flight during light rain, and system redundancy to improve reliability. The cockpit was more spacious to enable the pilot to fully lay on their back during flights that could last for five days and five nights [46].

Solar Impulse 1 flew all night in 2010. Solar Impulse 2 flew halfway around the world in 2015. It journeyed from Abu Dhabi in the United Arab Emirates (UAE) on 9th March 2015 to Oman, India, Myanmar, China, and Japan (eight stops). It flew nonstop for almost five days (117 hours 52 minutes) to arrive in Honolulu, Hawaii on July 3rd, 2015 at 5.55 am. The average speed was 47 km/h [47].

Extremely thin composite Si2 main and rear wing spars, body, and tail were thin-ply (or spread-tow) tapes (prepregs), constructed using individual carbon fibre tow spreads, which separate the flattened fibres into a wider and much thinner unidirectional tape. However, Si2 was grounded in Hawaii from July 3rd, 2015 to 2016, because of battery problems and not from composites failure [47].

Si2 72 m wingspan is longer than the 60 m wingspan of Boeing 787 Dreamliner. The plane's fibre architecture is strong, and lightweight, can withstand spar box torque resistance, and satisfy bend stiffness requirements. The cockpit was a low-density rigid polyurethane

foam of 180 μm cross-section, about 40% below the standard 300 μm cell density (or mass) [47]. The cockpit windshield of Covestro's transparent polycarbonate protected the pilot and instruments because the outside temperature could fall to -50^{0}C, and still able to maintain a planned temperature in the cockpit [47].

However, the worth of Si1 and Si2 solar aircraft industrialisation endeavours gained expertise, know-how, and developed network over the years in energy efficiency, ultralight materials, complex systems design, solar production, energy storage cycle, and electric motors. Solar-powered drones are developed and promoted by organisations like Google, Airbus, and Facebook, for internet access, disaster relief, environmental damage detection, and assessment [47].

4.9. Conclusions

The convex set was used to obtain optimal solutions to the bidirectional composite conductor software validation problem, in this thesis. Further, the local optimum was also the global optimum, for both the currents and gradients of the optimal bidirectional composite conductor design in the region of convexity. The materials and costs optimisation was so because the gradient shows the direction of the greatest change along the line of equipotential or equal energy. The Jacobian tracks the distortion, mirrors the symmetry, and measures the stretching, shrinking, or twisting of the changes to the new coordinate system. Also, the Hessian, as a minimiser analytically compares a derived gradient for correctness and evaluates the confidence interval values of parameters for maximum likelihood estimation.

Composite conductors commonly comprise two different wires with separate characteristics. They minimise corona effects, increase current-carrying capacity at higher temperatures, limit aeolian vibrations to safe levels, lower wind loading, reduce wind-induced galloping, acquire high electrical conductivity, and better sag-tension properties at high temperatures.

Cable and thermal sags occur when currents passing through the conductors exceed transmission capacity. The overheated wires elongate and cause sags, which potentially violate minimum ground clearances. Further, cable and thermal sags were implicated in the major blackouts of catastrophic proportions worldwide and their occurrences could be significantly reduced if the bidirectional composite conductors designed and software validated in this study could be deployed in future power systems networks worldwide.

Also, the CTC Global hybrid carbon/glass fibre ACCC and 3M's ACCR have low CTE and low sag. Their operational temperature ranges between 180^0 and 260^0C and can carry twice as much current as ACSR of similar dimensions. They are also able to carry currents between 300 and over 3500 A per line in their ampacity range.

The subsea composite cables have low weight and high stiffness/strength-to-weight ratio. They are used in deep off-shore for high stiffness/lower sag and lower elongation properties. The carbon-stiffened, hollow-umbilical cables carry electrical, fibre-optic sensing, and other service lines.

Current technological developments in composite conductors have led to frontiers in energy efficiency, ultralight materials, complex systems design, solar production, energy storage cycle, and electric motors. Other benefits include optimisation of production from existing assets, focus on innovation, cost-effective technology, delaying assets replacement, extending service life, better strength-to-weight ratios, lower thermal expansivity coefficients, higher moduli of elasticity (or stiffness), and lower electrical resistance.

Economically, longer spans between towers lead to a reduction in the number of towers, which carry the greater electrical load by close to 20% and significantly reduce installation costs.

However, the major drawbacks to composites conductor commercialisation include fibre availability, lack of standards, testing/inspection methodologies, customers continued adherence to the traditional ACSR cables, quality, and very high upfront costs.

Furthermore, the demerits of natural fibre composites include low impact strength, weather-dependent quality variability, hygroscopic swelling, limited maximum processing temperature, poor fire resistance, harvest-dependent price fluctuations, or based purely on agricultural politics, thinning, knots, ties, voids, cracks, and other imperfections.

Above all, the optimal bidirectional composite conductor design software validation proposed in this study shows one of the most innovative ways of using results of differential equations to make maximum use of the conductor materials in the design of using very tiny strips, and the advantage of minimising cross-sectional area, and possible total elimination of galvanic corrosion, and metal solution problems.

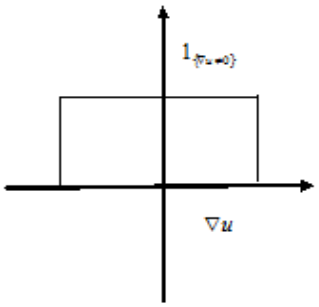

Figure 4. 1: The characteristic function of the unit square is used for the minimisation.

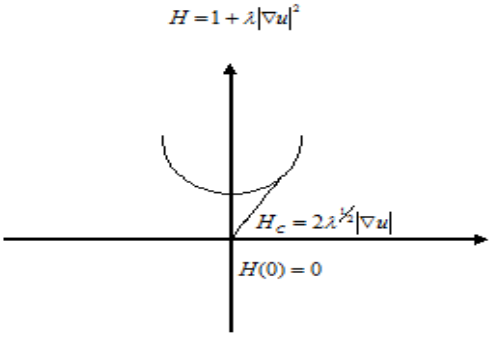

Figure 4. 2: Convexified function to obtain one minimum point in the interval of convexity.

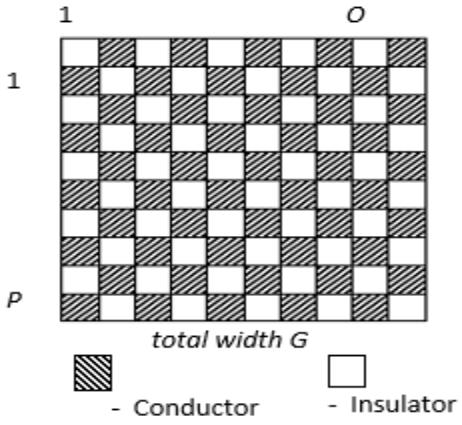

Figure 4. 3: Mat patterned approach to a truly homogenised composite: O > P.

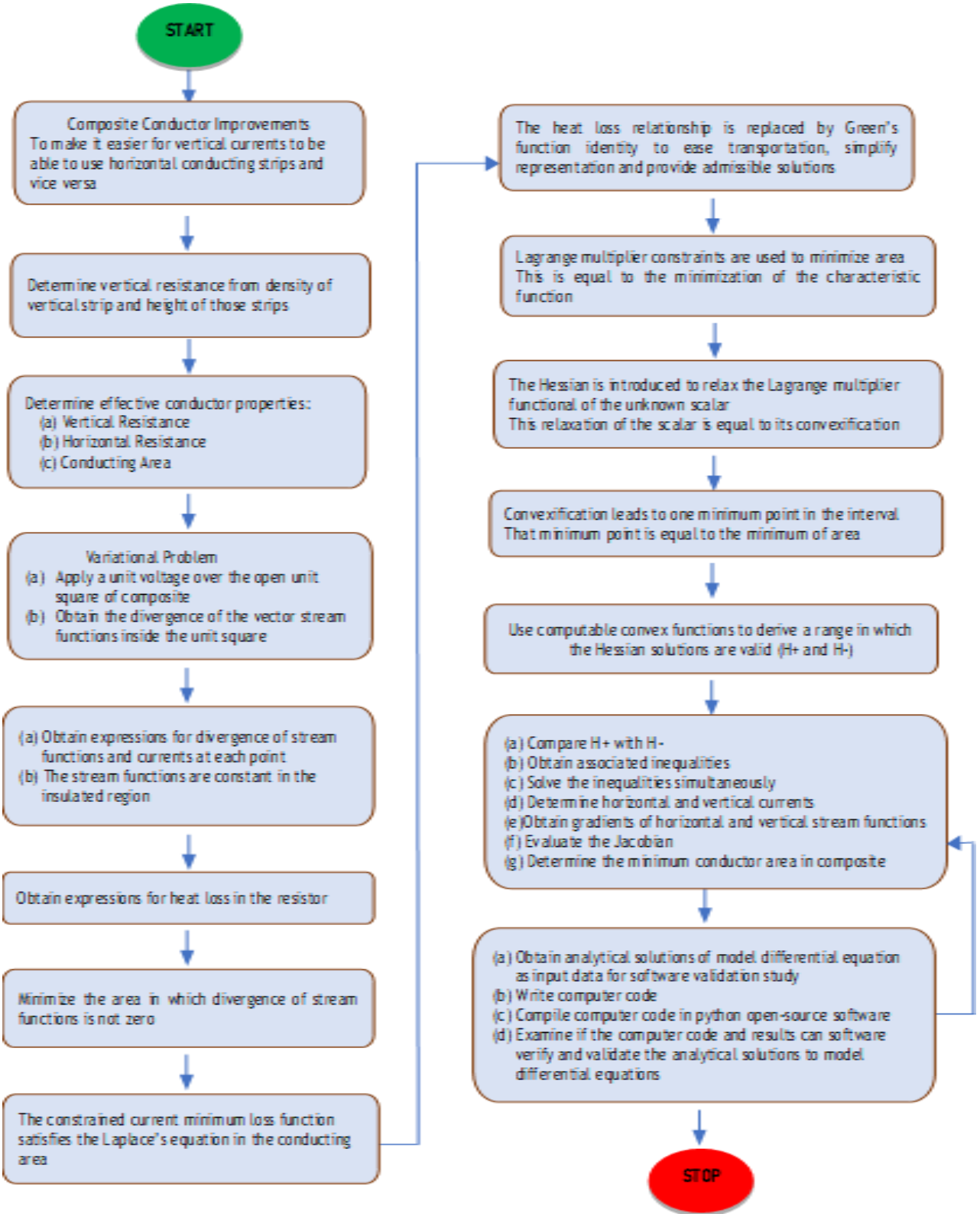

Figure 4. 4: Methodology flowchart

APPENDIX A

A.I. THE COMPILED PYTHON OPEN-SOURCE SOFTWARE PROGRAM

```
# The solution to the two-way optimal composite conductor problem
import math
m=0.5
n=0.5
grad_u=0.5
grad_w=0.5
C=D=0.5
Area=(C+D-2*C*D)/(1-C*D)
Jacobian=0.5*n
Lambda0=m-n
Lambda1=m+n
a=2*math.sqrt(m+n)-n
b=2*math.sqrt(m-n)+n
a>=b
if m>=n:
   if m>=0:
      if n>=0:
         (m+n)<=1
print('Positive Hessian comparison H+ =',a,'Negative Hessian comparison H- =',b,
    'The sum of squares of grad_u and grad_w =',m,'Twice the modulus Jacobian =',n,
    'The current following along the horizontal paths =', C,
    'The current following along the vertical paths =', D,
    'The optimized area A =', Area,
    'The Jacobian keeps track of the distortion from change in coordinate system =',Jacobian,
    'The Lambda0 (m-n)is the first solution condition of convexity =',Lambda0,
    'The second solution condition (m+n) for convexity =',Lambda1)
```

Table 4. 1: RESULTS OF PYTHON OPEN-SOURCE VALIDATION STUDY FOR THE BIDIRECTIONAL COMPOSITE CONDUCTOR DESIGN

Variable description obtained	Value
Positive Hessian comparison H_+	1.50
Negative Hessian comparison H_-	0.50
The sum of squares of grad_u and grad_w	0.50
Twice the modulus of Jacobian	0.50
Current flowing along the horizontal paths	0.50
Current flowing along the vertical paths	0.50
The optimised conductor area A	0.66’
The Jacobian (tracks the distortion from a change in a Coordinate system)	0.25
The Lambda0 $(m - n)$ is the first solution condition of convexity	0.00
The second solution condition $(m + n)$ for convexity	1.00

Table 4. 2: CONTRIBUTIONS OF OPTIMAL BIDIRECTIONAL COMPOSITE CONDUCTOR SOFTWARE VALIDATION STUDY DESIGN

Optimisation of production

Cost-effective technology

Delaying asset replacement

Extended service life

Increase in strength/weight ratio

Increase in current carrying capacity

Ability to carry both horizontal and vertical currents simultaneously using the same conductor

Ability to withstand high temperatures and high voltage stresses

Less sag/lower coefficient of thermal expansivities (CTEs)

Reduced overall installation costs

Ability to withstand higher corona breakdown voltages

Lower (about two-thirds) conductor materials requirements for commercialisation or manufacture

Time savings

Lower maintenance frequency and costs

Enhance machinability

Higher power carrying capacity/capabilities

Improved reliability

Less corrosion/corrosion resistance

Less weight/ultra-lightweight materials development

Ability to limit aeolian vibrations to safe levels

Better insulation capacity

Design and validation of complex systems using advanced mathematics and computer science

Higher moduli of elasticity or stiffness

Sustainable and less expensive alternatives in the longer terms

Less electrical resistance

Fewer losses

---

[3],[5],[31],[32],[33],[34],[35],[36],[37],[38],[39],[40],[41],[42],[43],[44],[45],[46],[47]

REFERENCES

[1] G. Strang and R. Kohn, "Optimal design of a two-way conductor," in *Topics in Nonsmooth Mechanics*, J. J. Moreau, P. D. Panagiotopoulus, and G. Strang, Eds. Basel: Birkhauser Verlag, 1988, pp. 143-155.

[2] G. N. O. Asemota," On a class of computable convex functions," *Can. J. Pure Appl. Sc.*, vol. 3, no. 3, pp. 959-965, 2009.

[3] G. N. O. Asemota, "Optimal two-way conductor design using computable convex functions approach," *Adv. Mat. Res.*, vol. 367, pp. 75-81, 2012, 10.4028/www.scientific.net/AMR.367.75.

[4] S. Takriti, "The unit commitment problem," in *Operational research in Industry,*T. A. Ciriani, S. Gliozzi, E. L. Johnson, and R. Tadei, Eds. London, UK: MacMillan, pp. 299 -322, 1999, 10.1057/9780230372924.

[5] G. N. O. Asemota, "Optimal two-way conductor design using computable convex functions approach," in *Proc. 3rd ICERD*, Benin City, Nigeria, 2010.

[6] J. J. Moreau, "Bounded variation in time," in *Topics in Nonsmooth Mechanics*, J. J. Moreau, P. D. Panagiotopoulus, and G. Strang, Eds. Basel: Birkhauser Verlag, 1988.

[7] C. H. Edwards and D. E. Penney, *Calculus*. New Jersey, NJ, USA: Prentice-Hall, 2002.

[8] Z. Hashin and S. Shtrikman , "A variational approach to the theory of the elastic behavior of Multiphase materials," *J. Mech. & Phys. Solids*., vol. 11, no. 2, pp. 127-140, Mar.-Apr. 1963, 10.1016/0022-5096(63)90060-7.

[9] F. Murat and L. Tartar, *Optimality conditions and homogenization: nonlinear variational problems.* (Isola de'Elba, 1983). London, UK: Roman Publishing, pp. 1-8, 1985.

[10] V. K. Mehta and R. Mehta, *Principles of Power System.* New Delhi, India: S. Chand, 2007.

[11] C. F. Gerald and P. O. Wheatley, *Applied Numerical Analysis.* Massachusetts, MA, USA: Addison-Wesley, 1999.

[12] M. S. Naidu and V. Kamaraju, *High Voltage Engineering*. 2nd ed. New Delhi, India: Tata McGraw-Hill, 2007.

[13] F. B. Hildebrand, *Advanced Calculus for Applications*. New Delhi, India: Prentice-Hall, 1977.

[14] T. Moon, "Convexity and Jensen's inequality," 2000. Accessed on: Dec. 5, 2007 [Online]. Available: http://www.neng.usu.edu/classes/ece/7860/lecture2/node5.html

[15] L. Potter, "Convexity," 2005. [Online]. Available: http://cnx.org/content/m10328/latest/ Accessed on: Dec. 5, 2007

[16] E. Fink and D. Wood, "Fundamentals of restricted-orientation convexity," 1996. Accessed on: Oct. 18, 2007 [Online]. Available: citeseer.ist.psu.edu/38250.html

[17] G. Lebanon, "Convex functions," 2006. Accessed on: Dec. 5, 2007 [Online]. Available: http://www.cc.gatech.edu/~lebanon/notes/convexFunctions.pdf

[18] C. M. Bishop, *Pattern Recognition and Machine Learning.* Singapore: Springer, 2008.

[19] Betterexplained, "Vector calculus: Understanding the gradient-better explained," [Online]. Available: https//betterexplained.com/articles/vector-calculus-understanding-the-gradient/, Accessed on: Nov. 17, 2018

[20] Whitman. "16 Vector calculus," Accessed on: Nov. 17, 2018. [Online]. Available: https://www.whitman.edu/mathematics/multivariable_16_Vector_Calculus.pdf

[21] P. A. Brodtkorb and J. D'Errico. Numdifftools Documentation Release 0.9.20.post0.dev144+ng9114a1a. 2018. Accessed on: Sep. 20, 2018. [Online]. Available: https://media.readthedocs.org/pdf/numdifftools/latest/numdifftools.pdf

[22] S. Bimenyimana, G. N. O. Asemota, and P. J. Ihirwe, "Optimization comparison of stand-alone and grid-tied solar PV systems in Rwanda," *Open Access Lib. J.*, vol. 5,

no.5, pp. 1-18, 2018a, 10.4236/oalib.1104603.

[23] S. Bimenyimana, G. N. O. Asemota, P. J. Ihirwe, and L. Li, "Clustering residential electricity consumption: a case Study," in *Proc. ACM Digital Library*, Tianjin, China, 2018b, pp. 121-128. ISBN: 978-1-4503-6541-3

[24] A. Papoulis and S. U. Pillai, *Probability, Random Variables and Stochastic Processes.* New Delhi, India: Tata McGraw-Hill, 2008.

[25] X. Meng, "Simulation CSCI 6337: advantages and disadvantages," Cited: Oct. 22, 2018. https://www.eg.bucknell.edu/~xmeng/Course/CS6337/Note/master/node3.html

[26] E. Winsberg, "Computer simulations in science. Stanford encyclopedia of Philosophy," 2015. Accessed on: Dec. 22, 2018. https://plato.stanford.edu/entries/simulations-science/

[27] D. Duzevik. Advantages and disadvantages of simulation. 2017. Cited on: Dec. 22, 2018. https://concentricmarket.com/blog/advantages-and-disadvantages-of- simulation/

[28] Y. Hu, Z. Bie, T. Ding, and Y. Lin, "An NSGA-II based multi-objective optimization for combined gas and electricity network expansion planning," *Appl. Energy*., vol. 167, pp. 280-293, 2016.

[29] M. Jakubcionis and J. Carlsson, "Estimation of European Union residential sector space cooling potential," *Energy Policy.* Vol. 101, pp. 225-235, 2017.

[30] S. Roy, "Recent advances in numerical methods for fluid dynamics and heat transfer," *J. Fluid Eng.*, vol. 127, no. 4, pp. 629-630, 2005.

[31] J. J. Burke and A. L. Clapp, "Power distribution," in *Standard Handbook for Electrical Engineers,*14th ed., D. G. Fink and W. H. Beaty, Eds. New York, NY, USA: McGraw -Hill, 2000, pp. 18-72-18-76.

[32] C. B. Rawlins, J. Tanaka, D. J. Barta, C. A. Harper, T. W. Dakin, J. Stubbins, and D. E. Lyon, "Properties of materials," in *Standard Handbook for Electrical Engineers,* 14th ed., D. G. Fink and W. H. Beaty WH, Eds. New York, NY, UAS: McGraw-Hill Handbooks, 2000, 4-2-4-39.

[33] D. Dawson, "Composite-cored conductors: Holding the line," 2013. Cited: Nov. 19, 2018 https://www.compositesworld.com/articles/composite-cored-conductorsholding-the-line

[34] J. R. Minkel, "The 2003 Northeast blackout-Five years later," 2008. Cited: Nov. 20, 2018 https://www.scientificamerican.com/article/2003-blackout-five-years-later/

[35] H. Pidd, "India blackouts leave 700 million people without power," 2012. Cited: Nov. 20, 2018. https://www.theguardian.com/world/2012/jul/31/india-blackout-electricity-power-cuts

[36] R. Bedi and R. Crilly, "World's biggest ever blackout as India is brought to a standstill,"

The Telegraph. (July) 2012. [Online]. Available: https://www.telegraph.co.uk/news/worldnews/asia/india/9441940/Worlds-biggest-ever-blackout-as-India-is-brought-to-a-standstill.html, Accessed on: Nov. 20, 2018

[37] G. N. O. Asemota and F. B. Gahimano, "Symmetrical fault currents determination at 70 -110 kV primary of Electrogaz grid in Rwanda," *Zambian Eng.*, vol. 41, no. 1, pp. 48 -55, 2008.

[38] D. Dawson, "Modeling software facilitates composite-for steel-cored cable conversion," 2006a. [Online]. Available: https://www.compositesworld.com/articles/modeling-software-facilitates-composite-for-steel-cored-cable-conversions, Accessed on: Nov. 19, 2018

[39] D. Dawson, "Composites connect with the world of cabling," 2006b. Cited: Nov. 19, 2018 https://www.compositesworld.com/articles/composites-connect-with-the-world-of-cabling

[40] G. N. O. Asemota, "Critical angle estimation of light in plantain fibres," *Can. J. Pure & Appl. Sc.*, vol. 5, no. 3, pp. 1693-1699, Oct. 2011.

[41] D. Dawson, "Composites extend service of oil and gas pipelines," 2015. [Online]. Available: https://www.compositesworld.com/articles/composites-extend-service-of-corrosion-prone-oil-and-gas-pipelines, Accessed on: Nov. 19, 2018

[42] J. Sloan, "Composite liner for subsea oil and gas nears readiness," 2017. [Online]. Available: https://www.compositesworld.com/news/composite-liner-for-subsea-oil-and-gas-nears-readiness, Accessed on: Nov. 19, 2018

[43] Staff, "In-field-liner installations helps to extend service life for Petronas subsea pipelines," 2016. Cited: Nov. 19, 2018, https://www.compositesworld.com/news/infield-liner-installations-helps-to-extend-service-life-for-petronas-subsea-pipelines-

[44] D. Dawson, "Focus on design: solar-powered composite car designed to win," 2007. [Online]. Available: https://www.compositesworld.com/articles/focus-on-design-solar-powered-composite-car-designed-to-win, Accessed on: Nov. 19, 2018

[45] S. Bimenyimana, G. N. O. Asemota, C. M. Kemunto, and L. Li, "Shading effects in photovoltaic modules: simulation and experimental results," in *Proc. 2017 2nd IEEE -ICPRE*, Chengdu, China, 2017, pp. 904-909, 10.1109/ICPRE.2017.8390665

[46] D. Dawson, "Spread-tow technology takes off," 2014. Accessed on: Nov. 19, 2018 https://www.compositesworld.com/articles/spread-tow-technology-takes-off-

[47] D. Dawson, "Solar impulse 2: pulse on the future," 2016. [Online]. Available: https://www.compositesworld.com/articles/solar-impulse-2-pulse-on- the-future Accessed on: Nov. 19, 2018

CHAPTER FIVE

5.0. Overall Conclusions

The proposed technological developments in composite conductors in this study could lead to frontiers in energy efficiency, more ultralight materials, more effective power systems design, enhanced solar production capacity, improved energy storage cycle, and more efficient electric motors. Other benefits include optimisation of production from existing assets, focus on innovation, cost-effective technology, delaying assets replacement, extending service life, better strength-to-weight ratios, lower thermal expansivity coefficients, higher moduli of elasticity (or stiffness), and lower electrical resistance.

Economically, longer spans between towers lead to a reduction in the number of towers, which carry the greater electrical load by close to 20.0%, and significantly reduce installation costs. Utilities can uprate their existing currents to achieve a twenty percent increase in power rating and be able to defer multibillion-dollar new installation costs for many years. The optimal bidirectional composite conductor proposed in the study can be beneficial to power utilities due to its higher thermal rating quality and power-carrying capabilities. Furthermore, uprating processes for raising the capacity of the existing power system infrastructure could use one or more of: (a) reconductoring, (b) dynamic rating for cables capable of operating above their nominal ratings for extended periods without exceeding their permissible limits, (c) adding forced cooling, (d) audit of the route of as-built-drawings and load shapes, and (e) thermal analysis. However, the major drawbacks to composites conductor commercialisation include fibre availability, lack of standards, testing/inspection methodologies, customers continued adherence to the traditional ACSR cables, quality, and very high upfront costs.

Furthermore, the demerits of natural fibre composites include low impact strength, weather-dependent quality variability, hygroscopic swelling, limited maximum processing temperature, poor fire resistance, harvest-dependent price fluctuations, or based purely on agricultural politics, thinning, knots, ties, voids, cracks, and other imperfections.

Natural fibres with low impact strength, when intertwined with metallic ribbons, could be abrased. The abrasion could lead to thinning, which eventually snaps the natural fibres, and consequent breakdown in the composite conductor matrix. The thinning of the natural fibres due to abrasion could equally lead to low corona breakdown voltages. As a result, the performance of the composite with low-impact strength natural fibres could be greatly compromised.

Natural fibres may be weather dependent. Whenever the quality and consistency of natural fibres depend on rain-fed growth, the regularity or variability of weather could affect the quality, quantity, and consistency of natural fibres production and availability. In extremes of weather conditions, the quality, quantity, and consistency of natural fibres cannot be guaranteed. Damage and ruin could be prevalent under these circumstances. As a consequence, there could be a tendency of not being able to produce composite conductors of the required standards.

Dry natural fibres are prone to absorbing water from the environment when they are exposed. Also, water is known to conduct electricity because it has some dipole moments. As long as the water absorbed by the formerly dry natural fibres is retained, the insulation capacity begins to decrease and renders the natural fibres unusable in the composite conductor matrix. In the worst-case scenario, the natural fibres begin to rot and could contaminate other natural fibres in the warehouse or stores. The damage and loss could be colossal.

One of the requirements of a composite conductor design is to be able to withstand high operating temperatures of more than 100^0C, and up to 260^0C, or even more. If the maximum processing temperature of any natural fibre is low, say below 100^0C, then it fails to meet one of the basic requirements of being a candidate for high temperature, high current, and high power carrying capacity composite conductor matrix component.

If any natural fibre does not have a high fire resistance, it would be subject to burning or degradation, then it fails to qualify as a component for high temperature, high current, high power, and low sag composite conductor material. Hence, the ability of any natural fibre not to have a high fire resistance quality would be a serious limitation that cannot be overlooked.

Also, the harvest quantity and quality of natural fibres are important for composite conductor manufacturing. Whenever harvest is good and there is no hoarding the price of natural fibres would be stable. Coincidentally, the cost of natural fibres would not be stable and prices could increase whenever supply reduces because of poor harvest or based purely on agricultural politics. Presently, a majority of the developing world is suffering from wheat and vegetable oils shortage because of the war between Ukraine and Russia that began on the 24^{th} of February 2022 and the end is not in sight (May 2023). The consequence of the war between Ukraine and Russia has brought skyrocketing inflation because of the blockade in the supply chains of wheat and vegetable oils and their byproducts. Cost-push inflation on basic food and petroleum products, and loss of revenues have seen many developing nations reeling from the devastating effects of the weakening of currencies against the major currencies as a

result of globalisation and interdependence on each other. Some of these occurrences have laid bare the fragility of the globalised world and how it is taking the progress and the productive sectors of African continent hostage.

The other problems of thinning, knots, ties, cracks, voids, wounding, and other imperfections in the core or periphery of natural fibres have different voltage withstand capacity constraints. These zones of weakness presented by these imperfect phenomena in natural fibres lead to diverse and variable breakdown voltages. The tests to carry out to be able to determine which and what kinds of breakdown voltages to expect from each manifestation of imperfections in natural fibres, would be frustratingly enormous. The enormity of the problems in handling imperfections, variabilities, and defects in natural fibres is better imagined than experienced. In contrast, carbon fibres which are about forty percent stronger than steel can prevent the Aluminium composite conductor core (ACCC) cable from elongation

Above all, the optimal bidirectional composite conductor design software validation proposed in the study shows one of the most innovative ways of using results of differential equations to make maximum use of the conductor materials in the design of using very tiny strips, and the advantage of minimising cross-sectional area, and possible total elimination of galvanic corrosion, and metal solution problems.

Using blinds, shutters, or shades significantly reduced inlet heat through windows in summer and heat outlets during winter, while daylighting reduced electricity consumption because electricity prices were stable, even during heavy, persistent, and widespread electricity consumption.

Both electricity price jump discontinuities and stepwise regression four-factor interaction analyses were 15 each, and the 0.5 Quetelet curve index at the median percentile was the optimal solution to the empirical electricity consumption and net pricing distribution patterns problem. Furthermore, the Quetelet index is used to create awareness, education, and behaviour modification, especially among the average citizens on energy efficiency for affordable, reliable, and sustainable supply.

Logistic and cubic interaction cross-lines show males prefer using blinds over windows than females. Blinds and day-lighting were the least costly and optimal strategies for

curtailing electricity consumption and latching price increases. Therefore, blinds and day-lighting could lead to optimal and more sustainable production, transmission, distribution, and utilisation of electrical power, worldwide.

Future research could consider actual electricity consumption measurements by electrical appliances category to ascertain quantifiable energy savings using any or a combination of the methods considered in the study. Consequently, actual electricity consumption measurements of appliances in households and other consumers could be used to better understand the cause-effect relationships and to determine specific energy savings from particular and specialised consumer categories.

Multivariate analyses were used to gauge the attitudes and behaviours of people toward electricity load management in the study. For all selected predictors, Hotelling's trace, Roy's largest root, and F-values were the same for each predictor class. There was no statistically significant predictor in the decoupled multivariate model. Small F-values less than unity suggest variance was due to error, which indicates Type-I errors in the sample.

Further, the many low Wilks' lambda values suggest substantial differences exist across gender in attitude toward optimal electricity load management practices and females were generally less likely to use electricity optimally. Lowering thermostats at night or anytime the house was vacant, drawing blinds over windows and doors, and locking all windows and doors tightly in winter were all seen to save energy, reduce overall energy costs and minimise inconveniences. Good and adequate house insulation, using shutters, and spreading underlay were seen to reduce sunlight into the house by between 50.0 and 75.0% in summer and reduce heat outlet by over 25.0% in winter.

Rarely opening refrigerator and freezer compartments in summer, cooking with little water, keeping the bottom of pots clean and shining, and boiling liquids in tight containers can minimise spoilage and save energy by over 20.0%, more than normally used. It is, therefore, strongly recommended for the least costs and minimal resources deployment in power utilities that the female gender could be sensitised, encouraged, prodded, and urged to adopt optimal multivariate electricity load management practices proposed in this study for affordable and sustainable electricity generation, supply, utilisation, growth, and overall development.

5.1 CONTRIBUTIONS TO KNOWLEDGE

5.2 Introduction

This section aims to make succinct statements of the contributions of this study to knowledge. These contributions are based on the analyses, investigations, and conclusions drawn from chapters two to four in this study.

5.3 Contributions to Knowledge

The research used multidimensional interactions of electricity consumers of a residential load management questionnaire designed and administered in Windhoek, Namibia to predict and modify electricity consumption styles and attitudes by gender of the average citizen, using the Quetelet curve index.

The investigation showed that the female gender and teenagers consumed about three times more electricity in the home, thereby increasing their carbon footprint. This assertion was also corroborated by other researchers in the United Kingdom and elsewhere.

The researcher also deduced the Quetelet curve index from the predictive analytics for the average citizen's behaviour modification, awareness, education, and targeted marketing to embrace optimal and lower electricity consumption so that they reap the benefits of lower energy cost, loss reduction, reliable supply, and enabling the utilities to supply more customers without stressing generation and network facilities.

Energy-efficient buildings that abated energy consumption using predictive analytics and integrated energy-efficient design procedures deployed drapes, daylighting, and heater regulators to lower energy demands, electricity consumption, and pricing arrangements of households, commercial, and industrial properties.

The validated optimal bidirectional composite conductor design with applications deployed the minimum conducting area of a conductor-insulator matrix to satisfy Laplace's equation. It together allowed noticeably high vertical and horizontal currents at high temperatures to flow through the composite conductor without local heating, galvanic corrosion, or metal solution problems.

The generation of the pyriform served as the globally optimised solution to the electricity consumption balanced loading problem. A balanced electrical power systems loading enables utilities to supply more customers, increases operational efficiencies, and places less stress on electricity generators, transmission, and distribution networks. Also, lower-cost operations and balanced light loading facilitates optimal unit commitment at lower economic and social costs. Consequently, service taxes are reduced because of cheaper electricity prices, utility witness flatter load curves, and avoided production costs across power systems operations, which further, lessens blackouts, and extends the life of utility facilities.

The Python open-source software was learned, wrote the software code, and used to validate the analytical correctness and robustness of the describing partial differential equations by simulation. The optimal bidirectional composite conductor design used Green's identity, Laplace's equation boundary conditions, and the minimum area principle. Again, the conductor component of the conductor-composite was proven to occupy about two-thirds of the unit square area, and the horizontal and vertical currents were a half each in this research.

The difference between the unit square and the area occupied by insulator strips is the savings in the conductor area that was achieved by homogenisation. That means a third of the unit area of the conductor was saved. It amounts to weight, cost, and materials optimisation, which also translates to reduced transmission tower foundation requirements.

Also, the local optimum was deduced to be equal to the global optimum in the convex domain. Consequently, both local maxima and global maxima occurred for the: (a) Horizontal currents, (b) Vertical currents, (c) Gradient of the vertical functional, (d) Gradient of the horizontal functional, and (e) Constraints.

Optimisation of composite conductor production used cost-effective technology to delay asset replacement and extend service life.

Optimisation of composite conductors increases the strength-to-weight ratio, increases the current carrying capacity, and can carry both horizontal and vertical currents together using the same conductor.

The optimised composite conductor can withstand high temperatures and high voltage stresses, less sag, or lower coefficient of thermal expansivities (CTEs), and reduced overall installation costs.

The optimised composite conductor has the ability to withstand higher corona breakdown voltages and lower (about two-thirds) conductor materials requirements for commercialisation or manufacture and time-saving operations.

The optimised composite conductor lowers maintenance frequency and costs, enhances machinability, noticeably higher power carrying capacity or capabilities, and improved reliability.

The optimised composite conductor has lesser corrosion or corrosion resistance, lower weight to ultra-lightweight materials development, the ability to limit aeolian vibrations to safe levels, and better insulation capacity.

The design and validation of more effective systems used advanced mathematics and computer science to obtain noticeably higher moduli of elasticity or stiffness, sustainable and less expensive alternatives in the longer terms, less electrical resistance, and fewer losses.

APPENDICES

The appendices section comprises published articles and unpublished manuscripts submitted for review in the South African Institute of Electrical Engineers – Africa Research Journal and Energy Engineering Journal, respectively.

Appendix D contains a Preview, entitled: "Rwanda's Off-Grid Solar Performance Targets" published in the first issue of the fifth volume of Joule Journal on the 20th of January 2021.

Appendix E consists of the published article which is an improved version of the accepted and presented conference paper in the second East African Community Regional Science, Technology, and Innovation (STI) Conference held in Bujumbura, Burundi between the 27th and 29th of October 2021. The aforesaid paper, entitled: "Optimisation of the eccentricity of the pyriform diagram for balancing electrical power systems loading" was published in The East African Journal of Science, Technology, and Innovation (EAJSTI), Vol. 3 (Special issue), in February 2022 (pp. 1-8. https://eajsti.org/index.php/EAJSTI/article/view/433).

Appendix F comprises the conference proceedings, entitled: "Shielding and Thermostatic Control for Optimal Electricity Load Management" of the thirteenth International Conference on Applied Energy 2021, held between November 29th and December 5th, 2021, in Bangkok, Thailand. The details include Energy Proceedings, vol. 23, 2021, pp. 1-4. ISSN 2004-2965. https://www.energy-proceedings.org/wp-content/uploads/icae/2021/1643308361.pdf

Appendix G contains the manuscript entitled: "Energy efficiency of a generalized optimal multidimensional electricity load management model", resubmitted to the South African Institute of Electrical Engineers – Africa Research Journal for Review on the 10th of May 2022.

Appendix H contains the manuscript entitled: "Multivariate Component Analysis Optimisation of Electricity Load Management". It was resubmitted to Energy Engineering for Review on the 9th of June 2022.

APPENDIX D

This part of the thesis presents the contents of a Preview entitled: Rwanda's Off-Grid Solar Performance Targets. The Preview was to assess solar energy penetration in Rwanda using synergies and their trade-offs based on the 17 sustainable development goals (SDGs) of the United Nations (UN). The analysis began by identifying the number of guidelines against the performance targets of the UN 2030 agenda. The study indicated that Rwanda could use off-grid solar energy to increase electricity access by deploying the Pay As You Go (PAYG) business prototype to collect real-time data for energy trend analysis, design enhancements, funding protocols, and upscaling. The study also showed that 16 out of 17 SDGs were applicable to Rwanda, except SDG 14 (Life Below Water) because Rwanda is a landlocked country without direct access to seas and oceans. Fortunately, Rwanda has been able to harness its solar energy resources to increase the stock of available renewable energy to its citizens. Furthermore, the Government had provided an enabling environment that ensures that none may be "left behind" in accessing energy among the citizens.

D.1 Preview

D.2 Rwanda's Off-Grid Solar Performance Targets

D.3 Abstract

The United Nations Statistical Commission's Inter-Agency and Expert Group on Sustainable Development Goals (IAEG-SDG) settled on 230 guidelines to assess the 17 SDGs and 169 Targets. The clause of "Leave No One Behind" and the scarcity of data in most deserving countries made the UN 2030 Agenda agree on 169 Targets. Recently in *Energy Policy*, Bisaga et al.[1] used synergies and trade-offs of SDG7 to assess Rwanda's off-grid solar energy sector performance against the 169 Targets of the UN 2030 Agenda.

D. 4 Body of the Preview

By 2015, the United Nations (UN) member states agreed to offer a successful, friendly, imperishable, and liveable world by 2030. The 17 sustainable development goals (SDGs) are individually inseparable interconnected systems, which are used to measure country-level preparedness for policy and financing.[1] Rwanda recognises the capacity of its off-grid solar energy sector to supply a large section of its population.

The study pinpoints the interdependencies between the solar energy market and SDGs to provide an analysis for future clean energy electrification and investment planning. Electricity

access has gradually increased, the Pay As You Go (PAYG) business model enables the collection of real-time energy use data to predict energy-demand trends, inform energy systems design improvements, and funding arrangements.[1,2]

The Economic Development and Poverty Reduction Strategy (EDPRSs I & II) enabled energy access scale-up through the implementation of the Electricity Access Rollout Programme (EARP) and Sector Wide Approach (SWAp) between 2009 and 2017 by the Rwanda Energy Group (REG), World Bank, Ministry of Infrastructure (MININFRA), and Rwanda Utilities Regulatory Authority (RURA) as key stakeholders.[1,3]

The Rwanda off-grid solar electrification strategy comprises solar lanterns,[1] solar home systems (SHSs), solar mini-grids, solar water pumps, and solar water heaters. Although a country-wide SHSs subsidy programme is underway, it is pertinent to evaluate how this unfolding energy market will configure and impact the execution of the SDGs in Rwanda.

The study used the global mapping of synergies and trade-offs[1,4] and structured it to Rwanda. The two study questions were whether: (a) the SDGs Target call for action related to off-grid solar systems in Rwanda and (b) synergies and trade-offs exist between the SDG target and decisions about off-grid solar systems in keeping with SDG7 in Rwanda?[1]

Responses to the first of the study questions indicate that 86 Targets (50.9%) were the activities satisfied by the off-grid solar energy in Rwanda, while those to the second question confirm that 85 Targets (50.3%) were the synergies and trade-offs achieved relative to the UN 2030 Agenda, respectively.

Also, only SDG14 (Life Below Water) was not satisfied by Rwanda because it is landlocked[1,2,5,6] and has no direct access to the seas and oceans. Furthermore, the majority of trade-offs involve SDG2 (Zero Hunger) and SDG12 (Responsible Consumption and Production). The results were clustered into three domains: (a) SDGs (1, 3, 4, 5, 10, and 16); (b) infrastructure and service delivery (SDGs 2, 6-9, 11, and 12), and (c) environment and other resources (SDGs 13-15).[1] Also, the quality of life and economic well-being of rural dwellers in Rwanda is rooted in Government's enhanced rural infrastructural development including energy.

About 44 Targets (44 synergies and 3 trade-offs) were pinpointed as SHSs upgraded the physical and economic well-being of households by removing kerosene-polluting lighting fuels (Targets 3.4 and 11.1) and increasing income generation possibilities (Targets 1.1 and 10.1). Additionally, the restricted capacity of the off-grid solar systems, places a constraint on using greater power agricultural machinery, thereby limiting some targets (Target 2.3).[1,6]

Rwanda's off-grid solar energy solutions are critical for realising healthy living that promotes well-being at household and community levels (Targets 3.1-3.4 and 3.9). Furthermore, they empowered and built friendly and inclusive communities by providing: secure living conditions (Target 11.1); equal access to information and communication technology (ICT), which connects people beyond their localities (Target 9.c); women with energy access decision-making and broader socioeconomic development (Target 5.5).[1]

Access to physical and social infrastructure is vital to poverty alleviation in Rwanda, and 58 Targets were authenticated in this category (58 synergies and 5 trade-offs).[1] SDG2 (Zero Hunger) depends on energy to drive agricultural equipment for effective and continuous food production. SDG2 trade-off with SDG7 leads to land competition for arable crops and solar energy mini-/micro-grid development and groundwater reduction because of rising solar irrigation (Targets 2.1-2.4).[1] Off-grid solar energy supports good health (SDG3) in health centres (Targets 3.1-3.3) and access to information and early warning signals in rural settlements (Target 3.d). It has enabled curriculum development in higher learning institutions (Targets 4.3-4.4). Clean electricity access has created profitable energy uses for the populace (Target 8.3) like mobile money, logistics, and real estate (Targets 8.5-8.6).[1]

Off-grid solar underpins Sustainable Cities and Communities (SDG11), enhanced the Environmental Footprint of Cities (SDG13), and supplying larger-power equipment like refrigerators using smart energy management of SHS-based mini-grids.[1] Twenty-one (21) Targets of synergies and trade-offs including SDG7 (17 synergies and trade-offs) are used to reduce natural resources dependency and maintain environmental continuance in Rwanda. Solar energy has also raised the proportion of renewables in the Rwanda energy mix (Target 7.1) mainly for electricity production, while solar cooking is in its infancy (Target 7.2).[1]

Solar energy has assisted resilient and sustainable industrialisation (SDGs 8, 9, 12) by applying mini-/micro-grids to drive cutting-edge business models (SDG9) in Rwanda. Solar irrigation boosts continual agricultural production and water resources management (Targets 2.4, 6.4). However, an e-waste management plant is necessary for handling obsolete, damaged, or faulty solar products, and devices in the country or nearby.[1,7]

The study spotted symbiosis and bargains among Rwanda's off-grid solar energy goals and targets in the context of the UN 2030 Agenda that satisfy clean energy development. Rwanda's off-grid solar energy success is attributed to the Government's unwavering support and realisation that energy (SDG7) is the prime mover and foundation for any meaningful sustainable development.

The endurance, disaster-reduction, and intra-family assessed gaps are difficult to measure, and cooling technologies are largely unnecessary because Rwanda is temperate.[1,8] Also, straightforward and coherent standards for disposing of obsolete, damaged, or faulty products, and using energy-efficient gadgets to optimise the benefits of clean energy past the rudimentary levels could be developed.

The study indicates that Rwanda's off-grid solar sector satisfactorily used SDG7 to account for 16 out of the 17 SDGs. Although a conducive environment by Government has favourably impacted electricity access and solar off-grid development, loss of livelihoods caused by the Coronavirus pandemic (COVID-19) could lead to energy poverty unless concrete cushioning measures are implemented to stem the tide.

Furthermore, the applied structural framework fails to competently track the fast-changing circumstances marked by volatile market-driven forces and new distribution patterns. Consequently, policy-makers can encourage data sharing between academia and industry practitioners by supplying funding, partnership intermediation services, and ordering a harmonised data reporting format.

The benefits of Rwanda's solar off-grid synergies and trade-offs study could be extended to other developing countries to reveal the gaps, disparities, and discontinuities that enable policymakers to use data and research results to inform decisions.

Above all, the recognition of synergies and trade-offs of using SDG7 as a metric against the UN 2030 Agenda supports the notion of concentrating on people, communities, most at-risk populations, and those "left behind".

References

1. Bisaga, I., Parikh, P., Tomei, J., and To, L.S. (2020). Mapping Synergies and Trade-Offs Between Energy and the Sustainable Development Goals: A Case Study of Off-Grid Solar Energy in Rwanda. Energy Policy. https://doi.org/10.1016/j.enpol.2020.112028
2. Niyonteze, J.D.D., Zou, F., Asemota, G.N.O., Bimenyimana, S., and Shyirambere, G. (2020). Key Technology Development Needs and Applicability Analysis of Renewable Energy Hybrid Technologies in Off-Grid Areas for the Rwanda Power Sector. Heliyon 6, 1-14. https://doi.org/10.1016/j.heliyon.2020.e03300
3. Bisaga, I., Parikh, P., Mulugetta, Y., and Hailu, Y. (2018). The Potential Performance Targets (imihigo) as Drivers of Energy Access Planning and Extending Access to Off-grid

Energy in Rural Rwanda. WIREs Energy and Environ. 2018 e310, 1-14. https://doi.org/10.1002/wene.310

4. Fuso-Nerini, F., Tomei, J., To, L.S., Bisaga, I., Parikh, P., Black, M., Borrion, A., Spataru, C., Castan Broto, V., Anandarajah, G., Milligan, B., and Mulugetta, Y. (2018). Mapping Synergies and Trade-offs between Energy and the Sustainable Development Goals. Nature Energy 10-15. https://doi.org/10.1038/s41560-017-0036-5
5. Kennedy, R., Numminen, S., Sutherland, J., and Urpeleinen, J. (2019). Multilevel customer segmentation for off-grid solar in developing countries from solar home systems in Rwanda and Kenya. Energy 186 (November 2019), 115728. https://doi.org/10.1016/j.energy.2019.07.058
6. Bimenyimana, S., Asemota, G.N.O., and Li, L. (2018). The State of the Power Sector in Rwanda: A progressive Sector with Ambitious Targets. Front. Energy Res. 6, 1-14. https://doi.org/10.3389/fenrg.2018.00068
7. Sinha Khetriwal, D., Magalini, F., and Mugabo, C. (2017). Sustainable Management of E-Waste in the Off-Grid Renewable Energy Sector in Rwanda. Energy Africa Compact – Rwanda Evidence on Demand. United Kingdom Department for International Development.
8. Bimenyimana, S., Asemota, G.N.O., Niyonteze, J.D.D., Nsengimana, C., Ihirwe, J.P., and Li, L. (2019). Photovoltaic Solar Technologies: Solution to Affordable, Sustainable, and Reliable Energy Access for All in Rwanda. International Journal of Photoenergy, Vol. 2019, 1-29. https://doi.org/10.1155/2019/5984206

APPENDIX E

This part of the thesis presents the contents of Optimisation of the eccentricity of the pyriform diagram for balancing electrical power systems loading. The study used the eccentricity of the ellipsoidal pyriform to optimise electricity consumption by drawing lines with subtended angles along and across the major and minor axes of the pyriform. The ratios of the lengths between the major and minor axes and the sine of each of the subtended angles were used to obtain the eccentricities. The eccentricities were subjected to Markov processes, Jordan Canonical transformations, and the Martingales to obtain the balanced loading of the electrical power system. The balanced loading derivable from the eccentricity optimisation was capable of changing the plant stock allocation, reducing peaking power plants assignment, and reduction in retail costs for goods and services.

E.1 Optimisation of the eccentricity of the pyriform diagram for balancing electrical power systems loading

E.2 Abstract - Electricity is a vital resource needed in any modern society for an enhanced lifestyle. Furthermore, electricity load management covers optimal power generation, transmission, distribution, and utilisation. Also, demand-side management is electricity consumption beyond the meter, and the ever-increasing electricity demand because of rising population and higher standards of living place a limitation and a constraint on its accessibility to all the citizens in any community.

The eccentricity of the pyriform scatter diagram data shape was used to characterise the statistical distribution of the electricity consumption data points around a common axis. The Markov process, the Jordan Canonical transformation, and the Martingales were used to generalise the independent electricity consumption to depend only on the outcome preceding it and not after it. The results show a balanced light loading of 50.0%. The pyriform was symmetrical, convex, and even about the midpoint, which served as the globally optimised solution to the electricity consumption balanced loading problem.

A balanced electrical power systems loading enables utilities to supply more customers, increases operational efficiencies, and places less stress on electricity generators, transmission, and distribution networks. It is recommended that the optimisation of electrical power systems loading will lead to energy efficiency, energy savings, and lower-cost operations for reliable and sustainable supply, growth, and development.

Balanced light loading of electrical power systems components facilitates optimal unit commitment at lower economic and social costs. Whenever service taxes are reduced because of cheaper electricity prices, utilities witness flatter load curves and avoided production costs across power systems operations. This further, lessens blackouts and extends the life of utility facilities.

E.3 Keywords

Balanced and light loading; energy efficiency; energy savings; Markov process; Martingales.

E.4 Introduction

Electricity load management (ELM) is used to control optimal power systems generation, transmission, distribution, and utilisation. Many scholars associate demand-side management (DSM) with ELM, but supply-side management (SSM) is included in ELM and should be considered for optimisation. This is so because inadequate energy resource optimisation at generation leads to poor power delivery down the value chain. These factors can cause large-scale inefficiencies, unstable grids, and incessant power failures that inconvenience the ultimate electricity consumer. Therefore, energy consumption increases, energy savings mechanisms with rising population, and quality of life directly impact the electricity consumption of households (Kerr, Gouldson, & Barret, 2017; Eid et al., 2016; Bimenyimana, Ishimwe, Asemota, Kemunto, & Li, 2018; Shiraki, Nakamura, Ashina, & Honjo, 2016).

Furthermore, DSM is associated with energy consumption after the electricity meter. It comprises government policies to control energy consumption for environmental sustainability, internal power security and social cohesion, demand response, and reduction of carbon footprint that could negatively impact climate change (Simoes, Nijs, Ruiz, Sgobbi, & Thiel, 2017; Warren, 2018).

A pyriform (pear-shaped) diagram is shown to be in hydrostatic stability when the flow velocity of the fluid is constant. In electrical power systems, it occurs when an external force like power is balanced by pressure gradient force, which is symmetrically rounded to an ellipsoid. It is a satisfactory approximation to flow speeds when acceleration is negligible. In astrophysics, the field compresses a star under gravitation to the most compact pyriform shape when the angular velocity is much greater than the critical angular velocity. Coincidentally,

the shapes aside from the pyriform are unstable (Wu & Karunamuni, 2014; Betterexplained, n.d.).

A pyriform scatter diagram is used to evaluate the correlation between two variables and predicts the behaviour of the dependent variable based on the measurement of the independent variable. The independent variable acts as the control because it influences the behaviour of the dependent variable. It is useful if one variable exhibits quantifiable change and the other does, not. It is also, the best approach to indicate nonlinear patterns because association points can either fall on a line or a curve as in the pyriform (Usmani, 2020).

However, the drawbacks of the scatter diagrams are that they do not provide the exact extent of correlation between variables. Also, they do not indicate the quantitative measurements of the association between variables nor indicate the associations beyond two variables.

In addition, the eccentricity of data shapes is used to characterise a statistical distribution of data points around a common axis. Eccentricity is interpreted as the fraction of the distance along the semi-major axis in which lies the focus. Eccentricity also ranges from 0 to infinity and the greater the eccentricity, the less the conic section resembles a circle (Lane & Ziemer, n.d.). Eccentricity is a measure of the deviation from being circular. It also measures how closely a conic resembles a circle. For any conic section, eccentricity is the condition of being eccentric (abnormal or irregular). It is equally the constant ratio of the distance from the directrix (a fixed-line) (Robinson, 2018; Kirkpatrick, Schwarz, Davidson, Seaton, Simpson, & Sherrard, 1983).

The objective of the study was to investigate how the eccentricity of the pyriform (pear-shaped) of the reduced electricity consumption pattern of a utility in Namibia can be used to balance electrical power systems loading.

E.5 Materials and Methods

A group of expert judges like electrical engineers, economists, and planners was used to validate a 5-point Likert scale residential electricity load management questionnaire used to gather survey data for statistical analysis in Windhoek City, Namibia. Out of the over 300 self-report questionnaires randomly distributed in Windhoek, Namibia, only 127 responses were returned. The sample size adequacy was proven in (Asemota, 2014). The statistical analysis yielded a pyriform (pear-shaped) of the reduced electricity consumption pattern that

was subsequently subjected to eccentricity analysis, the Markov process, Jordan canonical transformation, and the Martingales for balanced electrical power systems loading.

E.6 Eccentricity of the Pyriform

Lines were drawn along and across the major and minor axes of the pyriform in Figure E.1 and measurements were taken as shown in Figure E.2. Other tangent lines were also drawn to obtain angular measurements of the data points on the bimodal pyriform. The ratios between the major and minor axes lengths were used to obtain the eccentricities because the pyriform can be approximated to an ellipsoid.

The eccentricity e, is determined as (Robinson, 2018; Fun, n.d.; Weisstein, n.d.; Page, 2011):

For an ellipse, the length of the minor axis is:

$$\sqrt{(a+b)^2 - f} \tag{E.1}$$

where f is the distance between foci, a, b are the distances from each focus to any point on the ellipse.

The length of the major axis is:

$$a + b \tag{E.2}$$

where a, b were as earlier defined. Therefore:

$$e = \frac{c}{a} \tag{E.3}$$

where c is the distance from the centre of the conic section to the focus. Also,

$$e = \sqrt{1 + \frac{b^2}{a^2}} = \frac{c}{a} \tag{E.4}$$

For a hyperbola: $\left(e = \frac{c}{a} > 1\right)$; for a parabola: $(e = 1)$; for an ellipse: $(e < 1)$; for a circle: $(e = 0)$.

In addition, the eccentricity can also be calculated as (Fun, n.d.):

$$e = \frac{\sin\beta}{\sin\alpha} \tag{E.5}$$

where: $0 < \alpha < 90^0$; $0 < \beta < 90^0$.

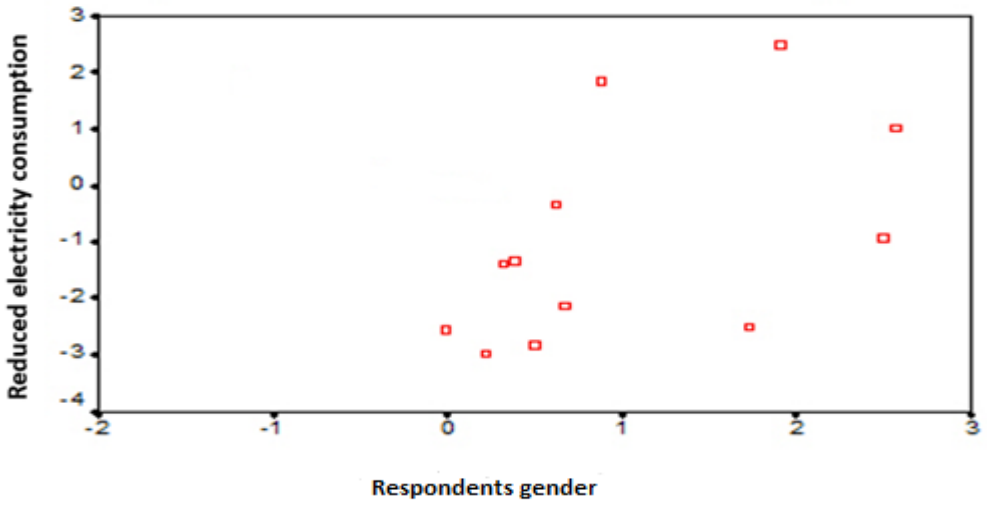

Figure E. 1: Scatter plot: Reduced electricity consumption pyriform (Asemota, 2013)

The determination of various eccentricities for the pyriform scatter diagrams are:

$$e_1 = \frac{c}{a} = \frac{6.7\ cm}{4.8\ cm} = 1.396;\ e_2 = \frac{\sin 62^0}{\sin 40^0} = \frac{0.88294759285}{0.64278760968} = 1.374;$$

$$e_3 = \frac{\sin 70^0}{\sin 40^0} = \frac{0.9396922078}{0.64278760968} = 1.462;\ e_4 = \frac{\sin 28^0}{\sin 40^0} = \frac{0.46947156278}{0.64278760968} = 0.730;$$

$$e_5 = \frac{\sin 77^0}{\sin 40^0} = \frac{0.97437006478}{0.64278760968} = 1.516;\ e_6 = \frac{\sin 45^0}{\sin 40^0} = \frac{0.70710678118}{0.64278760968} = 1.100;$$

$$e_7 = \frac{\sin 65^0}{\sin 40^0} = \frac{0.90630778703}{0.64278760968} = 1.410;\ e_8 = \frac{\sin 83^0}{\sin 40^0} = \frac{0.99254615164}{0.64278760968} = 1.544.$$

Mainly because the eccentricities calculated above were all almost greater than unity, it can be partially concluded that the pyriform (pear-shaped) scatter diagram is a hyperbola. A hyperbola is a smooth curve lying in a plane, which is defined by its geometric properties or by equations that form its solution set (Mathwarehouse, n.d.). Also, and because there was one of the eccentricities ($e_4 < 1 \approx 0.730$) less than unity, the pyriform scatter diagram can be best described as a platykurtic ellipsoidal bimodal pyriform. This is so because, there was a small tail, a dimple, two lobes, and an outer curve representing an ellipsoid (not shown, but can be gleaned from the shape of the pyriform).

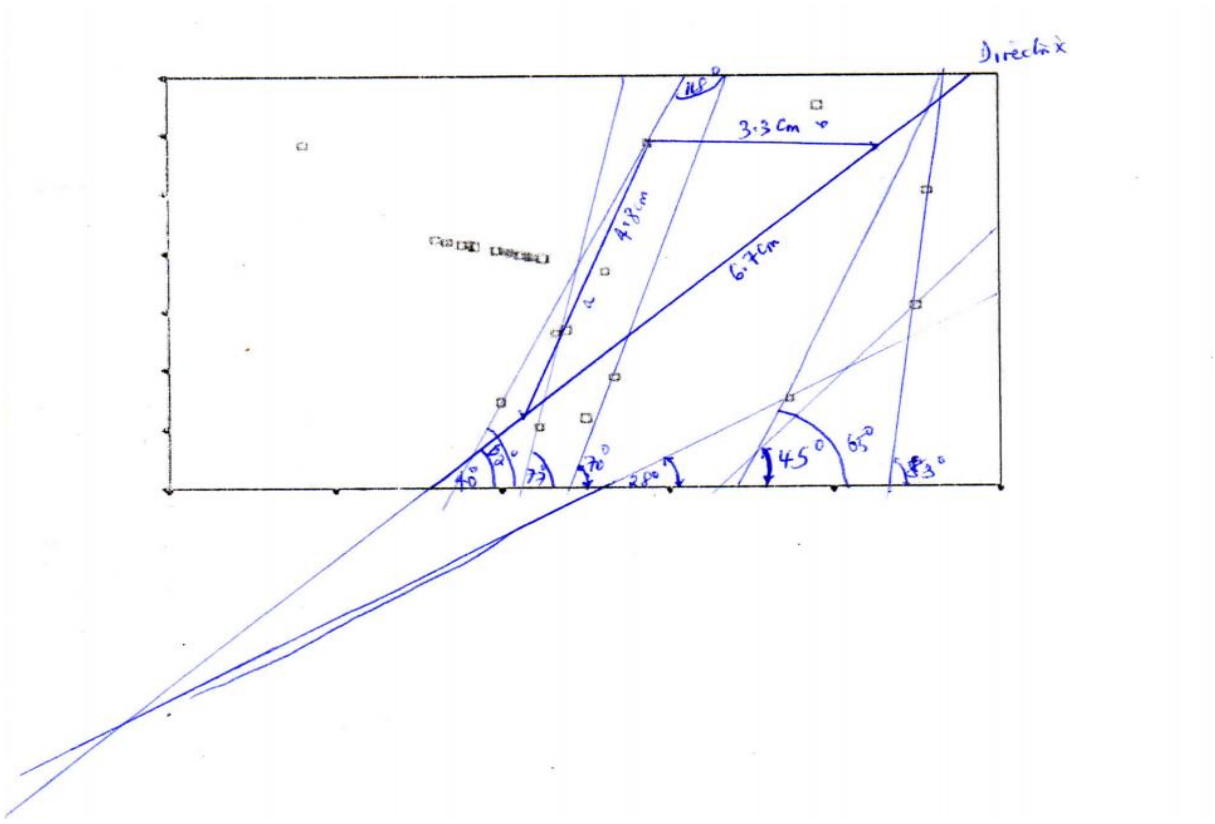

Figure E. 2: Eccentricity measurement lines for the reduced electricity consumption pyriform

E.7 Markov Process

Markov processes are the simplest generalisations of independent processes. They permit the outcome at any instant to depend only on the outcome preceding it and none before that. In a Markov chain, the system can occupy a finite or countably infinite number of states $e_1, e_2, \dots, e_k$. The future evolution of the process depends only on the present and not how it arrived at that state. A stochastic process is a non-countable infinity of random variables, one for each t (Papoulis & Pillai, 2008). The equation of the pyriform is (McGraw-Hill & Parker, 2003): $y = -ax^4 + bx^3$ (E.6)

Classification of states.

$$\begin{pmatrix} -ax^4 & 0 & 0 & 0 & 0 \\ 0 & bx^3 & 0 & 0 & 0 \\ 0 & 0 & 0 & 0 & 0 \\ 0 & 0 & 0 & 0 & 0 \\ 0 & 0 & 0 & 0 & 0 \end{pmatrix} \quad \text{(E.7)}$$

For given states e_k and e_l, if the probability $P_{kl}^{(n)} > 0$, for some n, there is a positive probability of getting to e_l starting from e_k in n steps. Hence, the state e_l is accessible from

e_k. If e_k and e_l are accessible from each other, then e_k communicates with e_l. If every Markov state is accessible from every other state, in many transitions, then it is an irreducible communicating chain (Papoulis & Pillai, 2008; Patil, Nagaraju, & Deasi, 2012).

For the 5×5 pyriform transition matrix,

$$Q = \begin{pmatrix} a_{11} & 0 & 0 & 0 & 0 \\ 0 & a_{22} & 0 & 0 & 0 \\ 0 & 0 & 0 & 0 & 0 \\ 0 & 0 & 0 & 0 & 0 \\ 0 & 0 & 0 & 0 & 0 \end{pmatrix} \tag{E.8}$$

where $a_{kl} > 0$ are positive probabilities. But a_{11} and a_{22} are the only nonzero entries in rows 1 and 2. By the Jordan canonical transformation, $a_{11} \equiv 1$ and $a_{22} \equiv 1$. Therefore, e_1 and e_2 are absorbing states. This is so because, both e_1 and e_2 are closed sets on themselves. They also communicate with each other, as irreducible communicating chains (Papoulis & Pillai, 2008; Patil et al., 2012).

In addition, $Q_1 = a_{11}, Q_2 = a_{22}, Q_3 = 0, Q_4 = 0$

$$Q_4 \triangleq [W, X] = 0 \tag{E.9}$$

$$\begin{pmatrix} 1 & 0 & 0 & 0 & 0 \\ 0 & 1 & 0 & 0 & 0 \\ 0 & 0 & 0 & 0 & 0 \\ 0 & 0 & 0 & 0 & 0 \\ 0 & 0 & 0 & 0 & 0 \end{pmatrix} \begin{pmatrix} -ax^4 \\ bx^3 \\ 0 \\ 0 \\ 0 \end{pmatrix} \tag{E.10}$$

Whenever the row sums and column sums are each unity, the transition matrix Q, is termed a doubly stochastic matrix. Therefore, the pyriform is an irreducible doubly stochastic communicating Markov chains with two absorbing states.

E.8 Martingales

A Markov chain is a martingale if for every k, the expectation of the probability distribution $\{q_{kl}\}$ equal k. Hence, in a martingale

$$\sum_l l q_{kl} = k \tag{E.11}$$

Let $e_0, e_1, \dots, e_N$ be states in a martingale, with $k = 0$ and $k = N$ in (E.11), we have

$q_{00} = q_{NN} = 1.$

Thus, e_0 and e_N are absorbing states. If we assume these to be persistent states in the chain, then $e_1, e_2, \dots, e_{N-1}$ are transient states (Papoulis & Pillai, 2008). The system is finally absorbed into e_0 or e_N. From (E.11), and by induction, we have

$\sum_l^N hq_{lh}^{(n)} = l$ (E.12)

for all n.

From the above equation (E.12), the expectation value becomes

$E\{\mathbf{x}_{n+m}|\mathbf{x}_m\} = \mathbf{x}_m$ for all n and m.

This is the definition of a martingale (Papoulis & Pillai, 2008).

Also, $q_{lh}^{(n)} \to 0$ for every transient state e_h, $h = 1,2,\dots,N-1$, for $l > 0$ in (E.12). Substituting appropriate values into (E.12) gives the only solution

$q_{lN}^{(n)} \to \frac{l}{N}$ (E.13)

Simply because there are only two absorbing states in the pyriform, we obtain

$q_{l.0}^{(n)} \to 1 - \frac{l}{N}$ (E.14)

If the system starts with e_l, the probability of the final absorption into e_0 and e_N are $1 - \frac{l}{N}$ and $\frac{l}{N}$, respectively (Papoulis & Pillai, 2008). If all states are equally likely, to begin with, then the probability of the final absorption into e_N is

$\lim_{n\to\infty} \sum_{l=0}^N q_l^{(0)} q_{l,N}^{(n)} = \sum_{l=1}^N \frac{1}{N+1} . \frac{l}{N} = ½$ (E.15)

Therefore, for a randomly chosen initial distribution, the final absorption into either e_0 or e_N are both equally likely events for a finite state of the martingale (Papoulis & Pillai, 2008). For the pyriform absorbing states, only a_{11} and a_{22} are admissible states. Regardless of the model formulation procedure, and beginning from an initial state e_l, the final absorption probabilities into e_0 and e_N are $1 - \frac{l}{N}$ and $\frac{l}{N}$, respectively.

Whenever this procedure is likened to breeding in genetics, only absorbing states (pure breeds) are allowed, while mixed breeds gradually go extinct (Papoulis & Pillai, 2008). Therefore, the probability of the final absorption into either a_{11} or a_{22} of the pyriform absorbing states is a half (0.5). This is also the optimal (best) solution to the pyriform electrical power systems balanced loading problem under investigation in this study. It also perfectly agrees with the Quetelet curve optimisation solution of the mid-point percentile (0.5) using the multivariate approach (Papoulis & Pillai, 2008; Jahoda, 2015). It was also found to be a convex set (Bishop, 2008; Asemota, 2009). This local optimum was equal to the global optimum in the interval of convexity.

E.9 Results

The eccentricities of the reduced electricity consumption pyriform were 1.396, 1.374, 1.462, 0.730, 1.516, 1.100, 1.410, and 1.544, respectively. Therefore, the pyriform scatter diagram can be best described as a platykurtic ellipsoidal bimodal pyriform. This is so because, there was a small tail, a dimple, two lobes, and an outer curve representing an ellipsoid (not shown, but can be gleaned from the shape of the pyriform). Also, the reduced electricity consumption pyriform is an irreducible doubly stochastic communicating Markov chains with two absorbing states. Above all, the probability of the final absorption into either a_{11} or a_{22} of the reduced electricity consumption pyriform absorbing states is a half (0.5).

This is also the optimal (or best) solution to the pyriform electrical power systems balanced loading problem in this study. The quantity of information we receive from a random variable depends on the amount of "surprise" we learn from the value. Thus, a less probable event contains more information than a very likely event. This is so because the certainty of an event occurring has no information content. Hence, the measure of the information content depends on the monotonic probability distribution function. Also, the information received is the sum of the information received from each of the events separately. If there are relatively fewer scores in the tails of the pyriform, the shape is platykurtic, otherwise, it is leptokurtic. If the distribution has short tails, it is platykurtic, because the distribution differs in kurtosis.

Furthermore, the eccentricity of data shapes describes the statistical distribution of data points around a common axis. Eccentricity is interpreted as the fraction of the distance along the semi-major axis in which lies the focus. Eccentricity also ranges from 0 to infinity and the greater the eccentricity, the less the conic section resembles a circle. Eccentricity is a measure of the deviation from being circular. It also measures how closely a conic resembles a circle.

For any conic section, eccentricity is the condition of being eccentric (abnormal or irregular). It is equally the constant ratio of the distance from the directrix (or a fixed line). In addition, if every Markov state is accessible from every other state, in a number of transitions, then it is an irreducible communicating chain.

E.10 Discussion

The pyriform (Figure 1) of the scatter diagram has a bimodal distribution because it has two peaks. If there are relatively fewer scores in its tails, the shape is platykurtic, otherwise, it is leptokurtic. If the distribution has short tails, it is platykurtic, because the distribution differs in kurtosis (Lane & Ziemer, n.d.). If e_k and e_l are accessible from each other, then e_k communicates with e_l. This is so because both e_k and e_l are closed sets on themselves. If every Markov state is accessible from every other state, in many transitions, then it is an irreducible communicating chain (Papoulis & Pillai, 2008; Patil et al., 2012).

Whenever the row sums and column sums are each unity, the transition matrix Q, is termed a doubly stochastic matrix (Papoulis & Pillai, 2008). Therefore, the reduced electricity consumption pyriform is an irreducible doubly stochastic communicating Markov chain with two absorbing states. A half $(1/2)$ is also the optimal and best solution to the pyriform electrical power systems balanced loading problem under investigation in this study.

It also perfectly agrees with the Quetelet curve optimisation solution of the mid-point percentile (0.5) using the multivariate approach (Papoulis & Pillai, 2008; Jahoda, 2015). It was also found to be a convex set. This local optimum is equal to the global optimum in the interval of convexity (Bishop, 2008; Asemota, 2009). The fifty percent average electrical power systems loading achieve optimal or balanced loading without hotspots or localised heating.

Further, any local optimum is also a global optimum, provided the constraints define a convex region. Also, these optimisation results describe linear functionals (Bishop, 2008), where the gradient indicates the direction of the greatest change along the line of equipotential or equal energy (Betterexplained, n.d.). The reduced electricity consumption pyriform optimisation is necessary for electricity network expansion planning because the utility can supply more electricity consumers.

Also, the transmission lines infrastructure can evacuate rising electricity generation and consumption capacities because of average and balanced loading. Balanced electrical power systems loadings can support, enhance, and strengthen optimal power systems operators' responses in emergencies (Asemota, 2012; Hu, Bie, Ding, & Lin, 2016). Electrical power systems balanced loading increase and maximise cost-benefit ratios, which enhance reliability improvements, and reduce operational costs against initially high optimal power generation, transmission, and distribution investments.

Further, to minimise total investment costs, transmission lines losses, and optimally and efficiently engage electricity production units that satisfy future load growth having additional security and operational constraints (Asemota, 2012; Hu et al., 2016). In addition, the Quetelet index is used to create awareness, education, and behaviour modification especially among the average citizens on energy efficiency for affordable, reliable, and sustainable electricity supply (Asemota & Ijumba, 2022).

E.11 Conclusion

The reduced electricity consumption pyriform optimisation is necessary for electricity network expansion planning because the utility can supply more electricity to consumers. Also, the transmission lines infrastructure can evacuate rising electricity generation and consumption capacities because of average and balanced loading. Balanced electrical power systems loadings can support, enhance, and strengthen optimal power systems operators' responses in emergencies. Electrical power systems balanced loading increase and maximise cost-benefit ratios, which enhance reliability improvements, reduce operational costs against initially high optimal power generation, transmission, and distribution investments. Further, to minimise total investment costs, transmission lines losses, and optimally and efficiently engage electricity production units that satisfy future load growth having additional security and operational constraints. In addition, the Quetelet index is used to create awareness, education, and behaviour modification, especially among the average citizens on energy efficiency for affordable, reliable, and sustainable electricity supply.

Also, the 50.0% or balanced electrical power systems loading proposed in this study could lead to a change in plant stock, increase base power plants, and reduce peaking power plants, tariffs, and fuel costs. Higher combustion efficiency and higher sunk capital costs could lead to reduced capacity costs, with costs spread across greater units of output. Other benefits include reduced transmission and distribution charges; retail costs of goods and services; service taxes; and gains from flatter load curves and avoided production costs across power systems operations.

References

Asemota, G. N. O. (2009). On a class of computable convex functions, *Canadian Journal of*

Pure and Applied Sciences, 3(3), 959-965.

Asemota, G. N. O. (2012). Optimal two-way conductor design using computable convex functions approach, *Advances in Materials Research, 367*, 75-81. doi:10.4028/www.scientific.net/AMR.367.75

Asemota, G. N. O. (2013). *Electricity Use in Namibia.* Indiana: iUniverse.

Asemota, G. N. O. (2014). Communality performance assessment of electricity load management model for Namibia, *IEEE-AIMS 2nd International Conference on Artificial Intelligence, Modelling and Simulation.* (pp. 252-257). New Jersey: IEEE.

Asemota, G. N. O., & Ijumba, N. M. (2022). Using blinds, day-lighting, and geyser temperature settings to reduce electricity consumption and pricing patterns in energy-efficient buildings, *South African Institute of Electrical Engineers-Africa Research Journal*, 113(1), 4-19. DOI: 10.23919/SAIEE.2022.9695422

Betterexplained. (n.d.). Vector calculus: Understanding the gradient- better Explained. Retrieved from: https//betterexplained.com/articles/vector-calculus-understanding -the-gradient/, Accessed on: Nov. 17, 2018

Bimenyimana, S., Ishimwe, A., Asemota, G. N. O., Kemunto, C. M., & Li, L. (2018). Web-based design and implementation of smart home appliances control system. (pp. 1-9). *IOP Conference Series: Earth Environmental Science, 168*.

Bishop, C. M. (2008). *Pattern recognition and machine learning.* Singapore: Springer.

Eid, C., Bollinger, A. L., Koirala, B., Scholten, D., Facchinetti, E., Lilliestan, J., & Hakvoort, R. (2016). Market integration of local energy systems: Is local energy management compatible with European regulation for retail competition? *Energy*, *114*, 913-922.

Fun, T. P. (n.d.). Bisection of the eccentricity. National University of Singapore. Retrieved from: www.math.nus.edu.sg/aslaksen/projects/tpf.pdf. Accessed on: Dec. 20, 2018

Hu, Y., Bie, Z., Ding, T., & Lin, Y. (2016) An NSGA-II based multi-objective optimization for combined gas and electricity network expansion planning, *Applied Energy*, *167*, 280-293.

Jahoda, G. (2015). Quetelet and the emergence of the behavioral sciences, *SpringerPlus, 4*, 473. Retrieved from: https://www.ncbi.nlm.nih.gov/pmc/articles/PMC4559562/, Accessed on: Jul. 30, 2018

Kerr, N., Gouldson, A., & Barret, J. (2017). The rationale for energy efficiency policy: Assessing the recognition of the multiple benefits of energy efficiency retrofit policy. *Energy Policy, 106*, 212-221.

Kirkpatrick, E. M., Schwarz, C. M., Davidson, G. W., Seaton, M. A., Simpson, J., & Sherrard, R. J. (1983). Chambers 20th Century Dictionary. Edinburgh: Chambers.

Lane, D. M., & Ziemer, H. (n.d.). Chapter 1: Introduction section-Distributions. Retrieved from: Onlinestatbook.com/2/introduction/distributions.html. Cited: Dec. 20, 2018

Mathwarehouse.com. (n.d.) Hyperbola. Accessed on: Dec. 22, 2018 Retrieved from: https://www.mathwarehousecom/hyperbola/graph-equation-of-a-hyperbola.php

McGraw-Hill., & Parker, S. P. (2003). *McGraw-Hill dictionary of scientific and technical terms* (6th ed.). New York: McGraw-Hill.

Page, J. (2011). Major/minor axes of an ellipse. Retrieved from: https:/www.mathopen.ref.coin/ellipse axes.html, Accessed on: Nov. 18, 2018

Papoulis, A., & Pillai, S. U. (2008). *Probability, random variables and stochastic processes* (4th ed.). New Delhi: Tata McGraw-Hill.

Patil, S., Nagaraju, P., & Deasi, S. (2012). Study of the behavior models based on probability and time using Markov process and transition. *International Journal of Computer Science & Engineering, 4*(3), 512-521. Retrieved from: www.enggjournals.com/ijcse/doc/IJCSE12-04-018.pdf, Accessed on: Nov. 10, 2019

Robinson, A. (2018). How to calculate eccentricity. Accessed: Dec. 20, 2018 Retrieved from: https://sciencing.com.com/how-to-calculate-eccentricity-12751764.html

Shiraki, H., Nakamura, S., Ashina, S., & Honjo, K. (2016). Estimating the hourly electricity profile of Japanese households-Coupling of engineering and statistical methods. *Energy, 114*, 478-491.

Simoes, S., Nijs, W., Ruiz, P., Sgobbi, A., & Thiel, C. (2017). Comparing policy routes for low-carbon power technology deployment in EU-an energy systems analysis. *Energy Policy, 101*, 353-365.

Usmani, F. (2020). What is a Scatter Diagram [A Correlation Chart?]. PM Study Circle. Retrieved from: https://pmstudycircle.com, Accessed on: Feb. 26, 2020

Warren, P. (2018). Demand-Side Policy: Global evidence base and implementation patterns. *Energy & Environment, 0*(0), 1-26.

Weisstein, E W. (n.d.). Eccentricity. mathworld-A wolfram web resource. Retrieved from: http://mathworld.woffram.com/Eccentricty.html, Accessed on: Dec. 22, 2018

Wu, J., & Karunamuni, R. J. (2014). Profile Hellinger distance estimation statistics. *Journal of Theory & Applied Statistics.* doi: 10.1080/02331888.2014.946928

APPENDIX F

This part of the thesis presents Shielding and Thermostatic Control for Optimal Electricity Load Management. The shielding and thermostatic control model was developed using the covariant-correlation procedure and logistic regression interaction cross lines through predictive analytics. There were no multicollinearity problems or biases in the data. However, the photo-electro-mechanical receptor and transduction processes are not well understood.

F.1. Shielding and Thermostatic Control for Optimal Electricity Load Management

F.2. ABSTRACT

Blinds systems, daylighting, natural convection, and shielding thermostats from heating appliances are known to reduce electricity consumption, reduce energy wastage, reduce energy bills, reduce spurious errors in thermostatic controls, reduces over-heating of compressors, reduces the incidence of burnt motors, and fire hazards. Predictive modeling using the multivariate logistic stepwise statistical procedure selects from a set of independent variables of electricity load management survey data gathered from Windhoek City, Namibia to develop the best and optimal model in the study. The results indicate that keeping heat-producing appliances away from the thermostat so that it can give accurate readings is highly interconnected to using blinds systems to reduce inlet heat in summer and heat loss in cold months. Also, small changes in data values can lead to large coefficient estimates and there is a perfect (100.0%) correlation between the dependent and independent variables. In addition, the proportion of the variance explained in the developed model was 97.0%. However, there were also no multicollinearity problems in the data and the developed model was optimal and fairly accurate.

F.3. Keywords: blinds systems, daylighting, energy balance, energy savings, energy consumption, waste reduction

F.4. INTRODUCTION

Electricity supply shortages in the Southern Africa Development Community (SADC) countries prompted demand-side management (DSM) programmes and load shedding that negatively impacted many countries' socio-economic development [1-2]. Namibia secured enough energy beyond August 2016's winter without expecting load shedding. It could

acquire 40.0% of energy locally and the remaining 60.0% from Zambia and Zimbabwe [3]. Namibia's electricity demand rose significantly in 2012 because of the mining sector, and Eskom supplies over 80.0% of the electricity [4]. Liquid fuel is over 63.0% of the total net energy consumption [5] and flat load curves in the energy sector because of expanding mining activities [6]. Also, Namibia's electricity price and industrial tariffs are high, and South Africa's rates are 20.0 to 25.0% lower [7].

The majority of the poor, unemployed, and rural Namibians cannot afford high electricity prices. Also, Namibia's harsh environment and water stress necessitated the Van Eck dry-cooling station in Windhoek [8], and the cooling water needed is the same as the United Kingdom's thermal electricity generation fleet [9]. Furthermore, 18.0% of the United Kingdom's households were fuel-poor in 2012. Blinds systems (curtains, shutters, and shade) over windows and doors reduce inlet heat by 50.0% in summer and 25.0% in heat outlets in winter [10]. Daylighting controls offer commercial benefits in the US because around 75.0% of the electricity was consumed in buildings nationwide. Daylighting reduces a third of total building energy costs [11].

The total electric energy consumed in commercial buildings is between 35.0% and 50.0%. Between 10.0% and 20.0% of the energy used for cooling buildings can be saved by daylighting [12]. Based on building architecture, usage, and energy consumption patterns, daylighting could trim electric lighting between 20.0% and 80.0% [13]. Turning off and dimming lights when not needed saves between 10.0% and 20.0% of the energy used for cooling a building. This also increases employees' productivity and improves the health of building occupants [14].

Also, above US$60 billion was expended annually for electric lighting which comprises over 37.0% average commercial building's total energy consumption [15]. Additionally, over 64 billion square feet of commercial buildings floor space is lit by fluorescent systems, and anywhere between 30.0% and 50.0% of the spaces can access daylight either by skylights or through windows. Consequently, millions of electric lighting fixtures can be turned off for some periods of the day for energy savings returns [16].

The United Kingdom and the United States of America have fully developed electricity markets, which effectively control their power systems' peak loads [17]. Also, negative pricing exists in all areas of the United States, which reflects a seasonal distribution and a raised frequency [18]. Price volatility caused by renewable energy injection with government incentives, negative price signals caused by over-supply, and price spikes caused by over-

demand, form the basis for electricity load management, future planning, and policy. To balance the impacts of electricity over-supply against over-demand, we formulate a shielding and thermostatic control model using the correlation-covariance method.

F.5. MATERIALS AND METHODS

F.5.1.Sample size adequacy

A 5-point Likert scale questionnaire designed for the residential electricity load management survey was validated by a panel of expert judges and used to gather electricity consumption data in Windhoek City, Namibia. Only 127 responses out of the over 300 questionnaires administered were analysed by the statistical analysis for the social sciences (SPSS). Also, the adequacy of the 127 sample size was proven in [19].

Alternatively, the sample size adequacy is proven using the Poisson distribution. The variance becomes:

$$\sigma = \left\{\frac{1}{N}\sum_{i=1}^{N}(l_i - \mu)^2\right\}^{\frac{1}{2}} \quad \text{(F.1)}$$

where μ is the sample average, l_i average results, and N sample size [20]. We invoke the Normal distribution if the errors are many and independent. The spread of the mean (μ) and the variance (σ), are good estimators of the distribution. For a normal distribution, the probability range is $[\mu - \sigma, \mu + \sigma]$:

$$A(\sigma) = \int_{\mu-\sigma}^{\mu+\sigma} P_G(\mu, \sigma, t)dt = 0.68 \quad \text{(F.2)}$$

where P_G is the probability function and t is time. For 100 measurements, each consisting of 127 measurements, 68.0% lie between $(\mu - \sigma)$ and $(\mu + \sigma)$.

Let $\mu \equiv Np$ (F.3)

As the probability: $p \to 0$, $N \to \infty$, μ is constant, the binomial distribution approaches a Poisson distribution:

$$P_p(n, \mu) = \frac{\mu^n}{n!}e^{-n} \quad \text{(F.4)}$$

However, the mean and the variance of the Poisson processes are equal. Hence, its occupancy for any sample is $(n)^{\frac{1}{2}}$ and 68.0% is the probability that the true value is within $\left[127 \mp (127)^{\frac{1}{2}}\right]$. The true sample size lies between 116 and 138, so the 127 samples used for the study are adequate for the study.

F.5.2 Correlation between dependent and independent variables

The correlation coefficient $r_{x,y}$ between $\{y_i\}$ and $\{x_i\}$:

$$r_{x,y} \equiv \frac{\sigma_{x,y}^2}{\sigma_x \sigma_y} = \frac{\sum_{i=1}^{N} \frac{1}{\sigma_i^2}(x_i-\mu_x)(y_i-\mu_y)}{\left\{\sum_{i=1}^{N} \frac{1}{\sigma_i^2}(x_i-\mu_x)^2\right\}^{1/2}\left\{\sum_{i=1}^{N} \frac{1}{\sigma_i^2}(y_i-\mu_y)^2\right\}^{1/2}} \quad \text{(F.5)}$$

where the mean values of y_i and x_i are given by:

$$\mu_x = \left(\sum_{i=1}^{N} \frac{1}{\sigma_i^2}\right)^{-1} \sum_{i=1}^{N} \frac{1}{\sigma_i^2} x_i = \frac{\beta}{\alpha} \quad \text{(F.6a)}$$

$$\mu_y = \left(\sum_{i=1}^{N} \frac{1}{\sigma_i^2}\right)^{-1} \sum_{i=1}^{N} \frac{1}{\sigma_i^2} y_i = \frac{\theta}{\alpha} \quad \text{(F.6b)}$$

From equations F.6a and F.6b, we have the variances for the distributions of $\{x_i\}$ and $\{y_i\}$:

$$\sigma_x^2 = \left(\sum_{i=1}^{N} \frac{1}{\sigma_i^2}\right)^{-1} \sum_{i=1}^{N} \frac{1}{\sigma_i^2} (x_i - \mu_x)^2 \quad \text{(F.7a)}$$

$$\sigma_y^2 = \left(\sum_{i=1}^{N} \frac{1}{\sigma_i^2}\right)^{-1} \sum_{i=1}^{N} \frac{1}{\sigma_i^2} \left(y_i - \mu_y\right)^2 \quad \text{(F.7b)}$$

The covariance between x and y:

$$\sigma_{x,y}^2 = \left(\sum_{i=1}^{N} \frac{1}{\sigma_i^2}\right)^{-1} \sum_{i=1}^{N} \frac{1}{\sigma_i^2} (x_i - \mu_x)\left(y_i - \mu_y\right) \quad \text{(F.8)}$$

That means, $r_{x,y}^2$ is related to the slope of y_i as a function of x_i [20].

F.6. RESULTS AND DISCUSSION

The results of the study are shown in Fig. F.1 and Tables F.1-F.3. Fig. F.1 is a combination of "H" cubic, growth, and logistic regression interaction cross-lines. The attribute of keeping heat-producing appliances from thermostats for accurate readings is independent of gender. This is so because the two parallel lines [21] are standing on 1.0 (male) and 2.0 (female) respectively on the $y-$axis. Similarly, the observed, cubic, logistic, and growth regression lines are horizontal. These cross-lines indicate that the respondents were rather indifferent in keeping heat-producing appliances away from thermostats, although their levels of agreement hovered around not sure (3) and agree (2).

Table F.1 indicates a perfect (100.0%) positive correlation of keeping heat-producing appliances away from thermostats occurring together with using blinds systems to reduce inlet heat in summer and heat loss in cold months. Also, the model covariance indicates the directional relationship of keeping heat-producing devices from thermostats for accurate readings vary concomitantly by 1.8% with the dependent variable. Also, the correlation measures the strength and direction of linear relationships [21].

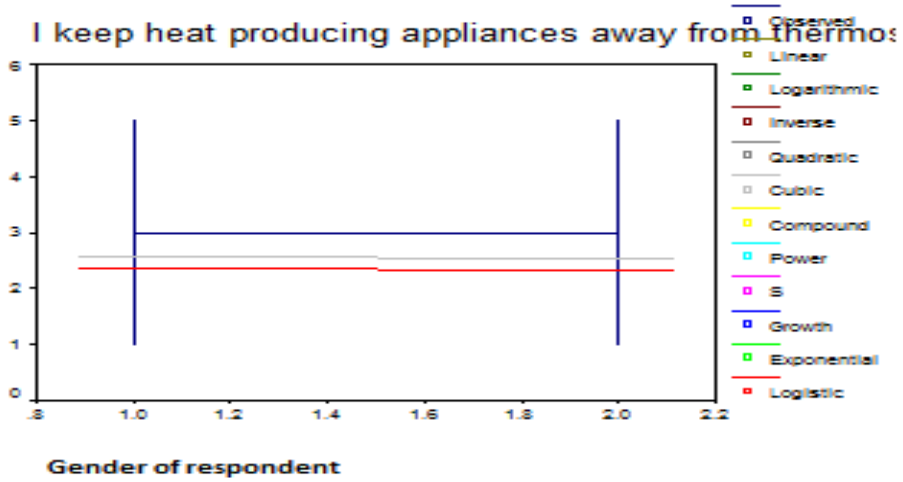

Figure F. 1: I keep heat-producing appliances away from the thermostat so that it can give accurate readings

Table F.2 tests whether there are severe problems of multicollinearity. The small changes in the data values can lead to large changes in the estimates of coefficients. The 0.064 eigenvalue of Dimension 2 that is close to 0.0, indicates that keeping heat-producing appliances away from thermostats and using blinds systems to reduce inlet heat in summer and heat loss in winter are highly interconnected operations. The condition index values greater than 15 indicate possible problems of collinearity [22]. But, Dimensions 1 and 2 of model 1 indicate that there are no collinearity problems in the data because the Condition indices are less than 15 [22]. That means, 3.0% of keeping heat-producing appliances from thermostats give accurate readings in the first Dimension while 97.0% was the explained variance in Dimension 2.

Table F.3 indicates the residual statistics of the model, which is the degree to which a model accounts for the variation in the observed data. Residuals check for bias. The standardised residual should be less than -2 or greater than 2. Ordinarily, we expect 95.0% of cases to have standardised residuals within ± 2.0 [22]. For a sample of 127, 6 cases (5.0%) are expected to have standardised residuals outside these limits: Therefore, our sample is what we expected it to be and that it conforms to a fairly accurate model.

Table F. 1: Coefficient Correlations(a)

Model			I keep heat-producing appliances away from the thermostat so that it can give accurate readings
1	Correlations	I keep heat-producing appliances away from thermostat so that it can give accurate readings	1.000
	Covariances	I keep heat-producing appliances away from the thermostat so that it can give accurate readings	.018

a Dependent Variable: Using blinds, shutters, shade can reduce inlet heat in summer and heat loss in cold months

Table F. 2: Collinearity Diagnostics(a)

Model	Dimension	Eigenvalue	Condition Index	Variance Proportions	
				(Constant)	I keep heat-producing appliances away from the thermostat so that it can give accurate readings
1	1	1.936	1.000	.03	.03
	2	.064	5.505	.97	.97

a Dependent Variable: Using blinds, shutters, shade can reduce inlet heat in summer and heat loss in cold months

Table F. 3: Residuals Statistics(a)

	Minimum	Maximum	Mean	Std. Deviation	N
Predicted Value	1.6958	3.6596	2.5154	.50464	121
Residual	-2.6596	3.3042	-.0361	1.04128	121
Std. Predicted Value	-1.5910	2.5270	.1280	1.05800	121
Std. Residual	-3.6010	4.4740	-.0490	1.41000	121

a Dependent Variable: Using blinds, shutters, shade can reduce inlet heat in summer and heat loss in cold months

F.7. CONCLUSION

Conclusively, shielding and thermostatic control are independent of the gender of respondents, and electricity consumers are either indifferent or oblivious of the costs of spurious dynamic thermostatic control due to energy wastage. There was a perfect (100.0%)

positive correlation between keeping heat-producing appliances away from thermostats. Also, using blinds systems to reduce energy loss and thermostatic controls are highly interconnected operations. Therefore, small changes in the data values can lead to large changes in the estimates of the coefficients. Because the condition indices are less than 15 it means that there are no collinearity problems in the data and a fairly accurate model was developed.

The 1.8% self-covariance core are single-valued, efficient, anonymous, and weak positive homogenous shifts that are solution vectors and their multipliers of the thermostatic control problem. The drag coefficients and wind profiles could lead to irregular compressor cooling, irregular and localised ambient temperatures. It is also a challenge to be able to trace the principle of "constant safety factor" in thermostatic adaptive response to photo-electro-mechanical stimuli. This is so because neither the photo-electro-mechanical receptor nor the signal transduction process is well understood.

Moreover, shielding thermostat from heat-producing appliances is a good optimal load management practice because incorrect temperature measurements by thermostats make air conditioners overwork and burn their motors as a result.

REFERENCES

[1] Bimenyimana S, Ishimwe A, Asemota GNO, Kemunto CM, Li L. Web-based design and implementation of smart home appliances control system. In: IOP Conf Series: Earth Environ Sci 2018; 168: 1-9.

[2] Shilamba PI. Update on the current power supply and progress made on NamPower projects and initiatives to ensure security of supply in Namibia. Media Briefing, Windhoek; 13 April, 2015.

[3] Anon. No power cuts expected in Namibia-Energy Minister. New Era Newspaper, Namibia; March 24 2016.

[4] Isaaks W. Energy situation in Namibia. Africa Energy Forum (AEF), Barcelona, Spain; 2013.

[5] Manuel V. Energy demand and forecasting in Namibia: Energy for economic development. Office of the President. Windhoek; 2013.

[6] Simshauser P, Downer D. Dynamic Pricing and the Peak Electricity Load Problem. The Australian Econ Rev 2012; 45(3): 305-324.

[7] Brandt E. Namibia's high electricity price. New Era Newspaper, Namibia; 14 November, 2014.

[8] Warren P. Demand-Side Policy: Global evidence base and implementation patterns. Energy & Env 2018: 1-26.

[9] Asemota GNO. Electricity use in Namibia. Indiana: iUniverse; 2013.

[10] Murrant D, Quinn A, Chapman L, Heaton C. Water use of the UK thermal electricity generation fleet by 2050: Part 2 quantifying the problem. Energy Policy 2017; 108: 859-874.

[11] Electricity Control Board. 2005 ECB annual report. Windhoek; 2006.

[12] von Oertzen D. Namibia's Electricity Supply. VO Consulting. Swakopmund: Namibia; 2009.

[13] Solatube. Daylighting Facts & Figures. 150516 Daylighting Facts & Figures-plain.pdf

[14] Ander G. Day-lighting: Whole building design guide. 2011.

[15] Stauffner N. Daylight device lightens electricity cost. MIT News 2007.

[16] Kozlowski D. Using daylighting to save on energy costs. FacilitiesNet 2006.

[17] Mocherniak T. Lighting technologies produce energy savings. Energy and Power Mgt 2006.

[18] Leslie RP, Raghavan R, Howlett O, Eaton C. The potential of simplified concepts for daylight harvesting. Lighting Res and Tech 2005.

[19] Asemota GNO. Communality performance assessment of electricity load management model for Namibia. In: 2nd IEEE-AIMS Int. Conf. 2014;252-257.

[20] Wong SSM. Computational methods in physics and engineering. 2nd ed. Singapore: World Scientific; 1997.

[21] Frost J. Understanding interaction effects in statistics. 2017.

[22] Field A. Discovering statistics. Linear models: Looking for bias. 2016.

APPENDIX G

This part of the thesis presents the Energy Efficiency of an Optimal Multidimensional Electricity Load Management Model. Energy management is important for understanding energy demand reduction and lessening carbon footprints. This is so because lower energy demand incentives are driven by measurements of supposedly negative quantities like energy savings, return on investment, and connected bias. The methods used in the analysis include log-likelihood ratio, asymptotes, Neyman-Pearson procedure, joint significance, charted likelihood ratio, amygdaloid diffused diagram analysis, and Durbin-Watson statistics. However, the amygdaloid is the most stable form of energy consumption that can help to determine lesser electricity utilisation patterns and reduce the amount spent on bills. Also, the proposed model could influence electricity costs, load growth, and lower carbon footprints.

G.1. Energy Efficiency of an Optimal Multidimensional Electricity Load Management Model

G.2. *Abstract*

Energy efficiency and energy management have a lot of benefits, but there is an understanding that demand-side energy programmes have been deemphasised for supply-side alternatives. Consequently, energy generation assets have been greater than those for lessening demand and carbon footprints. Therefore, an electricity load management questionnaire was drafted, authenticated, and used to gather data in Namibia. The response data were studied by the Statistical Package for Social Sciences. The sample size was also tested for adequacy and sufficiency. The log-likelihood ratio tests determined admissible probability results. The asymptotic properties of the random variables provided the chi-square distribution for the number of variables in the questionnaire. Convex functions, Lagrange multipliers, and amygdaloid (pear-shaped) analyses were also used for the investigation. The results indicate moderate electricity consumption (50%), a doubling of the power plants and operational efficiencies, as well as reasonably good and statistically significant inclusive system development. The proposed system was used to assess stable, least, and optimal electricity consumption models for energy efficiency and energy management. Overall, optimisation of the electricity amygdaloid leads to greater energy efficiency, reduction in utility operational and material costs, balanced power systems loading for better supply capabilities, and reduction in fuel, production, electricity consumption costs, and carbon

footprints. Substantial decreases in greenhouse gas emissions, lower power reserves capacity, more environmentally friendly power systems operations, sustainable plants, and facilities unit commitment suggest reliable electricity supply, societal growth, and enhanced development.

G.3. Keywords

Cost reduction, energy efficiency, energy resources conservation, foreign direct investment, industrialisation, optimal unit commitment.

G.4. Introduction

The rapidly rising load demand and growing pressures on novel and legacy generation capacities have intensified the increasing dependency on electricity imports in Namibia [1],[2]. Also, 2007 marked the beginning of electricity demand exceeding the power supply ability, which led to an increase in electricity tariffs [1],[2]. Although the energy consumption pattern has been soaring in Namibia, the high dependency on Southern Africa's electricity supply had severely restricted the domestic electricity supply situation [3].

Furthermore, Namibia imports up to 80.0% of the energy consumed at certain periods and its average is 60.0% [4]. Also, liquid fuel accounts for above 63.0% of final energy utilisation, 17.0% (electricity), 5.0% (coal), and 15.0% (other energy sources) [5].

The electricity supply in Namibia is dependable and relatively stable, but the very expensive tariffs negatively affect the country's manufacturing and industrialisation aspirations. Its industrial electricity tariffs are highest after Mauritius, and higher than South African rates by between 20.0 and 25.0% [6]. Also, electricity demand-side management (DSM) programmes were implemented in the SADC region because of the energy supply shortages it experienced.

The commissioned capital extensive power plants will supply the regional and domestic power shortfall, and possibly surpass future demands [7]. The Namibia power supply situation seems to be improving, as there was no visible risk of load shedding because the 630.0 MW expected maximum demand was provided for [8].

Also, NamPower internally obtains 40.0% of its electricity requirements from the hydro, coal, diesel, and solar power plants [8]. The remaining 60.0% of imports would come from

Eskom South Africa, Zambia (ZESCO), and Zimbabwe (ZPC) [8]. While Scorpion Zinc consumes around 18.0% of the total energy mix in Namibia, urban areas consume about 71.1%, and Windhoek City consumes the equivalent of an electro-winning smelter, and houses over 350,000 inhabitants, and large numbers of commerce and industries [9].

Namibia's average energy consumption rate exceeds 3000.0GWh/year and its generation capacity is about 1305.0GWh/year. Furthermore, electricity access is 53.9%, net energy import is 74.4% of energy use, and fossil fuel consumption is 66.7% of the total. The electricity supply deficit is imported from South Africa, Zambia, and Mozambique [10].

Whereas higher electricity tariffs were expected to cover new generation plant costs, other renewable energy sources, power infrastructure modernisation, and development, and realise Namibia's vision 2030 in terms of energy sufficiency, ordinary Namibians believe it was the cost of setting up the Regional Electricity Distributors (REDs) [11].

Energy efficiency and energy management systems have a lot of benefits, as demand-side energy policy alternatives have been deemphasised for supply-side alternatives. Thus, energy production assets are greater than energy demand decrease because of unexploited energy efficiency potential [12]. Therefore, energy demand-reduction investment support derives from measurements of perceived negative parameters like energy savings, unpredictable return on investment, and associated bias [12].

Distributed energy penetration growth opened up local energy management (LEM), from coordinated decentralised energy consumption, conversion, storage, supply, and transport within geographies [13]. Also, the liberalisation of European energy combined active pricing and local aggregators to achieve power systems expansion and retail competition. Self-organising control [14] and DSM permit LEM to use local heating to raise energy efficiency, lessen carbon emissions, and enhance energy independence [13].

Continual electricity consumption appliances such as a refrigerator or persons at home and awake determine the period that appliances are used and are vital for energy efficiency, energy management, and energy economy. Thus, energy utilisation has grown alongside population, gross domestic product (GDP), appliance multiplication, a lease on life, and electricity utilisation practices and behaviour [15].

The 2016 Wales project maximised community and locally-based generation. It explored community-based perception and participation in energy-saving schemes that incorporated

cultural norm changes [16]. Further, DSM is governmental policy for energy utilisation, environmental and energy security compliance, energy efficiency, demand response (DR), onsite generation, storage, and lessened carbon emissions [17],[18].

Also, the supply-side management (SSM) principles of utilities in China, France, the UK, and the USA comprise decoupling policies, information campaigns, loans and subsidies, achievement targets, production standards, and utility requirements [18].

Analyses of nations' reduced-carbon electricity conversion depend on economic, political, socio-technical, and technological developments. Hence, governmental energy policies derive from widely diffused social movements, able to shift policies, define national problems, and seek their solutions [19].

Although space cooling and heating demand are rising globally, space cooling demand statistics is not well established in Europe. While it is unknown how electricity is either used for cooling or lighting in Europe, greater cooling demand requires higher power generation and strengthened electricity transmission systems [20].

It is uncertain if wind power is capable of reducing demand-side power generation and shrinking greenhouse gas (GHG) emissions. It is difficult to estimate emissions displacement using unstable wind power outputs and this could increase emissions intensity in conventional power plants from fluctuating wind farm outputs [21]. That is why various energy efficiency and energy management modelling designs are used to drive strategies affecting the economic prosperity and future living of billions of people [22].

Renewable energy increases and greater electricity usage led to wider alterations in grid utilisation and expensive grid enlargements. Also, the motivation to reduce peaks and increase demand for charging electric cars causes network congestion. Hence, network tariffs are incentives to adjust peak shifting and balance the network by peak shedding through active pricing by requiring higher tariffs (peak pricing) during elevated network usage [23].

Urban energy flux stimulates the neighbourhood problems of urbanism that raise greenhouse gases. Hence, urban power outlooks indicate how energy is used for communications, lighting, thermal comfort, and transportation. Also, how direct fuels are used for heating or mechanical power, electricity generation, or gas to provide energy services [24].

Energy crises in Switzerland were addressed by reducing energy consumption by half, increasing 15-fold renewable energy production, reducing CO_2 emissions without jeopardising costs, security, and supply, and phasing out existing nuclear power reactors as their service lives end [25].

Many countries are changing their generation mixes and moving towards renewable sources such as hydro to reduce GHGs. For example in 2015, Switzerland met 59.9% of its electricity demand from hydropower [25]. For Namibia it was 67.0% in 2014 and Rwanda 48.0% in 2017 [26],[27],[28].

Furthermore, energy demand respecting climate change is heating-dependent and location-specific. Thus, warmth increases with climate change, the cooling load rises for warmer countries, and the heating load reduces for cooler countries. A study of energy use in supermarkets showed that open refrigeration shelves lead to air leakage and higher electricity demand, and about half the electricity consumed is due to lighting loads and is independent of weather [29].

The objective of this part of the thesis is to determine how the pyriformis of the curtailed utility electricity consumption equilibrium could lead to load balance for energy efficiency and energy management systems. Overall, optimisation of electricity consumption amygdaloid leads to greater energy efficiencies, reduced utility operational and material costs, balanced power systems loading for better supply capabilities, and reduced fuel, production, electricity consumption costs, and carbon footprints. Substantial decreases in greenhouse gas emissions, lower power reserves capacity, more environmentally friendly power systems operations, and sustainable plants, and facilities unit commitment lead to reliable electricity supply, societal growth, and enhanced development.

The investigation is subdivided into Prelude, Materials and Methods, Results and Discussion, Electricity load factor and Policy cost implications, and Conclusion.

G5. Materials and Methods

A questionnaire was drafted for the electricity load management survey and authenticated by a panel of expert judges like electrical engineers, economists, planners, and linguists. Five research assistants were trained and subsequently used to administer the questionnaires in Windhoek City, Namibia. The Cochran rule established the specimen size for the study and

only 127 responses were obtained from over 300 randomly distributed questionnaires. The data from the respondents were subsequently investigated by a statistical package for the social sciences (SPSS).

G.5.1. Sample Size Determination

For a 95% confidence interval, 5% precision, and maximum variability, the Cochran rule is:

$$n_0 = z^2 pq / e^2 \tag{G.1}$$

$$= \frac{(1.96)^2(0.5)(0.5)}{(0.05)^2} = 384.16 \approx 385$$

where Z is ± 1.96 (Z-score estimates), $p = q = 0.5$ are expectations, e is an inaccuracy (0.05), and an investigation for more than 10,000 population, the specimen size was 385. Furthermore, design heterogeneity reduces with rising specimen size, and acceptable response falls between 300 and 350 specimens [30], which is within the range of questionnaires administered in the study.

G.5.2. Statistical Adequacy and Sufficiency of Using the Obtained Sample Size

Reference [31] shows that the 127 specimens used in the thesis were statistically satisfactory and sufficient. Communality is the variance of any item from average factors. It is the proportion of the discrepancy each quantity assigns to other parameters in the study. It is characterised by a declared forecast, in which the deviation is described by average components [31],[32],[33],[34],[35].

Communality studies indicate the separate parts of compound designs. Their lesser limit examines and validates component analyses. In hindsight, they are used when either the analysis is completed or as an original contribution to data. In addition, communality studies separate multidimensional investigations into disparately calculated limit-value coefficients for each component in the model [31],[36].

Besides, aspects analysis exhibits the dimension of parameters, by lessening the assigned scope to a modest number of variables. Also, factor analysis is attractive because it measures

latent variables like electricity load, which cannot be directly measured as in the study [31],[36].

Using convergence limits to examine the asymptotes of the real number sequence employs Borel's and Bernoulli's laws of large numbers, and Chebyshev's bias to assess the sample size suitability:

$$P\{|x-a|<\varepsilon\}>1-\frac{\sigma^2}{\varepsilon^2}\text{ (Chebyshev's difference)} \quad \text{(G.2)}$$

where a is a value (survey variable) of inaccuracy υ, x is real number sequence, ε is a precision estimate, and σ^2 is the deviation. If $\sigma \ll \varepsilon$, the likelihood that $|x-a|$ is smaller than ε; approaches unity [31],[37].

The expectation P of the success rate equals k. Hence:

$$P\left\{\left|\frac{k}{n}-p\right|<\varepsilon\right\}\to 1 \text{ as } n\to\infty \quad \text{(G.3)}$$

Equation (G.3), is a random variables limit sequence [31],[37].

Also, the random variables sample mean approaches P as $n\to\infty$. But, the likelihood value $E\{.\}$, is:

$$E\{X_i\}=E\{\bar{x}_n\}=p;\ \sigma_{x_i}^2=pq$$

where p, q are likelihood outcomes, and $\sigma_{x_n}^2=\frac{pq}{n}$, is the discrepancy for any n [31],[37].

Also, for similarly anticipated events [31],[37]:

$$pq=q(1-q)\le ¼ \quad \text{(G.4)}$$

Therefore,

$$P\{|\bar{x}_i-q|<\varepsilon\}\ge 1-\frac{pq}{n\varepsilon^2}\ge 1-\frac{1}{4n\varepsilon^2}\to 1 \quad \text{(G.5)}$$

as $n\to\infty$.

Consequently, the sample means: $\bar{x}_n(\xi)=\frac{k}{n}$, if the event occurs k times.

For ease of analyses and better presentation, only those variables or sample sizes that are significant (at $p \leq 0.05$) or marginally significant (at $p \leq 0.10$), were considered. Hence, the sample size-frequency interpretation can determine q, and an error $[\varepsilon = 0.1]$, which allows for a marginal error of ten percent [2]. The change can be quantified and assigned to model the output replication process. The model uncertainty from the sampling and model selection processes compute the median and the 90.0% between-subjects bound (IQR90) among the *p0.95* and *p0.05* (*p0.90 = p0.95 - p0.05*) percentiles. Also, the greatest accepted differences involve broad neighbourhoods of elevated gradient information content [30].

Using the sample mean and $n \geq 127$, becomes [31]:

$$P\{|\bar{x}_n - p| < 0.1\} \geq 1 - \frac{1}{4 \times 127 \times 0.1^2} \geq ⅘$$

Repeating the investigation at least 127 times, and, in 4 out of 5 of the same experiments, the error is: $|\bar{x}_n - p| < 0.1$

Performing the survey very many times and determining the specimen average $\bar{x}_n$, Bernoulli's rule is effective and practicable. Hence, for any n the error $|\bar{x}_n - q|$ to exceed 0.1 [31] in such experiments equals $(1 - 1/5) = 4/5$. This implies that acceptable results will be generated in 80.0% of the experiments and the sample size used in the thesis is adequate.

Again, the specimen quantity can be determined using the Poisson dispersion. Furthermore, ambiguities are certain in data since they impact the results that can be drawn from the experiments. The deviations of the distribution function:

$$\sigma = \left\{\frac{1}{N}\sum_{i=1}^{N}(l_i - \mu)^2\right\}^{\frac{1}{2}} \tag{G.6}$$

where μ is sampling mean, l_i mean outcomes, and N specimen number [38]. How far do the mean approximate accurate assessments of the specimen population? Outside new data, we turn down the specimen mean μ as the average of the source allocation. The standard dispersion is used when the inaccuracies are separate and several [39]. When the specimens are real number sequences amid the original population, the dispersion average (μ) and the discrepancy (σ), are superior assessors of the classification [38].

Considering a typical classification, the likelihood interval

$[\mu - \sigma, \mu + \sigma]$:

$$A(\sigma) = \int_{\mu-\sigma}^{\mu+\sigma} P_G(\mu, \sigma, t)dt = 0.682 \quad \text{(G.7)}$$

where P_G is the likelihood operation and t is time. When the experiments are performed 100 times, 68.2% of the outcomes are within $(\mu - \sigma)$ and $(\mu + \sigma)$. For a feasible set of trials from the original classification, a Poisson classification is proposed [38].

When $\mu \equiv Nq$ (G.8)

The likelihood: q$\rightarrow 0$, $N \rightarrow \infty$, μ is fixed, and the binomial spread tends to a Poisson spread:

$$P_q(n, \mu) = \frac{\mu^n}{n!} e^{-n} \quad \text{(G.9)}$$

Additionally, the distribution of the measurements is Poisson for the electricity load management questionnaires. Furthermore, the average and the deviation of Poisson procedures are the same. Therefore, the unique value tends towards the standard classification. Accordingly, the holding capacity for any specimen is $(n)^{\frac{1}{2}}$ and 68.2% is the likelihood that the accurate value [38],[41] is inside $\left[127 - (127)^{\frac{1}{2}}, 127 + (127)^{\frac{1}{2}}\right]$. Hence, the accurate sample is inside 116 and 138. Consequently, the 127 trials used for this study are sufficient to obtain credible inferences from the research.

G.5.3. Other Methods and Procedures

The grounded theory uses the results generated from the data to derive the corresponding theories [38],[39]. The thesis addressed the questions: (a) How does the pyriformis of the lessened utility electricity consumption equilibrium lead to optimal electricity load balance? (b) To what extent does a lessened log-likelihood model differ from the full final model? (c) What is the optimum number of predictors suitable for the model development in this study?

The log-likelihood ratio analyses the optimisation of complete and looped models. Asymptotes of complimentary quantities indicate real number sequences are chi-square for all n. Also, lessened expectation value assesses the complete predictors of the inquiry. The joint significance forecasts the correct model and the Neyman-Pearson schema determines the

critical size of the rejection region. These works lead to the highest probability assessment, which is highest around the true value [37],[42],[43],[44],[45],[46],[47],[48],[49],[50].

G.5.4. Amygdaloid Diffuse Diagram

The diffuse diagram in Fig. G.1, uncovers a symmetrical amygdaloid, with a tangent $\{3.0-(-4.0)/(3.0-(-0.5))\}=2.0$, that approaches 63.4^0. The gradient was hand calculated and a more precise valuation is 60.0^0 to the horizontal, having $\pm 5.7\%$ (0.057) error. Also, the amygdaloid equation is:

$$y^2=-ax^4+bx^3 \tag{G.10}$$

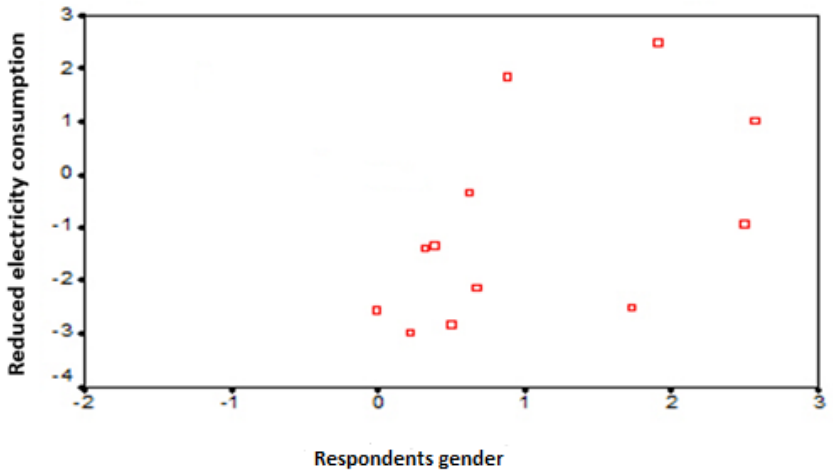

Figure G. 1: Scatter plot: Lessened electricity consumption [2]

Also, the simplest solutions to equation (G.10) in Fig. G.1 are: (i) 0 and (ii) 1 (for $a=b$), respectively [51],[52]. The $(0,1)$ problem is convex [53],[54], and convex functions are the smallest perfect solutions in the convexity interval, with one lowest point [53],[54],[55].

For emphasis, the negative quantities on each axis indicate the direction while the strength of the amygdaloid (pear-shaped) relationship is determined by the tangent. The variables shown in Fig. G.1 are the aggregated household electricity load management inquiry scores in Namibia. The outcome variable (reduced electricity consumption) on the vertical y-axis represents the levels of agreement with the household electricity load management questionnaire in Windhoek, and the predictor variable on the x-axis represents the gender of the respondents. Fig. G.1 shows how the gender of the respondents and electricity consumption in the households are related at the individual level for over 127 respondents.

The scatter diagram (amygdaloid) shows a general trend in electricity consumption patterns, each of which represents a single electricity consumption pattern. We can see a general downward scatter of electricity consumption pattern that is heavier towards the bottom of the amygdaloid. The scatter diagram (amygdaloid) shows that higher electricity consumption patterns are related to the female gender and lower electricity consumption pattern is related to the male gender.

This means that households with a higher number of females show greater electricity consumption patterns scatter. Overall, the data suggest that an average positive relationship exists between gender and electricity consumption patterns. Furthermore, we have assumed that the differences between the ordinal or Likert scale values are equivalent across the scale (weight) [38].

It can also be seen that the amygdaloid (pear-shape) lies in the right-hand-plane of the Respondents' gender vs Reduced electricity consumption scatter diagram (Fig. G.1). Therefore, the amygdaloid (pear-shape) is a cosine function (if we are to draw four quadrants in Fig. G.1 because only a cosine function is positive both in the first and fourth quadrants of a circle [56].

G6. Results and Discussion

Tables G.1 and G.4, and analyses are in the Appendix. Table G.1 indicates the likelihood ratio interpretation (LR) format. For LR greater than 10.0, it is for a large and convincing conclusion of an increase in the likelihood function. Whenever the LR lies between 5.0 and 10.0, it indicates that there is a moderate or modest increase in the likelihood function. For LR between 2.0 and 5.0, it reflects a slight or small likelihood. Also, if the LR ranges from 1.0 to 2.0, it shows a nominal rise in expectation. If the LR is equal to 1.0, it means there is no change in the likelihood function. Furthermore, whenever LR ranges from 0.5 to 1.0, it shows a nominal reduction in the expectation. If LR ranges from 0.2 to 0.5, it shows a miniature reduction in the expectation. When LR is between 0.1 and 0.2, it shows a limited reduction in the expectation. But, when the LR is below 0.1, it shows a slight reduction in the expectation [37],[42],[43],[44],[45],[46],[47],[48],[49],[50].

Fig. G.1 shows a diffused amygdaloid sketch of lessened electricity consumption drawn against respondents' gender. The females in the majority, disagree that lower electricity

consumption drastically decreases bills paid. Accordingly, special education and enlightenment programmes, incentives and stimulus packages, and marketing campaigns aimed at this people group can enhance efficient electricity uses. The female gender could be encouraged to embrace energy and money-saving schemes, loss, and waste mitigation for a more liveable environment. Furthermore, the female gender is implored to efficiently use energy because it can result in higher standards of living, and accelerate industrial progress, and socioeconomic development [2],[40].

Table G. 1: Model 1 Synopsis (b) (Adapted: [2])

Model	R	R Square	Adjusted R Square	Std. Error of the Estimate	Change Statistics					Durbin-Watson
					R Square Change	F Change	df1	df2	Sig. F Change	
1	1.000(a)	1.000	1.000	.	1.000	.	32	0	.	2.143

Note: Dependent Variable: Lessened power utilisation decreases money paid to Municipality or Utility

Table G. 2: ANOVA [2]

Model	Source of variance	Sum of Squares	Df	Mean Square	F	P-value
1	Regression	41.879	32	1.309	.	.
	Residual	.000	0	.		
	Total	41.879	32			

G6.1. Amygdaloid Scatter Diagram

The diffused sketch in Fig. G.1 indicates that the pyriform is a cluster of interdependent responses about the coordinates $\{(0.3,-3.0),(0.0,-2.5),(2.6,1.1),(1.9,2.6)\}$. The tangent of the diffused symmetrical amygdaloid was about 2.0 and subtends at around 63.4^0 to the horizontal. A more precise angle would be 60.0^0 and about $\pm 5.7\%$ (0.057) error.

Analogously, the 60.0^0 tangent of the amygdaloid lessens the quantity of the normal electricity demand to half of its usual value [57]. For a weight hastening down a 60.0^0 slope, its weight is halved (resultant) because its value is multiplied by cosine 60.0^0 (0.5).

Consequently, the 60.0^0 diffused symmetrical amygdaloid, indicates a 50.0% decrease in electricity utilisation. Thus, greater savings in the energy utilised reduces energy charges, electricity production resources, climate change, greenhouse gas emissions (GHGs), and carbon footprints.

Also, a 50.0% reduction in the amount of electricity consumed enables access to more electricity consumers at lower communal and economic expenses. Therefore, utilities can provide more than twice their general performance efficiencies for continuing development. Also, the power utility could use interim base-load power plants between 40.0 and 120.0 MW, to raise the current installed capacity in Namibia, and obtain over 60.0% power deficit through imports from other countries at 50.0% load factor [8].

Fig. G.2 shows the parameters included in the lessened electricity utilisation amygdaloid for the multidimensional tests. It also explains each of the variables used in the inquiry. Therefore, Q2-The gender of the respondents positively influences reduced electricity consumption and bills paid. Q10-Reduced electricity consumption and bills paid influence optimal electricity load management. Q10*Q2-The interaction component of reduced electricity consumption, bills paid, and gender of respondents positively influence optimal electricity load management. Q24-The opportunity or leeway of the utility to charge any amount for the electricity supply could induce more rational electricity consumption patterns, mitigate bills paid, and positively influence optimal electricity load management. Q25-Reducing wasted electricity positively influences development, reduces electricity consumption, and bills paid. Q26-Increasing electricity use directly and negatively impacts the environment and increases the bills paid.

Q27-Energy-efficient architecture and illumination conserve the earth's resources and positively influence optimal electricity load management. Q28-Uncontrolled electricity uses to make the utility raise prices, which negatively influences optimal electricity load management. Q29-Economical electricity utilisation defers the construction of additional electricity production plants and positively influences optimal electricity load management. Q30-Constructing fresh electricity facilities can only lessen worldwide heating and positively

influence optimal electricity load management, only if blue, green, and other alternative energy power plants are built.

Q31-Allowing the television to be on without anyone watching it negatively influences optimal electricity load management. Q32-Turning down heaters or closing air channels in visitors' suites positively influences optimal demand management. Q33-Lessening regulators at bedtime when the dwelling was unoccupied positively influence optimal electricity load management. Q34-Curtains covering windows at the eventide and opening them throughout the day positively influence optimal electricity load management. Q35-Locking every window securely throughout wintertime reduces high-temperature loss, and positively influences optimal electricity load management. Q36-Insulating houses to save energy and reduce money loss positively influence optimal electricity load management. Q37-Use curtains to lessen hot weather ingress in the hot season/warmth escape in the cold season positively influence optimal electricity load management.

Q39-Putting off air modifiers while departing home positively influences electricity load management. It also reduces fire hazards and risks, which forestalls colossal losses of property. Q40-Keeping air modifiers uncluttered without blocking them with curtains or household property positively influence optimal electricity load management. Q41-Keeping windows shut and opening exits rarely, when the air conditioner is on positively influences optimal electricity load management. Q42-Keeping heating equipment from thermostats for accurate readings undoubtedly impacts optimal electricity demand management. Q43-Keeping apartments' air modifiers and compressors safeguarded from sunlight for good thermostatic control positively influence optimal electricity load management.

Q44-Setting temperatures of water heaters at medium positively influence optimal electricity load management. Q45-Put-out radiators whenever travelled some days in winter positively influence optimal electricity load management. Q46-Opening the refrigerator/freezer compartment doors rarely in hot weather positively influence optimal electricity load management. The Q47-Keeping stable temperatures in the refrigerator/freezer compartments positively influence optimal electricity load management.

Q48-Cooking with as little water as possible positively influences optimal electricity load management. Q49-Boiling liquids in tightly closed pans and pots to save 20.0% energy positively influence optimal electricity load management. Q50-Keeping pot bottoms shining

to reduce energy waste and money paid on bills positively influence optimal electricity load management. Q51-Pots should be placed upon the same sizes as burners positively influence optimal electricity load management. Q52-Fluorescent lamps are used whenever it is practicable to positively influence optimal electricity load management. Q53-Automatic switches that cut-off lights when the door is closed positively influence optimal electricity load management. Q54-No switching of effulgent lamps within 15 minutes of turning them down positively influenced optimal electricity load management.

Fig. G.3 indicates the rationale for the optimal multidimensional electricity load management approach developed in this part of the thesis. The input of the questionnaire contains 34 parameters comprising Q2 (gender of the respondents), Q10 (reduced electricity consumption and bills paid), Q10*Q2 (interaction between gender and reduced electricity consumption and bills paid), and the interaction components of each question or parameter between Q24 and Q54 (inclusive).

The output or outcomes of the research led to high energy efficiency, low operations and maintenance costs, and balanced loading. Furthermore, it encourages a greater electricity supply base, lower production and consumption costs, lower greenhouse gases emission, optimal unit commitment, lower reserves capacity, and lower carbon footprints.

This energy efficiency and energy management study is useful to all tiers of Government, energy utilities, industry and commerce, households, financiers, insurers/assurers, and other professionals like Engineers, Economists, Planners, Architects, Accountants, and Energy experts.

The benefits of the study include reliable power generation and supply, lower incidence of power blackouts, optimal dispatch and savings in capital power plant costs, enhanced generation efficiencies, lower operating costs, and lesser carbon footprints.

The study also facilitates sustainable economic growth, energy sector development, energy efficiency, future energy research, higher percentage energy cost reduction, avoided energy production and avoided costs, foreign direct investment, and climate change mitigation.

G6.2. Durbin-Watson Statistics

Table G.2 indicates the parameter estimates of the model in Fig. G.1. The standard error reflects the model's precision. The R square change refines the R square if a second parameter is included in the analyses. $F-$ change are variables included in each stage of the analyses that materially enhanced the prediction. The $p-$estimate of the $F-$shift is the likelihood of adopting the other proposition or disallowing the null hypothesis. Whenever the $p-$value < 0.05, then there is statistical significance among the dependent and independent variables. The Durbin-Watson (DW) statistics determine the sufficiency, precision, significance, and autonomy of the autocorrelation results in the data of the developed load management model of Fig. G.1 [2],[29],[39],[58],[59],[60], [61].

Furthermore, the calculated 2.143 DW value was close to the unique 2.0 DW value, and that its difference from the maximum DW (4) value was above the uppermost term of the DW figures $(d_U = 1.73)$ for us to accept that no interdependence exists in the DW statistics (4.0 - 2.143 = 1.857>$d_U = 1.73$) [2],[29],[39],[62],[63],[64].

Also, there were a few exceptions to the absolute error conjecture and the errors were unrelated. The R coefficient determines the interdependence between the detected and forecast values of a standard energy variable. Therefore, the correlation coefficient indicates that the lesser power utilised lessens the amount paid by 100.0% of the respondents. Furthermore, the R square is a 100.0% proportion of the variation explained by lower electricity utilisation. It also reduces the amount paid for power as well as an optimal model. Moreover, the adjusted R square indicates that a 100.0% of the model was captured in the analyses.

Additionally, the accuracy from the accepted observation interval and regression line was 0.0001%. Also, the model accuracy indicates that 95.0% of the statistics lies between the regression line and +/-0.0002% of the lower electricity utilisation pattern. The R square indicates that the 100.0% improvement was achieved in Model 1 because of an additional forecast variable. This was so because model 1 is statistically significant $(F_{0,32} = 0.0001, p < 0.0001)$. There was also no significant F-change because a second variable will not significantly improve the prediction [58],[59],[60],[61]. Both the adjusted R^2 and R^2 shown in Table G.2 were 100.0% each, which indicates that an excellent model was developed.

G6.3. Analysis of Variance

Table G.3 indicates zero residuals, which suggests that there were no misalignments in the optimal multidimensional electricity load management model. Residuals are unresolved nonlinear segments of the dependent variable. Remainder statistics of the contingent criterion evaluate the disparity between the observed contingent criterion and its forecast. It suggests the precision of mathematical forecasts. The remainder properties gauge distortions in experiments as well as confirm the sufficiency of conjectures. Also, the model developed was perfect, indeed. The error sum of squares amount are departures of every observation from their average. The effective values are observations of deviations in the design. Furthermore, a 1.309 mean square value is the sample variance [2],[31],[39],[63],[65],[66]. Consequently, the approach was both fundamentally and statistically significant ($p < .0001$).

With each Effect, Error df, F, Hypothesis df, p-values, and values, respectively ".", then, $p < .0001$. Therefore, the model portrays very important results [39],[40],[41],[58],[59],[60], [61],[66]. Multidimensional investigations are fundamentally and statistically important because they provide dependable and honest results. Furthermore, little Fisher and significance test values support our assertion of advancing a superior model with interactions [39],[40],[41],[58],[59],[60],[61],[65], any power utility could realise.

G6.4. Likelihood Ratio

Table G.4 is shown in the Appendix. It indicates the probability proportion results: impact, -2 believability (-2LL), kurtosis (χ^2), df, and significance. The intercept indicates that the definitive pattern is the same as the reduced version. The effect of the -2 log-likelihood (-2LL) focuses on Q10 (Lower electricity utilisation lessens money paid to district or utility), Q21 (Lessening electricity utilisation lowers worldwide heating), Q18 (Raised electricity utilisation raises worldwide heating), Q3 (Age), and Q2 (Gender) as a basis for measuring the -2LL of other variables in the questionnaire. Consequently, the other data variable entries were to be used to deduce a reduced model. Since all the values of the -2LLs for the independent variables were zero, the deviance (or deviation) from the true and optimal algorithm was also zero. Therefore, the significance levels were very good, the developed model perfectly fits into the -2log likelihood metrics, and all the likelihood ratios were unity each. A perfect and optimal model was developed for the reduced electricity consumption

decreases the amount spent on bills either to the utility or municipality [2],[31],[39],[43],[63],[65], [66].

Kurtosis is the dissimilarity in -2LL between the definitive and discounted models. The discounted model was obtained by removing an influence from the definitive pattern, which indicates that no differences exist because all the parameter effects are zero. Therefore, both the final and reduced models are the same. The degree of freedom (DF) was zero. That means we need zero or no parameter variable change to describe the reduced model (lower power consumption reduces the amount paid). The model was not due to chance but noticeably attributable to lessened electricity utilisation because $p<0.0001$ (result of all 54 variables in the questionnaire) [2],[31],[39],[43],[63],[65],[66]. Furthermore, the lower model was equal to the full model because eliminating the parameter properties did not raise the df. Also, the -2 times log-likelihood is all zero, meaning that the likelihood is unity and a perfect model was developed [2].

Also, lower electricity consumption is important for propelling optimal electricity load management practices. This reduces electricity charges, lowers energy production inputs, extends the service lives of facilities, and reduces carbon footprints. It significantly reduces greenhouse gases. Furthermore, occasional and peak power plants are trimmed from generation, leading to reduced transaction expenses and fairer electricity rates [2],[55],[67],[68],[69],[70].

Conversely, rising electricity consumption leads to worldwide warming, melting ice, and rising sea level, leading to flooding in low-lying coastal cities and settlements. Flash floods, landslides, and bad weather, which cause colossal damage, death, and ruin, and power blackouts, become frequent [2],[55],[71],[72],[73].

Rising electricity expense occurs when need outstrips generation. Load removal, reduction, or rationing; load repositioning; load trimming; peak alteration; time of use (TOU) pricing, active pricing, and apex pricing, are incentives for handling network congestion problems [55],[64],[71],[72],[73].

The gender of respondents is a better impetus for electricity load management. Also, females more readily use electricity to operate household equipment. Hour of use, number of recurrences, and length of time are vital for load management because they influence electricity cost and load growth [2],[40],[55],[72].

The amygdaloid in Fig. G.1 indicates the tendency of females to use more electricity in households and in future planning. Similarly, the age of respondents is important because it

determines the technology in use, electricity consumption patterns due to the weather, and warmth for the elderly could be vital for applying load management principles [55],[64],[71],[72],[73].

Conclusively, stabilised loading is the major principle outlined in this part of the thesis, because it could be used to serve one of the superior electricity requirements of the citizenry.

In Table G.4, the chi-square statistics show that both the subordinated log-likelihood model and the full model were the same.

G7. Electricity Load Factor and Cost Policy Implications

G7.1. Electricity Challenge

The electricity challenge is increasing worldwide because of rising expendable incomes, population bang, and continuing urbanisation. Extreme weather makes household peak demand exceed 90% of the average daily demand, which necessitates using air conditioners or heaters [2].

Australia's growing electricity requirements and asset double created overcapitalisation, constant or decreasing fuel expenses from mining work rate profits, capital stock enlargement, material technological improvements for better fuel-efficient turbo-generators, and strengthened structural enhancements for superior grid interconnection. The inclusion of substantial extractive and manufacturing consumers having smooth and more stable load patterns caused the East Coast electricity sector to expand into economical base-load generators, stretch the bulky fixed costs of the sector over higher units of production, and reduce the complete organisation mean cost [71].

The range of changes occurring between households and commerce during peak loads demands a closer examination. This is so because digital meters (smart metering) replaced mechanical electricity meters to strengthen utility energy markets. Furthermore, both Australia and the USA doubled their energy demand, based on rising expendable earnings, vast household floor spaces, and declining appliance expenditures [71]. Although mechanical electricity meters were unable to identify nor disclose the hour-of-use pricing, the cardinal incentives for consumers to adjust maximum electricity demands are nonexistent [71],[72].

G7.2. Load Capacity and Expenses

Load capacity is the proportion of average demand to maximum demand, per annum. Load factors (LFs) between 0.30 and 0.40 are associated with extremely peaking family electricity

utilisation programmes. Favourable LFs are greater than 0.7 (> 0.70). They consist of both the industrial and extractive sectors of the economy. Consequently, the mean cost tariffs cause surplus capacity, unproductive load factors, and very expensive electricity tariffs. The 50.0% LF reorganises plant inventory levels, raises base power plants profile, and reduces peaking power plants utilisation frequency, tariffs, and fuel expenditures [8],[71],[72],[73],[74].

Harnessing greater combustion efficiencies and greater sunk capital expenditures enables the capital to be stretched over vast units of production. Others include reduced: transport expenses; retail expenses for outputs offered by businesses; service charges; profits from stable energy profiles, plus averted production gain [71].

Table G.5 shows the importance of the 50.0% electricity load factor on expenses, in the thesis. It indicates that the 50.0% electricity load factor was based on high and low-cost measures of electricity generation, transmission, distribution, utilisation, supply, and demand variables. Firstly, high base power plants utilised in the utility lead to low numbers of peaking and intermittent power plants in service, low tariff structure, and low fuel costs. Secondly, engaging higher combustion efficiency generation capacities to reduce capacity costs, spread equipment costs among larger generation units for reduced tariffs, transportation, and delivery levies decrease the cost of making it cheaper to transfer power along the power systems backbone with lower costs and also strengthened to carry larger amounts of power able to sustainably supply more consumers with lesser blackouts [2],[55],[71],[72],[73],[74].

Furthermore, retail costs of goods and services decline because electricity tariffs are lower, which leads to lower commodity prices across the board. Larger mining and industrial electricity consumption lead to flatter load curves with more predictability and lesser frequencies of peaking demand. This situation leads to engaging larger baseload unit commitment, and balanced loading than using more high-cost peaking, and intermittent generation plants. Additionally, avoided production reduces electricity and energy generation costs, reduces GHG emissions, and leads to lengthening the exploitable life of energy resources, and AUS$1.7 Billion a year from the household sector was gained through avoided production alone. This equally leads to mitigating climate change repercussions that enable citizens to live in healthier environments, and reduce the consumption rates of fossil fuel energy resources for electricity generation, which leads to lower pollutants released to the environment [2],[55],[71],[72],[73],[74].

Thirdly, higher sunk capital expense and high price shock periods tend to encourage the utility to charge higher tariffs to cover their generation, transmission, distribution, and

utilisation of infrastructural development costs. The high price fluctuations tend to discourage more electricity consumption, especially for the average citizen. This is so because a majority of this group of consumers cannot continually absorb rising electricity tariffs. Also, engaging a high price suppression period would lead to behaviour change in the utilisation of electric appliance stock. This is so because if the cost of kWh is significantly reduced for a while, consumers would be quick to take advantage of such incentives. This could change dwelling appliance selection, enhancement, and strategies for practically deploying electrical equipment around the home [2],[55],[71],[72],[73],[74].

Moreover, the length of the public education period or advertising campaign could help electricity consumers imbibe energy savings, energy efficiency, and energy management behaviour modification to consciously decide to reduce their demand for their perceived energy, financial, and other benefits for consumers to deliberately decide to reduce electricity consumption, and wastage [2],[55],[71],[72],[73],[74].

However, high tariff increases would naturally lead to lower aggregate demand and could be inconveniencing to the poor, weak, infirm, and elderly people who might not be able to afford the cost of electricity and might freeze to death in winter if smart or prepaid meters, which automatically switch off if the electricity units loaded onto the prepaid meter are exhausted [2],[55],[71],[72],[73], [74].

Dynamic pricing on the other hand has a lot of models like TOU, shifting average to TOU tariff, up to real-time pricing. Therefore, the traditional TOU or off-peak tariff, TOU, and judicious price structure, and transferring mean to TOU tariff all lead to peak demand reduction, respectively. Also, both the technology plus automatic-demand response, and peak-time rebate trials lead to demand reduction, respectively. While the strategic maximum pricing valuations are extremely promising maximum demand reduction methods, the automated demand response (DR) leads to a substantial peak demand reduction [2],[55],[71],[72],[73],[74].

Above all, the real-time dynamical pricing technique is not popular with electricity consumers because it places material installation and other financial strains on electricity consumers as the tariffs change with the power demand and supply constraints in the power systems network at every time instant. This is so because the price for each kWh is time-dependent, and swings or continuously changes with time [2],[55],[71],[72],[73],[74].

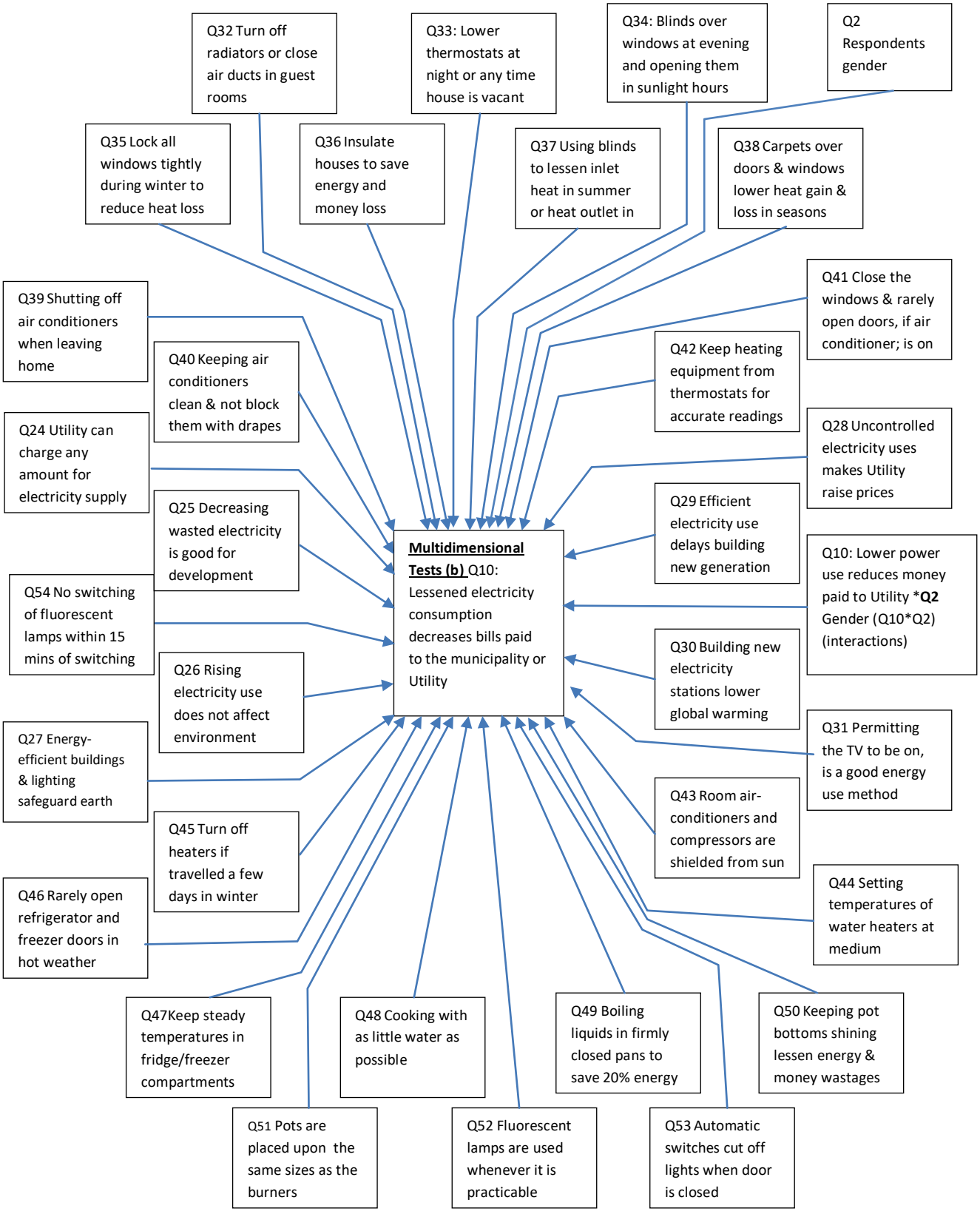

Figure G. 2: Lessened electricity utilisation (Adapted: [2])

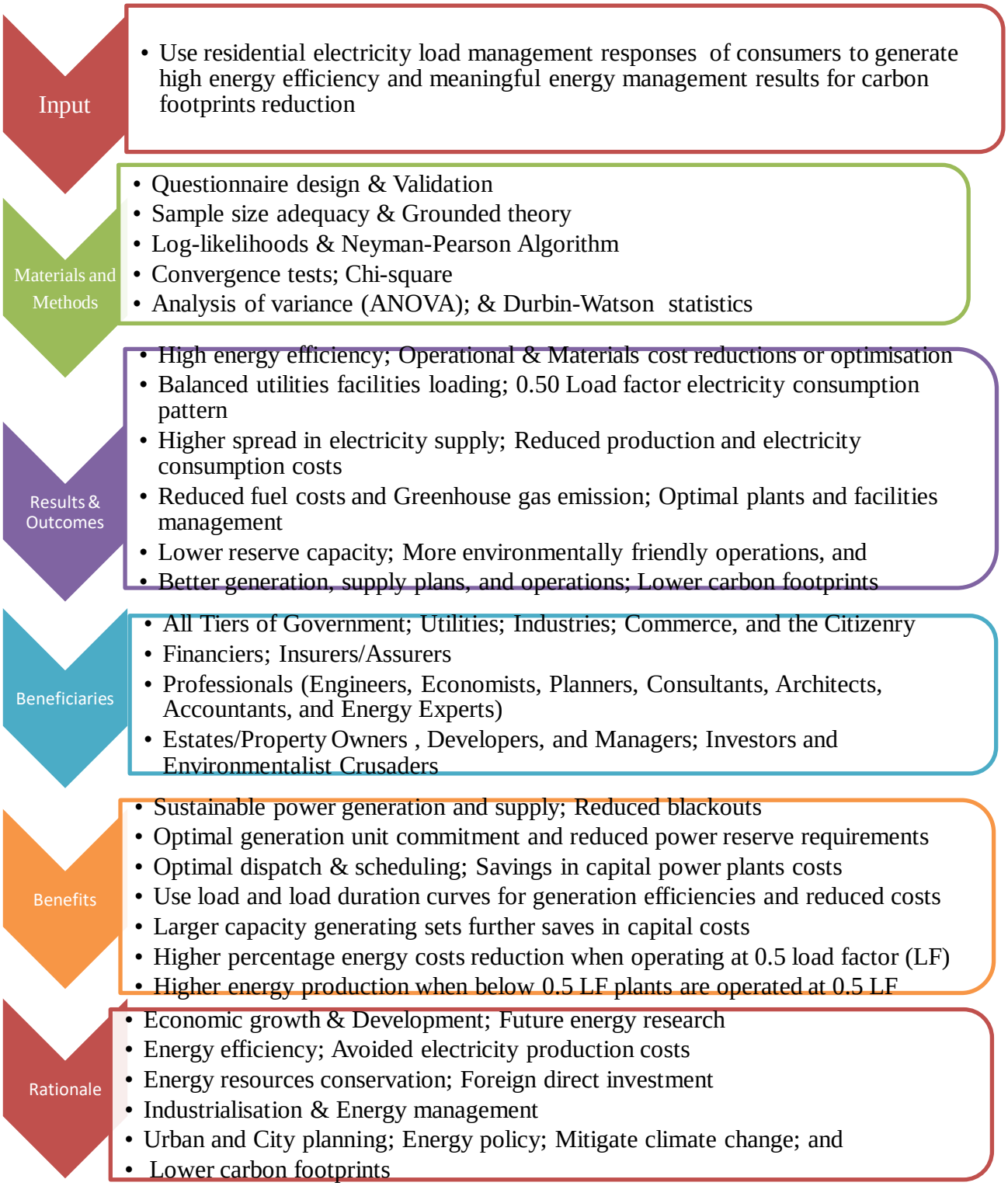

Figure G. 3: Rationale for the Optimal Multidimensional Electricity Load Management System

Table G. 3: Sources:[2],[55],[71],[72],[73],[74] Importance of 50.0% electricity load capacity on expenses

High	Low
Base power plants	$\begin{cases} Peaking\ plants\ in\ service \\ Tariffs \\ Fuel\ costs \end{cases}$
Higher combustion efficiency	$\begin{cases} Reduced\ capacity\ costs \\ Costs\ spread\ across\ greater\ units\ of\ output \\ Transmission\ and\ distribution\ charges\ decline \\ Retail\ costs\ of\ goods/services\ decline \\ Service\ taxes\ are\ reduced \\ Gains\ from\ flatter\ load\ curves \\ Avoided\ production\ costs \\ Aus\$1.7 Billion\ a\ year\ in\ the\ household\ sector\ (avoided) \end{cases}$
Greater sunk capital expenses	
Extreme price shock period	$Average\ household\ consumption\ declines$
Price suppression period	$\begin{cases} Change\ in\ appliance\ stock, dwelling\ improvement\ or \\ Changes\ in\ utilization\ decisions \end{cases}$
Public education period or advertising	$Demand\ reduction$
Tariff increases	$Demand\ reduction\ (aggregate)\ with\ inconveniences$
<u>Active pricing</u>	
Traditional TOU or Off-peak tariff	$Peak\ demand\ reduction$
TOU and judicious price structure	$Peak\ demand\ reduction$
Transferring mean to TOU tariff	$Peak\ demand\ reduction$
Technology plus automated demand response	$Demand\ reduction$
Peak-time rebate trials	$Demand\ reduction$
Judicious peak pricing trials	$Most\ promising\ demand\ peak\ reduction\ method$
Technology-driven demand response	$Large\ peak\ demand\ reduction$
Real-time pricing	$\begin{cases} Unpopular - places\ material\ or \\ financial\ burden\ on\ customers \end{cases}$

5.0 Conclusion

An important contribution of this research is to demonstrate how the pyriform diffused diagram was used to deduce lesser electricity utilisation behavioural patterns, and by extension, could substantially decrease the amount spent on bills. The reduced electricity consumption behaviour could be used to double both the industrial and functional efficiencies of utilities and cause stabilised loading (50.0%) to be implemented in the grid.

The amygdaloid in Fig. G.1 indicates the tendency of females to use more electricity in households and it is useful in future planning. Similarly, the age of respondents is important because it determines the technology in use, electricity consumption patterns due to the weather, and warmth for the elderly could be vital for applying humane load management principles. Also, hours of use, recurrence number, and length of time are important for load management because they influence electricity cost, load growth, and carbon footprints.

Additionally, the proposed model was used to assess stable, least, and optimal electricity consumption for energy efficiency, energy management, operational and material costs reduction, balanced loading, enhanced supply capabilities, lower GHG emissions, lower fuel and production costs, lower reserve capacity, sustainable plants unit commitment, and more environmentally friendly power systems operations.

The overarching demonstration of a 50.0% lower amount of electricity utilised enables power services to access more consumers, reduce peaks, decrease tariffs, minimise fuel costs, and a windfall to trade, business exchange, industry, and better conditions of living for healthier dwelling environments.

Therefore, special education and enlightenment programmes, incentives and stimulus packages, and marketing campaigns aimed at each people group can enhance efficient electricity use. The female gender could be encouraged to embrace energy and money-saving schemes, and loss, and waste mitigation practices for a more liveable environment. Furthermore, the female gender is implored to efficiently use energy because it can result in higher standards of living, and accelerate industrial progress, and socioeconomic development.

References

[1] Electricity Control Board, 2005 ECB annual report. Windhoek; 2006.

[2] G.N.O. Asemota, Electricity Use in Namibia, first ed., iUniverse, Indiana, 2013.

[3] D. von Oertzen, Namibia's Electricity Supply. https://www.voconsulting.net/pdf/Namibia's%20Electricity%20Supply%20-%20VO%20CONSULTING.pdf/, 2009 (accessed 29 March 2017)

[4] W. Isaaks, Energy situation in Namibia. www.energynet.co.uk/system/files/Private_23/, 2013 (accessed 29 March 2017)

[5] V. Manuel, Energy demand and forecasting in Namibia: Energy for economic development, Office of the President, National Planning Commission, Windhoek, 2013.

[6] E. Brandt, Namibia's high electricity price. http://allafrica.com/stories/201411140794.html/, 2014 (accessed 29 March 2017)

[7] P.I. Shilamba, Update on the current power supply and progress made on NamPower projects and initiatives to ensure security of supply in Namibia, Media Briefing, Windhoek, 13 April, 2015.

[8] Anon, No power cuts expected in Namibia-Energy Minister. https://www.newera.com.na/2016/03/24/power-cuts-expected-namibia energy-minister/, 2016 (accessed 29 March 2017)

[9] N.A. Kgabi, The Namibian electrical energy mix and its implications for air quality and climate variability, 2016. J. Power and Energy Engg., 4 (2010) 19-30. http://dx.doi/10.4236/jpee.2016.43003

[10] Energypedia, Namibia Energy Situation. Energypedia.info/wiki/Namibia Energy_Situation/, 12 February 2020. (accessed 27 March 2021)

[11] P. Shilamba, NAMPOWER tariffs to go up in July. http://www.economist.com.na/2004/25june/06-25-07.htm/, 2004. (accessed 17 July 2006)

[12] N. Kerr, A. Gouldson, J. Barret, The rationale for energy efficiency policy: Assessing the recognition of the multiple benefits of energy efficiency retrofit policy. Energy Policy, 106 (2017) 212-221.

[13] C. Eid, A.L. Bollinger, B. Koirala, D. Scholten, E. Facchinetti, J. Lilliestan, R. Hakvoort, Market integration of local energy systems: Is local energy management compatible

with European regulation for retail competition? Energy, 114 (2016) 913-922.

[14] S. Bimenyimana, A. Ishimwe, G.N.O. Asemota, C.M. Kemunto, L. Li, Web-based design and implementation of smart home appliances control system, Proc. IOP Conf Series: Earth Environ. Sci. 168 (2018) 1-9.

[15] H. Shiraki, S. Nakamura, S. Ashina, K. Honjo, Estimating the hourly electricity profile of Japanese households-Coupling of engineering and statistical methods, Energy. 114 (2016) 478-491. .

[16] D.H. Llewellyn, M. Rohse, R. Day, H. Fyfe, Evolving energy landscapes in the South Wales Valleys: Exploring community perception and participation, Energy Policy. 108 (2017) 818-828.

[17] S. Simoes, W. Nijs, P. Ruiz, A. Sgobbi, and C. Thiel, Comparing policy routes for low -carbon power technology deployment in EU-an energy systems analysis, Energy Policy. 101 (2017) 353-365.

[18] P. Warren, Demand-Side Policy: Global evidence base and implementation patterns, Energy & Environ. 2018, pp. 1-26.

[19] A. Cherp, V. Vinichenko, J. Jewell, M. Suzuki, M. Antal, Comparing electricity transitions: A historical analysis of nuclear, wind and solar power in Germany and Japan, Energy Policy. 101 (2017) 612-628.

[20] M. Jakubcionis, J. Carlsson, Estimation of European Union residential sector space cooling potential, Energy Policy. 101 (2017) 225-235.

[21] C.R. Thomson, G.P. Harrison, J.P. Chick, Marginal greenhouse gas emissions displacement of wind power in Great Britain, Energy Policy. 1010 (2017) 201-210.

[22] S. Pfenninger, J. Decarolis, L. Hirth, S. Quoilin, I. Stafell, The importance of open data and software: Is energy research lagging behind?, Energy Policy. 101 (2017) 211-215.

[23] S. Neuteleers, M. Mulder, F. Hindriks, Assessing fairness of dynamic grid tariffs, Energy Policy. 108 (2017) 111-120.

[24] C.V. Broto, Energy landscapes and urban trajectories towards sustainability, Energy Policy. 108 (2017) 755-764.

[25] P. Diaz, C. Adler, A. Patt, Do stakeholders perspectives on renewable energy infrastructure pose a risk to energy policy implementation? A case of a hydropower plant in Switzerland, Energy Policy. 108 (2017) 21-28.

[26] M. Rama, E. Purseheimo, T. Lindroos, K. Koponen, Development of Namibian energy

sector, VTT Technical Research Centre of Finland, Finland. Research Report VTT-R -07599-13, 2014, pp. 1-69.

[27] S. Bimenyimana, G.N.O. Asemota, J.P. Ihirwe, C.M. Kemunto, L. Li, Performance estimation of Ntaruka hydropower plant and its comparison with the prediction obtained by SPSS, Energy & Environ. 2018, 1-18. https://doi.org/10.1177/0958305X18765961

[28] S. Bimenyimana, G.N.O. Asemota, L. Li, 2018. The state of the power sector in Rwanda: A progressive sector with ambitious targets, Front. Energy Res. 6 (68) 1-14. https://doi.org/10.3389/fenrg.2018.00068

[29] M.R. Braun, H. Altan, S.B.M. Beck, Using regression analysis to predict the future energy consumption of a supermarket in the UK, Appl. Energy. 130 (2014) 305-313.

[30] T. Heckmann, K. Gegg, A. Gegg, M. Becht, Sample size matters: investigating the effect of sample size on a logistic regression susceptibility model for debris flow, Nat. Hazards Earth Sys. Sc. J. 14 (2014) 259-278. https://doi.org/10.5194/nhess-14-259-2014.

[31] G.N.O. Asemota, Communality performance assessment of electricity load management model for Namibia, Proc. IEEE-AIMS. 2014, pp. 252-257. https://doi.org/10.1109/AIMS.2014.20

[32] Statsoft.com, Principal components and factor analysis, pp. 1-4, 2010. http://www.statsoft.com.texrbook/principal-componenets-factor-analysis (accessed 4 September 2013)

[33] N. O'Rouke, L. Hatcher, A step-by-step approach to using SAS for factor analysis and structured equation modeling, second ed., SAS Institute Inc., North Carolina, 2013.

[34] B. Thompson, Communality, in: I.M.S. Lewis-Beck, A.E. Bryman, T.F. Liao (Eds.), Sage encyclopedia of social science research methods, 1, Sage, London, 2004, pp. 145 -147.

[35] N. Blunch, Introduction to structural equation modelling using IBM SPSS Statistics and Amos, Sage, London, 2013.

[36] UNESCO.ORG. 6.3 Factor analysis. (accessed 12 December 2015) http://www.unesco.org/webworld/idams/advguide/chap6_3.htm

[37] A. Papoulis, S.U. Pillai, Probability, random variables and stochastic processes, fourth ed., Tata McGraw-Hill, New Delhi, 2008.

[38] S. S. M. Wong, Computational methods in physics and engineering, World Scientific, Singapore, 1997.

[39] G.N.O. Asemota, A prediction model of future electricity pricing in Namibia, Adv. Mat. Res. 824, 2013, pp. 93-99. https://doi.org/10.4028/www.scientific.net/AMR.824.93.

[40] G.N.O. Asemota, N.M. Ijumba, Gender mediated optimal multivariate electricity load management model, Proc. IEEE PES/IAS Power Africa 2020. https://doi.org/10.1109/PowerAfrica49420.2020.9219796.

[41] O.O. Asemota, G.N.O. Asemota, Time series modelling of academic employee commitment of a sub-Saharan African University, 2020. Asian J. Econ. Bus. Acctg. 19 (3) 60-76. https://doi.org/10.9734/AJEBA/2020/v19i330308

[42] P.D. Leedy, J.E. Omrod, Practical research: Planning and design, tenth ed., Pearson, Merrill, Prentice Hall, New Jersey, 2010.

[43] G.N.O. Asemota, Multivariate parsimony model of electricity load management, Proc. WSEAS 2015, *pp. 77-86, Energy & Environ 10th Int'l Conf. Energy & Environ*., Budapest, Hungary.

[44] EBP.UGA.EDU, Likelihood ratios, n.d. (accessed 6 December 2015) http://ebp.uga.edu/courses/Chapter 4 - Diagnosis I/6 Likelihood ratios.html

[45] HU-Berlin.De, Likelihood ratio test. n.d. (accessed 6 December 2015) Sfb649.wiwi.huberlin.de/fedc_homepage/xplore/tutorial/mvahtmlnode49.html.

[46] Z. Huang, 5 Likelihood ratio tests. 2009. (accessed 6 December 2015) http://www.math.uah.edu/stat/hypothesis/index.html

[47] A. Kyle, How are the likelihood ratio, Wald, and Lagrange multiplier (score) tests different and/or similar? 2012. http://www.ats.ucla.edu/stat/mult_pkg/faq/general/citingats.htm

[48] NIST/SEMATECH, Engineering statistics handbook: e-Handbook of statistical methods, 2013. http://www.itl.nist.gov/div898/handbook/ (accessed 6 December 2015)

[49] Penn State University, Reduced Likelihood Ratio Tests, 2015. https://onlinecourses.science.psu.edu/Stat504 (accessed 6 December 2015)

[50] S.F. Zheng, Likelihood Ratio Tests, n.d. (accessed 6 December 2015) http://people.missouristate.edu/songfengzheng/Teaching/MTH541/Lecture Notes/LRT.pdf.

[51] McGraw-Hill, S.P. Parker, McGraw-Hill dictionary of scientific and technical terms, sixth ed., McGraw-Hill, New York, 2003.

[52] T. Kancharla, P. Kharade, S. Gindi, K. Kutty, V.G. Vaidya, Edge based segmentation for

Pedestrian detection using NIR camera, IEEE. 2011. https://doi.org/10.1109/ICIIP.2011.6108965

[53] C. M. Bishop, Pattern recognition and machine learning. Springer, Singapore, 2008.

[54] G.N.O. Asemota, 2009. On a Class of Computable Convex Functions, Can. J. Pure & Appl. Sci. 3 (3) 959-965.

[55] G.N.O. Asemota, Optimal two-way conductor design using computable convex functions approach, Adv. Mat. Res. 367 (2012) 75-81. https://doi.org/10:4028/www.scientific.net/AMR.367.75

[56] F.B. Hildebrand, Advanced Calculus for Applications, Prentice-Hall of India, New Delhi, 1977.

[57] The Physics classroom: Inclined planes, 2015. http://www.physicsclassroom.com/class/vectors/Lesson-3/Inclined-Plane (accessed 29 January 2016)

[58] J. Frost, Standard error of the regression vs r-squared. 2017a. (accessed 23 January 2019) Statisticsbyjim.com/regression/standard-error-regression-vs-r-squared

[59] J. Frost, How to interpret r-squared in regression analysis. 2018. Statisticsbyjim.com/regression/interpret-r-squared-regression/ (accessed 23 January 2019)

[60] J. Frost, How to interpret adjusted–r-squared and predicted r-squared in regression analysis. 2017b. Statisticsbyjim.com/interpret-adjusted-r-squared-predicted-r-squared -regression/ (accessed 19 January 2019)

[61] J. T. Newsom, Lecture 20: more on multiple regression. 2007. Web.pdx.edu/~newsomj/PR551/lecture20.htm (accessed 29 January 2019)

[62] J. Netter, M.H. Kutner, C.J. Nachtsheim, W. Wasserman, Applied linear regression, third ed., Irwin, USA, 1996.

[63] N. Brace, R. Kemp, and R. Snelgar, SPSS for Psychologists: A guide to data analysis using SPSS for windows, Lawrence Erlbaum, New Jersey, 2000.

[64] A.H. Kvanli, S.C. Guynes, R.J. Pavur, Introduction to business statistics: A computer integrated approach, fourth ed., West Publishing Company, St. Paul, Minneapolis, 2002.

[65] J.J. Foster, Data analysis using SPSS for windows: A beginner's guide, Sage, London, 1998.

[66] Weibull.com, Reliability hot wire: Analysis of variance.

https://www.weibull.com/hotwire/issue95/relbasics95.htm (accessed 11 February 2019)

[67] W.B. Boast, H.W. Hale, E.C. Jones, Jr., A.L. Day, Electric and magnetic circuits, in: D.G. Fink, W.H. Beaty (Eds.), Standard Handbook for Electrical Engineers, fourteenth ed., McGraw-Hill, New York, 2000, Section 2, pp. 2-1-2-99.

[68] G. Strang, R. Kohn, Optimal design of a two-way conductor, in: J.J. Moreau, P.D. Panatogiopoulos, G. Strang (Eds.), Topics in nonsmooth mechanics, Birhauser Verlag, Basel, 1988.

[69] S. Takriti, The unit commitment problem, in: T.A. Ciriani, S. Gliozzi, E.L. Johnson, R. Tadei (Eds.), Operational research in industry, MacMillan, London, 1999, pp. 299-322.

[70] G.N.O. Asemota, Optimal two-way conductor design using computable convex functions approach, Proc. ICERD 2010, third Int'l Conf. Engg. Res. Dev., Benin City, Nigeria.

[71] P. Simshauser, D. Downer, 2012. Dynamic Pricing and the Peak Electricity Load Problem, The Australian Econ. Rev. 45 (3) 305-324.

[72] S. Bimenyimana, G.N.O. Asemota, 2018 Traditional Vs Smart Electricity Metering Systems: A Brief Overview, J. Mar. & Consum. Res. 46 (2018) 1-8.

[73] W. Cao, J. Wu, N. Jenkins, C. Wang, T. Green, Benefits analysis of Soft Open Points for electrical distribution network operation, Appl. Energy, 165 (2016) 36-47.

[74] D.M. Murray, J. Liao, L. Stankovic, V. Stankovic, Understanding usage patterns of electric kettle and energy saving potential, Appl. Energy, 171 (2016) 231-242.

[75] C.H. Edwards, D.E. Penney, Calculus, Prentice-Hall, New Jersey, 2002.

[76] R.B. Stull, Meteorology for Scientists and Engineers, second ed., Brooks/Cole, USA, 2000.

[77] F.M. White, Pressure distribution in a fluid: Fluid Mechanics, McGraw-Hill, New York, 2008.

APPENDIX

1. APPENDIX G.A

G.A. Analyses

The analyses support the foundation for the optimal electricity load management system, using likelihood ratio, asymptotes, subdued likelihood ratio, shared meaning measurements,

Neyman-Pearson algorithm, and multidimensional probability evaluation, in the following sub-sections.

G.A.1. Log-likelihood ratio and Convergence tests

The likelihood ratio (LR) evaluates simple or composite hypotheses [37]. LR checks for discrepancies in looped models, streamlines, or suggests more ideal or parsimonious models [46]. They decide which diagnoses to accept [41],[42],[43],[44]. There are at least two possibilities (affirmative or invalidating), [37],[41],[42],[43],[44],[45],[46], [47].

The affirmative expectation (LR+) states how greatly to raise the likelihood if it is in the affirmative. The invalidating expectation (LR-) indicates how little to lessen the likelihood if it is negating [41].

The generalised LR equations:

$$\text{LR} = \frac{Probability\ that\ the\ condition\ \ has\ \ true\ test\ result}{Probability\ \ without\ the\ condition\ has\ a\ true\ test\ result} \quad \text{(G.A.1a)}$$

$$\text{Positive LR} = \text{LR+} = \frac{Probability\ that\ the\ condition\ has\ a\ positive\ test\ result}{probability\ without\ the\ condition\ has\ a\ positive\ test\ result} \quad \text{(G.A.1b)}$$

$$\text{Negative LR} = \text{LR-} = \frac{probability\ that\ the\ condition\ \ has\ a\ negative\ test\ result}{probability\ without\ the\ condition\ has\ a\ negative\ test\ result} \quad \text{(G.A.1c)}$$

We define LR+ and LR- by their responsiveness and definiteness, respectively [41]. LR+ (responsiveness) is the expectation that an individual with a "definite" condition has an affirmative test. Therefore,

$$\text{LR-} = (\text{responsiveness})/(1 - \text{definiteness}) \quad \text{(G.A.2a)}$$

$$\text{LR+} = (1 - \text{responsiveness})/\text{definiteness} \quad \text{(G.A.2b)}$$

Consequently, LR+ is the "accept" condition, and LR- is the "reject" condition. Hence, LR+ and LR- are not altered as the odds fluctuate. They are positions and ranks that provide abundant and more practical advice [41].

Thus, LR+ and LR- are established attributes of an assessment, like responsiveness and definiteness, which are simple to adapt and use. Hence, the odds are as shown in Table G.1:

Table G.2 [41]

LR	Interpretation
>10.0	Substantial rise in the expectation
5.0-10.0	Modest rise in the expectation
2.0-5.0	Minor rise in the expectation
1.0-2.0	Token rise in the expectation
1.0	No alteration in the expectation
0.5-1.0	Nominal reduction in the expectation
0.2-0.5	Miniature reduction in the expectation
0.1-0.2	Limited reduction in the expectation
<0.1	Slight reductions in the expectation

All the assessments are divided into two (Yes or No, affirmative/negating). Many assessment types exist.

One model is complete and the looped model is achieved from the alternative by permitting some values to become zero [41],[42],[43],[44],[45],[46],[47]. This makes the design have a lesser expectation.

We assess the observed deviations if the design is statistically significant [44].

A real number sequence $\boldsymbol{x}$ has a density operation $f(x, \theta)$, where θ is any quantity, scalar, or vector. The sets Θ_0 and Θ_1 are subsets of the parameter space (test the hypothesis $H_0: \theta \in \Theta_0$, against $H_1: \theta \in \Theta_1$)

$$\Theta = \Theta_0 \cup \Theta_1 \tag{G.A.3}$$

Furthermore, θ_{m0} is the highest likelihood (ML) of $f(\boldsymbol{X}, \theta)$, for the sequence Θ_0 [37]. Therefore,

$$\lambda = \frac{f(\boldsymbol{X}, \theta_{m0})}{f(\boldsymbol{X}, \theta_m)} \tag{G.A.4}$$

where $0 \leq \lambda \leq 1$. This is so because $f(\boldsymbol{X}, \theta_{m0}) \leq f(\boldsymbol{X}, \theta_m)$, and, λ is intense near 1 if H_0 is true.

If H_0 is the simple hypothesis $\theta = \theta_0$, then,

$$\alpha = P\{\lambda \leq c|H_0\} = \int_0^c f_\lambda(\lambda, \theta_0)d\lambda \quad \text{(G.A.5)}$$

Using trials x_i of $\boldsymbol{x}$ to form the expectation operation $f(X, \theta)$. We evaluate θ_m and θ_{m0} and obtain the ratio $\lambda = \frac{f(X,\theta_{m0})}{f(X,\theta_m)}$:

Reject H_0 iff $\lambda < \lambda_\alpha$ (G.A.6)

where λ_α is the hundredth of the investigation statistic λ included in proposition H_0 [37]. When H_0 is a compound assumption, c is a fixed quantity, and $P\{\lambda \leq c\} < \lambda_\alpha$ for all $\theta \in \Theta_0$.

Consider, $f(x, \theta) \sim \theta e^{-\theta x} U(x)$. We investigate the proposition:

$H_0: 0 < \theta \leq \theta_0$ versus $H_1: \theta > \theta_0$. (G.A.7)

Also, Θ_0 is in a portion $0 < \theta \leq \theta_0$ of the authentic border and Θ is midway of $\theta > 0$. But, we have two compound propositions and the expectation operations are:

$$f(\boldsymbol{X}, \theta) = \theta^n e^{-n\bar{x}\theta} \quad \text{(G.A.8)}$$

whenever $\bar{x} > 1/\theta_0$ including $\bar{x} < 1/\theta_0$ [37].

In the half plane $\theta > 0$, the operation in equation (G.A.8) is highest when $\theta = 1/\bar{x}$. In the space $0 < \theta \leq \theta_0$, is highest as $\theta = 1/\bar{x}$ provided that $\bar{x} > 1/\theta_0$, while $\theta = \theta_0$, when $\bar{x} < 1/\theta_0$. As a result,

$$\theta_m = 1/x, \ \theta_{m0} = \begin{cases} 1/\bar{x}, & \bar{x} > 1/\theta_0 \\ \theta_0, & \bar{x} < 1/\theta_0 \end{cases} \quad \text{(G.A.9)}$$

The probability equals:

$$\lambda = \begin{cases} 1, & \bar{x} > 1/\theta_0 \\ (\theta_0 \bar{x})^n \left(e^{n\theta_0(1-\bar{x})}\right), & \bar{x} < 0 \end{cases} \quad \text{(G.A.10)}$$

Accordingly, we discard H_0 when $\lambda < c$, because $\bar{x} < c_1$, and c_1 balances the α portions of the real number sequence $\overline{\boldsymbol{x}}$ [37]. Therefore, the density of λ is evaluated, using asymptotes for large n to streamline the problem.

G.A.2. Asymptotes

Using m and m_0 to express the numbers of free quantities in Θ and Θ_0. These quantities can take on several values. Also, if $m > m_0$, the real number sequence assignment $\boldsymbol{w} = -2\log\lambda$ approaches a χ^2 distribution with $m - m_0$ df as $n \to \infty$ [37].

The function $w = -2\log\lambda$ is monotone decreasing, therefore, $\lambda < c$ iff $w > c_1 = -2\log c$. Consequently, $\alpha = P\{\lambda < c\} = P\{\boldsymbol{w} > c_1\}$, where

$c_1 = \chi^2_{1-\alpha}(m - m_0)$, and equation (G.A.10) yields this test:

Reject H_0 iff $-2\log\lambda > \chi^2_{1-\alpha}(m - m_0)$ (G.A.11)

Using the $N(\eta, 1)$ real number sequence $\boldsymbol{x}$ to assess the plain proposition $\eta = \eta_0$ against $\eta \neq \eta_0$, for asymptotes and any n [37]. Also, $\eta_{m0} = \eta_0$, and

$$f(X,\eta) = \frac{1}{\sqrt{(2\pi)^n}} exp\left\{-\frac{1}{2}\sum(x_i - \eta)^2\right\} \quad \text{(G.A.12)}$$

Equation (G.A.12) is highest if the identity sum

$$\sum(x_i - \eta)^2 = \sum(x_i - \bar{x} + \bar{x} - \eta)^2$$

$$=\sum(x_i - \bar{x})^2 + n(\bar{x} - \eta)^2$$

is least, when $\eta = \bar{x}$. For n identically separately dispersed (i.i.d) $N(\eta, \sigma)$ real number sequence $\boldsymbol{x_i}$, the specimen variance and specimen mean:

$$s^2 = \frac{1}{n-1}\sum_{i=1}^{n}(x_i - \bar{x})^2;\ \bar{x} = \frac{1}{n}\sum_{i=1}^{n} x_i \quad \text{(G.A.13)}$$

But, $\sum(x_i - \bar{x}) = 0$, and simplifies to,

$$\sum_{i=1}^{n}\left(\frac{\bar{x}-\eta}{\sigma}\right)^2 = \sum_{i=1}^{n}\left(\frac{x_i-\bar{x}}{\sigma}\right)^2 + n\left(\frac{\bar{x}-\eta}{\sigma}\right)^2 \quad \text{(G.A.14)}$$

Also, the two real numbers sequences $\bar{\boldsymbol{x}}$ and $\bar{\boldsymbol{s}}^2$ are separate. Therefore, the two terms to the right-hand side of equation (G.A.14) are separate [37].

Thus, $\eta_m = \bar{x}$, and the assessment λ, is:

$$\lambda = \frac{exp\left\{-\frac{1}{2}\sum(x_i-\eta_0)^2\right\}}{exp\left\{-\frac{1}{2}\sum(x_i-\bar{x})^2\right\}} = exp\left\{-\frac{n}{2}(\bar{x}-\eta_0)^2\right\} \quad \text{(G.A.15)}$$

Also, $\lambda > c$ if and only if $|\bar{x}-\eta_0| < c_1$. The expectation of the average real number sequence is equal to the strategic regional assessment, (q_u hundredth) evaluated at the approved normal hundredth z_u by:

$H_1: \eta \neq \eta_0$, Accept H_0 iff $z_{\alpha/2} < q < z_{1-\alpha/2}$ (G.A.16)

Additionally, when $m = 1$ and $m_0 = 0$:

$$w = -2\log\lambda = n(\bar{X}-\eta_0)^2 = \left(\frac{\bar{x}-\eta_0}{1/\sqrt{n}}\right)^2 \quad \text{(G.A.17)}$$

Equation G.A.17 is a real number sequence with kurtosis $\chi^2(1)$. The real number sequence $\boldsymbol{w}$ has a kurtosis $\chi^2(m-m_0)$ and is asymptotically assigned for all n [37].

G.A.3. Abated likelihood ratio

Two alternative models were considered (parsimonious and complete models) [46]. Furthermore, looped models are derived from the full models, by permitting some values to be zero [37],[46].

H_0: abated pattern is correct, H_a: Present version l is false

The no relationships and alternate propositions were different. Also, the no differences assumption was tested by setting a band of k factors from the design to nought [44],[46].

The two models were fitted, as:

(a) Abated model eliminates k estimates

(b) Complete pattern has k estimates

The expectation becomes:

$\Delta G^2 = -2\log L$ of lower design $-$ ($-2\log L$, of present version) (G.A.18)

where $G^{2\prime}s$ are general integrity statistics, and k is df (factors in the inquiry). The p-estimate is $P(\chi^{2k} \geq \Delta G^2)$. The abated design is the no differences approach. The current fitted model

contains the intercept and covariates model [44],[46]. This is akin to the null hypothesis being an accurate and smaller model [44].

G.A.4. Joint significance

The null hypothesis is tested by setting all the coefficients simultaneously to zero:

$$\log(\pi_1 - \pi) = a_0 + a_1X_1 + a_2X_2 + \cdots, a_kX_k \quad \text{(G.A.19)}$$

The assessment is:

$H_0 = a_1 = a_2 = \cdots = a_k = 0$, against the alternate proposition that at least a factor: $a_1, a_2 \ldots., a_k \neq 0$ [46].

The foregoing is akin to the comprehensive F-test in continuous regression. It equates to the no differences only assumption, which is acceptable:

$$\log(\pi_1 - \pi) = a_0 \quad \text{(G.A.20)}$$

This is opposed to the proposition that the present design (full design) is acceptable:

$$\log(\pi_1 - \pi) = a_0 + a_1X_1 \quad \text{(G.A.21)}$$

The assessment has k df (number of factors, except intercept) [46]. Thus, huge χ^2 kurtosis provides slight p-estimates and favors the current approach [37],[44],[46].

Consider a real number sequence X taking on values in S. For n trials from a population (recorded measurements), then,

$X = (X_1, X_2, \ldots, X_f, \ldots, X_n)$, where X_i is the i^{th} object vector [43].

Special cases occur when $(X_1, X_2, \ldots, X_n)$ are i.i.d. Consequently, the common distribution of size n.

If X has only two distributions, then:

H_0: X has pdf f_0 (G.A.22a)

H_1: X has pdf f_1 (G.A.22b)

If we observe that $X = X_1$, then the condition $f_1(X) > f_0(X)$ favours the alternative hypothesis. Also, the opposite inequality favors the null hypothesis [43].

We further let:

$$L(X) = f_0(X)f_1(X), X \in S \quad \text{(G.A.23)}$$

The functional L is the odds quotient operation for the proposition and $L(X)$ is the probability figure. Further, discard H_0 iff $L \leq j$, where j is a constant [43].

The significance level test is $\alpha = P_0 \ (L \leq j)$. We construct an assessment tool to choose j so that α is defined. When α lies within the distribution function $L(X)$, X has a discrete distribution [43].

The distribution of X depends on quantity θ, which has two possibilities [40],[41],[42],[43],[44],[45,[46]. The value space:

$\Theta = \{\theta_0, \theta_1\}$, and f_0 is probability density function (pdf) of X at $\theta = \theta_0$, and f_1 is the pdf of X, at $\theta = \theta_1$ [43],[47].

Accordingly, the propositions become:

$$H_0: \theta = \theta_0 \text{ opposed to } H_1: \theta = \theta_1 \quad \text{(G.A.24)}$$

G.A.5. The Neyman-Pearson schema

It is operational if it is within the exclusion region [43],[47]. Let,

$$R = \{X \in S: L(X) \leq j\} \quad \text{(G.A.25)}$$

where R is the exclusion region.

Additionally, the exclusion regions R are given by equation (G.A.25) and $A \subseteq S$. When R somewhat equals A, the exclusion area R is superior to the exclusion area A [43]. When

$P_0(X \in R) \geq P_0(X \in A)$, then

$$P_1(X \in R) \geq P_1(X \in A) \quad \text{(G.A.26)}$$

Proof of equation (G.A.26), and from L and R, the imparity holds:

$P_0(X \in A)P_0(X \in A) \leq jP_1(X \in A)$, because

$A \subseteq R \geq jP_1(X \in A)$, along with $A \subseteq R_C$.

For random $A \subseteq S$, we have:

$R = (R \cap A) \cup (R \backslash A)$, and $A = (A \cap R) \cup (A \backslash R)$.

From the additivity of the expectation and the imparities:

$$P_1(X \in R) - P_1(X \in A) \geq j[P_0(X \in R) - P_0(X \in A)]$$

Hence, if $P_0(X \in R) \geq P_0(X \in A)$, then,

$P_1(X \in R) \geq P_1(X \in A)$ (As was to be shown)

The foregoing Neyman-Pearson schema is more practicable than envisaged [42]. Hence, it is satisfactory for a range of alternatives, especially for the spectrum considered in this study [42],[43],[45],[47].

G.A.6. Charted likelihood ratio

Using the pdf f_0 of the data X, based on the value θ, and in the quantities space Θ. The propositions are:

$\theta \in \Theta_0$ against $\theta \notin \Theta_0$ (G.A.27)

where $\hat{\Theta} \subseteq \Theta$, and $\Theta_0 \subseteq \Theta$.

But,

$L(X) = max\{f_0(X): \theta \in \Theta_0\} max\{f_0(X): \theta \in \Theta\}$ (G.A.28)

where both L and $L(X)$ were as before. Therefore, modest $L(X)$ values favour the alternative hypothesis.

Log-likelihood ratio test (LRT) is generalised for optimal tests of null and alternative hypotheses. It depends on the expectation operation: $f_n(X_1, \ldots, X_n \mid \theta)$ [47]. But, the likelihood function is greatest adjacent to the precise θ value, and it is fundamental to maximum likelihood estimation:

$$\lambda = \frac{L(\hat{\omega}_0)}{L(\hat{\omega})} = \frac{k^{-1}(\hat{\theta})^{n\bar{x}+n\bar{y}} e^{-2n\hat{\theta}}}{k^{-1}(\theta_1)^{n\bar{x}}(\hat{\theta}_2)^{n\bar{y}} e^{-n\theta_1 - n\theta_2}} = \frac{(\hat{\theta})^{n\bar{x}+n\bar{y}}}{(\bar{x})^{n\bar{x}}(\bar{y})^{n\bar{y}}} \quad \text{(G.A.29)}$$

Because the abated and satiated (complete) systems are equal, $\bar{x} = \bar{y}$. The realised quantities are $\hat{\theta} = \frac{1}{2}(\bar{x} + \bar{y})$. Since, $\bar{x} = \bar{y}$. Then,

$$\hat{\theta} = \frac{1}{2}(2\bar{x}) = \bar{x} \quad \text{(G.A.30)}$$

Consequently,

$$\lambda = \frac{(\hat{\theta})^{n\bar{x}+n\bar{y}}}{(\bar{x})^{n\bar{x}}(\bar{y})^{n\bar{y}}} = \frac{(\hat{\theta})^{2n\bar{x}}}{(\hat{\theta})^{n\bar{x}}(\hat{\theta})^{n\bar{x}}} = \frac{(\hat{\theta})^{2n\bar{x}}}{(\hat{\theta})^{2n\bar{x}}} = 1 \quad \text{(G.A.31)}$$

Thus,

$$-2\ \log\lambda\ =\ -2\log 1 = 0 \quad \text{(G.A.32)}$$

Consequently, the sum of independent values in $\Theta\ = \{(\theta_1, \theta_2): \theta_1 > 0, \theta_2 > 0\}$ is $r\ =\ 2$. The specification in $\Theta_0 = \{(\theta_1, \theta_2 : \theta_1 = \theta_2 = \theta)\}$ is $r_0 = 1$. Therefore, $-2\log\lambda$ is a chi-square (χ^2) distribution having an $r - r_0 = 1$ degree of freedom. Since λ values are for large $-2\log\lambda$ in the rejection region [37],[41],[42],[43],[44],[45],[46],[47], the α test level consists of $-2\log\lambda$ and surpasses $\chi^2_{1(1-\alpha)}$. Again, 3.841 is the χ^2 analytical estimate at $\alpha = 0.05$ significance. It cuts off 0.95 area of the one-tailed χ^2_1 location [47].

Since $-2\log\lambda$ is below 3.841, the no differences conjecture is accepted $(H_0: \theta_1 = \theta_2)$. Therefore, the lessened – 2 log-probability design, is the same as the satiated model.

G.A.7. Amygdaloid diffused diagram using convex functions

It can also be seen that the pyriform lies in the right-hand-plane of the Respondents' gender vs Reduced electricity consumption scatter diagram (Fig. G.1). Therefore, the amygdaloid (pear-shape) is a cosine function (if we are to draw four quadrants in Fig. G.1 because only a cosine function is positive both in the first and fourth quadrants of a circle) [56].

Let us analyse this scenario.

We define the Hessian (H), H_r the relaxed Hessian, L the Lagrangian, and L_r the relaxed Lagrangian (greatest functional lower than L). The optimal electricity consumption problem is solved because H_r is convex, and the energy bulk β flows through a square area (A) [68].

Therefore, the energy bulk ($\beta = A = W$), where W is the lowest electricity demanded. Hence, the most favorable electricity utilisation arrangement has M estimates, in the minimised square, because:

$$M = \{\nabla u \neq 0\} \cup \{\nabla \mathrm{v} \neq 0\} \tag{G.A.33a}$$

$$Minimise\ surface\ area\ (M) = \iint 1_M dxdy, \tag{G.A.33b}$$

Based on: $\iint |\nabla u|^2 dxdy \leq E;\ \iint |\nabla v|^2 dxdy \leq F;\ u(x,0) = 0;\ u(x,1) = E;\ v(0,y) = 0;$ $v(1,y) = F$

Where E and F are either flow of charges or, potential differences; even though $E \leq 1$ and $F \leq 1$; $u(x,y)$ and $v(x,y)$ are extremals [56],[69],[70],[75],[76].

It has been shown by [55],[68] that the minimal area is:

$$W = \frac{E+F-2EF}{1-EF} \tag{G.A.34}$$

The $0-1$ electricity consumption problem is not convex because the controlled Lagrange factors λ and μ convert it into constrained operations:

$$L(u,v,\lambda,\mu) = \iint [1_M + \lambda|u|^2 + \mu|v|^2] dxdy - \lambda E - \mu F \tag{G.A.35}$$

Equation (G.A.35) is convex and the least L_c is below L. The pseudoconvexity L_r is the greatest operative below L that leads to fragile half-continuous and lower relaxation. Pseudoconvexity is burdensome to prove, but it exists and it is proven [55],[56],[68],[69],[70],[75]. The relaxation $L_r = \iint H_r(\nabla u, \nabla v) dxdy$ is polyconvex because H_r is convex in $|\nabla u|$ and $|\nabla v|$, and the Jacobian derivation, is

$$J = |\nabla u \nabla v| \tag{G.A.36}$$

Also, the optimal electricity consumption problem is solved because H_r is convex, and a unit square is considered:

$$Minimise\ \iint H_r dxdy \tag{G.A.37a}$$

Depending on: $\begin{cases} \bar{u}(x,0) = 0;\ \bar{u}(x,1) = \lambda^{½} E \\ \bar{v}(0,y) = 0;\ \bar{v}(1,y) = \mu^{½} F \end{cases}$ (A.37b)

The foregoing are satisfied by continuous operations: $\bar{u} = \lambda^{½} Ey$; $\bar{v} = \mu^{½} Fx$. Again, the Jacobian operations are fixed, since pseudoconvexity provides solutions to the boundary conditions. Fortunately, it is the smallest solution. Therefore, the least $\iint H_r dxdy$ is obtained from:

$$2\beta - 2|\bar{J}| = 2(\lambda E^2 + \mu F^2 + 2\lambda^{½}\mu^{½} EF)^{½} - 2EF = 2(\lambda^{½} E + \mu^{½} F - \lambda^{½}\mu^{½} EF) \quad \text{(G.A.38)}$$

Equation (G.A.38) was derived using the ending items of equation (G.A.34) and maximised upon λ and μ. Therefore,

$$W' = \max_{\lambda,\mu} \min_{u,v} L_r = \max_{\lambda,\mu} 2\left(\lambda^{\frac{1}{2}} E + \mu^{\frac{1}{2}} F - \lambda^{\frac{1}{2}}\mu^{\frac{1}{2}} EF\right) - \lambda E - \mu F \quad \text{(G.A.39)}$$

Differentiating equation (G.A.39) about λ and μ, and reshuffling, show: $\lambda^{½} = \frac{1-F}{1-EF}$; $\mu^{½} = \frac{1-E}{1-EF}$. Substituting utilities into equation (G.A.39) becomes:

$$W' = \frac{E+F-2EF}{1-EF} \quad \text{(G.A.40)}$$

The foregoing corresponds with the lowest electricity used W.

Additionally, $H_{\pm}(\nabla u, \nabla v, J)$

$$= d\left(\left[|\nabla u|^2 + |\nabla v|^2 \pm 2det[\nabla u \nabla v]\right]^{½}\right) \mp 2J \quad \text{(G.A.41)}$$

Also, $d(\nabla u, \nabla v, det[\nabla u \nabla v])$ is convex.

The least energy consumed arises when $\beta \leq 1$. Then: (a) Least energy utilisation W' is not greater than generated power W, since $H_r \leq H$ and $L_r \leq L$ for every positive Lagrangian coefficient λ and μ, (b) H_r are convex because its operative is the least, (c) Controlled least energy utilisation W' is equal to W.

Additionally, the smallest functions are within the fragile oscillation boundaries for L. But H_r is polyconvex when $H_r \leq H$ [55],[56],[70]. Polyconvexity shows that multilinear functions are minimum H_r envelopes that are less than H. Thus:

$$d(\sigma) = \begin{cases} 2\sigma, & 0 \leq \sigma \leq 1 \\ 1 + \sigma^2, & \sigma \geq 1 \end{cases} \quad \text{(G.A.42)}$$

The square root of σ, $d(\sigma)$ and constituents of $d(\sigma(\nabla u, \nabla v))$ are convex. The Jacobian values $\mp 2J$, make $H_{\pm}$ convex functions with supplementary parameters. But, H_r is the larger of either function, $H_{\pm}$ and when J is equal to $det[\nabla u \nabla v]$, H_r is polyconvex [55],[68],[70]. Since, $d\sigma = 1 + \sigma^2$ and for sizeable σ, the $H_{\pm}$ operations are $1 + |\nabla u|^2 + |\nabla v|^2$. For modest σ, the difference among H_+ and H_- hinges on:

$$2(l+n)^{1/2} - n \geq 2(l-n)^{1/2} + n \tag{G.A.43}$$

Equation (G.A.43) exists when $l \geq n \geq 0$ and $l + n \leq 1$. Thus, $l = |\nabla u|^2 + |\nabla v|^2$ and $n = 2|J|$.

The largest value of $\pm det[\nabla u \nabla v]$ equals $|J|$. The parameter σ is equal to φ in H_r because max $H_{\pm}$ is equal to H_r [54],[55]. However, H_r is below H since 2σ is below $1 + \sigma^2$ (for substantial σ). The benefits of multilinearisation are savings in electricity consumption and avoided production costs obtained by homogenisation. Consequently, the above arguments propose the realisation of the energy management of the charted optimal multidimensional electricity load management system.

Alternatively, an amygdaloid develops in hydrostatic equilibrium at balance or when the outflow velocity of every fluid parcel is static or unchanging. It occurs as a symmetrically rounded ellipsoid. Also, it satisfactorily approximates small flow velocities that cause insignificant acceleration.

In Astronomy, the field squeezes a star to the best-condensed design achievable. Consequently, whenever the trajectory of a star's angular velocity is much faster than the critical angular velocity, it produces or traces an amygdaloid. Further, shapes beyond the amygdaloid are unstable. Also, in hydrostatic equilibrium, there are no net forces, nor acceleration [76],[77]. Let us attempt some formalism.

We consider a cuboid parcel of fluid with density ρ, height dz, and surface area dA. The mass of the parcel is:

$$m = \rho \cdot dA \cdot dz \tag{G.A.44}$$

Using Newton's second law,

$$F = m \cdot a \tag{G.A.45}$$

where F is force and a is acceleration. We evaluate a pressure difference dP (assumed only in the z-direction) to obtain the force [76],[77]. Thus,

$$F = -dP.dA = \rho \cdot dA \cdot dz \cdot a \tag{G.A.46}$$

The acceleration from the pressure gradient is

$$a = -\frac{1}{\rho}\frac{dP}{dz} \tag{G.A.47}$$

The general expression for acceleration as a function of pressure is

$$\vec{a} = -\frac{1}{\rho}\vec{\nabla}P \tag{G.A.48}$$

The hydrostatic balance for Fig. G.1, occurs when the sum of forces in one direction is equal and opposite the sum of forces in the opposing direction. We divide the cuboid volume into volume elements and use an element to derive the action on the fluid [76],[77]. The force acting downwards on top of the fluid cuboid from pressure P is:

$$F_{top} = -P_{top} \cdot A \tag{G.A.49}$$

The volume element force acting upwards from below the fluid pressure is

$$F_{bottom} = P_{bottom} \cdot A \tag{G.A.50}$$

For the downward force of the volume element weight (V is volume element and g is standard gravity), then

$$F_{weight} = -\rho \cdot g \cdot V \tag{G.A.51}$$

The volume of the cuboid equals the area of the top or bottom element multiplied by height (h):

$$F_{weight} = -\rho \cdot g \cdot Ah \tag{G.A.52}$$

Balancing forces,

$$\sum F = F_{bottom} + F_{top} + F_{weight}$$

$$= P_{bottom} \cdot A - P_{top} \cdot A \quad \text{(G.A.53)}$$

For constant fluid velocity and dividing equation (G.A.53) by A, we have

$$0 = P_{bottom} - P_{top} - \rho \cdot g \cdot h$$

$$P_{top} - P_{bottom} = -\rho \cdot g \cdot h \quad \text{(G.A.54)}$$

Thus, $P_{top} - P_{bottom}$ is a pressure change.

Using pressure to be analogous to power in Fig. G.1, and power density is the time rate of energy per unit volume or power per unit volume (Wm^{-3}). At balance and without acceleration, the right-hand side of equation (G.A.54) equals zero. Hence,

$$Power_{top} - Power_{bottom} = 0$$

$$Power_{top} = P_{bottom} \quad \text{(G.A.55)}$$

For convexity condition (0,1), it means:

$$Power_{top} - P_{bottom} = 0 \quad \text{(G.A.56a)}$$

$$Power_{top} + Power_{bottom} = 1 \quad \text{(G.A.56b)}$$

We can easily solve equations (G.A.56a) and (G.A.56b), from hindsight of the convexity conditions of equation (G.A.43) above,

$$l \geq n \geq 0 \text{ and } l + n \leq 1 \quad \text{(G.A.57)}$$

Then,

$$l - n = 0, l + n = 1$$

$$l = n = ½ \quad \text{(G.A.58)}$$

Hence, using the same convexity corollary for equations (G.A.56a) and (G.A.56b),

$$Power_{top} = Power_{bottom} = ½ \quad \text{(G.A.59)}$$

The conditions in equations (G.A.55) and (G.A.59) can only be satisfied along the long diagonal of the amygdaloid at 50.0 percentile (0.5) and balanced loading because the amygdaloid is convex. Therefore, (½) or 50.0% load factor is the most economical operational solution to the charted multidimensional optimal electricity load management system.

G.A.8. Durbin-Watson (DW) statistic

Durbin-Watson (DW) evaluates the mutual interdependence of set forecast variables, applying first-order autoregressive error models. Also, the ordinary least squares (OLS) fit the regression operation in DW Statistic using ordinary residuals. They determine whether the mutual interdependence quantity ρ is zero. The errors e_t are unrelated if $\rho = 0$. Furthermore, the perturbations δ_r are unrelated [2],[43],[62],[63],[64].

The proposition assessments are:

$$H_0: \rho = 0; H_a: \rho > 0, \tag{G.A.60}$$

where n is the specimen, H_o is no difference assumption, and H_a is the alternate premise. Accurate DW indices are laborious to achieve. They are evaluated between two limits (higher (d_U) and lesser limits (d_L)), and D values exterior to these limits establish a definite conclusion.

The conclusions were arrived at using these two premises:

For $D > d_U$, we conclude H_0. If $D < d_L$, we deduce H_a. But, when $d_L \leq D \leq d_U$, the DW test is inconclusive [2],[43],[62],[63],[64].

Therefore, the DW statistic was determined from each leftover quantity, e_t, and its former value, e_{t-1}:

$$DW = \frac{\sum_{t=2}^{T}(e_t - e_{t-1})^2}{\sum_{t=1}^{T} e_t^2} \tag{G.A.61}$$

where T are observations in time sequences. But, slight D quantities show that $\rho > 0$, since adjacent inaccuracy items e_t and e_{t-1} are comparable in magnitude. Also, residual deviations $e_t - e_{t-1}$, are little when $\rho > 0$, so that D values are small in value [2],[43],[62],[63],[64].

Moreover, DW statistics is unable to manage the wrong specifications of a model. Thus, DW cannot recognise or discover self-organising interdependence errors linked with second-order interdependence patterns [2],[43],[62],[63],[64].

Table 2 indicates: $DW = 2.143$; $n = 32\ (33-1)$; α = 0.05; $k = 4$ (four estimates dependent on y_t) [2],[43],[62],[63],[64]. The test assumptions used DW statistic table values:

Jettison H_0: if $DW < 1.18$,

Accept H_0: if $(4 - DW) > d_U\ (d_U = 1.73)$

The analysis is vague if $d_L \leq (4 - DW) \leq d_U$

Also, $4 - DW = 4 - 2.143 = 1.857$

Already, $4 - DW\ (= 1.857) > d_U\ (= 1.73)$.

We adopt the No relationships assumption because there was no mutual interdependence. Consequently, we admit that the lessened energy utilisation amygdaloid is an optimal solution to the multidimensional electricity load management problem, which by extension can also decrease the money paid to the municipality or utility among other benefits [29],[43].

2. APPENDIX G.B

G.B.1. Log-likelihood ratio tests

A random number $\boldsymbol{x}$ has a density function $f(x, \theta)$, where θ is any quantity, scalar, or vector. To evaluate the premise $H_0: \theta \in \Theta_0$, versus $H_1: \theta \in \Theta_1$. The series Θ_0 and Θ_1 are subseries of the quantity space:

$$\Theta = \Theta_0 \cup \Theta_1. \tag{G.B.1}$$

Furthermore, θ_m is the θ when, $f(\boldsymbol{X}, \theta)$ is the highest in the interval Θ and θ_m. It is the Highest Expectation of θ. Thus, θ_{m0} is the best of $f(\boldsymbol{X}, \theta)$, in the sequence Θ_0 [26]. Accordingly,

$$\lambda = \frac{f(\boldsymbol{X}, \theta_{m0})}{f(\boldsymbol{X}, \theta_m)} \tag{G.B.2}$$

where $0 \leq \lambda \leq 1$. This is so because $f(\boldsymbol{X}, \theta_{m0}) \leq f(\boldsymbol{X}, \theta_m)$. Therefore, λ is condensed near 1 if H_0 is accurate.

The ML evaluation θ_m of θ approaches the accurate θ^* as $n \to \infty$. For the null assumption, θ^* is in the sequence Θ_0, hence, $\lambda \to 1$ when $n \to \infty$. We jettison H_0 when $\lambda < c$. The constant c is evaluated using the significance level α of the assessment [26].

When H_0 is the classic assumption $\theta = \theta_0$,

$$\alpha = P\{\lambda \leq c | H_0\} = \int_0^c f_\lambda(\lambda, \theta_0) d\lambda \tag{G.B.3}$$

From the above, we apply specimens x_i of $\boldsymbol{x}$ to build the expectation function $f(X, \theta)$.

We evaluate θ_m and θ_{m0} and build the ratio $\lambda = \frac{f(X, \theta_{m0})}{f(X, \theta_m)}$:

Reject H_0 iff $\lambda < \lambda_\alpha$ (G.B.4)

where λ_α is the hundredth of the assessment statistic λ using proposition H_0 [26].

Whenever H_0 is a compound proposition, c is fixed, and $P\{\lambda \leq c\} < \lambda_\alpha$ for all $\theta \in \Theta_0$.

Considering that, $f(x, \theta) \sim \theta e^{-\theta x} U(x)$. We can analyse the assumption:

$H_0: 0 < \theta \leq \theta_0$ opposed to $H_1: \theta > \theta_0$. (G.B.5)

Thus, Θ_0 is in section $0 < \theta \leq \theta_0$ of the true lane and Θ is midway of $\theta > 0$. For compound assumptions, the expectation operation is:

$$f(\boldsymbol{X}, \theta) = \theta^n e^{-n\bar{x}\theta} \tag{G.B.6}$$

as long as $\bar{x} > 1/\theta_0$ and $\bar{x} < 1/\theta_0$ [26].

In the half plane $\theta > 0$, the operation in equation (G.B.6) is highest for $\theta = 1/\bar{x}$. The interval $0 < \theta \leq \theta_0$, is highest at $\theta = 1/\bar{x}$ provided that $\bar{x} > 1/\theta_0$, and for $\theta = \theta_0$, then $\bar{x} < 1/\theta_0$. Hence,

$$\theta_m = 1/x, \ \theta_{m0} = \begin{cases} 1/\bar{x}, & \bar{x} > 1/\theta_0 \\ \theta_0, & \bar{x} < 1/\theta_0 \end{cases} \tag{G.B.7}$$

The probability equals:

$$\lambda = \begin{cases} 1, \ \bar{x} > 1/\theta_0 \\ (\theta_0 \bar{x})^{\,n}\left(e^{n\theta_0(1-\bar{x})}\right), \ \bar{x} < 0 \end{cases} \quad \text{(G.B.8)}$$

Additionally, we jettison H_0 if $\lambda < c$, which is equal to $\bar{x} < c_1$, where c_1 is identical to the α percentile of the real number sequence $\bar{\boldsymbol{x}}$ [26]. To achieve the foregoing, the density λ is evaluated, using asymptotes for large n.

3. APPENDIX G.C

Table G. 4: Likelihood Ratio Tests [2]

Effect	-2 Log Likelihood of Reduced Model	Chi-Square	Df	P-value
Intercept	.000(a)	.000	0	.
Q10RCDPN	.000(a)	.000	0	.
Q21RECRG	.000(a)	.000	0	.
Q18IECIG	.000(a)	.000	0	.
GENDER	.000(a)	.000	0	.
AGE	.000(a)	.000	0	.
Q4ELEENJ	.000(a)	.000	0	.
Q5SWIOFF	.000(a)	.000	0	.
Q6SGACHA	.000(a)	.000	0	.
Q7ESRCEC	.000(a)	.000	0	.
Q8LIVEAW	.000(a)	.000	0	.
Q9ESNBC	.000(a)	.000	0	.
Q11SCHNP	.000(a)	.000	0	.
Q12UEELS	.000(a)	.000	0	.
Q13LWABL	.000(a)	.000	0	.
Q14LSAWA	.000(a)	.000	0	.
Q15NRECP	.000(a)	.000	0	.
Q16PDCWD	.000(a)	.000	0	.
Q19BEEER	.000(a)	.000	0	.
Q20WANDN	.000(a)	.000	0	.
Q22EPEEM	.000(a)	.000	0	.
Q23MDLRE	.000(a)	.000	0	.
Q24NCAAC	.000(a)	.000	0	.
Q25RWEGD	.000(a)	.000	0	.
Q26IEUDN	.000(a)	.000	0	.
Q27EEBLP	.000(a)	.000	0	.
Q28EUNCN	.000(a)	.000	0	.
Q29EEUDP	.000(a)	.000	0	.
Q30BNEGS	.000(a)	.000	0	.

Q31TVOWP	.000(a)	.000	0	.
Q32TODRG	.000(a)	.000	0	.
Q33LTWHV	.000(a)	.000	0	.
Q34DCEOD	.000(a)	.000	0	.
Q35LWTDW	.000(a)	.000	0	.
Q36IHSEM	.000(a)	.000	0	.
Q37DSRHM	.000(a)	.000	0	.
Q38UCWDR	.000(a)	.000	0	.
Q39SOACO	.000(a)	.000	0	.
Q40KACFB	.000(a)	.000	0	.
Q41KWCDA	.000(a)	.000	0	.
Q42KHAAT	.000(a)	.000	0	.
Q43RACCP	.000(a)	.000	0	.
Q44STHAM	.000(a)	.000	0	.
Q45TOHAD	.000(a)	.000	0	.
Q46OFFDR	.000(a)	.000	0	.
Q47MPTRF	.000(a)	.000	0	.
Q48CWLWP	.000(a)	.000	0	.
Q49BLQTC	.000(a)	.000	0	.
Q50KBPPS	.000(a)	.000	0	.
Q51PPSSB	.000(a)	.000	0	.
Q52UFLWP	.000(a)	.000	0	.
Q53ASCLD	.000(a)	.000	0	.
Q54NSFWF	.000(a)	.000	0	.

Note:

The kurtosis is the difference in -2 log-probabilities between the satiated pattern and an abated model. The lessened approach is modelled by leaving out an effect from the satiated model. The no differences assumption is that all parameters of that effect are 0.

a. The abated model is equivalent to the full model because neglecting the effect does not increase the degrees of freedom.

APPENDIX H

This part of the thesis presents Multivariate Component Analysis Optimisation of Electricity Load Management in which principal component analysis (PCA) uses lower bound convex functions to assess the patterns of deviations that indicate interrelationships among household characteristics and household electricity consumption behaviours. PCA is a straightforward explanatory statistical procedure that elicits meaning from competing dimensionless arguments or propositions. The results show that seventeen components were extracted from the load management predictors that assign distinctive importance or weights to the number of load management variables (between 1 and 32) extracted and included for each component. Furthermore, every component extract depicts fewer energy losses, waste reduction, and money and energy-saving mechanisms. The extracted component factors can be used to device efficient, resilient, and smart grids and smart cities of the future.

H.0 Multivariate component analysis optimisation for electricity load management

H.1 ABSTRACT

The principal component analysis (PCA) is a more precise technique for finding valuable electricity load management patterns in high-dimension data. The new variable components measure many variations that reflect strong relationships between household characteristics and household electricity consumption behaviours. The lower-bound communality solutions are similar to convex functions used for determining high-quality optimisation solutions without resorting to laborious mathematical algorithm computations. Furthermore, PCA provides an unbiased statistical description of electricity load management behaviours because it enables contrast between dimensionless quantities. A validated 5-point Likert scale residential electricity load management questionnaire gathered the survey data for component analysis in Windhoek City, Namibia, deploying the statistical package for social sciences (SPSS). The results indicate that the eigenvalues varied between 8.229 and 1.020. The average communality was around 88.8%, and the communality ranged between 0.762 and 0.955. The 17 components extracted using the PCA assessed all the electricity load management metrics to varying degrees. Also, between 1 and 32 parameters were extracted in each of the 17 components selected. Generally, each extracted component indicates lesser losses, waste minimisation, and energy and money savings. In addition, the results show that building new generation stations would not reduce global warming unless building blue,

green, and other alternative energy generation stations. Also, the outcome or findings of the study can streamline data heterogeneity, over-time variability of distribution networks, and territorial factors of electricity consumption variability by geography. These factors can be used to implement the efficient, resilient, and smart grids of the future that can withstand the weather, especially in the face of climate change and its consequences on the environment.

H.2 KEYWORDS

Communality; energy savings; factor analysis; principal component analysis; waste minimisation

H.3 Introduction

Load management (LM) effectively optimises the successful operation of any power utility. Load growth, expanding generation ability constraints, mounting electricity imports, and electricity demand above supply ability allowed new generation facilities or LM to supply the deficit [1]. High energy absorption caused surging electricity tariffs in Namibia [2]. Cost thoughtful electricity tariffs were proposed in 2011/2012. But, large supply dependency on South Africa has confined the Namibian electricity supply sector [3]. Namibia's electricity demand doubled in 2012 by investing in the mining sector. It imports 80.0% of the energy consumed at certain periods and its average is 60.0% [4]. Liquid fuel accounted for over 63.0% of the total net energy consumption [5]. Namibia's electricity supply is dependable and relatively stable, but its industrial electricity tariffs are the highest after Mauritius, and higher than South African rates by between 20.0 and 25.0% [6]. Namibia generates about 1305.0GWh/year and consumes over 3000.0GWh/year. The electricity supply deficit is imported from South Africa, Zambia, and Mozambique [7].

Power demand response (DR) presents as electricity prices, incentives, or changes in power consumption patterns. It combines electricity, heat, natural gas, and other forms of energy to reduce energy consumption [8,9]. Both the UK and the US have effectively controlled their peak loads, and the European electricity markets have used DR to reduce peak loading by 2.9% on average in each country [10].

Negative pricing exists in the US and some electricity generators like nuclear, hydroelectric, and wind energy pay their customers to consume more power for economic and technical reasons, even during electricity supply shortages [10]. Price volatility from renewable energy injection [11], over-supply, and over-demand in energy result in price spikes that form

the basis for electricity load management, future planning, and policy. The principal component analysis (PCA) model was formulated to balance the impacts of electricity over-supply against over-demand [12]. PCA separates peak-load spikes into individual principal components (PCs) and explains how they precisely influence the electricity load fluctuation in the power system. Although the electricity market experiences more power shortage problems than power excess [10,13], electrical energy storage (EES), transmission capacity upgrade, and DR can reduce power shortage [1,10,14].

PCA assesses the dimensions of variability and aids hypotheses testing [15]. Also, irregular load behaviours occur at numerous points along with the transmission system having highly amassed load shapes, load clustering, load forecasting, and load modelling applications. Besides, robust principal component analysis (RPCA) decouples the annual load profiles in low-rank and sparse components. It also reduces data quality problems resulting from corrupted data or missing values [1,16,17].

A building's energy consumption is influenced by climate, building characteristics, user characteristics, building services, and building occupants' behaviour and activities. Others include social and economic factors and indoor environmental quality [18]. Load forecasting accuracy with a backpropagation neural network is obtained through planning, power consumption, and dispatching [12,19].

Energy efficiency has a lot of benefits but energy generation investment is higher than energy demand reduction because about two-thirds of the energy efficiency potential will remain untapped by 2035 [20]. Distributed energy penetration growth opened up local energy management (LEM), and decentralised energy supply, storage, transport, conversion, and consumption within geographical areas [21]. Automated control [9] and demand-side management (DSM) enabled LEM to use local heating to increase energy efficiency, reduce carbon emissions, and improve energy independence [21].

Hourly electricity consumption appliances in households save energy. Also, energy consumption increases with population, gross domestic product (GDP), appliance proliferation, quality of life, and electricity consumption behaviour [22]. Governments use DSM to manage energy consumption, environment, energy security, energy efficiency, demand response, onsite generation, energy storage, and carbon emissions reduction [23-24].

Supply-side management (SSM) uses utility business models in the USA, UK, France, and China to achieve performance targets, decoupling policies, information campaigns, loans and

subsidies, utility obligations, and performance standards for low carbon incentives and environmentally sustainable energy systems [24]. Analyses of nations' low-carbon electricity transition depend on technological, economic, political, and socio-technical processes [25].

Also, the demand for space heating and cooling is growing globally. More cooling demand requires greater power generation capacity and a fortification of the electricity transmission systems [26].

Rising intermittent renewable energy and greater electricity usage drive strong variations in network management, costly network expansion, peak reduction, and network congestions [27]. Urban energy transition drives urbanisation and rising carbon emissions. Further, the urban energy outlook indicates how people use energy for lighting, thermal comfort, communications, and transportation. Also, it indicates how electricity generation, gas, direct use of fuels for heat, or mechanical power are provided [28]. A major policy shift to address energy crises in Switzerland comprises reducing energy consumption by half, increasing 15-fold renewable energy production, reducing CO_2 emissions without compromising supply, security, and costs, and phasing out existing nuclear power reactors at the end of their service lives [29].

Several countries are changing their generation mixes and moving towards renewable sources such as hydro to reduce greenhouse gas emissions (GHGs). For example in 2015, Switzerland met 59.9% of its electricity demand from hydropower [29]. For Namibia it was 67.0% in 2014 and for Rwanda 48.0% in 2017 [13,30,31].

Blinds systems over windows and doors trim inlet heat by 50.0% in summer and 25.0% in heat outlets in winter [1]. Daylighting regulates natural light and trims electric lighting, and saves energy. Day-lighting controls commercially benefit the United States (US) because 75.0% of the electricity is consumed in buildings nationwide. Platinum-level tubular skylights use daylighting to achieve uniform light distribution including 25.0% less energy than traditional lighting fixtures. Limited electric lighting supports a 24.0% energy reduction in Los Angeles schools and trims a third of total building energy costs [32].

Also, between 10.0% and 20.0% of the energy used for cooling buildings can be saved by daylighting and trimming total energy costs by a third [33]. Further, the building architecture, usage, and energy consumption habits, day-lighting can reduce electric lighting between 20.0% and 80.0% [34]. Day-lighting at utility peak demand hours trims demand charges, raises employees' productivity, and improves the health of building occupants [35].

Additionally, above US$60 billion was expended annually on electric lighting in commercial buildings' [36] while between 30.0% and 50.0% of the over 64 billion square feet of commercial buildings' floor spaces can access daylight either by skylights or through windows. Therefore, millions of electric lighting fixtures can be turned off for some periods of the day for energy savings [37].

However, principal component factor analysis demands that variables included are metric level or dichotomous – nominal level (coded). The sample size must be greater than 50 (preferably 100), and the ratio of cases to variables must be 5 to 1 or higher (at least a 5-point Likert scale). The correlation matrix for variables must contain 2, or more correlations of 0.3, or greater [38]. Furthermore, PCA reduces survey data into factors that account for maximum variance using algorithms that generate conceptual and mathematical understanding of the construct under investigation [39]. Besides employing the covariance matrix, the variables are in their original metrics. PCA assumes each original measure was obtained without measurement error. The drawbacks are that PCA needs a large sample size and depends on the correlation matrix of the variables under investigation. Also, correlations require a large sample size before they stabilise [40].

The remaining parts of this thesis consist of the methodology, results and discussion, and conclusion.

H.4 Methodology

A validated 5-point Likert scale residential electricity load management questionnaire gathered survey data for analysis in Windhoek City, Namibia. Only 127 (42.3%) completed and duly received responses from over 300 questionnaires administered were subjected to statistical analysis for the social sciences (SPSS). Also, the 127 sample size sufficiency was proven in [41]. Reference [42] advises on sample sizes to indicate that 300 is good, 500 is very good, and 1000 or more is excellent. A minimum of 10 observations per variable is required to avoid computational difficulties, but without stating the population to determine the appropriate success rates. Reference [43] indicates that the average questionnaire response was 52.7% when 1607 studies were analysed for 400,000 individual respondents. Furthermore, the standard deviation was 20.4 meaning that the response rate lay between 32.3% and 73.1%, respectively. Reference [44] obtained around 33.0% response rate for online surveys and 43.0% for agricultural science teachers in Texas [45]. Therefore, the 42.3% response rate obtained in this study is within acceptable limits [43-45].

H4.1 Sample Size Adequacy

Alternatively, the sample size adequacy can use the Poisson distribution. We can conclude data with finite sample sizes using the root mean square deviations (RMSD) of the distribution function [46,47]. If one sampling set from the parent distribution is considered, the Poisson distribution approaches a binomial distribution.

Also, the mean and variance of Poisson processes are equal for infinite samples of 127 electricity load management surveys. In addition, the sufficient sample size is represented by one value when the degrees of freedom (DF), is large. Since the occupancy for any sample is $(n)^{\frac{1}{2}}$, the correct sample size [47,48] lies between $\left[127-(127)^{\frac{1}{2}}\right]$ and $\left[127+(127)^{\frac{1}{2}}\right]$. That means, any sample size between 116 and 138, is sufficient to obtain trustworthy conclusions from the research.

H4.2 Principal Component Analysis

PCA is a widely used procedure in multivariate statistical inference [49]. Mathematically, PCA transforms a related series of variables into the same number of uncorrelated variables. For n random variables $x=[x_1,x_2,\dots,x_n]^T$, the mean vector is a zero vector $[E[\boldsymbol{x}]=0]$. The covariance matrix is $\boldsymbol{C}=\left[Cov[x_i,x_j]\right]_{\{1\le i,j\le n\}}$ $E[\boldsymbol{x}\boldsymbol{x}^T]$, and is not a zero vector ($\boldsymbol{C}\neq\boldsymbol{0}$). It is positive definite, and all the n separate variables $(Var[x_i],i=1,\dots,n)$ are positive values [10]. Also, PCA uncovers which variables describe the highest variance. It also simplifies most of the overall variability or total spread.

Mathematically, we determine the non-zero column vector $\boldsymbol{A}=[a_1,a_2,\dots,a_n]^T$ that satisfies $\boldsymbol{A}'\boldsymbol{A}=1$ to maximise the variance of the linear combination, $\boldsymbol{A}'\boldsymbol{x}$:

$$Var[\boldsymbol{A}'\boldsymbol{x}]=E[\boldsymbol{A}'\boldsymbol{x}]^2=E[(a_1x_1+\cdots+a_nx_n)^2] \quad \text{(H.1)}$$

Since the covariance matrix of $\boldsymbol{x}$ is $\boldsymbol{C}$, the variance of $\boldsymbol{A}'\boldsymbol{x}$ is

$$Var[\boldsymbol{A}'\boldsymbol{x}]=\boldsymbol{A}'\boldsymbol{C}\boldsymbol{A} \quad \text{(H.2)}$$

To evaluate $\boldsymbol{A}$ we solve the following Lagrange function

$$L=\boldsymbol{A}'\boldsymbol{C}\boldsymbol{A}-\lambda(\boldsymbol{A}'\boldsymbol{A}-1) \quad \text{(H.3)}$$

where λ is a Lagrange multiplier [10]. In the first-order condition (FOC), the vector of the partial derivative becomes

$$\partial L/\partial\boldsymbol{A}=2\boldsymbol{C}\boldsymbol{A}-2\lambda\boldsymbol{A}=2(\boldsymbol{C}-\lambda\boldsymbol{I})\boldsymbol{A}=0 \quad \text{(H.4)}$$

For admissible solutions in the FOC, the Lagrange multiplier λ must satisfy the characteristic equation $[\boldsymbol{C} - \lambda I] = 0$. The polynomial $[\boldsymbol{C} - \lambda \boldsymbol{I}]$ comprises n degrees of λ and will have n λs $(\lambda_1, \lambda_2, \dots, \lambda_n)$. We can interpret λs by rearranging the FOC into the equation $\boldsymbol{CA} = \lambda \boldsymbol{A}$ that agrees with the eigenvalue description. Hence, λ is the eigenvalue to the covariance matrix $\boldsymbol{C}$, and $\boldsymbol{A}$ is the associated eigenvector. The λs of $\boldsymbol{C}$ can be ranked as $\lambda_1 \geq \lambda_2 \geq \cdots \geq \lambda_n > 0$ [10].

The highest variance is equal to λ_1, so the associated representative eigenvector $\boldsymbol{A_1}$ maximises the variance of $\boldsymbol{A'x}$, and comprises most of the total variability. But, $\boldsymbol{A'x}$ is the principal component (PC) of $\boldsymbol{x}$ linear combinations with variance λ_1. Correspondingly, the second PC is $\boldsymbol{A_2'x}$, which depicts the second largest variance that is equal to λ_2 which has not been allowed for by the first PC [10].

We have a total of n PCs used to describe the variability. Also, any two different PCs are independent and can be expressed as

$$\begin{aligned} PC_1 &= \boldsymbol{A_1'x} = a_{11}x_1 + a_{12}x_2 + \cdots + a_{1n}x_n \\ PC_2 &= \boldsymbol{A_2'x} = a_{21}x_1 + a_{22}x_2 + \cdots + a_{2n}x_n \\ &\vdots \\ PC_n &= \boldsymbol{A_n'x} = a_{n1}x_1 + a_{n2}x_2 + \cdots + a_{nn}x_n \end{aligned} \quad \text{(H.5)}$$

Consequently, the PCs retain most of the essential information embedded in the original variables $\boldsymbol{x}$. In the cell of $\boldsymbol{A'}$, a_{ij} is the measure of the j^{th} variable in the i^{th} PC, which is the factor loading. Hence, a_{ij} satisfies the requirements [10]:

$$a_{i1}^2 + a_{i2}^2 + \cdots + a_{in}^2 = 1 \text{ for } i = 1,2, \dots, n \quad \text{(H.6)}$$

and

$$a_{i1}a_{j1} + a_{i2}a_{j2} + \cdots + a_{in}a_{jn} = 0 \text{ for } i \neq j \quad \text{(H.7)}$$

Equation (H.6) is used to specify the scale of the PCs as a necessary condition while equation (H.7) guarantees that any two PCs are orthogonal to each other. In one PC, the a_{ij} coefficients are significantly different between x_js. The parameters x_js with higher coefficients have dominant power in the PC. But, the coefficient a_{ij} on the j^{th} variable x_j shows different values in separate PCs. To uncover and explain the hidden meaning communicated by PCs, we focus our attention on the coefficients with relatively higher PCs than others on the same PC [10]. Since the eigenvalue and variance λ_s are in descending order, we only retain PCs with large λ_s

and eliminate the remaining PCs with smaller λ_s. In sum, we can use PCA to identify a set of new orthogonal factors called the PCs. The general properties of PCs include: each PC is a linear mix of the original parameters. The first PC describes the largest variance in the data, which equals the highest eigenvalue of the covariance. The second PC describes the largest variance in the data that was not described by the first PC. The i^{th} PC continues to describe the largest variance in the data that was not described by the previous $(i-1)$PCs. The number of PCs is equal to the number of the original variances. However, any two of the PCs are uncorrelated (orthogonal), and only PCs with large variance values are necessary for PCA use [10].

H4.3 Data Normalisation

Upon collecting load data N^I, each load area i is a column vector $x_i \in R^{N^I}$ of historical annual load data with N^T measurements. Disparate load areas normally have different peak loads X_i^{max}. For stability in computation and ease of differentiation, the load profiles are normalised for the scales to be 0 and 1. The load data matrix M of size $N^T \times N^I$is obtained. Each column $y_i \in R^{N^T}$ is a normalised load profile [16].

$$y_i = \left(x_i - X_i^{min}\right)/\left(X_i^{max} - X_i^{min}\right) \quad \text{(H.8)}$$

PCA is used for data reduction and feature extraction. PCA is formulated for optimisation to determine a rank-k component L to minimise the l_2-form of reconstruction errors connecting the original data M and low-rank component L. The SVD is used to solve the optimisation problem [16]:

$$\text{Minimise } \|M - L\| \quad \text{(H.9)}$$

$$\text{Subject to } \quad \text{rank}(L) \leq k$$

Although PCA cannot perform well if the data is not well cleaned, corrupted measurements may lead to poor reduction results.

In power systems, robust PCA (R-PCA) is a filter that decouples the normalised load data into low-rank and sparse components. But PCA is a linear mapping method that transforms data, keeps data integrity, and is suitable for load time series analysis [16]. The principal component pursuit (PCP) form of the R-PCA minimises the weighted sum of the nuclear norm of the low-rank matrix L, and l_1-norm of the sparse matrix S, subject to the original matrix

conditions. The nuclear norm assesses the sum of the singular matrix values of equation (H.11), and the l_1-norm imposes sparsity in the S matrix of the equation (H.12) [16]:

Minimise $\|L\|_* + \mu\|S\|_1$ (H.10)

Subject to $L + S = M$

$\|L\|_* = \sum_i \sigma_i(L)$ (H.11)

$\|S\|_1 = \sum_{ij}|S_{ij}|$ (H.12)

Fortunately, no tuning parameter is necessary. The weighting factor μ is theoretically determined using equation (H.13) under lenient conditions.

$\mu = 1/\sqrt{max(N^T, N^I)}$ (H.13)

This controllable convex optimisation problem is solved to competently recover the PCP form of the original data matrix. Also, the iterative threshold, accelerated proximal gradient, and augmented Lagrangian multipliers can be used to solve the problem [16].

H5 Results and Discussion

Figure H.1 is the scree plot that indicates the eigenvalues graphed against the number of components obtained from the factor analysis. It describes the correlations between each response to every question on the administered questionnaire. The eigenvalue is the solution to the parameter equation that is compatible with the boundary conditions. The component is one of the elements into which any algorithmic equation could be resolved. Furthermore, a scree graph is an exponential decay curve for which the eigenvalues decrease with component numbers. Both the eigenvalue and component are dimensionless, and can, therefore, fit into any reference frame [1,40,41].

The first eigenvalue in Figure H.1 is slightly greater than 8 (8.227). The elbow to the leeward side of the slope had about 19 components until the eigenvalues are almost indistinguishable. Seventeen components were selected by the component matrix because the Kaiser criterion allows only unity eigenvalues or greater as components. This means that a factor extracts at least one variable, otherwise it must be discarded [1,40,41]. Thus, only two, or three, or four, or five factors, or more are required when using a scree plot. Although the scree graph returns very few factors, the Kaiser criterion can return too many components for which interpretation could be difficult [1,40,41,50,51].

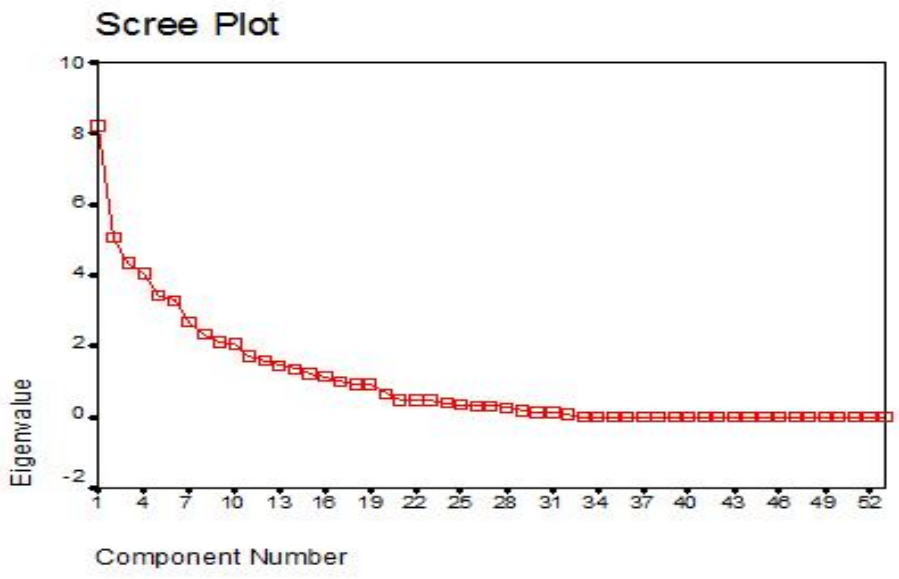

Figure H. 1: Eigenvalue as a function of principal component number [4].

Table H.1 indicates the communalities, ranging between 0.762 and 0.955, while 0.888 was the average communality. Communalities are lower-bound optimisation solutions similar to convex functions for obtaining optimal high-quality results without engaging laborious mathematical algorithms [41,52,53]. Communality is the property of an observed variable having a variance of common factors. Thus, large communality reflects a strong influence by at least one common factor. It is how much variance it has in common with hidden variables in the model. The symbol of the communality coefficients is h^2. The essential initial communalities are the variances of each parameter, which are common variances of the components [1,40,41,48,53].

Table H.2 depicts the total variance explained comprising component numbers (17 for which eigenvalues are greater than or equal to unity), initial eigenvalues, and extracted sums of squared loadings. Furthermore, the initial eigenvalues are the variances of the PCs because the PCA was conducted on the correlation matrix [40]. The Total column consists of eigenvalues (8.229 to 1.020). The first column accounts for the most variance or highest eigenvalue and the second component accounts for the rest or leftover variance as it can. Each successive component accounts for smaller and smaller variance [1,40]. The percentage variance is the variance percent accounted for by each principal component (15.527%-1.924%). The cumulative percentage variance accounts for the current or overall or all preceding principal components (15.527%-88.792%). The extraction of sums of square loadings has three columns

of the half of the table that exactly reproduce the values or metrics given on the same rows on the left side of the table [40].

Table H.3 shown in Appendix A depicts the component analysis matrix composed of components with their respective loadings and constituting parameters. Component scores are variables added to the dataset for observing the dimensionality of data. If two components are extracted and those two components accounted for 68.0% of the total variance, then the two dimensions in the component space account for 68.0% of the variance [40]. Therefore, Table H.3 accounted for 17 extracted components that amounted to 88.8% of the variance. The component matrix has component loadings, which are the correlations between the variable and the component. The SPSS does not consider any of the correlations that are below 0.3 (whether positive or negative) because it makes the interpretation easier to read by removing the low correlations that are not very meaningful [40]. Furthermore, negative loading is just as strong as positive loading. Negative loading means an inverse or negative relationship [38].

Further, all the component matrix values of Table H.3 shown in Appendix H.A were compared using the strength of the relationships or association [54] with optimal electricity load management. Also, component 1 comprises 32 electricity load management metrics and each has loadings 0.3 or greater. As a result, only those parameters exhibiting moderate or strong relationships were considered for the brevity of the analysis of each component.

For Component 1, the metrics exhibiting moderate relationships include electricity is to be enjoyed (-0.433); reduced electricity consumption decreases money paid to the utility or municipality (0.569); smaller electricity use helps the utility supply regular power to all (0.572); I do not need to reduce the electricity consumed since I can pay for it (-0.402); controlled power consumption reduces stress on utility facilities (0.638); I will like to buy energy-efficient equipment to reduce the amount spent on bills (0.524); reducing wasted electricity is good for development (0.520); I draw curtains over all windows in the evenings and open them during sunlight hours (0.498); I insulate my house as much as possible to save energy and money (0.453); blinds, shutters, and shade reduce inlet heat in summer and heat loss in cold months (0.413); keeping air conditioners clean and not block them with drapes or furniture (0.541); I should open refrigerator and freezer doors rarely especially in hot weather (0.422); and my pots and pans should be the same sizes as the sizes of burners I put them upon (0.568). However, strong relationships include lowering the thermostat at night or anytime the house is vacant (0.661); I lock all windows tightly during winter to cut down on heat loss (0.633); I shut off my

air conditioner whenever I leave the home for more than one hour or two (0.658); I maintain proper temperature in refrigerator and freezer compartments (0.644); setting the temperature of the water heater (geyser) at medium (0.668), and I keep the bottom of my pots and pans shining to reduce energy wastage (0.601).

Component 2 summary results indicating moderate relationships include I can live in some areas of Windhoek city if asked to do so by law or legislation (0.560); reducing electricity consumption reduces global warming (-0.708); increasing electricity use does not affect the environment (0.523); lowering the thermostat at night or any time the house is vacant (0.424); installing underlay or carpets over windows and doors can reduce about 75.0% of sunlight heat from getting into the house (-0.482); I set the temperature of my water heater (geyser) at medium (-0.449); my pots and pans should be the same sizes as the sizes of burners I put them upon (-0.498); I install automatic switches in closets for the lights to go off whenever the door is closed (0.503), and I should not switch on fluorescent lamps within 15 minutes of switching off (0.425). However, a strong inverse relationship exists between if electricity use is not controlled the utility will continue to increase the cost of electricity (-0.639).

Component 3 summary results indicating moderate relationships include I can only live in some areas of Windhoek city if asked to do so by law or legislation (-0.484); controlled electricity consumption reduces stress on utility facilities (0.403); whatever affects the utility does not necessarily affect me (0.536); building new electricity generation stations to reduce global warming, only if blue, green, or other alternative energy generation plant technologies are installed (0.583); keeping heat-producing appliances away from the thermostat so that it can give accurate readings (0.412); I boil liquids quickly in tightly closed pans and save about 20.0% of the energy, if otherwise (0.457). However, using blinds, shutters, or shades can reduce the heat coming through windows by 50.0% during summer and reduce heat loss by 25.0% in cold months. These actions can save me money and reduce energy wastage (0.604).

Component 4 summary results indicating moderate relationships include the age of the participants (-0.468); I feel I can live comfortably anywhere in Windhoek city (-0.449); energy-efficient buildings and lighting protect the globe and earth resources (-0.536); allowing my television to be “on” without anyone watching it, is a good energy use method (0.552); installing underlay or carpets over windows and doors can reduce about 75.0% sunlight heat from getting into the house (0.476); I boil liquids quickly in tightly closed pans and save about 20.0% of the energy, if otherwise (0.436); I keep the bottom of my pans and

pots shining to reduce energy wastage (0.436) and I install automatic switches in closets for the lights to go off whenever the door is closed (0.446).

Component 5 summary results indicating moderate relationships include gender of the respondents (0.462); I will only use efficient lighting bulbs or lamps if supplied by the Electricity Control Board (ECB) or Municipality (0.505); engineers are there to produce enough energy for me to enjoy (0.430); I insulate my house as much as I can to save energy and money (-0.479) and installing underlay or carpets over windows and doors to reduce about 75.0% sunlight heat from getting into the house (0.407). However, a strong inverse relationship exists between I turn off radiators or closing air ducts in rooms used for guests (-0.714) and optimal electricity load management.

Component 6 summary results indicating moderate relationships include I should always switch off lights that I am not using (0.462); I do not need to reduce the electricity consumed since I can pay the amount charged by the Municipality or ECB or utility (-0.437); I prefer to use a dryer than the clothesline in drying my clothes (0.430); the utility should be allowed to charge any amount for electricity supply to consumers (-0.412) and I should not switch on fluorescent lamps within 15 minutes of switching off (-0.467).

Component 7 summary results indicating moderate positive relationships include electricity is meant to be enjoyed as long as I can pay for it (0.559); utility should be allowed to charge any amount for electricity supply to consumers (0.490); efficient use of electricity will enable the delay in building new power generation stations (0.585) and I keep heat-producing appliances away from the thermostat so that it can give accurate readings (0.422).

Component 8 summary results indicate a strong positive relationship. That means, energy savers are not bright enough and are very costly (0.602); while moderate relationships include I draw curtains over all windows in the evenings and open them during sunlight hours (0.431); I turn off the heater if I go away for more than a few days in winter (0.428) and I boil liquids quickly in tightly closed pans and save about 20.0% of the energy, if otherwise (-0.404).

Component 9 summary results indicating moderate relationships include gender of the respondents (-0.495); the age of the respondents (0.417) and energy-savers reducing the cost of electricity consumed (-0.464).

Component 10 summary results indicating moderate relationships include control switches are used on geysers, air conditioners, and other high energy consuming house

appliances (-0.461); and I prefer to use a dryer than the clothesline in drying my clothes (-0.433).

Component 11 summary results indicating moderate positive relationships include reduced electricity consumption decreases money paid to the Municipality or utility (0.420) and increased electricity consumption increases global warming (0.408). However, a strong inverse relationship exists between more day-lighting in buildings reducing electricity use (-0.613) and optimal electricity load management.

Component 12 indicates that a moderate inverse relationship exists for using fluorescent lamps whenever practicable. Component 13 indicates that a moderate inverse relationship exists for keeping windows closed and only open doors when necessary if the air conditioner is operating (-0.423). Component 14 implies that a moderate positive relationship exists because building new electricity generation stations can reduce global warming if blue, green, and other renewable power stations were installed (0.476). However, there were neither moderate nor strong electricity load management metrics extracted by components 15 to 17, respectively.

Table H. 1: Communalities

	Initial	Extraction
gender of respondent	1.000	.870
age of participant	1.000	.879
electricity to be enjoyed	1.000	.955
switch off light not using	1.000	.901
switch controls for geysers, a/c, etc	1.000	.896
energy savers reduce cost of electricity consumed	1.000	.886
I feel I can live comfortably anywhere in Windhoek	1.000	.947
energy savers are not bright enough and are very costly	1.000	.914
reduced consumption decreases money paid to Municipality/Utility	1.000	.921
smaller electricity use helps Utility supply regular power to all	1.000	.914
I will only use efficient lighting bulbs if supplied by ECB or the municipality	1.000	.920
I can only live in some areas of Windhoek if asked by law or legislation	1.000	.932
I can live in some areas of Windhoek city if asked to do so by Law or legislation	1.000	.930
I do not need to reduce the electricity consumed since I can pay for it	1.000	.865
I prefer to dry my clothes with a dryer rather than the clothesline	1.000	.889
Controlled power consumption reduces stress on Utility facilities	1.000	.882
Increased electricity consumption increases global warming	1.000	.820
I will like to buy energy-efficient equipment to reduce the bills paid	1.000	.853
Whatever affects Utility does not necessarily affect me	1.000	.852
Reducing electricity consumption reduces global warming	1.000	.885
Engineers are there to produce enough energy for me to enjoy	1.000	.919
More day light in buildings reduce electricity use	1.000	.861
The utility should be allowed to charge any amount for electricity supply to consumers	1.000	.928
Reducing wasted electricity is good for development	1.000	.844
Increasing electricity use does not affect the environment	1.000	.762

Energy-efficient buildings and lighting protect the globe and earth resources	1.000	.935
If electricity use is not controlled Utility will continue to increase cost for electricity	1.000	.902
Efficient electricity use delays building of new power stations	1.000	.798
Building new electricity generation stations reduce global warming	1.000	.896
Putting television on without anyone watching it is a good energy use method	1.000	.934
I turn off radiators or close air ducts in rooms used for guests	1.000	.790
I lower the thermostat at night or anytime the house is vacant	1.000	.913
I draw curtains over all windows in the evenings and open them during sunlight hours	1.000	.881
I lock all windows tightly during winter to cut down on heat loss	1.000	.846
I insulate my house as much as possible to save energy and money	1.000	.922
Using blinds, shutters, shade can reduce inlet heat in summer and heat loss in cold	1.000	.877
Installing underlay, carpets over windows, doors can reduce 75% sunlight heat getting	1.000	.873
I shut off my air conditioners whenever I leave home for more than one hour or two	1.000	.865
I keep air conditioners clean and do not block them with drapes or furniture	1.000	.906
I keep windows closed and only open doors when necessary if the air-conditioner is	1.000	.853
I keep heat-producing appliances away from the thermostat so that it can give accurate	1.000	.888
All rooms air conditioners and outside compressors are protected from the sun	1.000	.892
I set the temperature of my water heater at a medium	1.000	.894
I turn off the heater if I go away for more than a few days in winter	1.000	.931
I should open refrigerator and freezer doors rarely, especially in hot weather	1.000	.951
I maintain proper temperature in refrigerator and freezer compartments	1.000	.782
I cook with as little water as possible	1.000	.878
I boil liquids quickly in tightly closed pans to save about 20% energy, if otherwise	1.000	.890
I keep the bottom of my pots and pans shining to reduce energy wastage	1.000	.913
My pots and pans should be the same sizes as the sizes of burners I put them upon	1.000	.872
I use fluorescent lamps whenever possible	1.000	.945
I install automatic switches in closets for the lights to go off whenever the door is	1.000	.916
I should not switch on fluorescent lamps within 15 minutes of switching off	1.000	.894

*Extraction Method: Principal Component Analysis.

Table H. 2: Total Variance explained [1]

Component	Initial Eigenvalues			Extraction Sums of Squared Loadings		
	Total	% of Variance	Cumulative %	Total	% of Variance	Cumulative %
1	8.229	15.527	15.527	8.229	15.527	15.527
2	5.049	9.527	25.054	5.049	9.527	25.054
3	4.335	8.179	33.233	4.335	8.179	33.233
4	4.043	7.628	40.861	4.043	7.628	40.861
5	3.442	6.494	47.355	3.442	6.494	47.355
6	3.276	6.181	53.535	3.276	6.181	53.535
7	2.691	5.078	58.613	2.691	5.078	58.613
8	2.303	4.346	62.959	2.303	4.346	62.959
9	2.123	4.005	66.964	2.123	4.005	66.964
10	2.079	3.922	70.886	2.079	3.922	70.886
11	1.722	3.248	74.135	1.722	3.248	74.135
12	1.567	2.957	77.091	1.567	2.957	77.091
13	1.444	2.724	79.815	1.444	2.724	79.815
14	1.363	2.571	82.386	1.363	2.571	82.386
15	1.232	2.325	84.711	1.232	2.325	84.711
16	1.143	2.156	86.867	1.143	2.156	86.867
17	1.020	1.924	88.792	1.020	1.924	88.792
18	.923	1.741	90.533			
19	.904	1.705	92.238			
20	.647	1.220	93.459			
21	.492	.927	94.386			
22	.479	.903	95.289			
23	.455	.858	96.147			
24	.372	.702	96.850			

25	.351	.662	97.511
26	.309	.583	98.094
27	.299	.564	98.659
28	.239	.451	99.110
29	.182	.344	99.454
30	.130	.244	99.699
31	.098	.186	99.884
32	.061	.116	100.000
33	5.675E-16	1.071E-15	100.000

*Extraction Method: Principal Component Analysis.

H6.2 A Brief Research Overview

The need to use the variants of the PCAs proposed in this study depends on the ability to digitalise, select, and optimise the most significant electricity load growth parameters critical to optimal electricity generation and supply mix, smart grids, and smart cities. Decoupling the power systems analysis cycle using the PCAs indicates that the standard matrix formulation is made constant to reduce the computation time, computer memory space requirements, the number of iterations, increase algorithms convergence rates, and increase the accuracy of solutions [55]. The above factors reduce time delays, reduce the incidence of power failures, and enhance online supervisory computer control and data acquisition (SCADA) operating, and restoration systems. Also, to strengthen electric power generation plants, transmission, and distribution networks, and resolves short supply problems.

Also, data heterogeneity, over-time variability of distribution networks, and territorial factors of electricity consumption variability by geography can be streamlined by the PCAs for the ordered implementation of digital and smart systems, smart grids, and smart cities. These are the basis for the power systems of the future [56]. The data reduction capabilities of the PCAs are vital because they denote the ingredients that form the backbone, foundation, and frameworks for the implementation of efficient, resilient, and smart grids of the future that can withstand the weather in the face of climate change and its unpredictable consequences on the environment [57].

Furthermore, peak electricity consumption and peaking generating units can be shaved from the power system's energy mix using the PCAs. These factors will result in the economy, energy savings, waste minimisation, avoided generation, reduced greenhouse gas emissions, systems optimisation, deferred installation of new generation and transmission systems, and modulate electricity consumption patterns [58,59].

H7 Conclusion

All the estimated PCs reproduced the total system variability, which can be accounted for by a small number of uncorrelated PCs. The first PC contains as much variability in the data as possible. Each succeeding component accounts for as much of the remaining variability as possible. The PCA also assessed the diversity and grouping of variables based on the characteristics of the parameters measured.

The scree plot has 17 components with eigenvalues greater than unity. The communalities ranged between 0.762 and 0.955, while the average was 0.888 or 88.8%. Furthermore, communalities are lower-bound optimisation solutions similar to convex functions for obtaining high-quality optimal results without engaging laborious mathematical algorithms.

The analysis explains that the 17 component eigenvalues range between 8.229 and 1.020. The cumulative variance indicates that the 17 extracted components amount to 88.8% variance. Each of the 17 components comprises between 1 and 32 electricity load management variables having at least 0.3 loadings each. Also, all the constituting electricity load management variables in each of the extracted components show a moderate relationship with the variable under study. Therefore, only those variables having strong relationships with optimal electricity load management are enumerated.

Hence, a strong positive relationship exists for energy savers that are not bright enough; controlled electricity consumption reduces stress on utility facilities; reducing electricity consumption reduces global warming; more day-lighting in buildings reduces electricity use and if electricity use is not controlled the utility will continue to increase the cost of electricity. Also, I turn off radiators or close air ducts in rooms used for guests; lower the thermostat at night or any time the house is vacant; lock all windows tightly during winter to cut down on heat loss; blinds, shutters, or shades to reduce the heat coming through windows by 50.0% during summer and reduce heat loss by 25.0% in cold months; shutting off my air conditioner whenever I leave home for more than one hour or two; setting the temperature of my water heater (geyser) at medium; maintain proper temperature in the refrigerator and freezer compartments and keeping the bottom of my pans and pots shining to reduce energy wastage.

It is recommended that the PCAs in this study can digitalise, select, and optimise critical electricity load growth parameters for optimal electricity load management, smart grids, and smart cities infrastructure development. Also, the outcome or findings of the PCAs in the study can streamline data heterogeneity, over-time variability of distribution networks,

and territorial factors of electricity consumption variability by geography. Furthermore, the ordered implementation comprises the backbone of efficient, resilient, and smart grids of the future that can withstand the weather, especially in the face of climate change and its consequences on the environment.

References

1. Asemota, G. N. O. (2013). *Electricity use in Namibia*. USA: iUniverse.
2. Electricity Control Board. (2006). *2005 Electricity Control Board Annual Report.* Namibia: ECB.
3. von Oertzen, D. (2009). *Namibia's Electricity Supply.* Namibia: VO Consulting. https://www.voconsulting.net/pdf/Namibia's%20Electricity%20Supply%20-%20VO%20CONSULTING.pdf, Accessed on: Mar. 29, 2017
4. Isaaks, W. (2013). Energy situation in Namibia. *Africa Energy Forum (AEF),* Barcelona, Spain. www.energynet.co.uk/system/files/Private_23, Accessed on: Mar. 29, 2017
5. Manuel, V. (2013). Energy demand and forecasting in Namibia: Energy for economic development. Office of the President. *National Planning Commission,* Windhoek.
6. Brandt, E. (2014). Namibia's high electricity price. Namibia: *New Era Newspaper.* 14 November. http://allafrica.com/stories/201411140794.html, Accessed: Mar. 29, 2017
7. Energypedia. (2020). Namibia Energy Situation. Energypedia.info/wiki/Namibia_Energy_Situation. Accessed: Mar. 27, 2021
8. Huang, W., Zhang, N., Kang, C., Li, M., Huo, M. (2019). From demand response to integrated demand response: review and prospect of research and application. *Protection & Control of Modern Power Systems, 4(12),* 1-13.
9. Bimenyimana, S., Ishimwe, A., Asemota, G. N. O., Kemunto, C. M., Li, L. (2018). Web-based design and implementation of smart home appliances control system. *IOP Earth & Environmental Science Conference, 168,* 1-9.
10. Li, K., Cursio, J. D., Sun, Y. (2018). Principal component analysis of price fluctuation in the smart grid electricity market. *Sustainability, 10(4019),* 1-16.
11. Asemota, G. N. O. (2021). Rwanda's off-grid solar performance targets. *Joule, 5,* 22-23.
12. Asemota, G. N. O., Ijumba, N. M. (2020). Gender mediated optimal multivariate electricity load management model. *IEEE PES/IAS Power Africa Conference,* 1-5.
13. Bimenyimana, S., Asemota, G. N. O., Li, L. (2018). The state of the power sector in

Rwanda: a progressive sector with ambitious targets. *Frontiers in Energy Research, 6(68),* 1-14.

14. Asemota, G. N. O. (2013). A prediction model of future electricity pricing in Namibia. *Advances in Materials Research, 824,* 93-99.
15. Isebrands, J. G., Chow, T. R. (1975). Introduction to uses and interpretation of principal component analysis in forest biology. *North Central Forest Experimental Station Forest Service, U. S. Department of Agriculture, Forest Service General Technical Report NC-17*.
16. Wang, Y., Lu, X., Xu, Y., Shi, D., Yi, Z., et al. (2019). Submodular load clustering with robust principal component analysis. *arXiv:1902.07367v1 [cs.LG] 20 Feb 2019,* 1-5.
17. Bimenyimana, S., Asemota, G. N. O., Ihirwe, P. J., Li, L. (2018). Clustering residential electricity consumption: a case study. *International Conference in Electrical & Electronics Engineering Technology*, 44-51.
18. Burgas, L., Melendez, J., Colomer, J. (2014). Principal component analysis for monitoring Electrical consumption of academic buildings. *International Conference on Sustainability in Energy and Buildings, SEB-14, Energy Procedia*, *62,* 555-564.
19. Fahim, M., Silliti, A. (2019). Analyzing load profiles of energy consumption to infer household characteristics using smart meters. *Energies, 12(773),* 1-15.
20. Kerr, N., Gouldson, A., Barret, J. (2017). The rationale for energy efficiency policy: Assessing the recognition of the multiple benefits of energy efficiency retrofit policy. Energy Policy, 106, 212-221.
21. Eid, C., Bollinger, A. L., Koirala, B., Scholten, D., Facchinetti, E., Lilliestan, J., Hakvoort, R. (2016). Market integration of local energy systems: Is local energy management compatible with European regulation for retail competition? *Energy*, *114*, 913-922.
22. Shiraki, H., Nakamura, S., Ashina, S., Honjo, K. (2016). Estimating the hourly electricity profile of Japanese households-Coupling of engineering and statistical methods. *Energy, 114,* 478-491.
23. Simoes, S., Nijs, W., Ruiz, P., Sgobbi, A., Thiel, C. (2017). Comparing policy routes for low-carbon power technology deployment in EU-an energy systems analysis. *Energy Policy, 101,* 353-365.

24. Warren, P. (2018). Demand-Side Policy: Global evidence base and implementation patterns. *Energy & Environment 0(0),* 1-26.
25. Cherp, A., Vinichenko, V., Jewell, J., Suzuki, M., Antal, M. (2017). Comparing electricity transitions: A historical analysis of nuclear, wind and solar power in Germany and Japan. *Energy Policy, 101,* 612-628.
26. Jakubcionis, M., Carlsson, J. (2017). Estimation of European Union residential sector space cooling potential. *Energy Policy, 101*, 225-235
27. Neuteleers, S., Mulder, M., Hindriks, F. (2017). Assessing fairness of dynamic grid tariffs. *Energy Policy, 108,* 111-120
28. Broto, C. V. (2017). Energy landscapes and urban trajectories towards sustainability. *Energy Policy, 108,* 755-764.
29. Diaz, P., Adler, C., Patt, A. (2017). Do stakeholders perspectives on renewable energy infrastructure pose a risk to energy policy implementation? A case of a hydropower plant in Switzerland. *Energy Policy, 108,* 21-28.
30. Rama, M., Purseheimo, E., Lindroos, T., Koponen, K. (2014). Development of Namibian energy sector. *VTT Technical Research Centre of Finland, Finland*. Research Report VTT-R-07599-13, 1-69.
31. Bimenyimana, S., Asemota, G. N. O., Ihirwe, J. P., Kemunto, C. M., Li, L. (2018). Performance estimation of Ntaruka hydropower plant and its comparison with the prediction obtained by SPSS. *Energy & Environment, 0(0),* 1-18.
32. Solatube. (n.d.). Daylighting Facts & Figures. 150516 Daylighting Facts & Figures-plain.pdf, Accessed on: Feb. 24, 2020
33. Ander, G. (2011). Day-lighting: Whole building design guide. http://www.wbdg.org/resources/daylighting.php, Accessed on: Feb. 24, 2020
34. Stauffner, N. (2007). Daylight Device Lightens Electricity Cost. *MIT News*. http://newsoffice.mit.edu//2007/techtalk51-26.pdf, Accessed on: Feb. 24, 2020
35. Kozlowski, D. (2006). Using daylighting to save on energy costs. *FacilitiesNet.* http://www.facilitiesnet.com/energyefficiency/article/Harnessing-Daylight-For-Energy Savings-Facilities Management-EnergyEfficiency-Feature—4267#, Accessed on: Feb. 24, 2020
36. Mocherniak, T. (2006). Lighting technologies produce energy savings. *Energy and Power Mgt.* www.highbeam.com/doc/1G1-146346289.html, Accessed on: Feb. 24, 2020

37. Leslie, R. P., Raghavan, R., Howlett, O., Eaton, C. (2005). The potential of simplified concepts for daylight harvesting. *Lighting Research and Technology*. http://www.lrc.rpi.edu/programs/daylighting/pdf/simplifiedConcepts.pdf, Accessed on: Feb. 24, 2020
38. Anon. (n.d.). Factor analysis: phases and rule of thumb. https://avesis.ege.edu.tr, Accessed on: Oct. 27, 2020
39. Scalelive. (2020). Principal component analysis. Accessed on: Oct. 27, 2020 https://scalelive.com/principal-components-analysis.html
40. UC Regents. (2020). Principal components: SPSS annotated output. https://stats.idre.ucla.edu/spss/output/principal_components/, Accessed on: Oct. 27, 2020
41. Asemota, G. N. O. (2014). Communality performance assessment of electricity load management model for Namibia. *IEEE Artificial Intelligence, Modelling, and Simulation Conference,* 252-257.
42. Tabachnick, B. G., Fidell, L. S. (2001). *Using Multivariate Statistics.* USA: Allyn & Bacon.
43. Baruch, Y., Holtom, B. C. (2008). Survey response rate levels and trends in organizational research. *Human Relations, 61(8),* 1139-1160.
44. Hamilton, M. B. (1999). Online survey response rates and times: background and guidance for industry. http://www.Supersurvey.com/papers/supersurvey_white_paper_response_rate.htm
45. Fraze, S. D., Hardin, K. K., Brashears, M. T., Haygood, J. L., Smith, J. H. (2003). The effects of delivery mode upon survey response rate and perceived attitudes of Texas agric-science teachers. *Journal of Agricultural Education, 70(5),* 646-675.
46. Papoulis, A., Pillai, S. U. (2008). *Probability, random variables, and stochastic processes.* India: Tata McGraw-Hill.
47. Wong, S. S. M. (2008). *Computational methods in physics and engineering.* Singapore: World Scientific.
48. Asemota, O. O., Asemota, G. N. O. (2020). Time series modeling of academic employee commitment of a sub-Saharan African University. *Asian Journal of Economics, Business & Accounting, 19(3),* 60-76.
49. Asemota, G. N. O. (2015). Multivariate parsimony model for electricity load management. *WSEAS Energy & Environment Conference,* 77-86.

50. Foster, J. J. (1998). Data analysis using SPSS for Windows: a beginner's guide. UK: Sage.
51. Brace, N., Kemp, R., Snelgar, R. (2000). *SPSS for psychologists: a guide to data analysis using SPSS for Windows.* USA: Lawrence Erlbaum Associates.
52. Asemota, G. N. O. (2009). On a class of computable convex functions. *Canadian Journal of Pure & Applied Sciences, 3(3),* 959-965.
53. Asemota, G. N. O. (2012). Optimal two-way conductor design using computable convex functions approach. *Advances in Materials Research, 367,* 75-81.
54. LaMorte, W. W. (2021). PH717 Module 9- Correlation and regression: evaluating association between two continuous variables. https://sphweb.bumc.bu.edu.otlt/MPH-Modules/PH717-QuantCore/PH717-Module9- Correlation-Regression/PH717-Module9-Correlation-Regression4.html, Accessed: Mar. 29, 2022
55. Asemota, G. N. O. (2010). *Application of modern load flow techniques to electric power systems.* Germany: Lambert Academic Publishing.
56. Bimenyimana, S., Asemota, G.N.O. (2018). Traditional vs smart electricity metering systems: a brief overview. *Journal of Marketing & Consumer Research, 46,* 1-7.
57. Bimenyimana, S., Wang, C., Nduwamungu, A., Asemota, G. N. O., Utetiwabo, W., et al. (2021). Integration of microgrids and electric vehicle technologies in the national grid as the key enabler to the sustainable development for Rwanda. *International Journal of Photoenergy, 2021(9928551),* 1-17.
58. Ihirwe, J. P., Li, Z., Sun, K., Bimenyimana, S., Wang, C., et al. (2021). Solar PV Minigrid Technology: Peak Shaving Analysis in the East African Community Countries. *International Journal of Photoenergy, 2021(5580264),* 1-40.
59. Niyonteze, J. D. D., Zou, F., Asemota, G. N. O., Nsengiyumva, W., Hagumimana, N., et al. (2021). Applications of Metaheuristic Algorithms in Solar Air Heaters Optimization: A Review of Recent Trends and Future Prospects. *International Journal of Photoenergy, 2021(6672579),* 1-36.

APPENDIX H.A

Table H.3: Component Matrix a

	Component																
	1	**2**	**3**	**4**	**5**	**6**	**7**	**8**	**9**	**10**	**11**	**12**	**13**	**14**	**15**	**16**	**17**
gender of respondent	-.045	.330	-.167	-.033	.462	-.355	-.114	-.051	-.495	.154	.197	-.062	.120	.001	-.141	.075	-.153
age of participant	-.141	-.128	.184	-.468	.133	.140	-.110	-.301	.417	.152	-.024	.071	.387	.110	-.022	-.289	.035
electricity to be enjoyed	-.433	-.211	.007	.016	.005	-.220	.559	.356	.079	-.218	.042	-.123	-.026	-.257	-.262	-.025	.169
switch off light not using	.383	.100	.247	.304	-.205	.462	-.091	-.031	-.257	.041	.192	.193	-.042	-.280	-.049	-.077	.311
switch controls for geysers, a/c, etc	.333	.272	.224	.251	-.007	-.107	.266	.086	.259	-.431	-.166	.236	.203	-.059	-.042	.243	.256
energy savers reduce cost of electricity consumed	.378	.294	.081	-.072	.107	.185	.124	-.268	-.464	-.227	.142	.056	.027	-.057	.240	-.361	.171
I feel I can live comfortably anywhere in Windhoek	.123	.052	.328	-.449	-.016	-.392	-.225	-.136	.213	-.109	-.015	.240	-.383	.273	.048	.191	.147
energy savers are not bright enough and very costly	-.119	-.201	-.319	.390	.050	.295	.055	.602	.197	-.060	.042	.111	-.064	-.256	.133	-.070	.035
reduced consumption decreases money paid to Municipality/Utility	.569	.019	-.384	.131	.164	.221	-.046	-.129	.070	.071	.420	-.069	.096	.097	.259	.149	.197
smaller electricity use helps Utility supply regular power to all	.572	-.314	.005	.106	.352	.178	-.149	-.068	.070	-.242	-.309	.101	.053	-.041	.066	.221	-.261
I will only use efficient lighting bulbs if supplied by ECB or municipality	-.227	.126	.105	-.120	.505	.373	.124	.309	-.123	-.055	.068	.333	-.222	.200	.225	.178	.129
I can only live in some areas of Windhoek if asked by law or legislation	-.202	.359	-.484	.334	-.096	.339	.059	-.172	.089	.383	.227	-.054	-.070	.087	-.105	.155	.054
I can live in some areas of Windhoek city if asked to do so by Law or legislation	-.143	.560	-.311	.251	-.341	.211	.317	-.125	-.115	.168	.109	-.042	.187	.030	-.148	.214	.039
I do not need to reduce electricity consumed since I can pay for it	-.402	.125	.254	.245	-.350	-.437	.115	.190	-.262	.098	.084	-.159	.024	.181	.222	.070	.049
I prefer to dry my clothes with dryer rather than the line	-.232	.275	-.112	.082	.017	.430	-.215	.213	.367	-.433	.061	-.007	-.210	.197	-.171	-.149	.050
Controlled power consumption reduces stress on Utility facilities	.638	.190	-.316	-.251	.167	.308	.166	-.082	-.155	-.044	-.065	.148	-.001	-.079	.114	.214	.034
Increased electricity consumption increases global warming	.341	-.185	.403	-.348	-.200	.159	.100	.160	-.114	-.057	.408	.147	.206	.056	-.164	.086	-.008
I will like to buy energy efficient equipment to reduce amount of money spent on bills	.524	.006	-.344	.215	.237	-.213	.169	-.157	-.114	-.037	-.074	.073	-.145	.186	-.394	-.091	.120
Whatever affects Utility does not necessarily affect me	-.248	.370	.536	.182	.180	-.057	-.174	-.114	.289	-.022	.032	.306	.147	.007	-.205	.025	.102
Reducing electricity consumption reduces global warming	.216	-.708	.371	-.175	.093	.164	-.099	-.023	-.198	.000	-.015	.095	.021	-.080	.138	.150	-.161
Engineers are there to produce enough energy for me to enjoy	-.222	.223	-.199	.247	.430	-.357	-.040	.371	-.049	.187	.204	.209	.012	.181	.235	-.175	.161
More day light in buildings reduce electricity use	.003	.290	.087	.212	.097	.363	-.235	.188	-.157	.102	-.613	-.140	-.079	.125	.120	-.100	.127
Utility should be allowed to charge any amount for electricity supply to consumers	-.046	.299	-.044	-.150	.133	-.412	.490	.076	.337	-.095	.121	.008	.204	.004	.339	.120	-.265
Reducing wasted electricity is good for development	.520	.065	-.291	-.277	.221	.228	.274	-.094	.183	-.145	.089	-.328	-.036	.188	-.121	.031	-.023
Increasing electricity use does not affect the environment	-.394	.523	.127	.187	-.327	.227	-.089	.058	.099	.081	-.001	.219	.061	-.012	-.022	-.043	-.206
Energy efficient buildings and lighting protect the globe and earth resources	.248	.199	.374	-.536	.395	.278	.044	-.010	.007	.081	.184	-.120	.072	-.181	-.073	-.241	-.123
If electricity use is not controlled Utility will continue to increase cost for electricity	.320	-.639	-.371	.286	-.180	-.043	.038	.071	-.073	-.125	-.002	-.010	-.164	.180	.020	-.195	-.109
Efficient electricity use delays building of new power stations	.106	-.033	.249	-.308	-.018	.178	.585	.301	-.099	-.048	-.219	-.129	.084	.204	-.137	.117	.072
Building new electricity generation stations reduce global warming	.060	-.059	.583	.269	-.320	-.063	.139	.041	-.041	.176	-.199	.031	.193	.476	.031	-.064	.082
Putting television on without anyone watching it is a good energy use method	-.277	-.261	.386	.552	.248	-.039	-.241	-.171	-.038	-.013	.171	.072	.232	-.217	.095	.195	.032
I turn off radiators or close air ducts in rooms used for guests	.310	.160	.149	-.074	-.714	-.051	-.079	.018	-.006	-.175	.151	-.191	-.014	-.017	.090	-.149	-.008
I lower thermostat at night or anytime the house is vacant	.661	.424	.013	-.274	-.242	.043	.145	.035	-.061	-.084	-.010	-.007	-.143	.020	.316	-.081	-.003
I draw curtains over all windows in the evenings and open them during sunlight hours	.498	.338	-.077	-.251	-.226	-.284	-.054	.431	.207	.216	.049	.019	-.014	-.146	.113	-.039	.021
I lock all windows tightly during winter to cut down on heat loss	.633	-.053	-.309	.351	-.158	-.195	.064	-.061	.055	.141	-.166	.159	.114	-.166	.015	-.154	-.111
I insulate my house as much as possible to save energy and money	.453	-.389	.195	-.014	-.479	-.177	.265	-.048	-.053	.274	.011	.214	-.051	-.141	-.132	.123	.121
Using blinds, shutters, shade can reduce inlet heat in summer and heat loss in cold months	.413	.043	.604	.020	.345	-.096	.102	.118	-.102	.215	.182	-.033	-.166	.146	-.109	-.184	.042
Installing underlay, carpets over windows, doors can reduce 75% sunlight heat getting into house	.158	-.482	.167	.476	.407	.050	.051	.214	-.165	.144	-.027	-.160	.123	.217	-.082	.023	-.038
I shut off my air conditioners whenever I leave home for more than one hour or two	.658	.106	-.276	.262	.168	-.236	-.176	.002	.172	.330	-.033	.029	.062	.104	-.046	.050	.041
I keep air conditioner clean and not block them with drapes or furniture	.541	.333	.042	.216	.181	-.143	.031	-.064	.312	.096	-.227	-.234	.358	-.020	.109	-.124	.163
I keep windows closed and only open doors when necessary if air conditioner is operating	.039	.336	.295	.397	.177	-.216	.099	-.026	.289	-.012	.208	-.007	-.423	-.180	-.123	-.127	-.187
I keep heat producing appliances away from thermostat so that it can give accurate readings	.369	.139	.412	-.028	.269	-.032	.422	.144	-.013	.375	-.167	8.143E-05	-.187	-.265	.052	.052	-.101
All rooms air conditioners and outside compressors are protected from the sun	.386	.222	.370	.171	-.198	.300	-.238	-.071	.105	.149	-.191	-.358	-.207	-.155	.069	.254	.048
I set the temperature of my hot water heater at medium	.668	-.449	-.101	.133	-.126	-.185	-.203	.140	.211	-.005	.054	.178	-.015	.028	.120	-.114	-.001
I turn off heater if I go away for more than a few days in winter	.379	.281	-.026	-.101	-.106	.386	-.262	.428	.141	.157	.204	.130	.156	.211	-.135	.151	-.269
I should open refrigerator and freezer doors rarely, especially in hot weather	.422	.323	.155	.065	-.312	.002	-.281	.396	-.354	-.189	-.037	.143	.196	.054	-.149	-.080	-.232
I maintain proper temperature in refrigerator and freezer compartments	.664	.131	-.176	-.388	.058	-.012	-.004	.096	.019	.274	-.133	.040	-.019	-.047	-.167	-.045	.053
I cook with as little water as possible	-.060	-.331	.151	.278	-.249	.321	.374	-.203	.182	.265	.178	-.040	-.238	.251	.144	-.010	-.204
I boil liquids quickly in tightly closed pans to save about 20% energy, if otherwise	.264	.147	.457	.436	.036	.174	.295	-.404	.109	-.244	.104	.016	.015	.093	.115	-.082	-.080
I keep the bottom of my pots and pans shining to reduce energy wastage	.601	-.222	-.172	.436	.027	.106	.320	-.025	-.025	-.306	.034	.176	.103	.044	-.081	-.099	-.115
My pots and pans should be the same sizes as the sizes of burners I put them upon	.568	-.498	.188	-.054	-.066	-.101	-.267	.027	.214	.166	.209	-.062	-.099	-.005	-.099	.071	.174
I use fluorescent lamps whenever possible	.369	-.100	.127	.080	.063	-.180	-.290	.247	.001	-.383	.275	-.568	.117	.020	.022	.157	.104
I install automatic switches in closets for the lights to go off whenever the door is closed	.364	.503	.396	.446	.202	-.117	-.104	.025	-.069	-.088	.005	-.185	-.150	-.040	-.087	.021	-.175
I should not switch on fluorescent lamps within 15 minutes of switching off	.377	.425	-.182	-.057	-.109	-.467	-.120	-.266	-.204	-.280	-.039	.176	-.156	.108	-.053	.161	-.065
Extraction Method: Principal Component Analysis.																	

*a17 components extracted